Planet Formation

Jürgen Blum

Institut für Geophysik und extraterrestrische Physik

Technische Universität zu Braunschweig

Germany

Contents

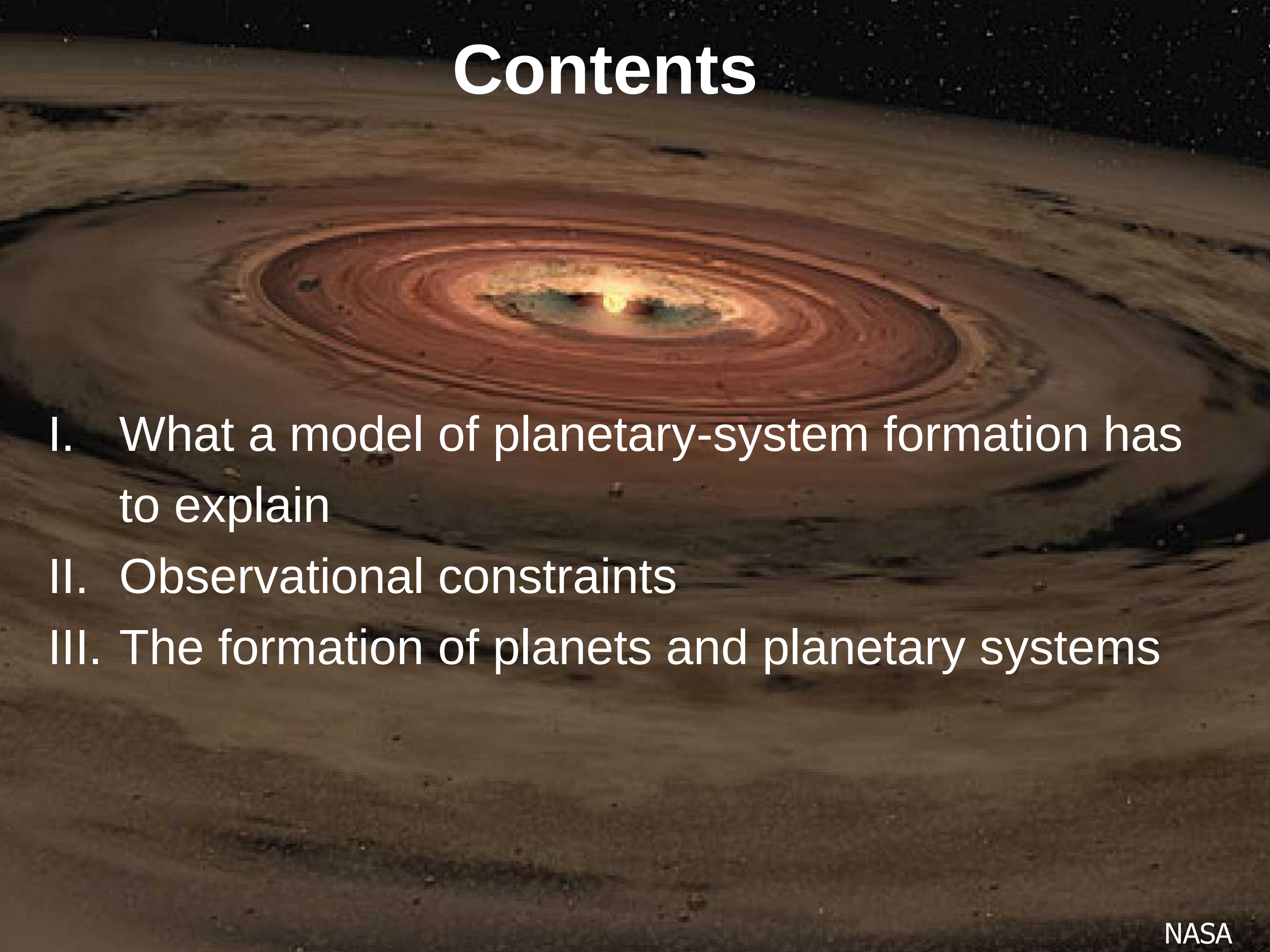

NASA

A small chronology of the world

13,7 Gyr	Big bang; formation of the elements H and He
13,4 Gyr	First stars and galaxies; first supernova explosions produce the heavy elements (C,N,O,Si,Fe,…)
12 Gyr	Formation of the milky way
4,567 Gyr	Formation of the solar system; at this point in time the interstellar medium has been enriched with 1% heavy elements
4,5 Gyr	Formation of the earth and the moon
4,45 Gyr	Layer structure of the earth
4,4 Gyr	Solid earth crust
4,2 Gyr	Early ocean
4 Gyr	Plate tectonics
>3,5 Gyr	Earth's magnetic field
>3,5 Gyr	Origin of life
2,3 Gyr	Formation of oxygen-rich atmosphere; formation of ozone
1 Gyr	"Freeze-out" of inner earth core
0 Gyr	Today

I.
What a model of planetary-system formation has to explain

I. What a model of planetary-system formation has to explain

a. The architecture of our Solar System

- Terrestrial planets in the inner system, gas giants in the outer system
- The occurrence of an asteroid belt between the terrestrial and gaseous planet region
- Kuiper belt
- Oort cloud

The planets of the solar system

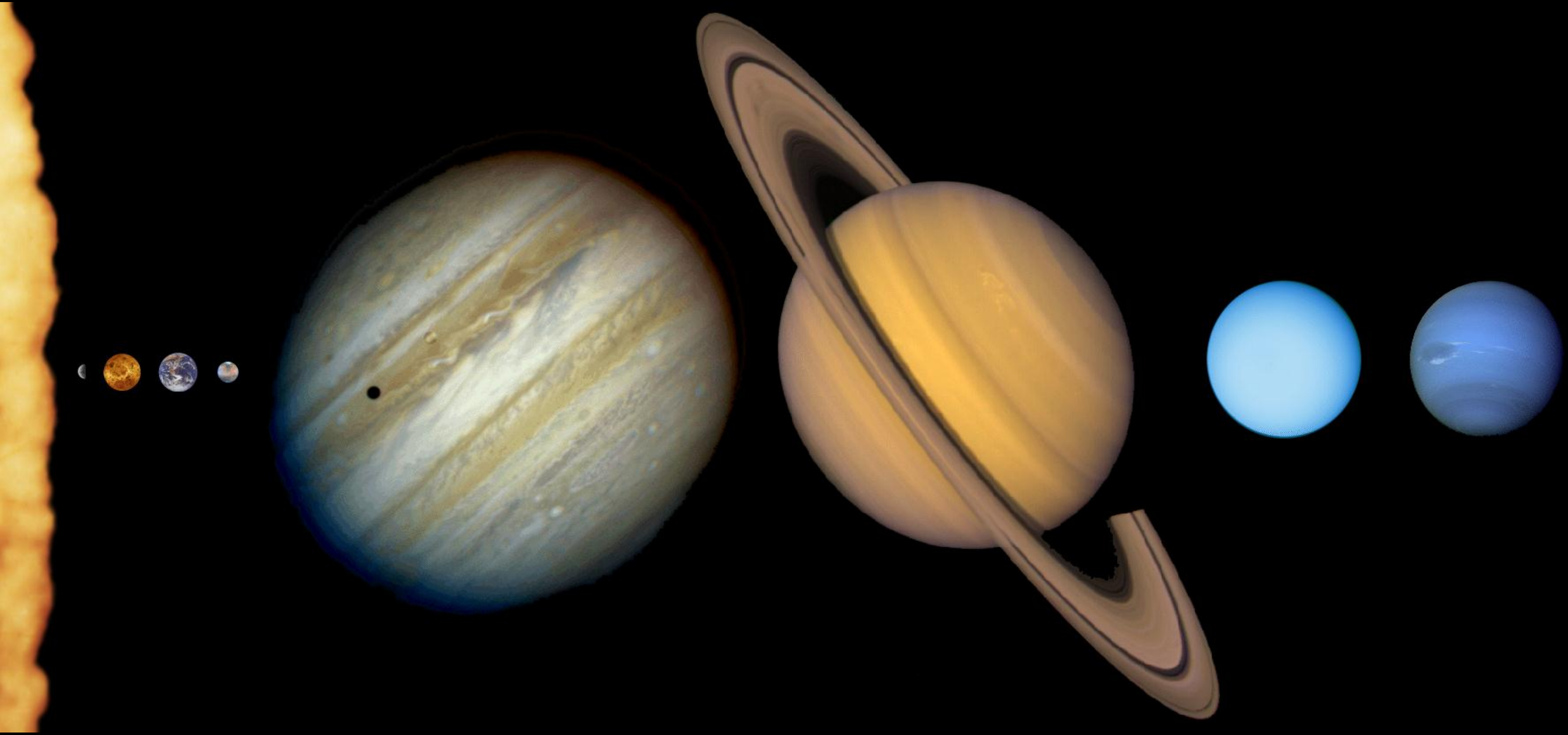

Terrestrial vs. gaseous planets

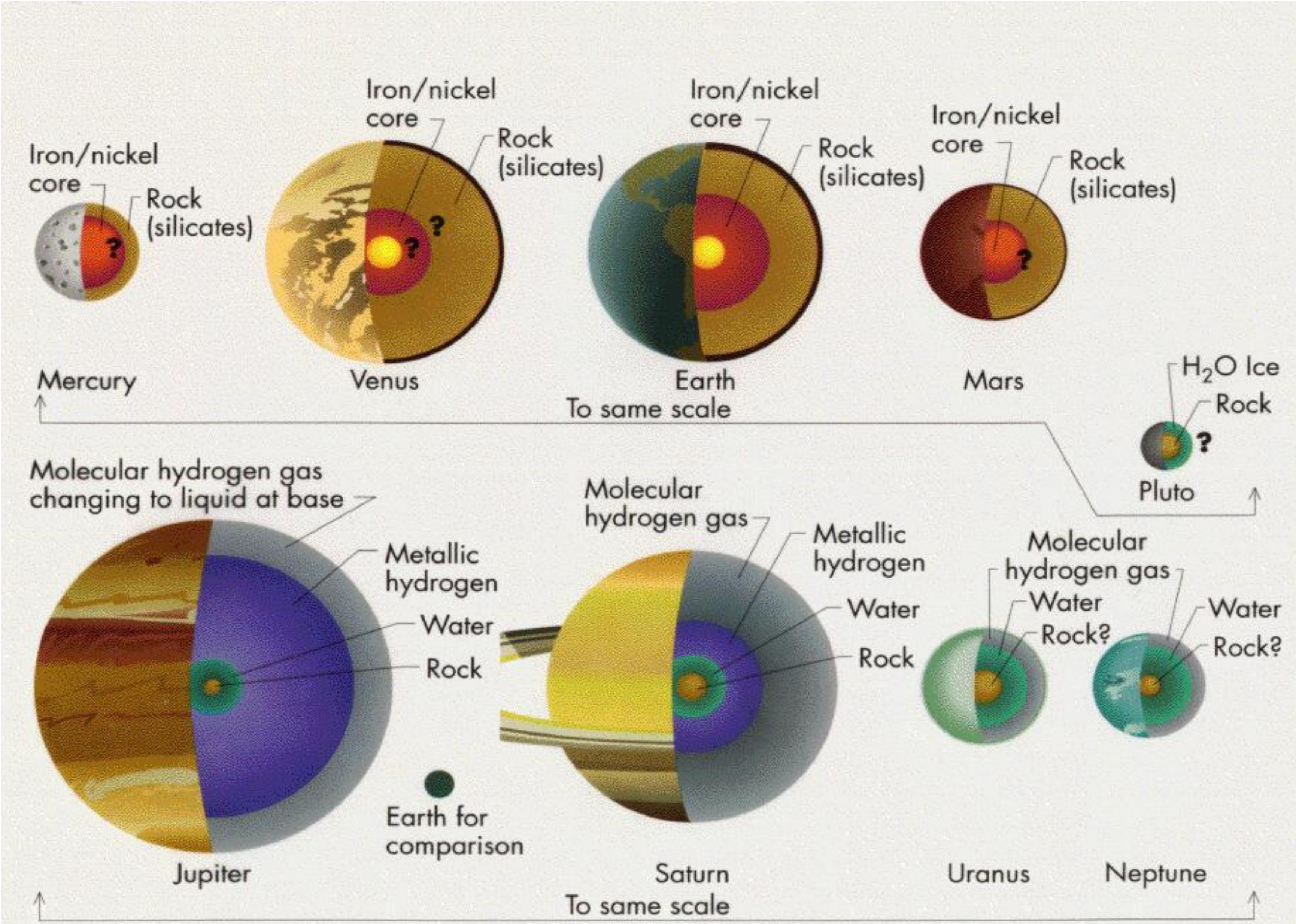

Comparative Planetology

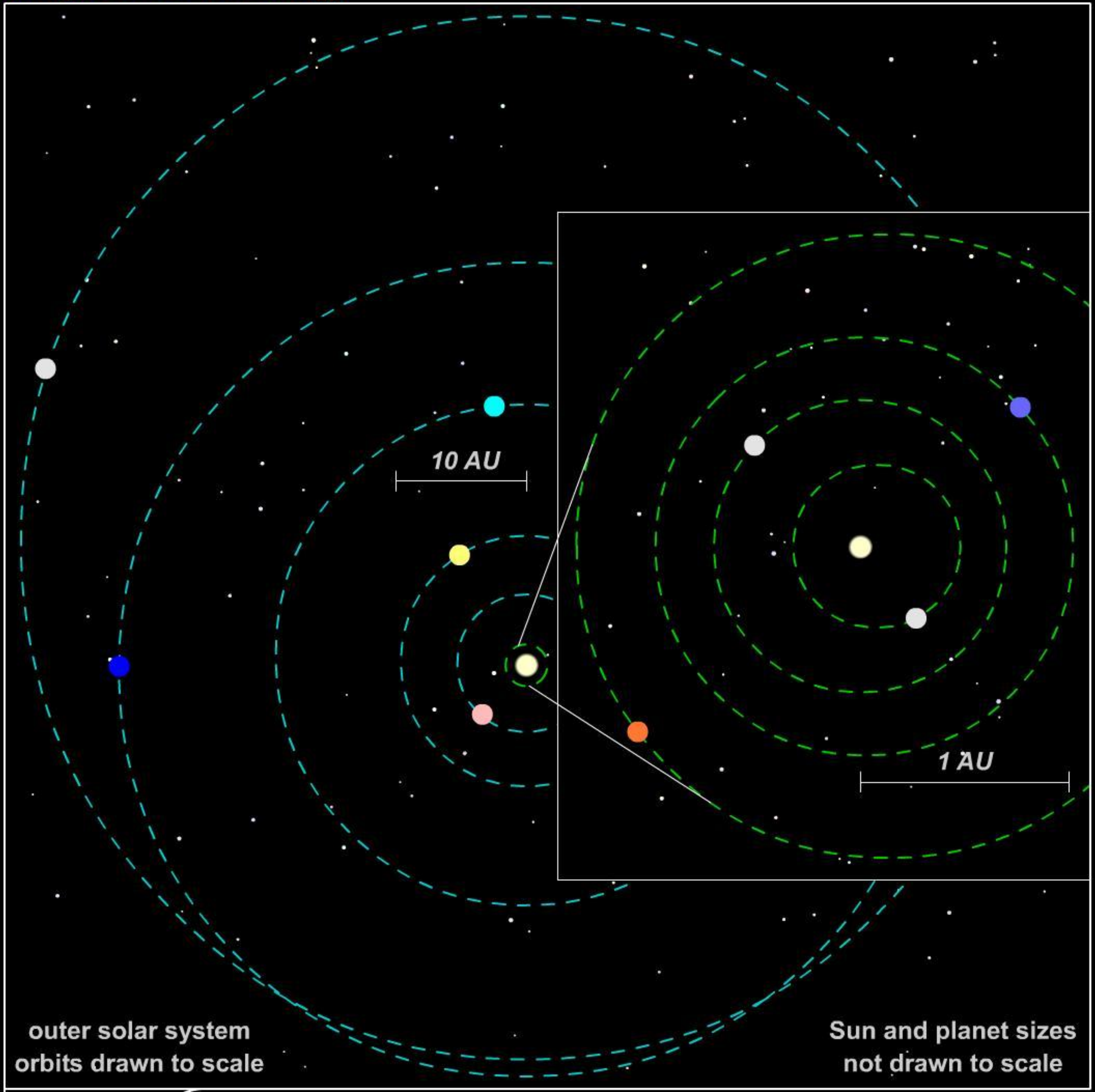

Asteroid belt, Kuiper belt

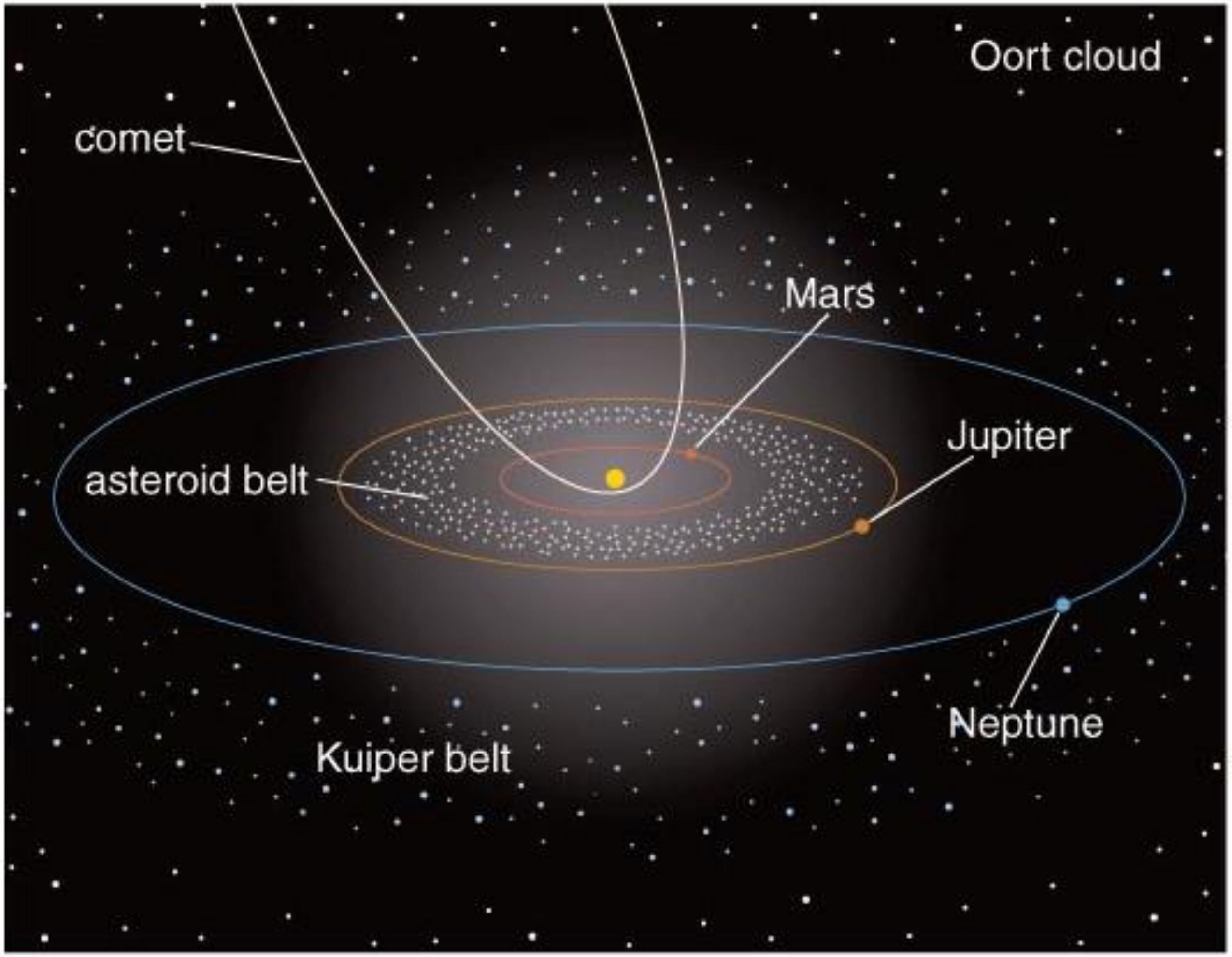

3. Swarms of asteroids and comets populate the solar system. Asteroids are concentrated in the asteroid belt, and comets populate the regions known as the Kuiper belt and the Oort cloud.

Oort cloud

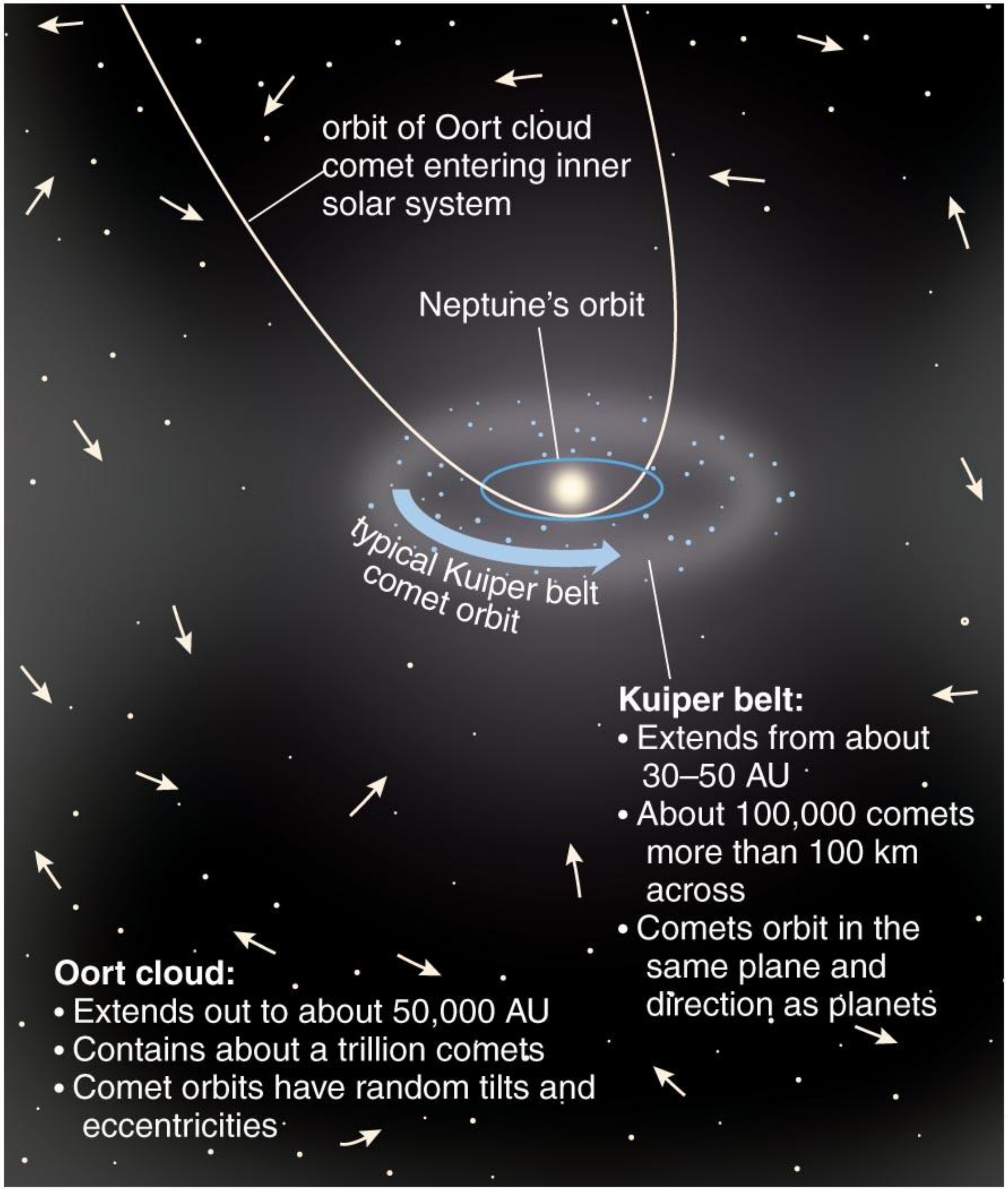

orbit of Oort cloud comet entering inner solar system
Neptune's orbit
typical Kuiper belt comet orbit
Kuiper belt:
• Extends from about 30–50 AU
• About 100,000 comets more than 100 km across
• Comets orbit in the same plane and direction as planets
Oort cloud:
• Extends out to about 50,000 AU
• Contains about a trillion comets
• Comet orbits have random tilts and eccentricities

I. What a model of planetary-system formation has to explain

b. The existence and formation scenario of the Moon

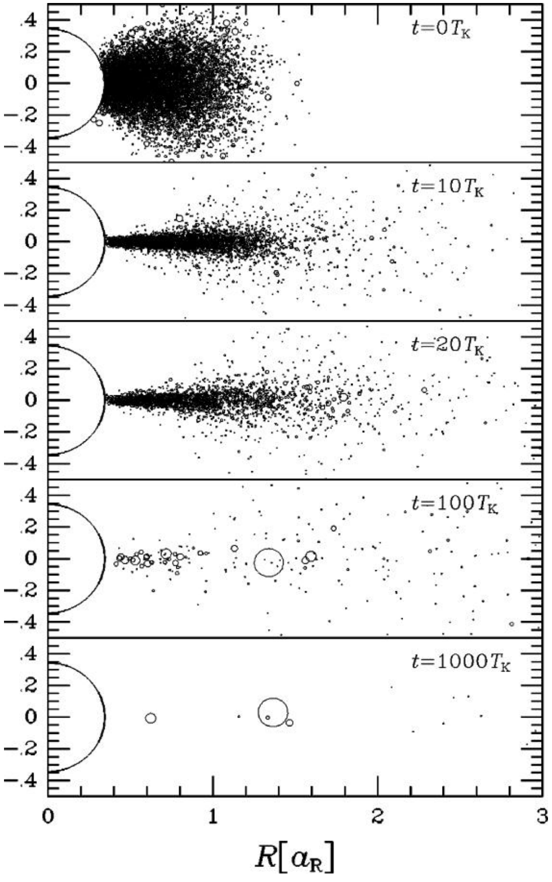

Kokubo et al. 2000

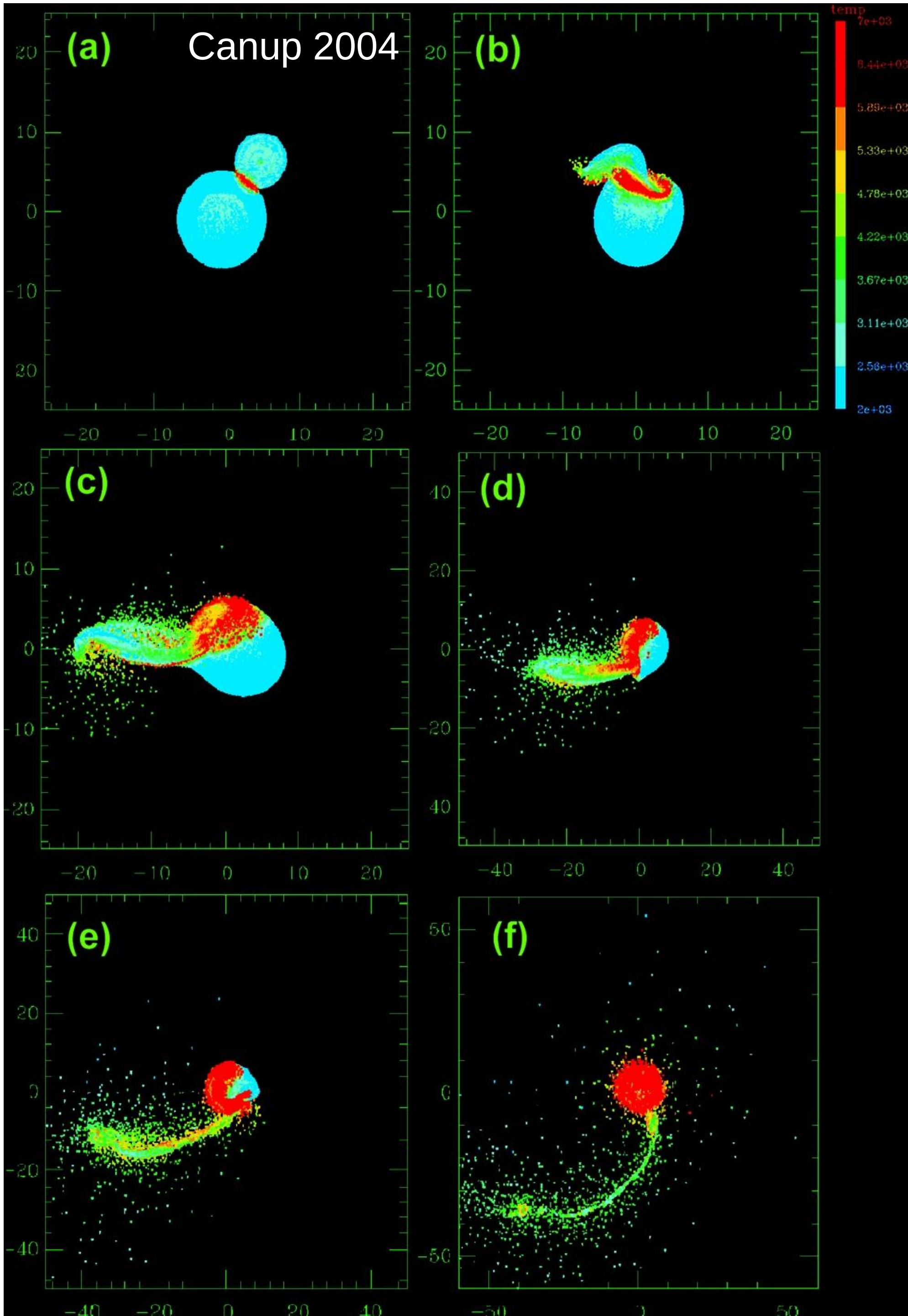

I. What a model of planetary-system formation has to explain

c. The architecture of other solar systems

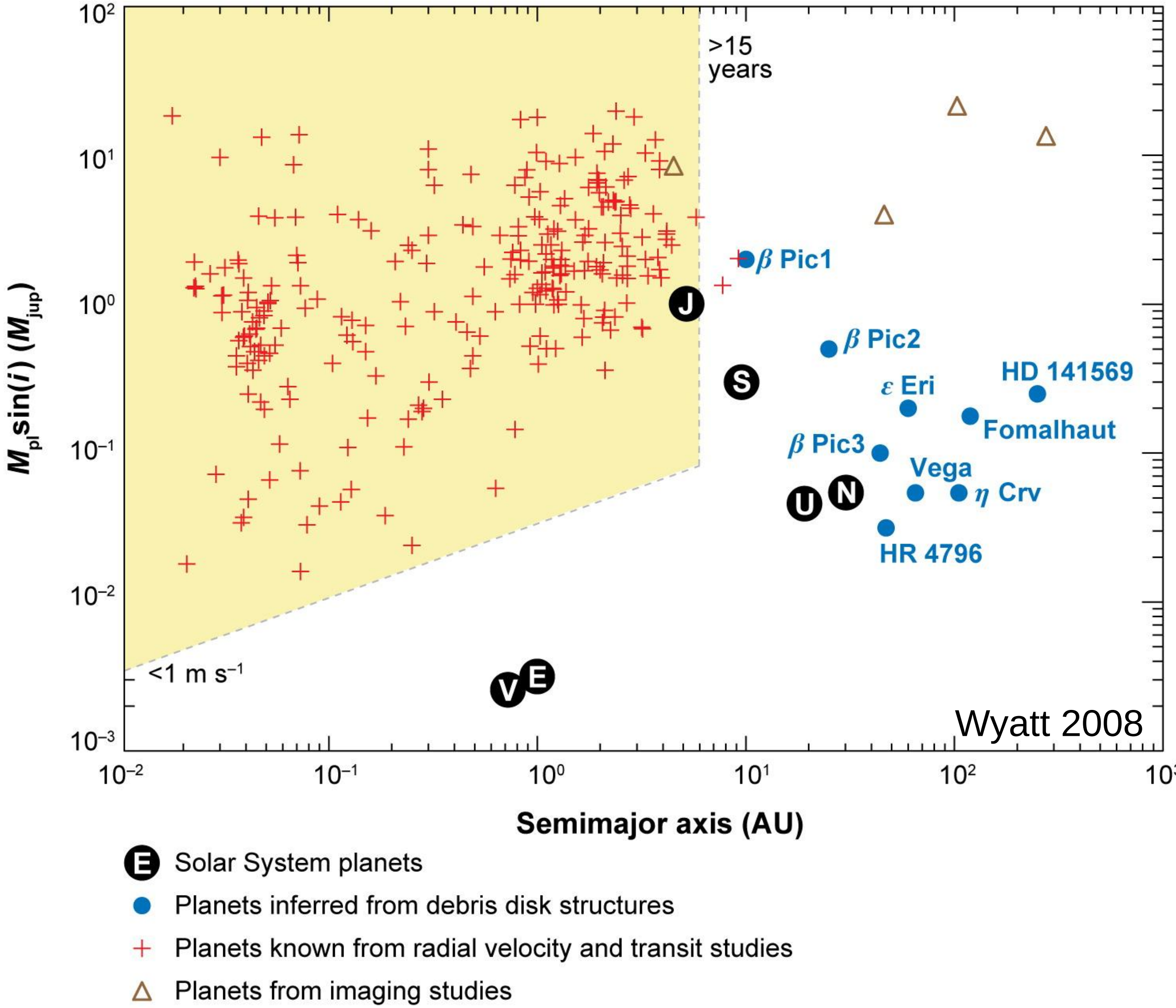

I. What a model of planetary-system formation has to explain

d. The gaseous-disk lifetime constraint

Maximum lifetime of protoplanetary disks 10^7 years

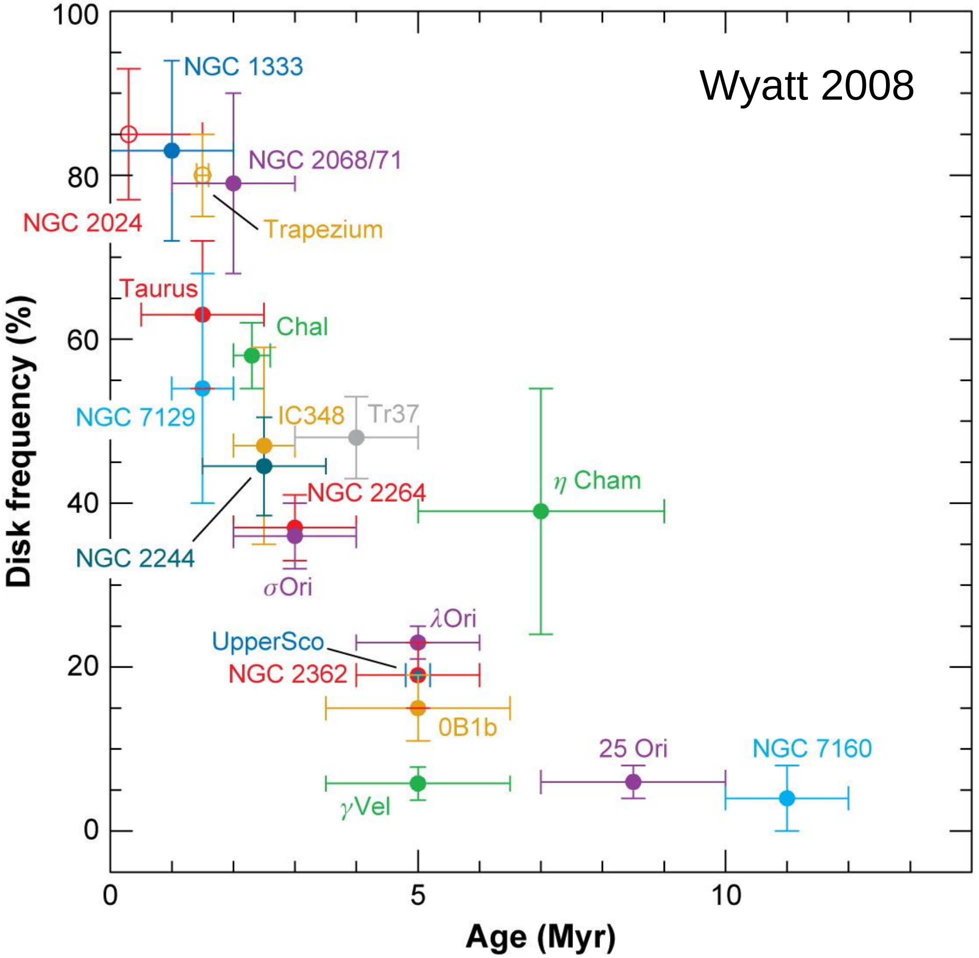

I. What a model of planetary-system formation has to explain

e. Meteoritic constraints

© E. Zinner, Washington University, St. Louis, Missouri (USA)

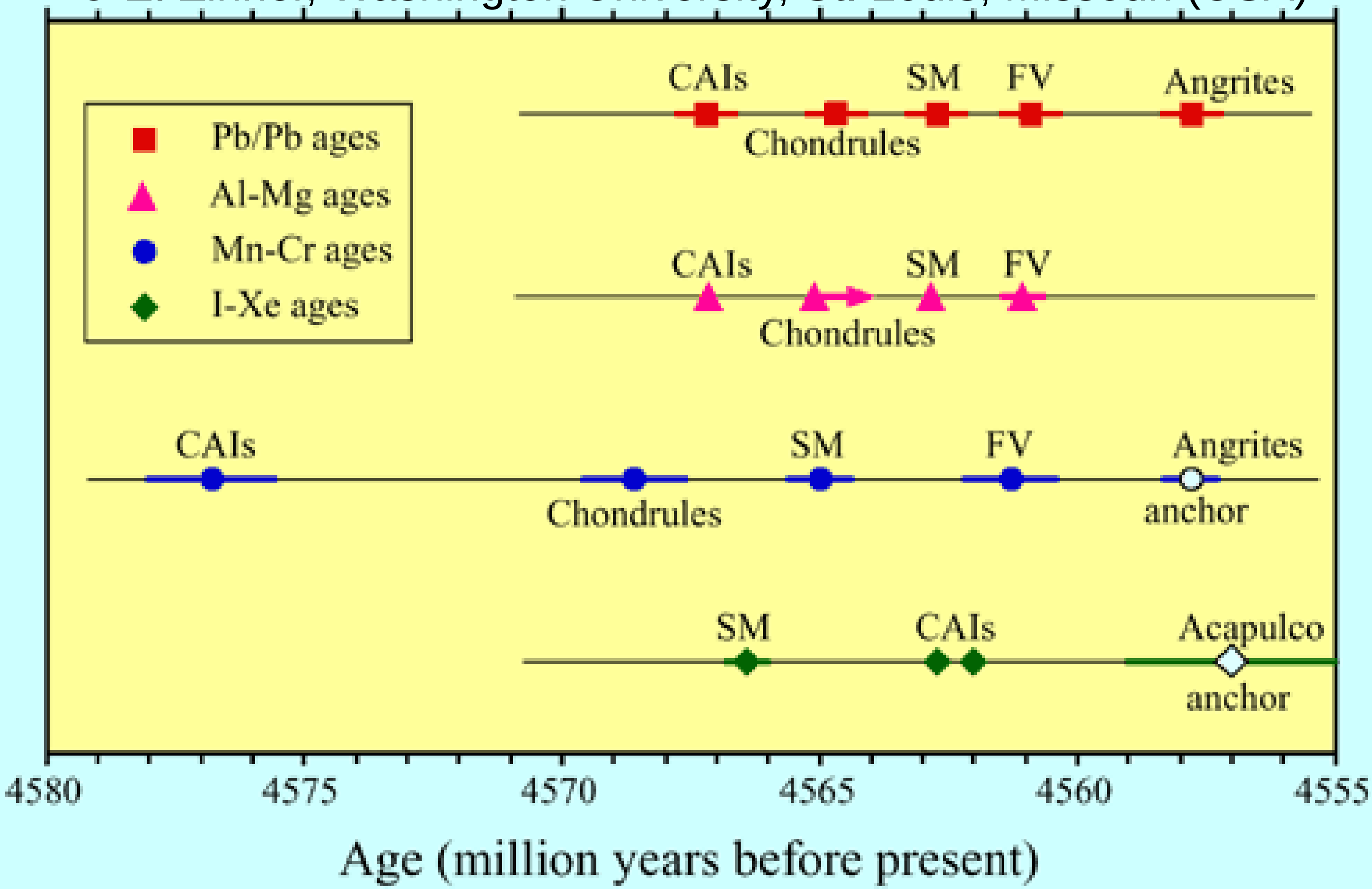

I. What a model of planetary-system formation has to explain

f. Debris disks

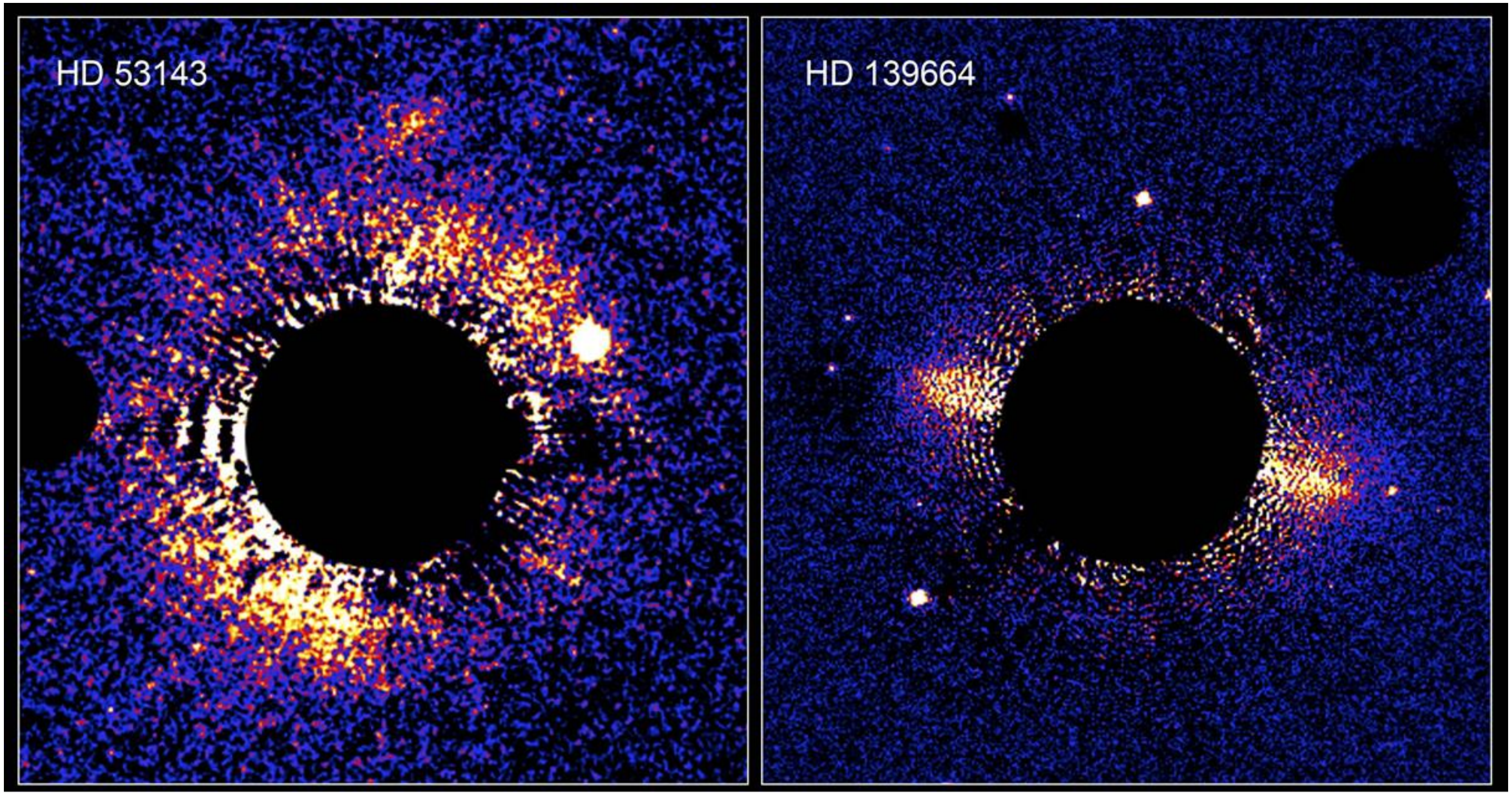

http://upload.wikimedia.org/wikipedia/commons/3/3a/Kuiper_belt_remote.jpg

I. What a model of planetary-system formation has to explain

g. The late heavy bombardment

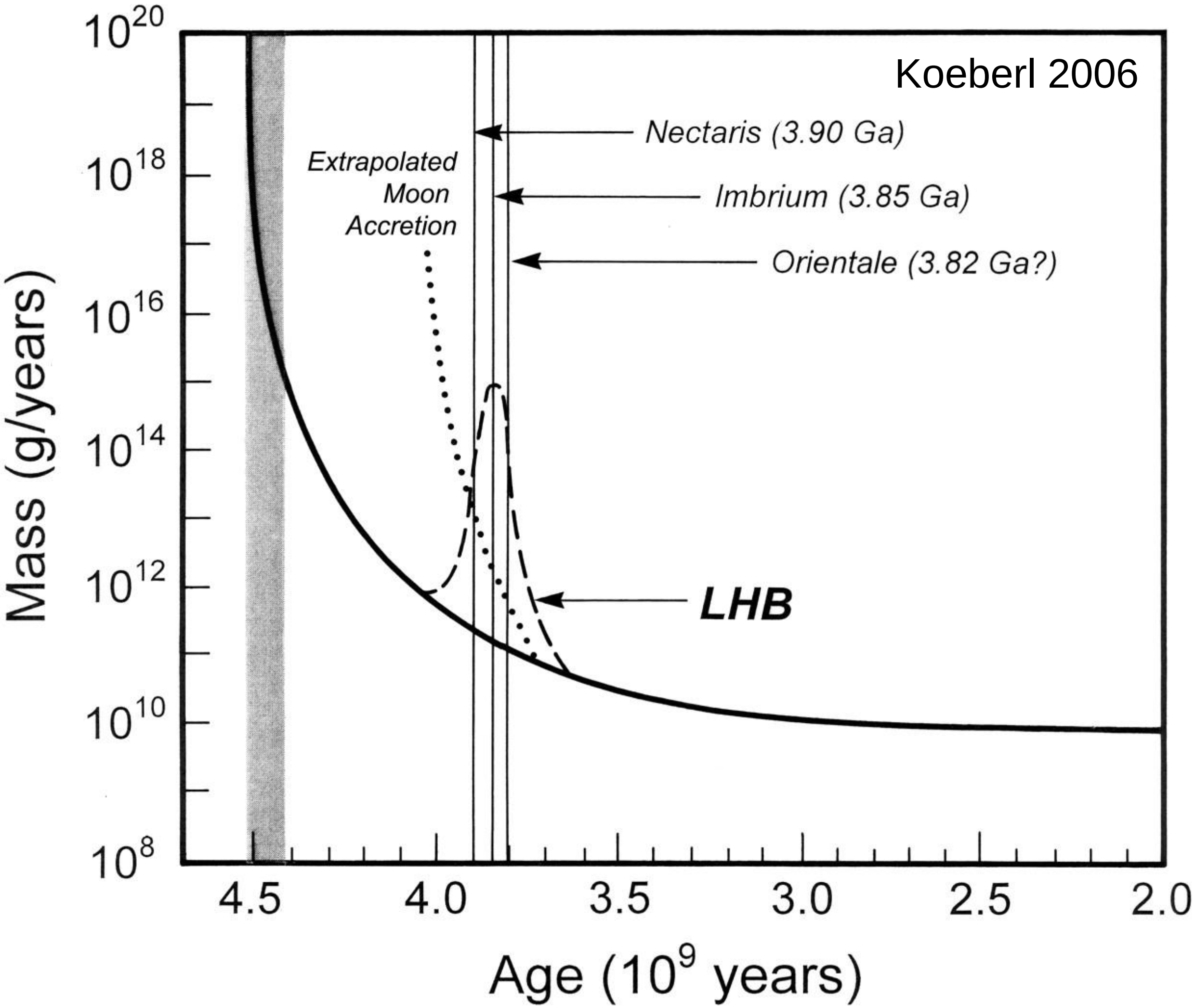

I. What a model of planetary-system formation has to explain

h. The stability over Gyrs

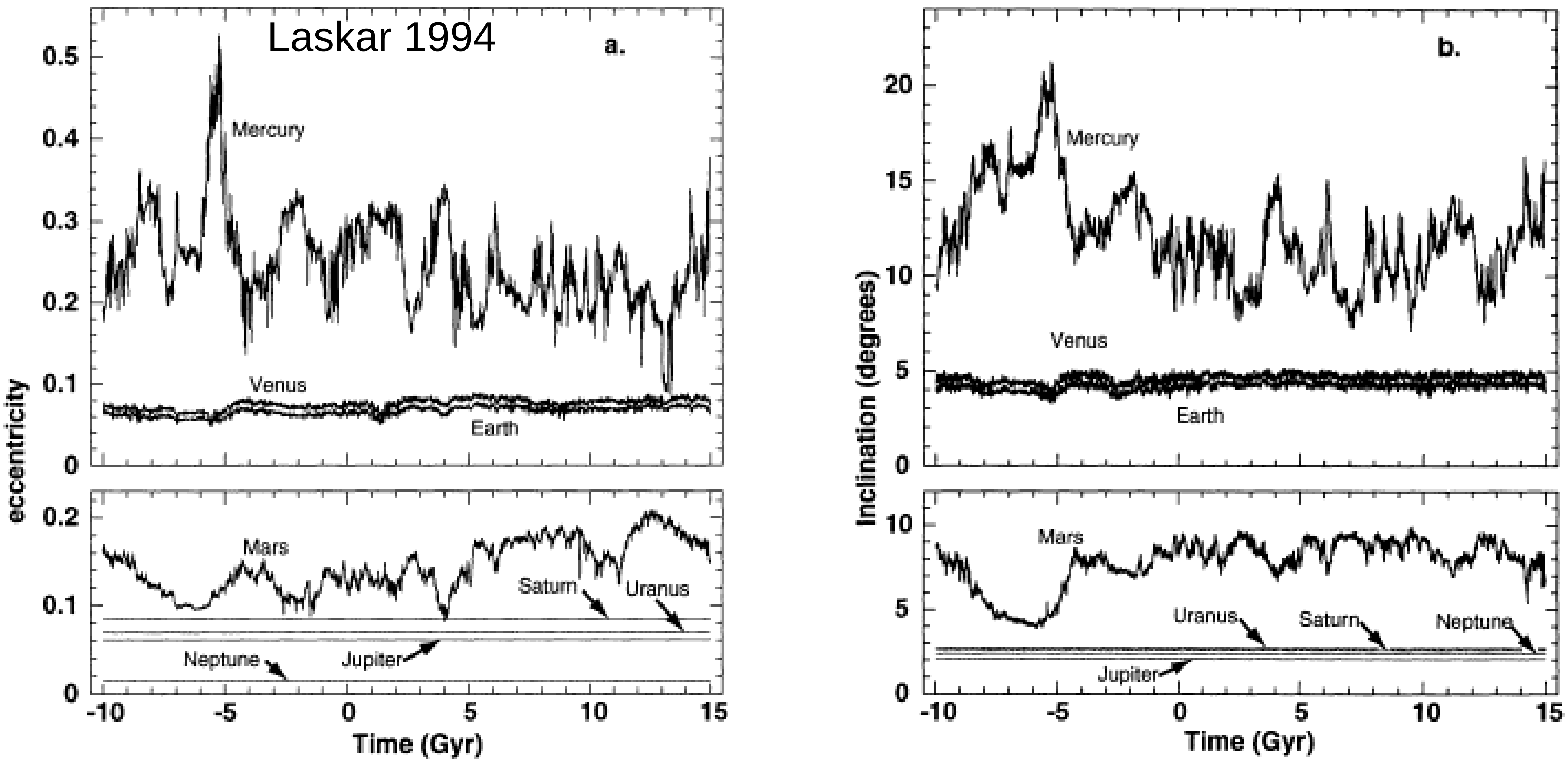

Fig. 1a and b. Numerical integration of the averaged equations of motion of the solar system 10 Gyr backward and 15 Gyr forward. For each planet, the maximum value obtained over intervals of 10 Myr for the eccentricity (a) and inclination (in degrees) from the fixed ecliptic J2000 (b) are plotted versus time. For clarity of the figures, Mercury, Venus and the Earth are plotted separately from Mars, Jupiter, Saturn, Uranus and Neptune. The large planets behavior is so regular that all the curves of maximum eccentricity and inclination appear as straight lines. On the contrary the corresponding curves of the inner planets show very large and irregular variations, which attest to their diffusion in the chaotic zone.

II.
Observational constraints

II. Observational constraints

a. Solar System has disk shape

Inclination				
	Name	Inclination to ecliptic	Inclination to Sun's equator	Inclination to invariable plane[3]
Terrestrials	Mercury	7.01°	3.38°	6.34°
	Venus	3.39°	3.86°	2.19°
	Earth	0°	7.155°	1.57°
	Mars	1.85°	5.65°	1.67°
Gas giants	Jupiter	1.31°	6.09°	0.32°
	Saturn	2.49°	5.51°	0.93°
	Uranus	0.77°	6.48°	1.02°
	Neptune	1.77°	6.43°	0.72°

http://en.wikipedia.org/wiki/Inclination#cite_note-meanplane-2

II. Observational constraints

b. Co-formation of Sun and planets

The sun and the planets of our solar system formed at the same time and from the same material reservoir:

- ▷ Elementary abundances
- ▷ Age of the meteorites = age of the sun
- ▷ Parallel angular momentum of sun and planets

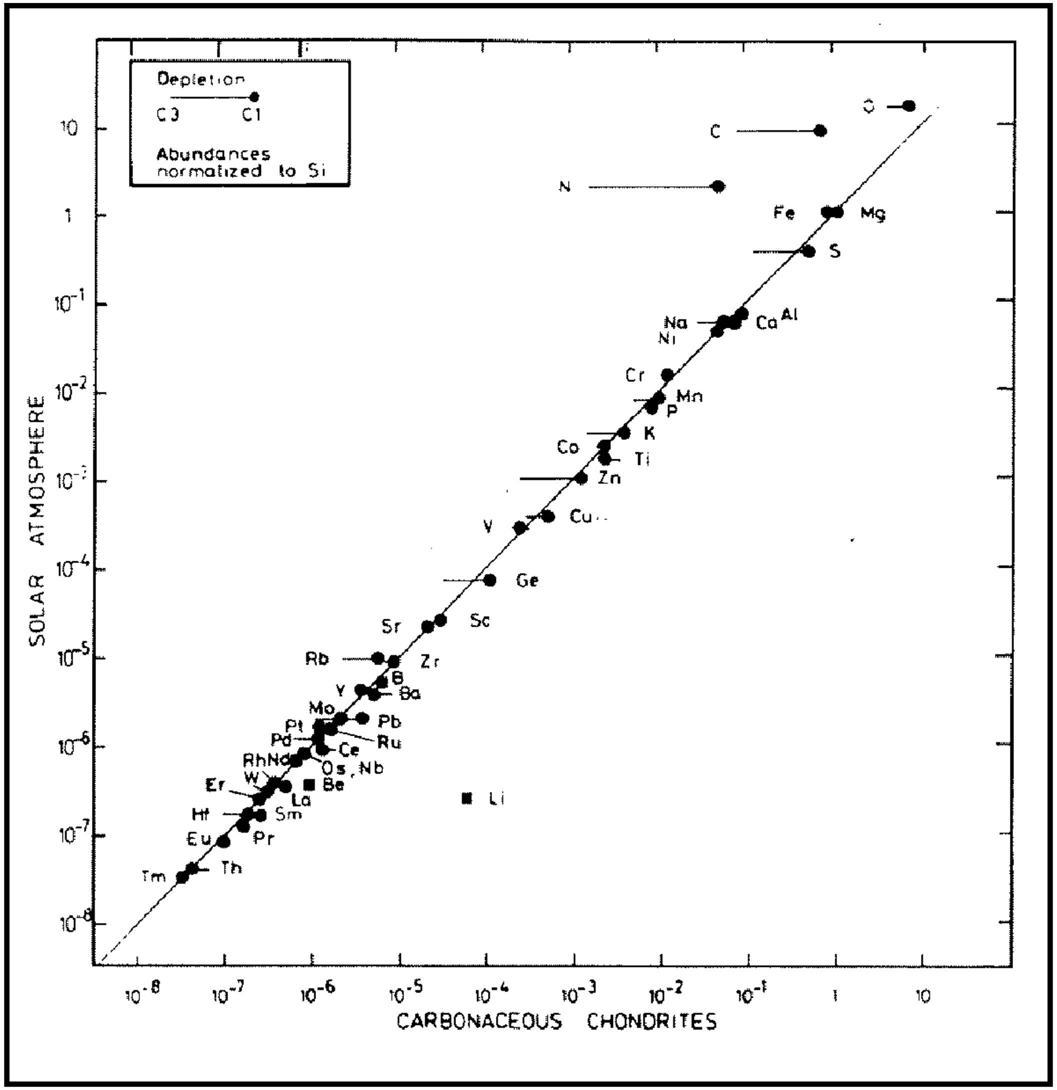

Cowley 1995

II. Observational constraints

b. Co-formation of Sun and planets

The sun and the planets of our solar system formed at the same time and from the same material reservoir:

- ▷ Elementary abundances
- ▷ Age of the meteorites = age of the sun
- ▷ Parallel angular momentum of sun and planets

Radiometric dating:

Material	Age
Earth (Zircon, Australia)	4.40 Gyr
Moon (highland rocks)	4.1-4.4 Gyr
Meteorite (oldest from Mars)	4.5 Gyr
Meteorite (chondrules)	4.564 Gyr
Meteorite (CAI)	4.567 Gyr

Age determination of the sun (evolutionary models and helioseismology data):

Authors	Age
Guenther & Demarque 1997	4.5±0.1 Gyr
Bonnano, Schlattl & Paterno 2002	4.57±0.11 Gyr
Houdek & Gough 2007	4.68±0.02 Gyr

II. Observational constraints

c. Existence and lifetimes of PPDs

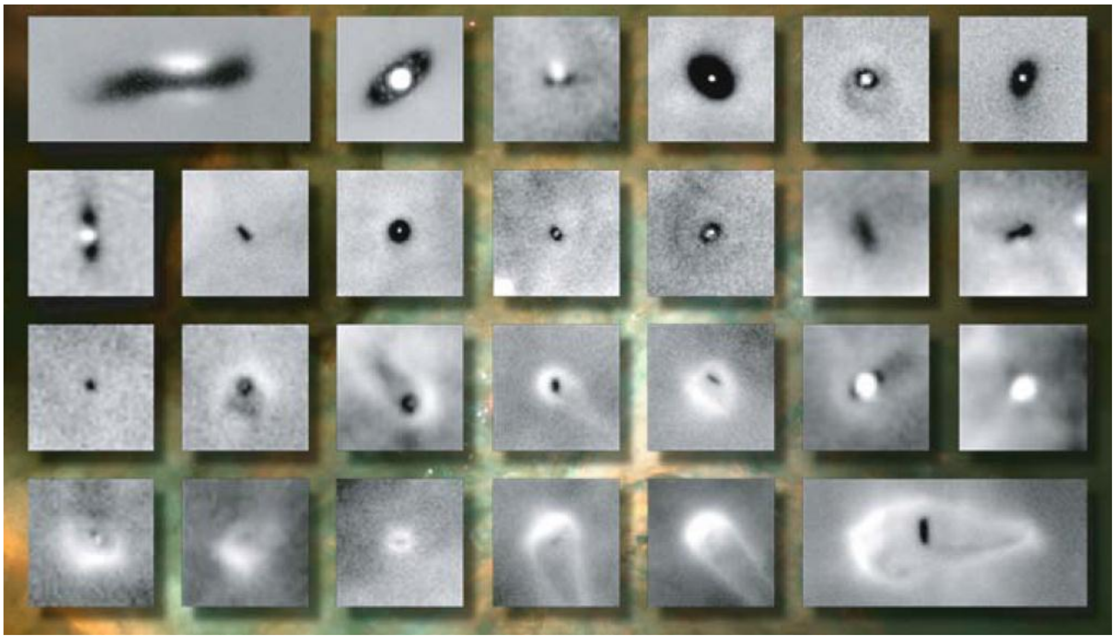

Gardner et al. 2006

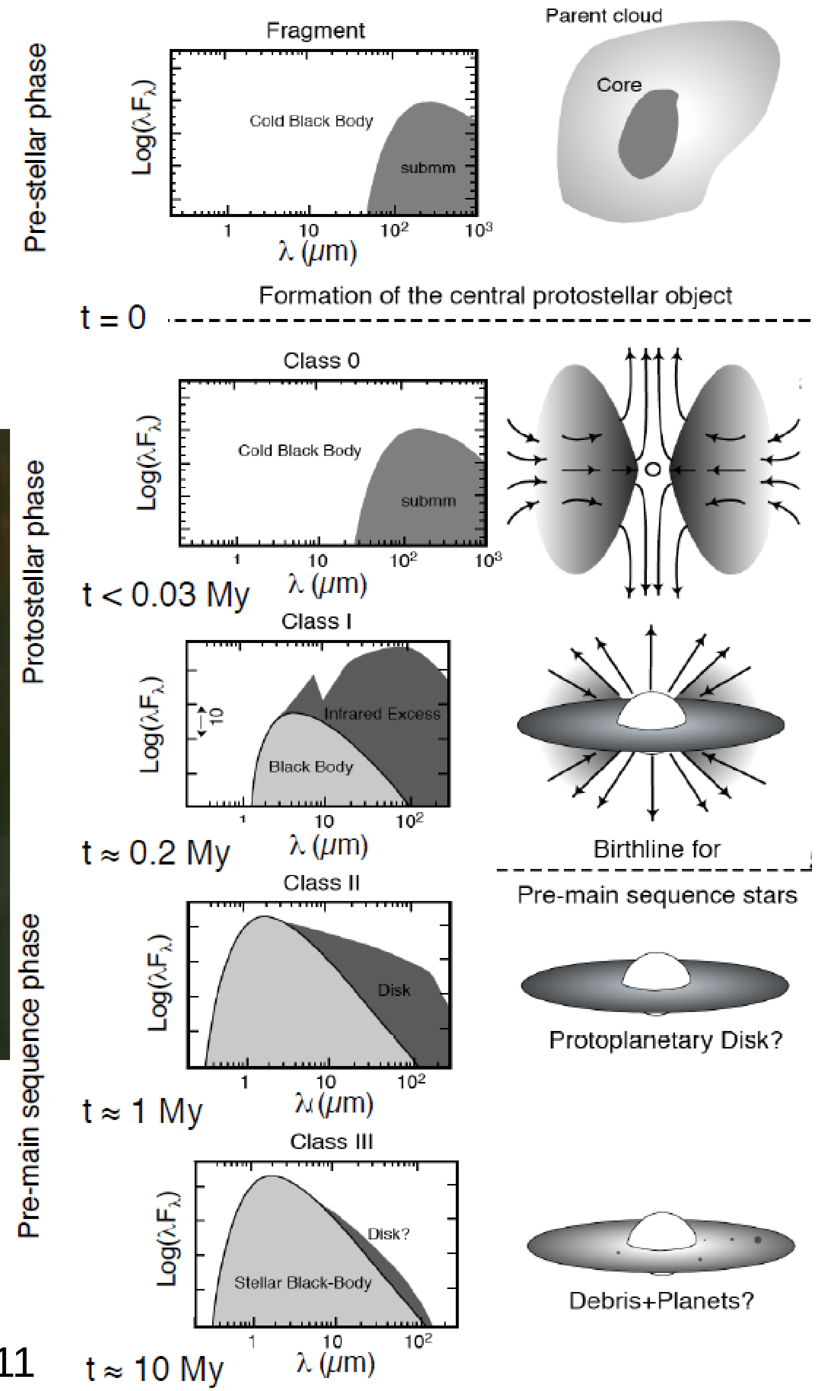

Dauphas & Chaussidon 2011

Molecular clouds I

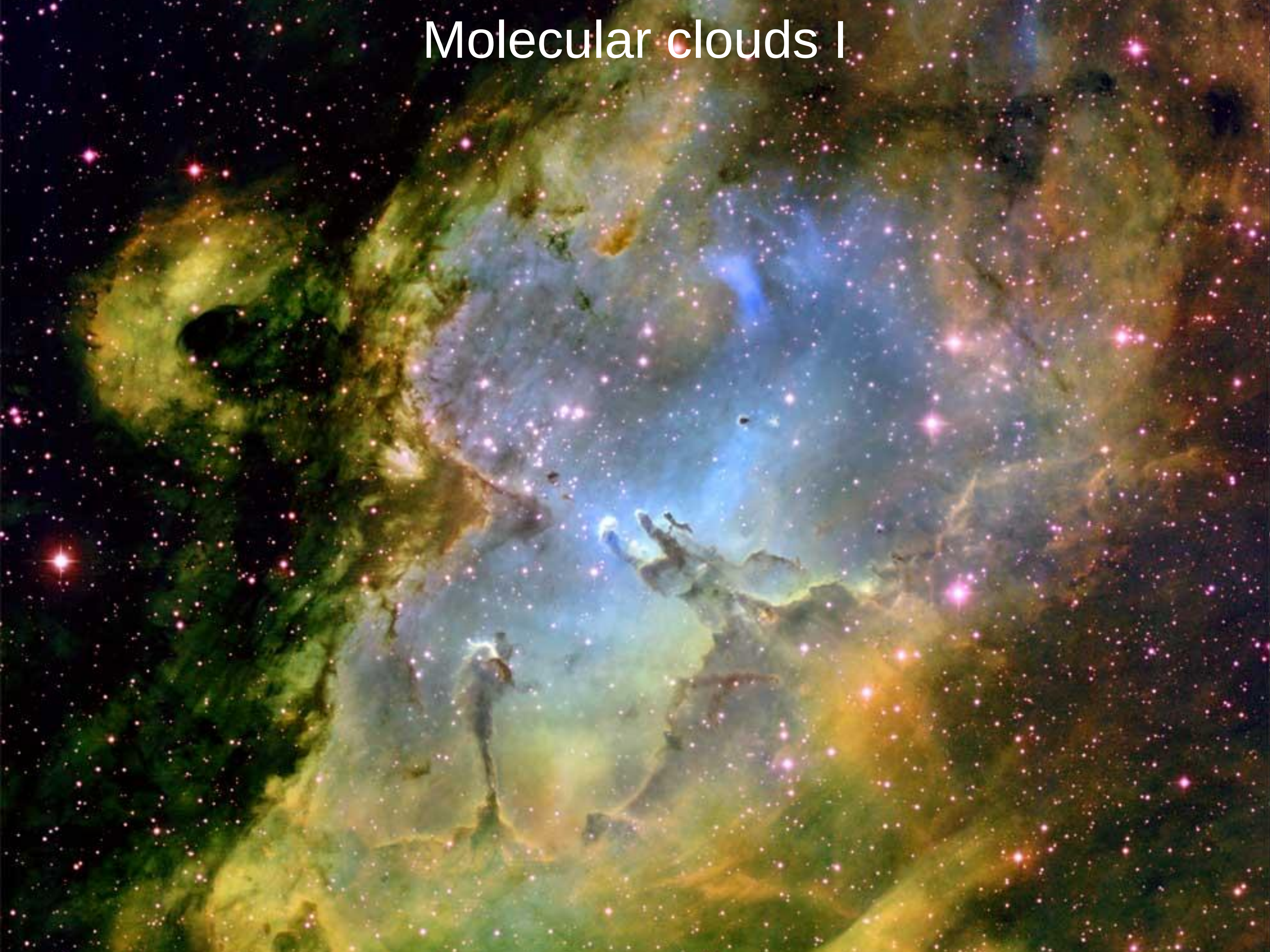

Molecular clouds II

Molecular clouds III

Molecular clouds IV: dust and gas

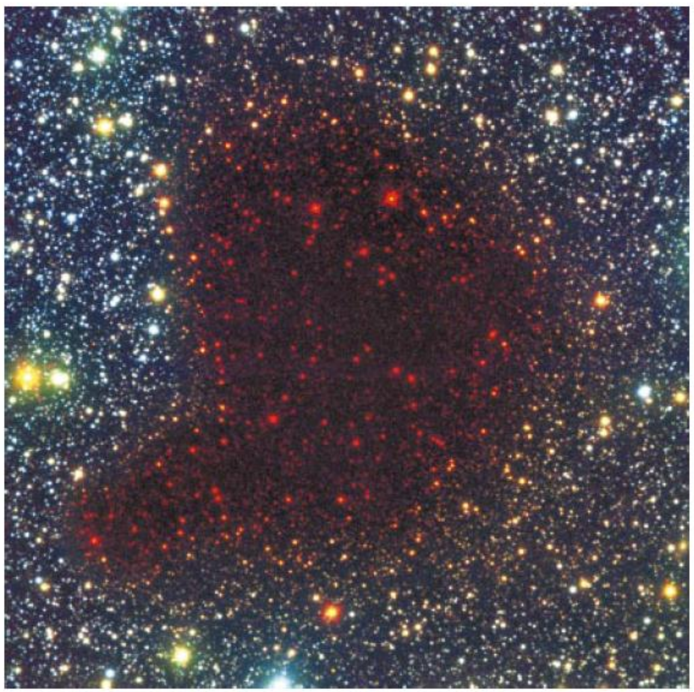

Figure 1 Visible and near-infrared images of Barnard 68. Top, deep B,V,I band (0.44 μm, 0.55 μm, 0.90 μm) image (~7′ × 7′) of the dark molecular cloud Barnard 68 taken with ESO's Very Large Telescope (VLT) located in the Chilean Andes. The cloud is seen in projection against the Galactic bulge. At these optical wavelengths the cloud is completely opaque owing to extinction of background starlight caused by small interstellar dust particles that permeate the cloud. The complete absence of foreground stars projected onto the cloud is a result of the proximity of the cloud to the Solar System (125 pc). The outer radius of the cloud is comparable to the inner size of the Oort cloud of comets that surround the Sun ($\sim 10^4$ AU). The mass of the cloud is about twice that of the Sun. Bottom, deep B,I,K band image of the cloud constructed by combining an infrared K band (2.2 μm wavelength) image with the B and I images. The K band image was obtained with ESO's New Technology Telescope (NTT) in the Chilean Andes. At near-infrared wavelengths the cloud becomes transparent and the stars located behind the cloud clearly appear in the image. Because these stars are observed only in the longest of the three wavelength bands, they appear very red in this three-colour image. These are the stars that provide measurements of dust extinction directly through the cloud.

Molecular clouds V: the interior

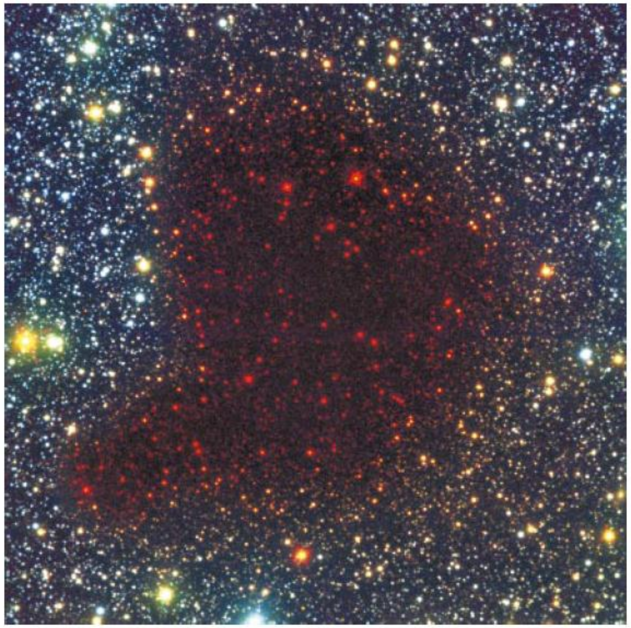

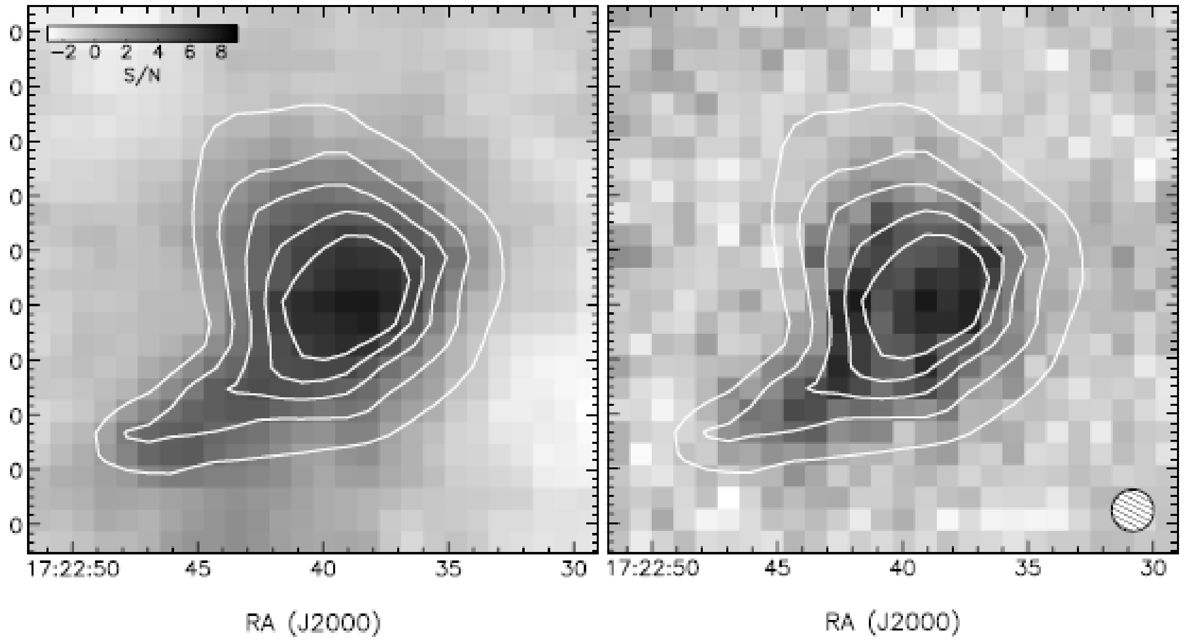

Fig. 1. SCUBA map at 850 μm (left) and SIMBA map at 1.2 mm (right) of Barnard 68, with superimposed A_V contours. The A_V and SCUBA maps have been smoothed to match the SIMBA resolution ($FWHM = 24''$; the beamsize is shown on the right image). All images have been resampled to a pixel size of $12''$. The field of view is $5' \times 5'$. A_V contours start at 4 mag and are spaced by 4 mag. For both images, the grayscale in units of S/N.

Molecular clouds VI: gravitational collapse

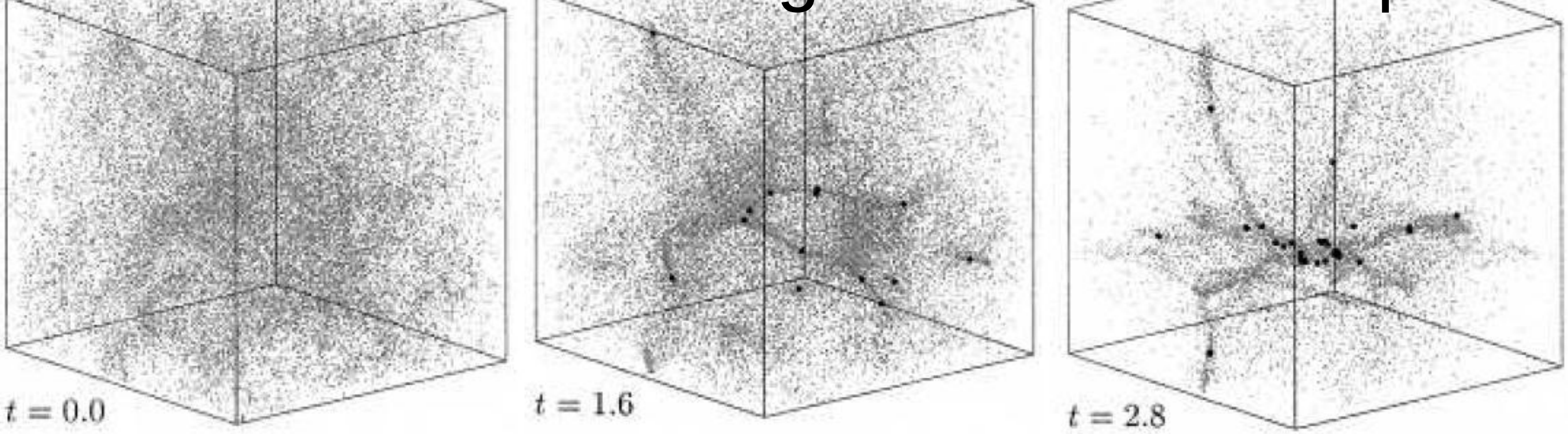

Fig. 2.— The gravitational fragmentation of molecular cloud is shown from a simulation containing initial structure (*Klessen et al.*, 1998). The gravitational collapse enhances this structure producing filaments which fragment to form individual stars. The time t is given in units of the free-fall time.

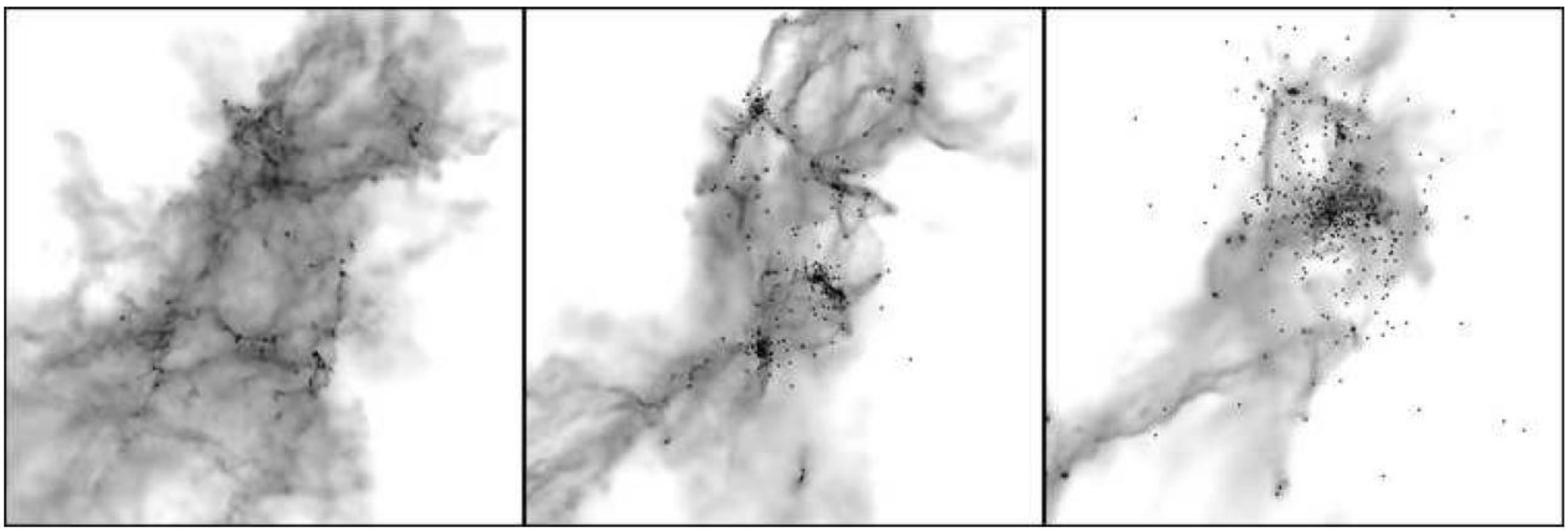

Fig. 8.— The fragmentation of a 1000 $M_\odot$ turbulent molecular cloud and the formation of a stellar cluster (*Bonnell et al.*, 2003). Note the merging of the smaller subclusters to a single big cluster.

Stars form in clusters:
the open clusters h und χ Persei

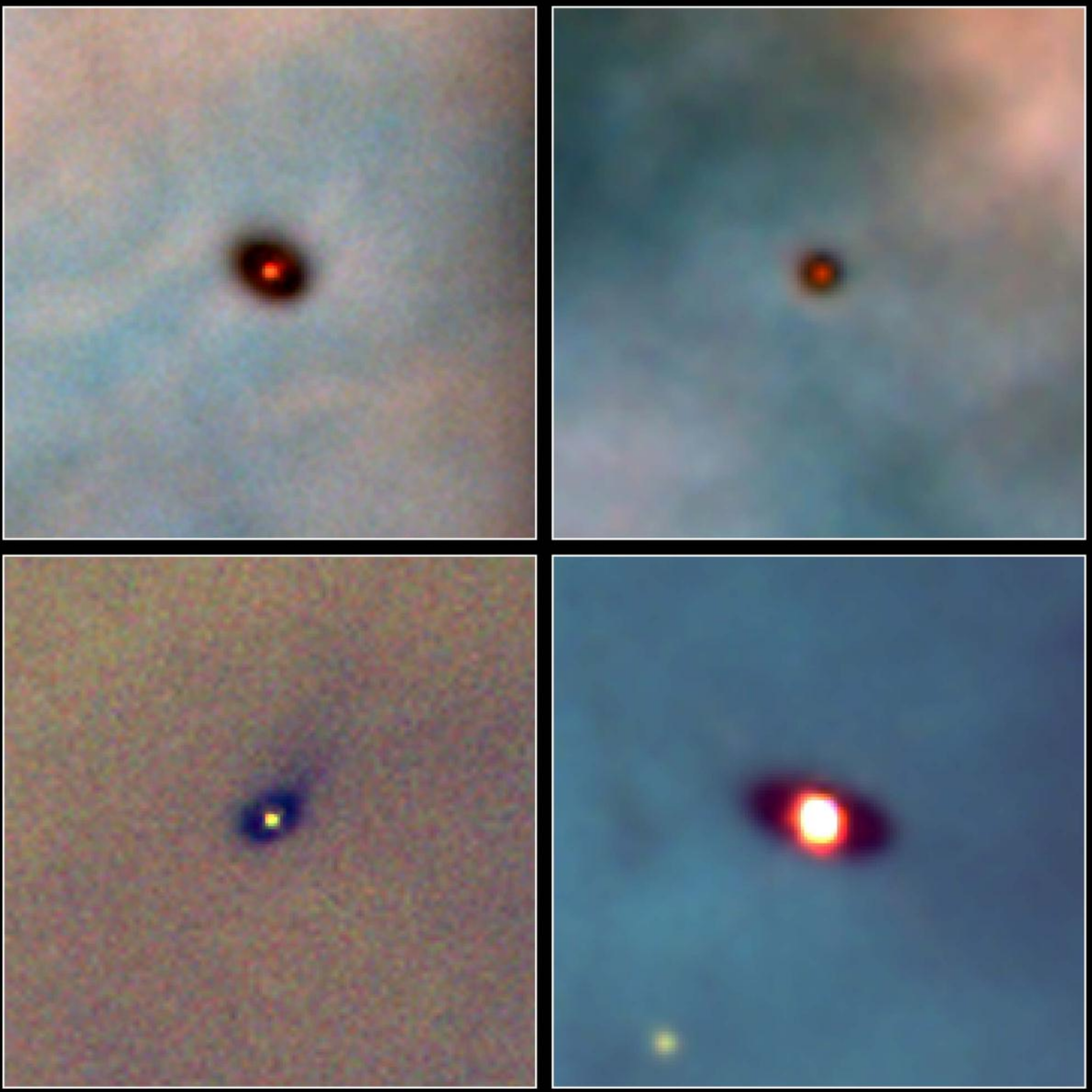

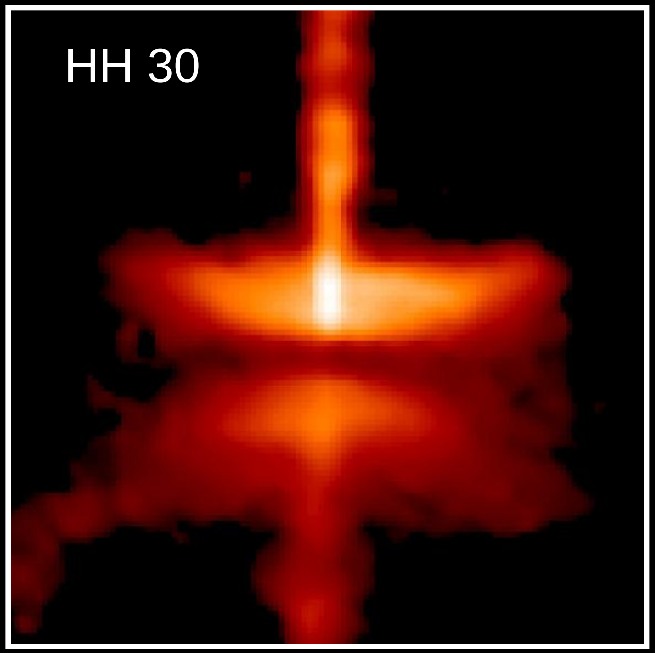

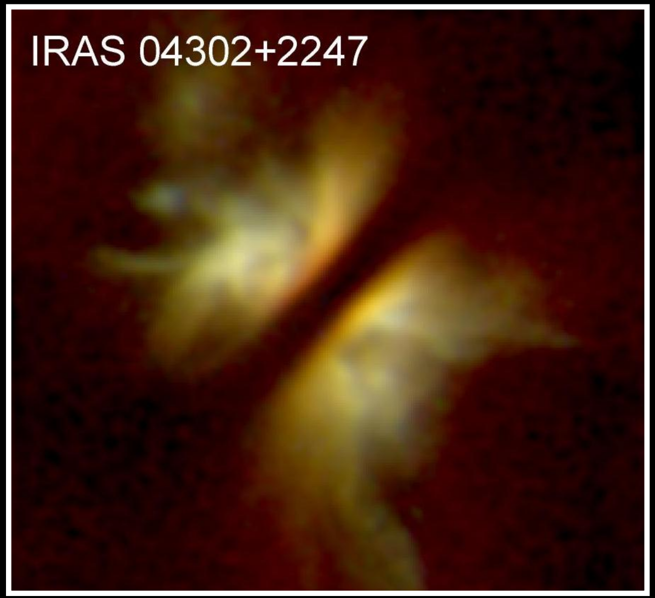

Protoplanetary Disks • Orion Nebula

Hubble Space Telescope • WFPC2

PRC95-45b • ST ScI OPO • November 20, 1995 • M. J. McCaughrean (MPIA), C. R. O'Dell (Rice University), NASA

Planet formation must be a (relatively) fast process!

Maximum lifetime of protoplanetary disks 10^7 years

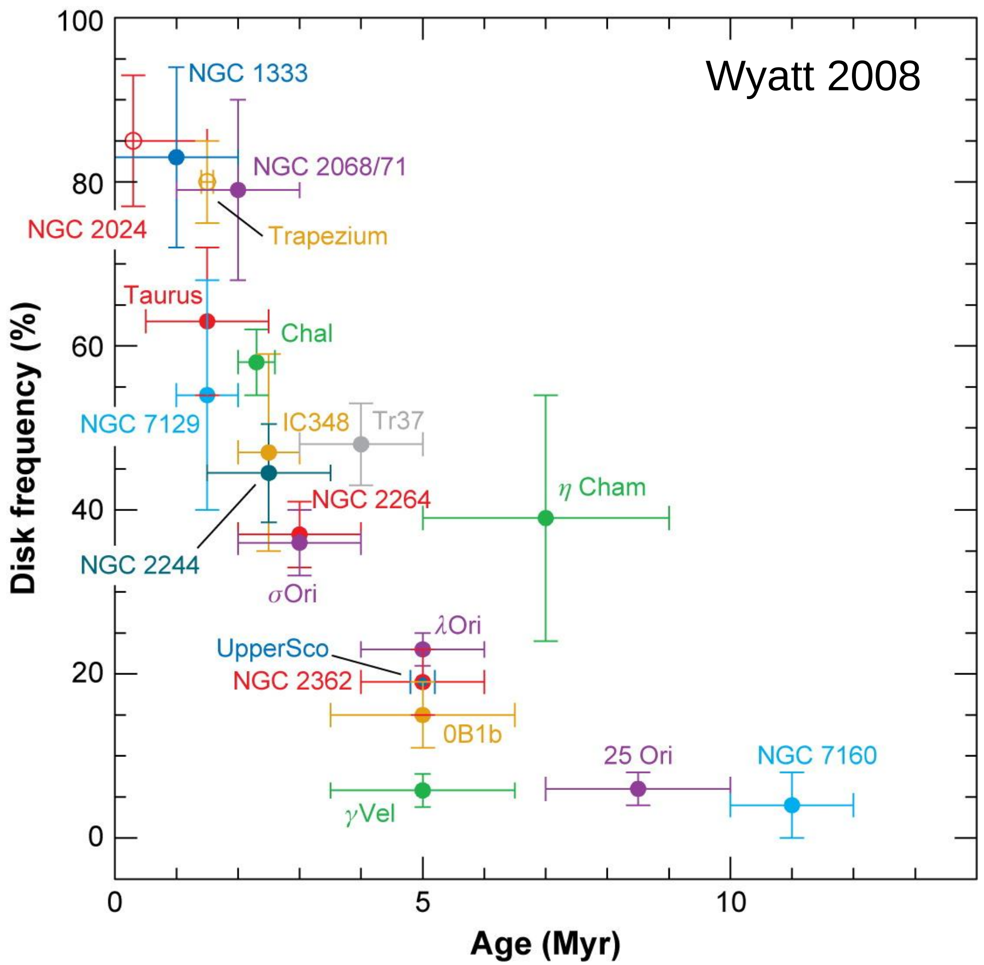

II. Observational constraints

d. Dust growth within PPDs

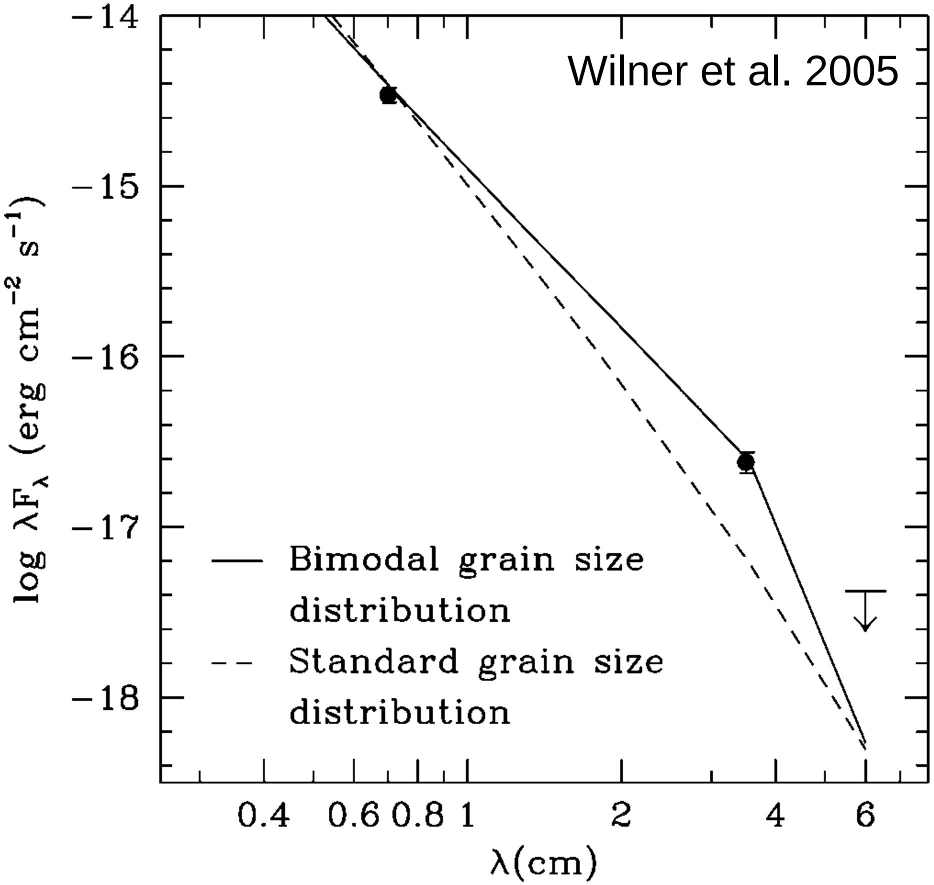

Fig. 3.—*Circles*, VLA measurements at 7 mm and 3.5 cm; *arrow*, an upper limit at 6 cm. The long-wavelength spectrum of TW Hya is better fitted by a model in which nearly all of the mass in solids is in centimeter-size grains (*solid line*) than by the model of Calvet et al. (2002) based on a single-power power-law grain size distribution (*dashed line*).

II. Observational constraints

e. Existence and lifetimes of debris disks

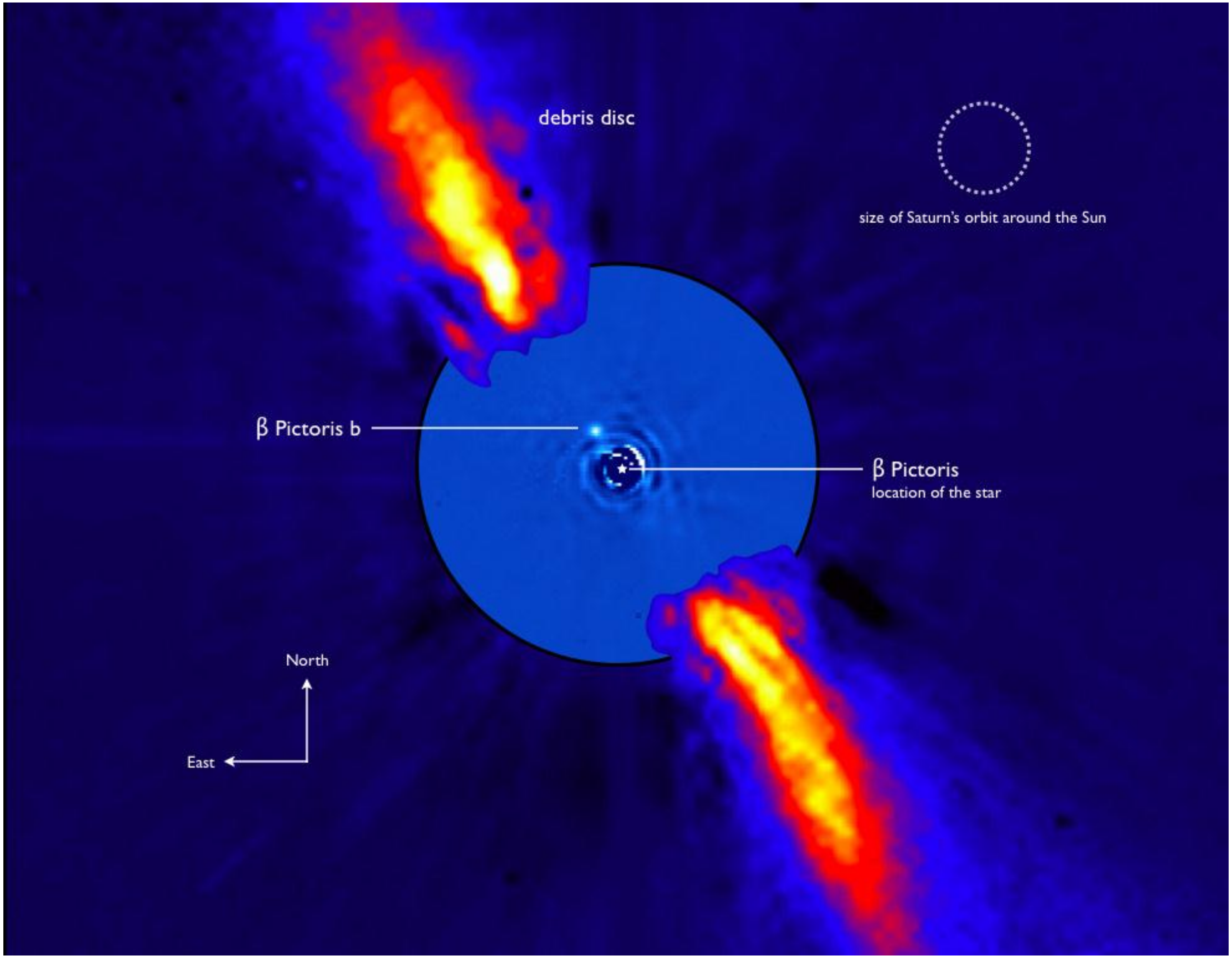

ESO

II. Observational constraints

e. Existence and lifetimes of debris disks

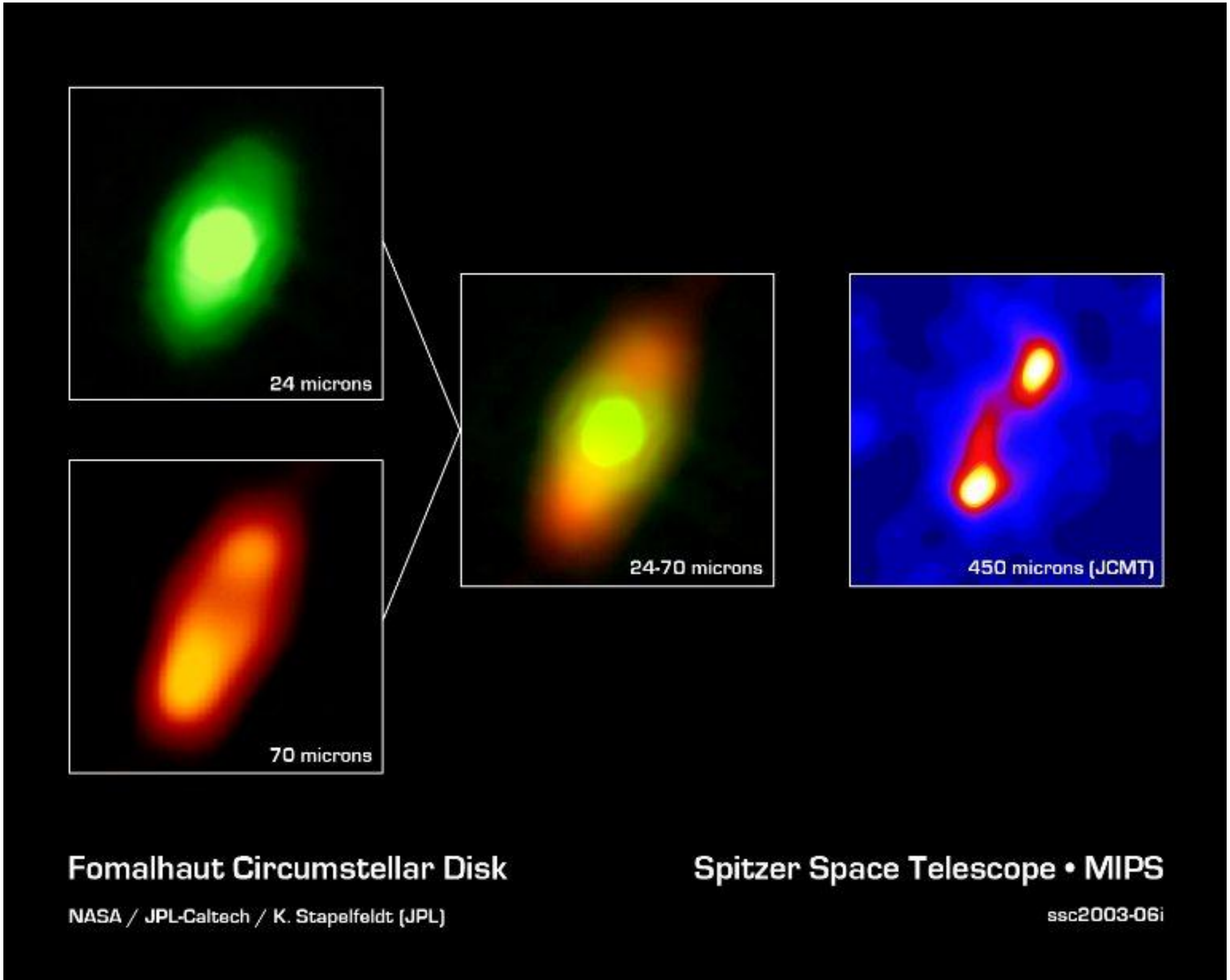

II. Observational constraints

e. Existence and lifetimes of debris disks

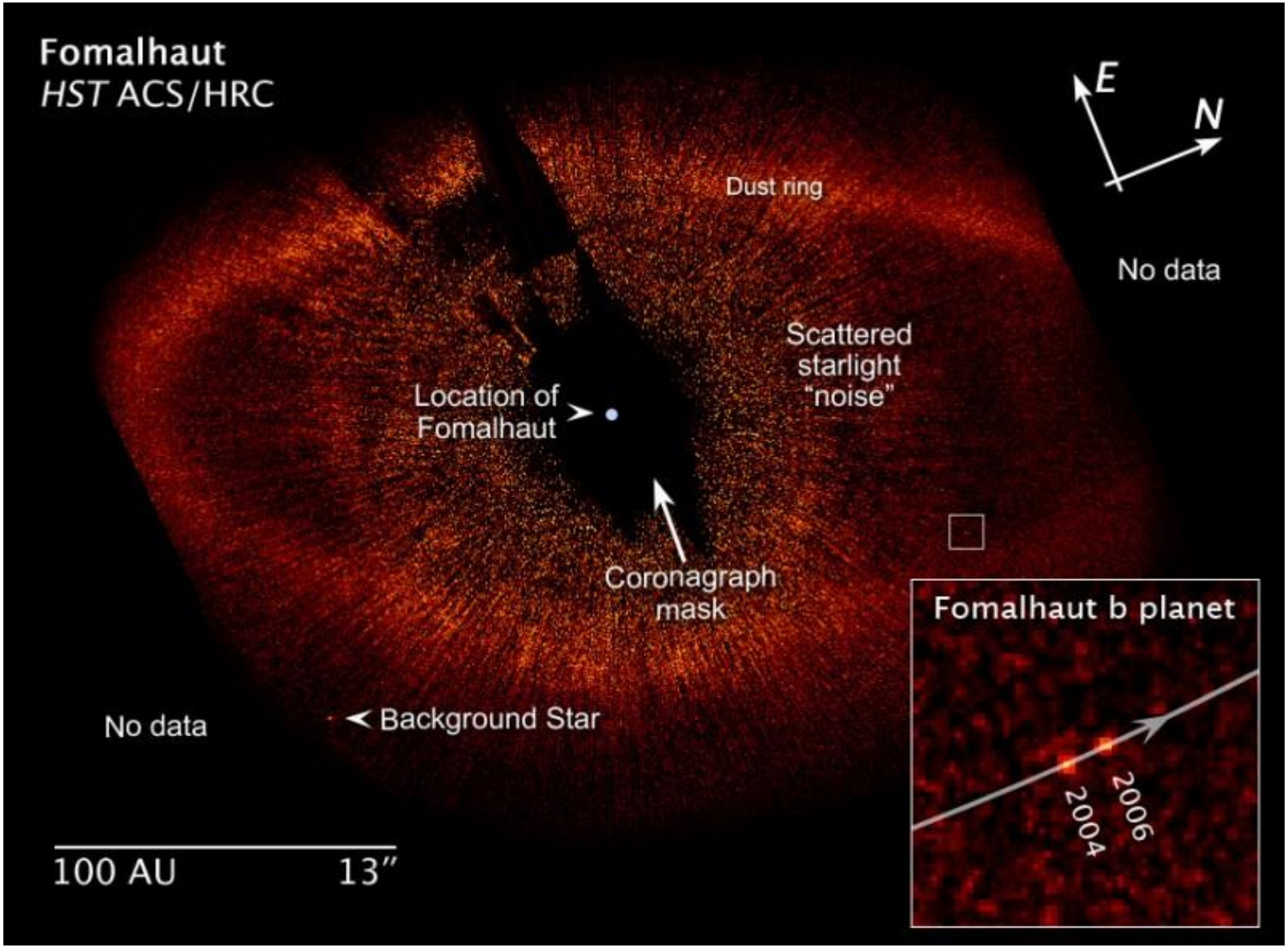

II. Observational constraints

e. Existence and lifetimes of debris disks

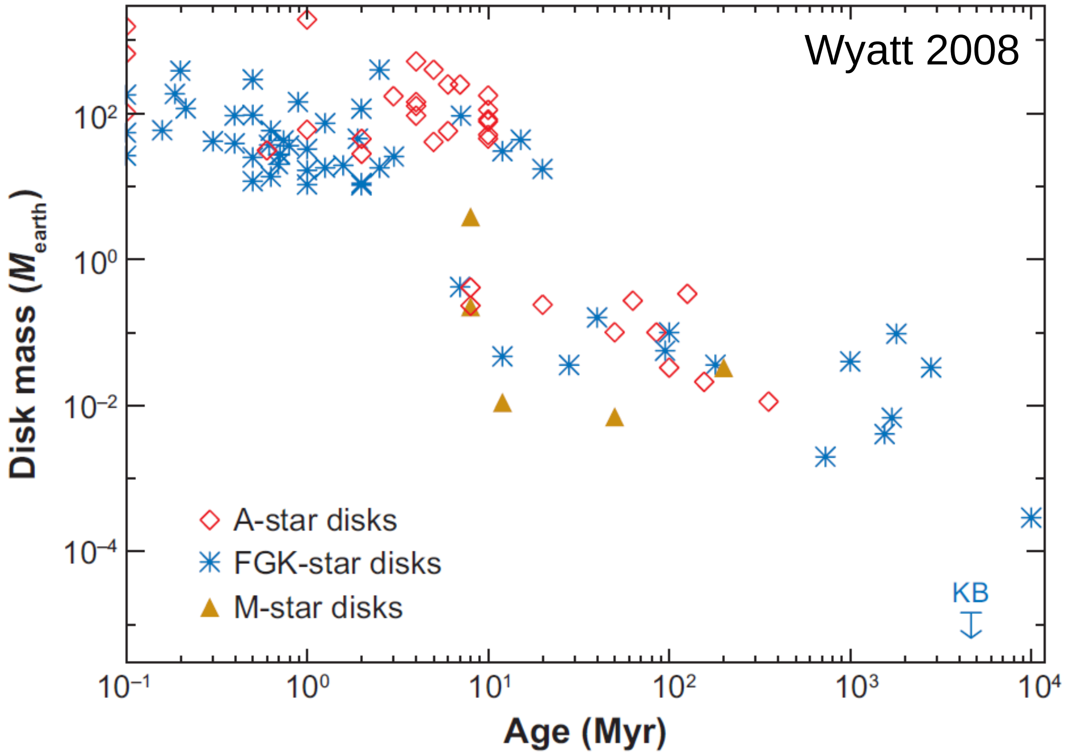

Figure 3

Evolution of disk mass derived from submillimeter observations. This plot extends the compilation of ages and masses of Wyatt, Dent & Greaves (2003) to include all debris disks currently detected at submillimeter wavelengths (Greaves et al. 2004b; Liu et al. 2004; Sheret, Dent & Wyatt 2004; Najita & Williams 2005; Wyatt et al. 2005; Lestrade et al. 2006; Williams & Andrews 2006; Matthews, Kalas & Wyatt 2007). The same (representative) sample of protoplanetary disks is included from Wyatt, Dent & Greaves (2003), and an opacity of 45 AU^2 $M_\oplus^{-1}$ is assumed for both protoplanetary and debris disks. The upper limit on the Kuiper belt dust mass from submillimeter observations (see Greaves et al. 2004b) is also plotted.

II. Observational constraints

f. Extrasolar planetary systems

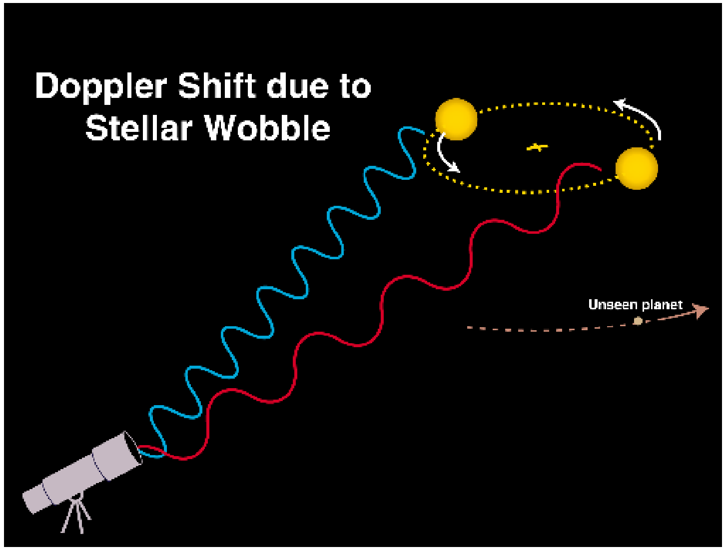

- ▷ Planets around solar-type stars
- ▷ Total of 556 extrasolar-planet candidates (8 June 2011)
  - ▶Spectroscopically detected: 507
  - ▶Transits: 135
- ▷ Kepler candidates: 1235 (confirmed: 16)
- ▷ System with 2 or more planets: 127
- ▷ Fraction of stars with planets: 0-25% (depending on metallicity of the star)

II. Observational constraints

f. Extrasolar planetary systems

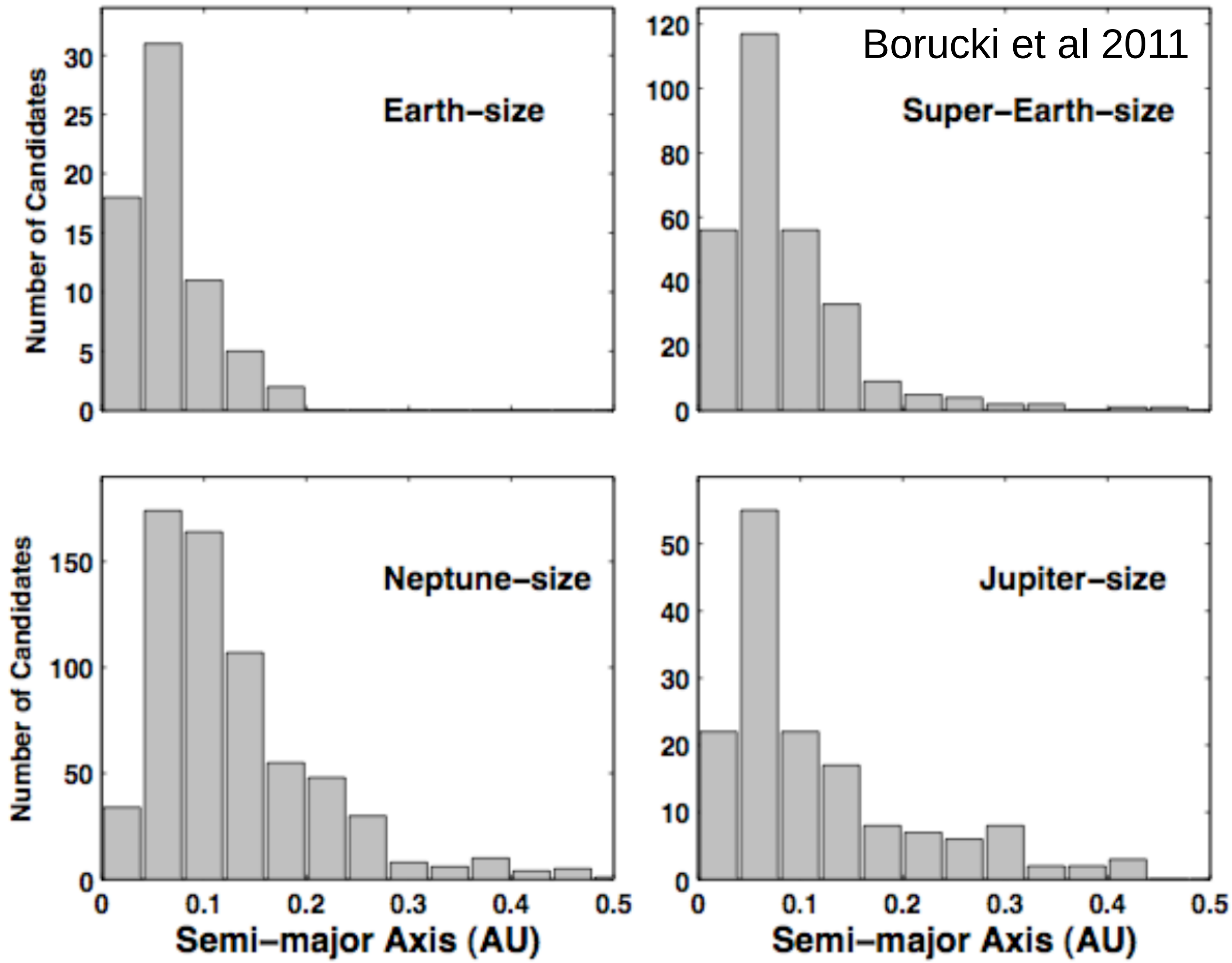

Figure 7. Number of observed candidates versus semi-major axis for four candidate size ranges. As defined in Table 6, Earth-size refers to $R_p < 1.25\ R_\oplus$, super-Earth-size to $1.25\ R_\oplus < R_p < 2\ R_\oplus$, Neptune-size to 2 $R_\oplus$, $< R_p < 6\ R_\oplus$, and Jupiter-size refers to $6\ R_\oplus < R_p < 15\ R_\oplus$. Bin size for the semi-major axis is 0.04 AU.

II. Observational constraints

f. Extrasolar planetary systems

Mass distribution of extrasolar planets

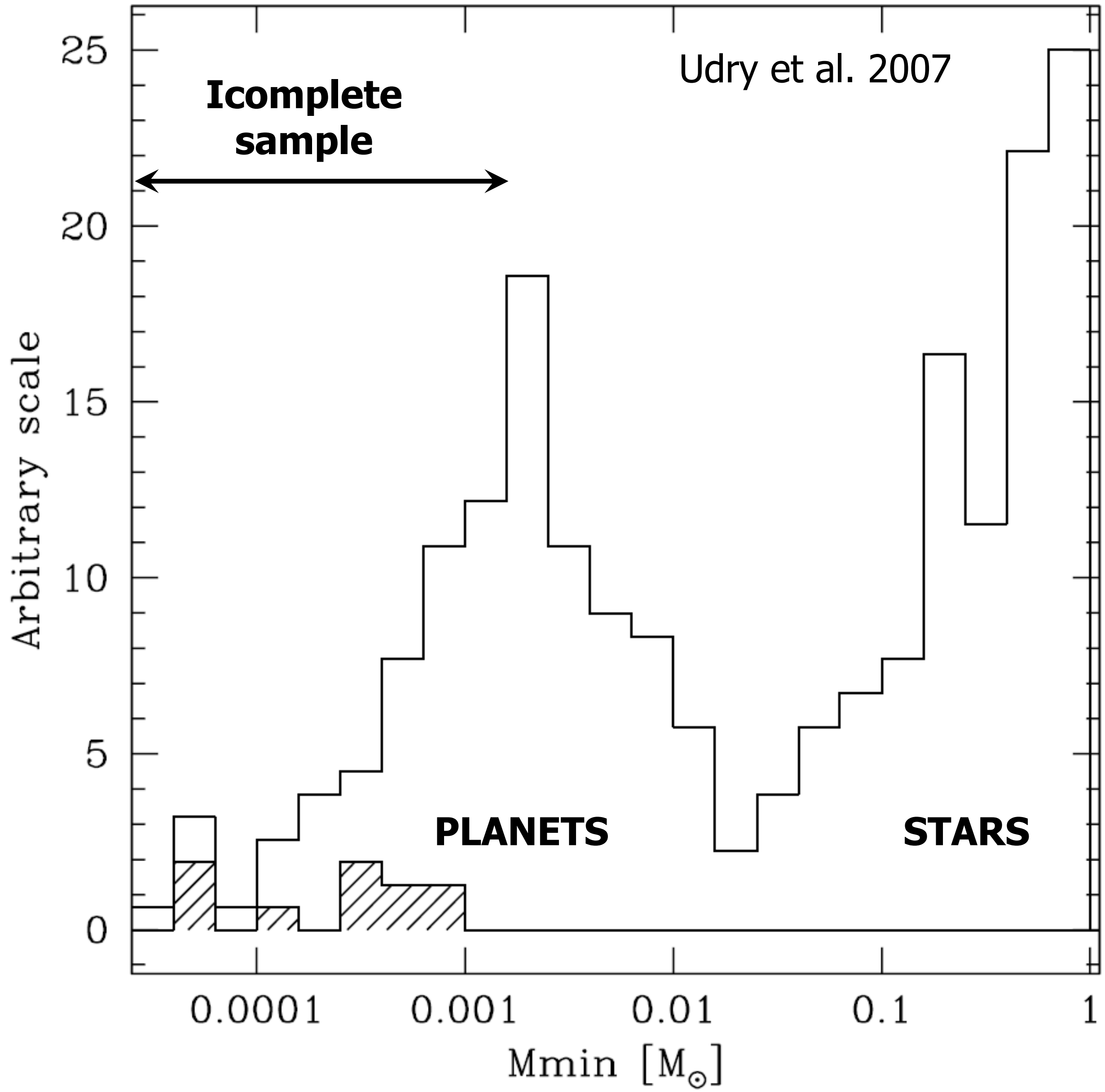

Orbits of extrasolar planets

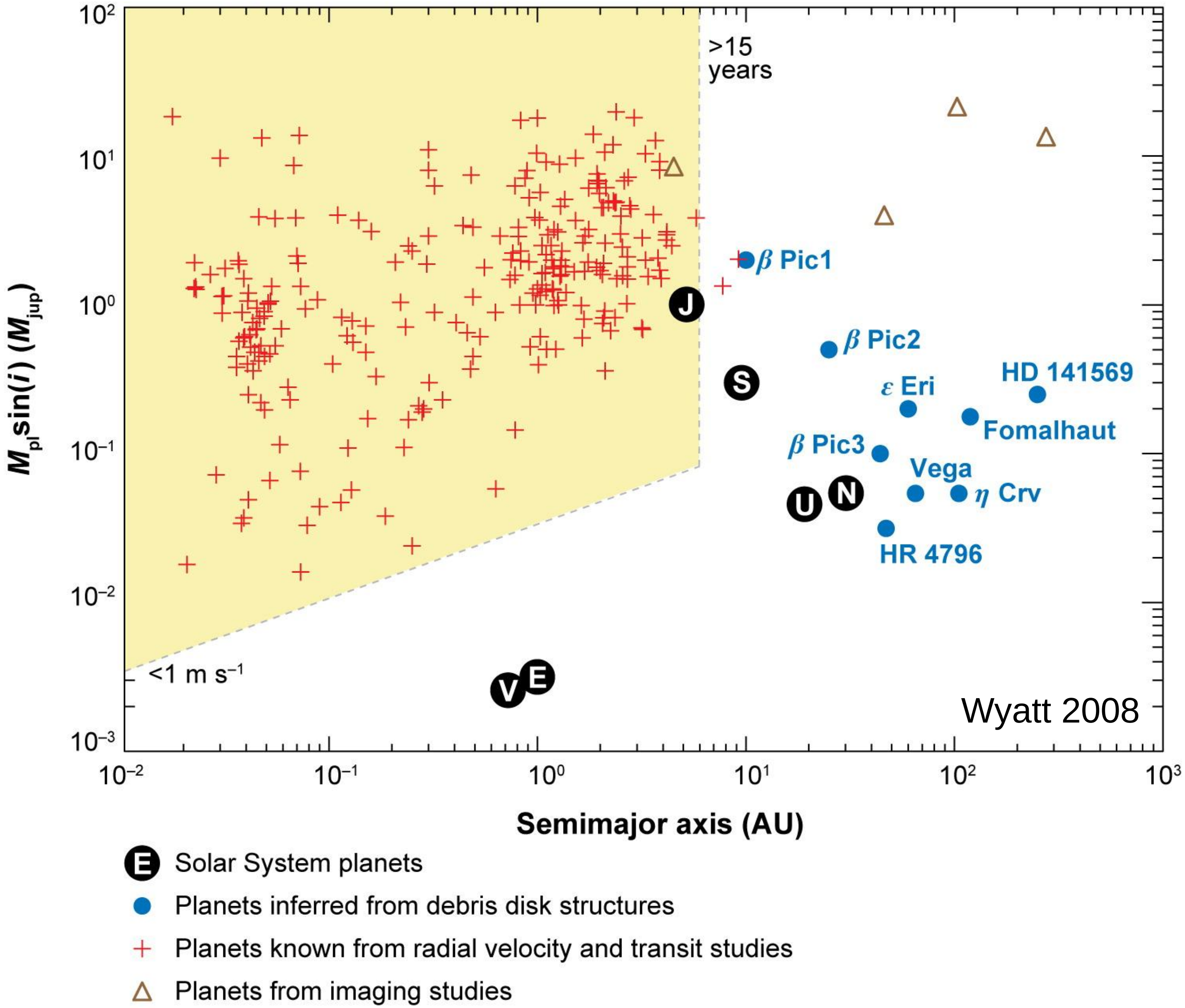

About the metallicity of stars and the connection to planets

- ▷ The search for planets around stars in globular cluster has so far been unsuccessful; stars in globular clusters possess metallicities «1%.
- ▷ The sun possesses a metallicity of ~1%.
- ▷ The mean metallicity of stars with extrasolar planets is >1%.

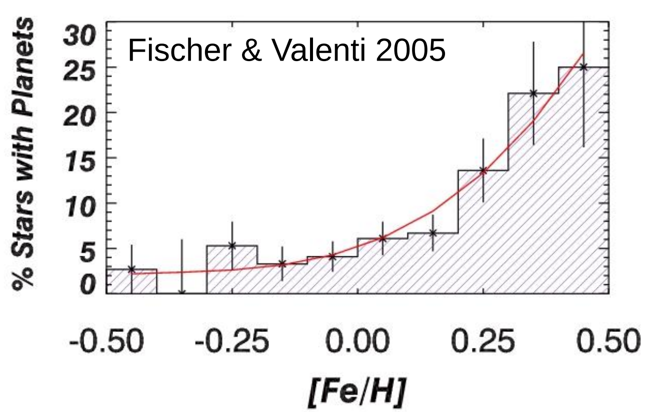

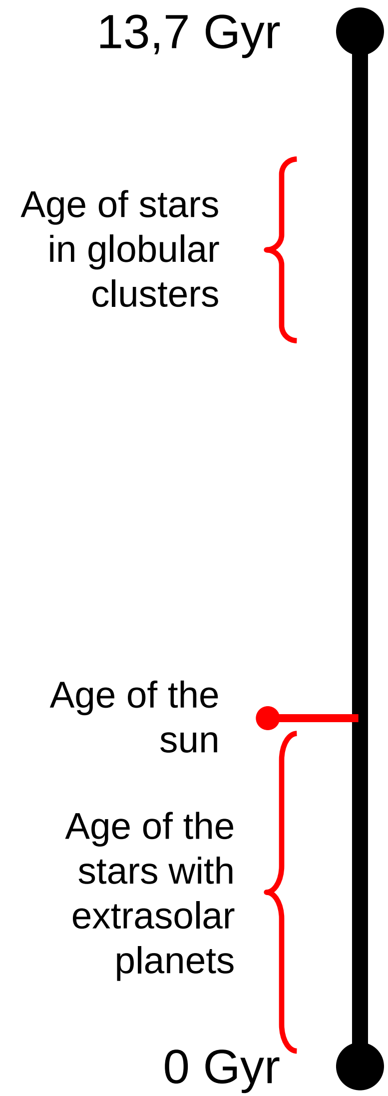

II. Observational constraints

f. Extrasolar planetary systems

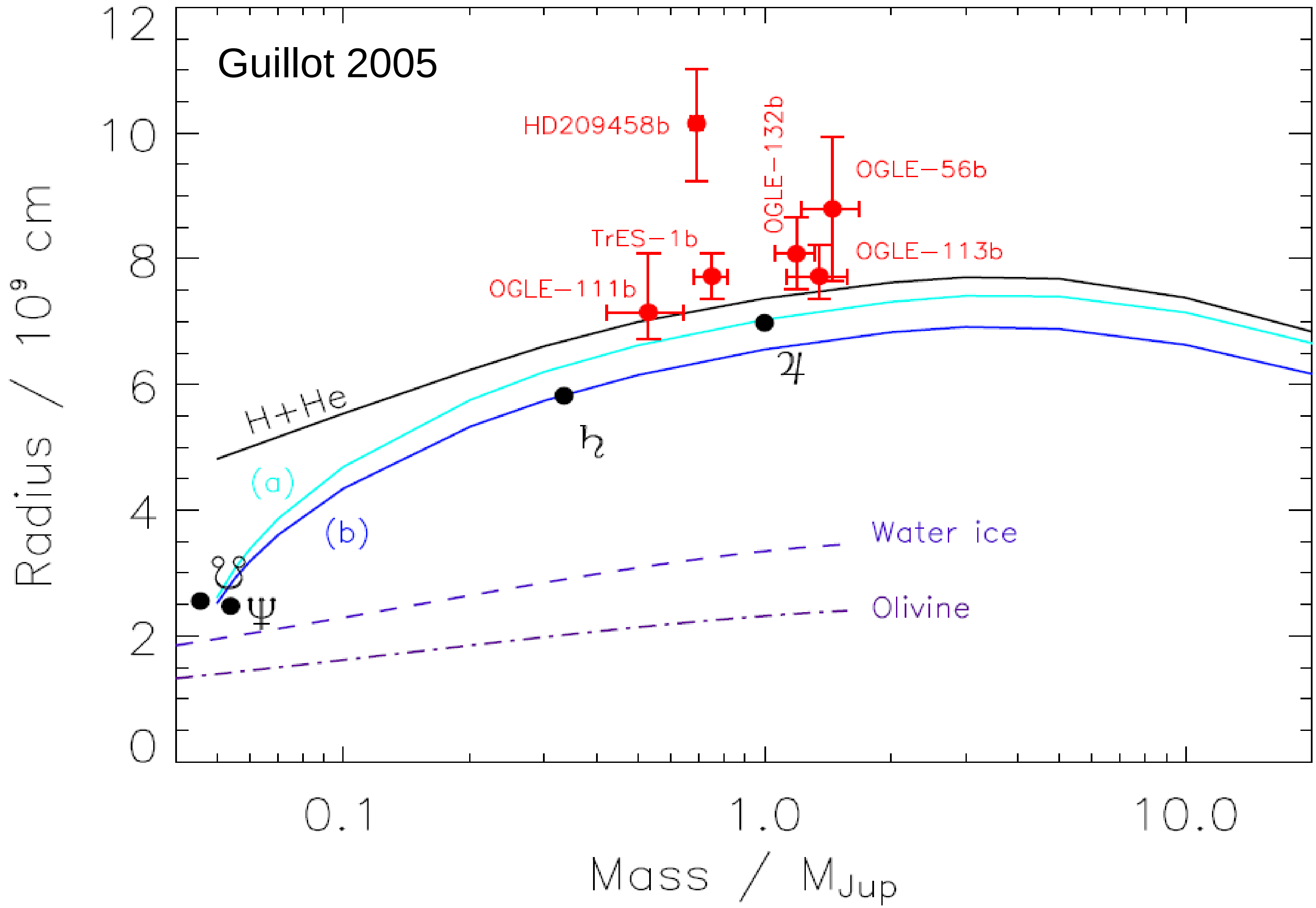

Figure 3: Radius versus mass for giant planets after 4.5 Ga of evolution compared to measured values for our four giant planets and four known extrasolar planets. As in fig. 2, the lines correspond to: H+He: a pure, $Y = 0.25$, hydrogen-helium composition (Y=0.25); (a): a model with $Y = 0.30$ and a 15 $M_\oplus$ core; (b): the same model but with $Y = 0.36$. An approximate mass-radius relation for zero-temperature water and olivine planets is shown as dashed and dash-dotted lines, respectively (Courtesy of W.B. Hubbard).

II. Observational constraints

f. Extrasolar planetary systems

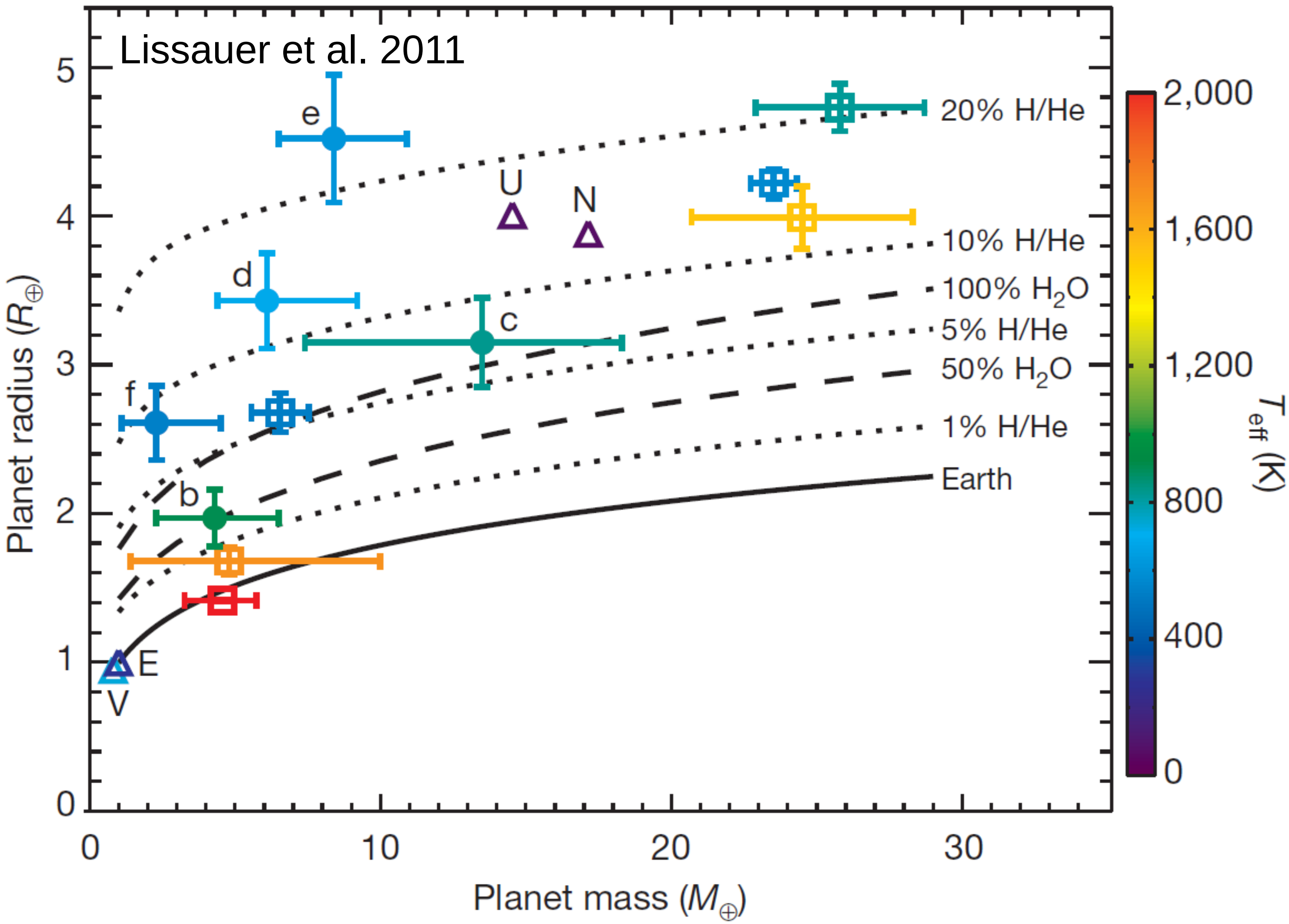

II. Observational constraints

g. The existence of chondrules

Chondrule formation

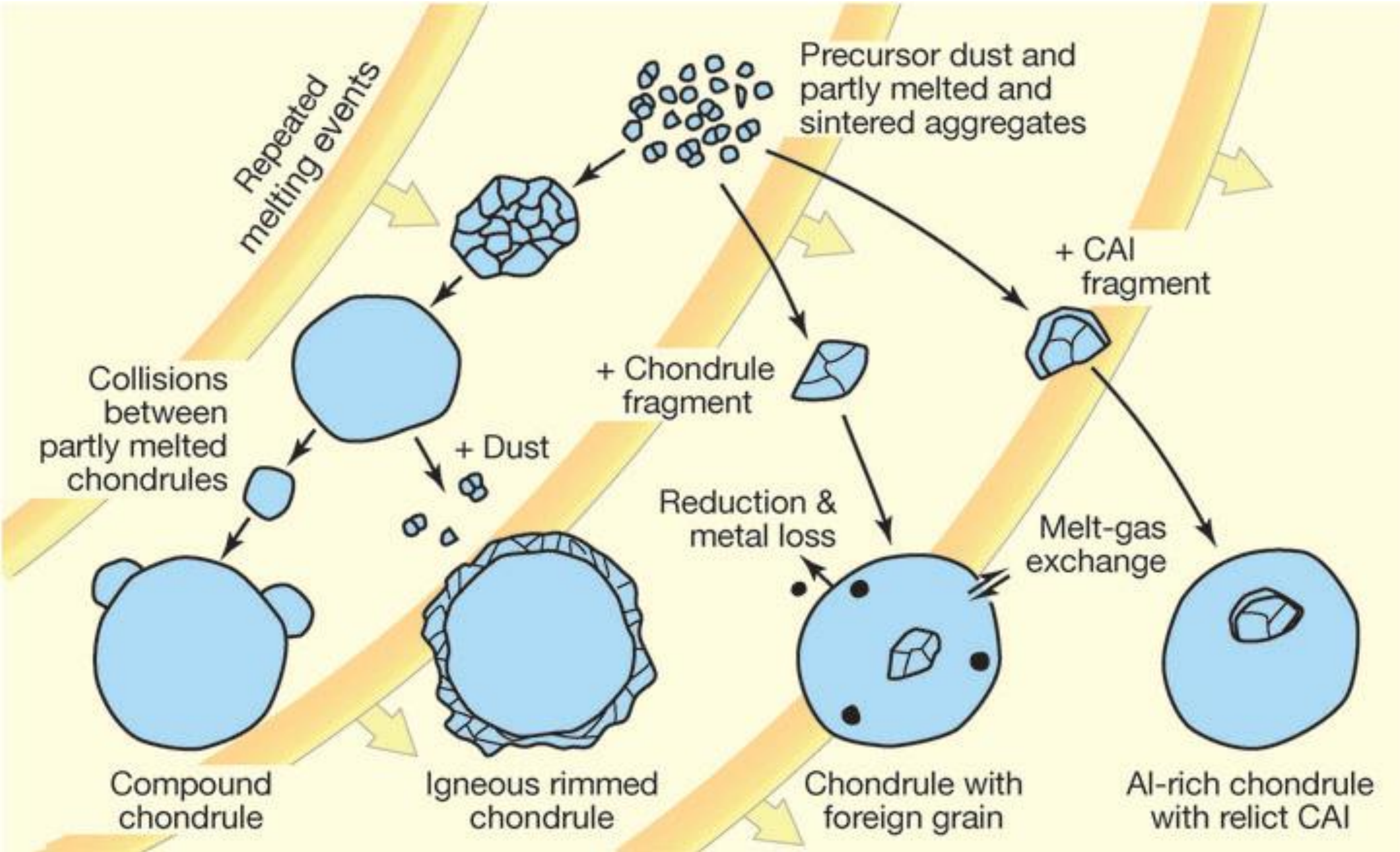

Scott 2007

Chondrule size distribution

Miura & Nakamoto 2006

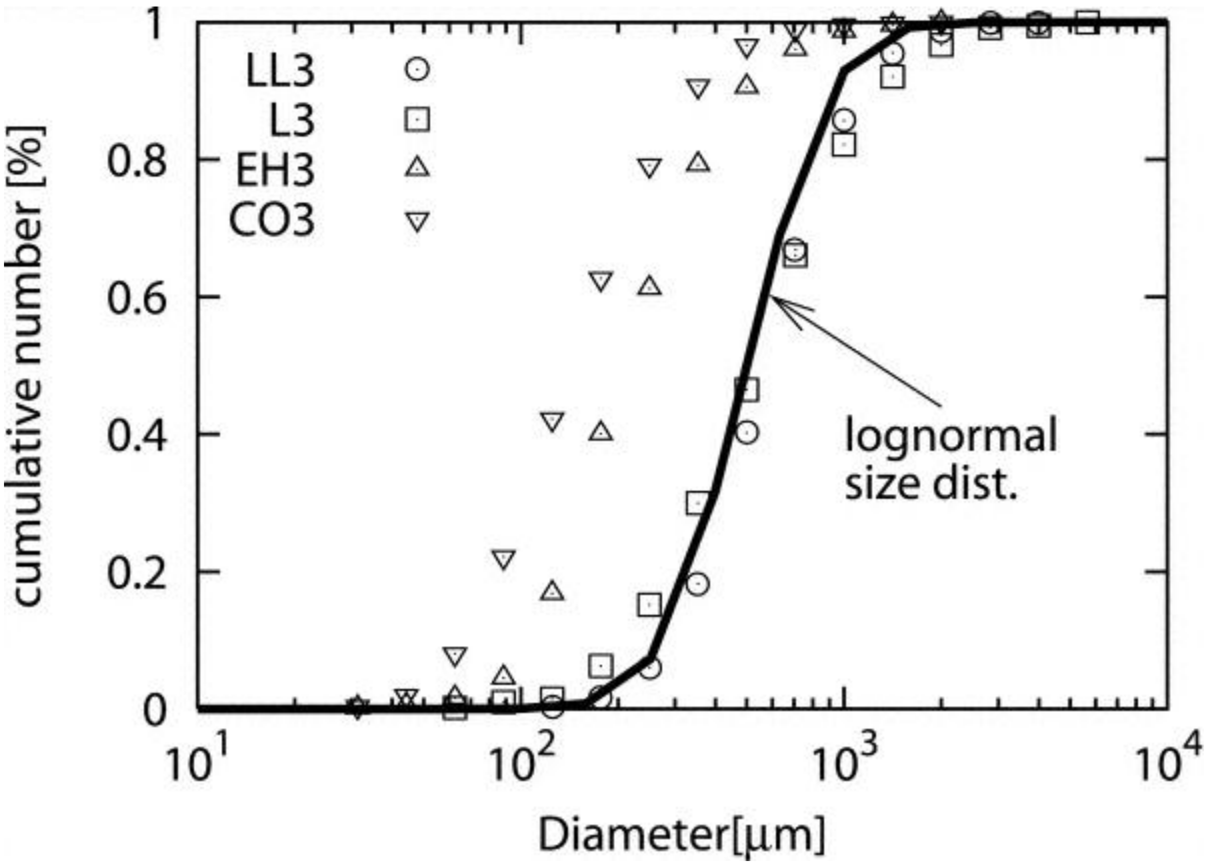

II. Observational constraints

h. Meteoritic evidence of formation timescales

NWA 5932, carbonaceous chondrite, CV3

Source: http://tw.strahlen.org/fotoatlas1/meteorite_chondrite1.html

Radiometric dating of meteorites - long half lives

Radioactive Isotope (Parent)	Product (Daughter)	Half-Life (Years)
Samarium-147	Neodymium-143	106 billion
Rubidium-87	Strontium-87	48.8 billion
Rhenium-187	Osmium-187	42 billion
Lutetium-176	Hafnium-176	38 billion
Thorium-232	Lead-208	14 billion
Uranium-238	Lead-206	4.5 billion
Potassium-40	Argon-40	1.26 billion
Uranium-235	Lead-207	0.7 billion

http://www.asa3.org/ASA/resources/wiens.html

Absolute ages – the Pb-Pb method

$$\left(\frac{^{207}Pb}{^{204}Pb}\right)_P = \left(\frac{^{207}Pb}{^{204}Pb}\right)_I + \left(\frac{^{235}U}{^{204}Pb}\right)\left(e^{\lambda_{235}t} - 1\right)$$

$$\left(\frac{^{206}Pb}{^{204}Pb}\right)_P = \left(\frac{^{206}Pb}{^{204}Pb}\right)_I + \left(\frac{^{238}U}{^{204}Pb}\right)\left(e^{\lambda_{238}t} - 1\right)$$

$$\left[\frac{\left(\frac{^{207}Pb}{^{204}Pb}\right)_P - \left(\frac{^{207}Pb}{^{204}Pb}\right)_I}{\left(\frac{^{206}Pb}{^{204}Pb}\right)_P - \left(\frac{^{206}Pb}{^{204}Pb}\right)_I}\right] = \left(\frac{1}{137.88}\right)\left(\frac{e^{\lambda_{235}t} - 1}{e^{\lambda_{238}t} - 1}\right)$$

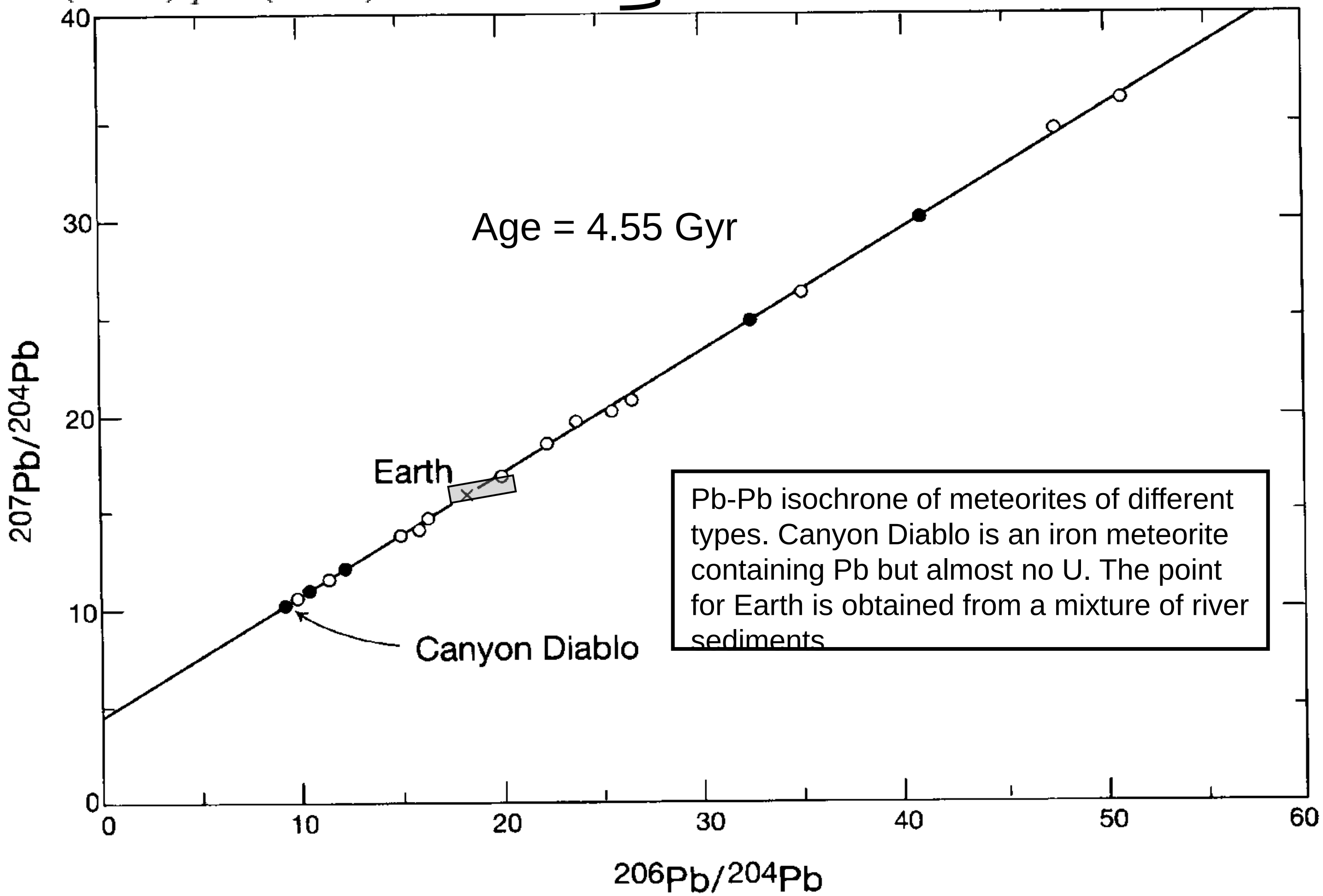

Pb-Pb isochrone of meteorites of different types. Canyon Diablo is an iron meteorite containing Pb but almost no U. The point for Earth is obtained from a mixture of river sediments

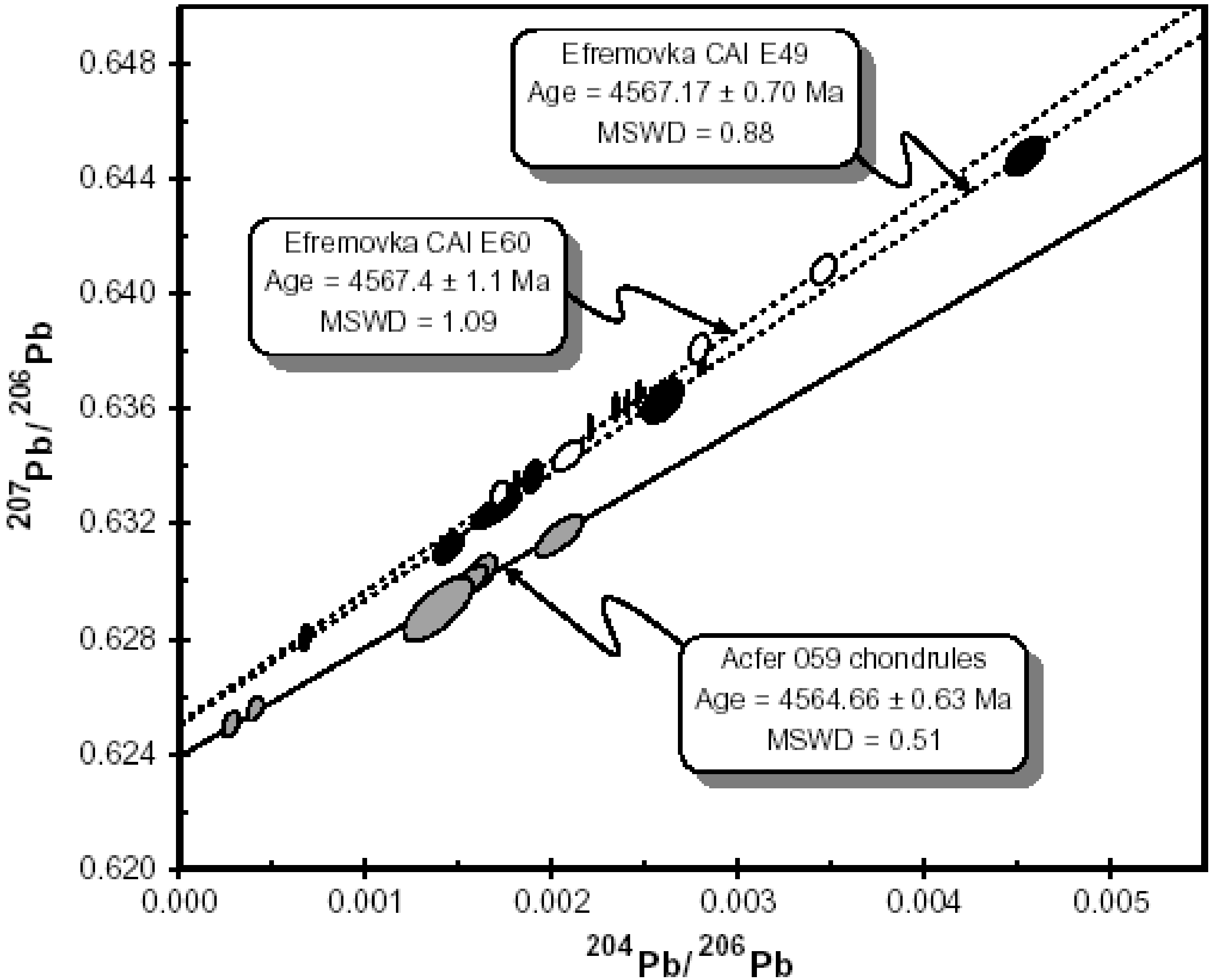

Fig. 1. Pb-Pb isochrons for the six most radiogenic Pb isotopic analyses of acid-washed chondrules from the CR chondrite Acfer 059 (solid line), and for acid-washed fractions from the Efremovka CAIs (dashed lines). $^{207}Pb/^{206}Pb$ ratios are not corrected for initial common Pb. Error ellipses are 2σ. Isochron age errors are 95% confidence intervals.

Amelin et al. 2002

Radiometric dating of meteorites
- short half lives

Table 1. Extinct radioactivities in meteorites

Parent nuclide	Half-life (My)	Decay constant (My^{-1})	Daughter nuclide	Estimated initial abundance
Samarium-146	103	0.00673	Neodymium-142	$^{146}Sm/^{144}Sm=(8.4\pm0.5)\times10^{-3}$
Plutonium-244	80	0.0087	Fission products	$^{244}Pu/^{238}U=(6.8\pm1.0)\times10^{-3}$
Iodine-129	15.7	0.0441	Xenon-129	$^{129}I/^{127}I=(1.19\pm0.20)\times10^{-4}$
Hafnium-182	8.9	0.078	Tungsten-182	$^{182}Hf/^{180}Hf=(9.72\pm0.44)\times10^{-5}$
Manganese-53	3.74	0.185	Chromium-53	$^{53}Mn/^{55}Mn=(6.28\pm0.66)\times10^{-6}$
Beryllium-10	1.385	0.500	Boron-10	$^{10}Be/^{9}Be=(7.0\pm0.8)\times10^{-4}$
Aluminum-26	0.717	0.967	Magnesium-26	$^{26}Al/^{27}Al=(5.23\pm0.13)\times10^{-5}$
Niobium-92	34.7	0.0200	Zirconium-92	$^{92}Nb/^{93}Nb=(1.6\pm0.3)\times10^{-5}$
Palladium-107	6.5	0.11	Silver-107	$^{107}Pd/^{108}Pd=(5.9\pm2.2)\times10^{-5}$
Iron-60	2.62	0.265	Nickel-60	$(7.9\pm2.8)\times10^{-9}<^{60}Fe/^{56}Fe<(6.3\pm2.0)\times10^{-7}$
Chlorine-36	0.301	2.30	Sulfur-36 (1.9 %), argon-36 (98.1 %)	$^{36}Cl/^{35}Cl>(17.2\pm2.5)\times10^{-6}$
Curium-247	15.6	0.0444	Uranium-235	$^{247}Cm/^{238}U=(5.5\pm2.0)\times10^{-5}$
Lead-205	15.1	0.0459	Thallium-205	$^{205}Pb/^{204}Pb=(1.0\pm0.4)\times10^{-3}$
Cesium-135	2.3	0.30	Barium-135	$^{135}Cs/^{133}Cs=(4.8\pm0.8)\times10^{-4}$
Calcium-41	0.102	6.80	Potassium-41	$^{41}Ca/^{40}Ca=(1.41\pm0.14)\times10^{-8}$
Beryllium-7	1.46×10^{-7}	6.86×10^{6}	Lithium-7	$^{7}Be/^{9}Be=0.0061\pm0.0013$
Technetium-97	4.21	0.16464	Molybdenum-97	$^{97}Tc/^{92}Mo<3\times10^{-6}$
Technetium-98	4.2	0.17	Ruthenium-98	$^{98}Tc/^{96}Ru<2\times10^{-5}$
Tin-126	0.23	3.0	Tellurium-126	$^{126}Sn/^{124}Sn<7.7\times10^{-5}$

Dauphas & Chaussidon 2011

Relative ages – the decay of ^{26}Al

CHUR = chondritic uniform reservoir

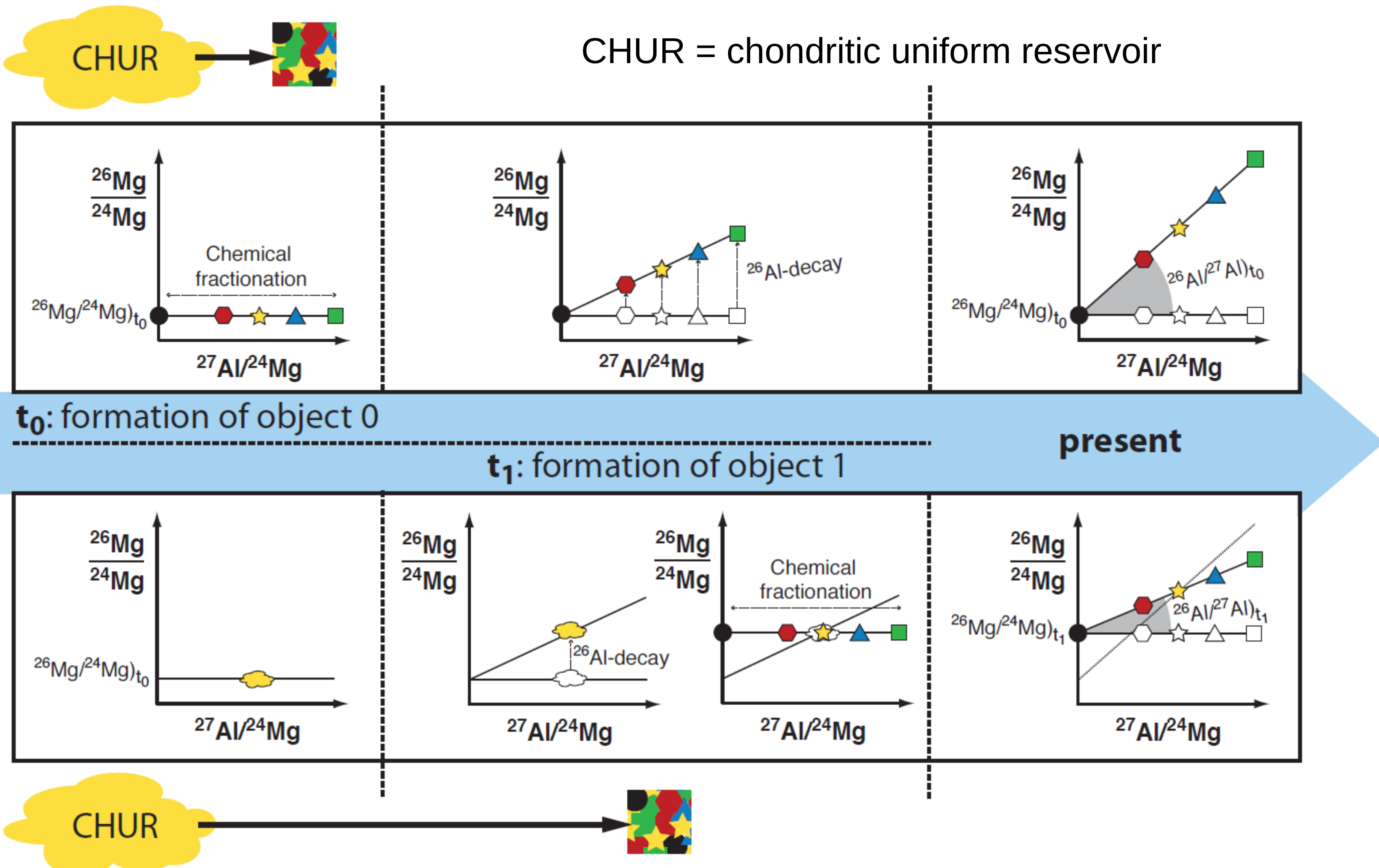

Dauphas & Chaussidon 2011

Condensation of 1-10 μm dust from nebular gas

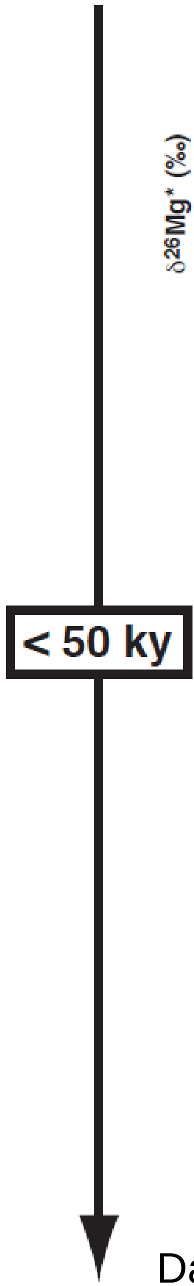

Bulk isochron of CAIs
(Jacobsen et al., 2008)

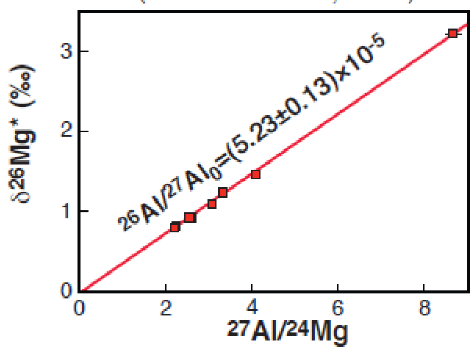

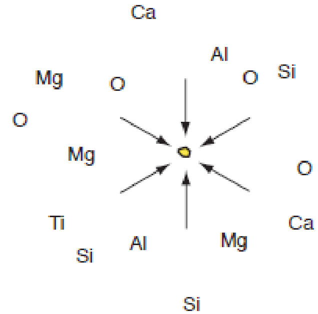

Internal isochron of a fine-grained CAI
(MacPherson et al., 2010a)

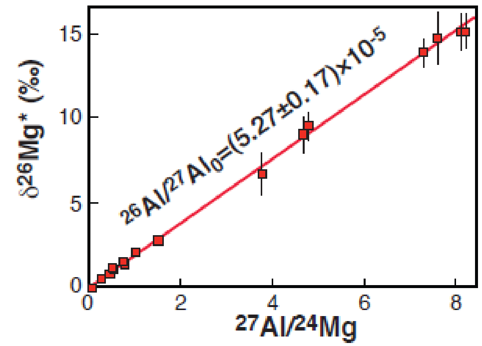

Agglomeration into mm-cm objects

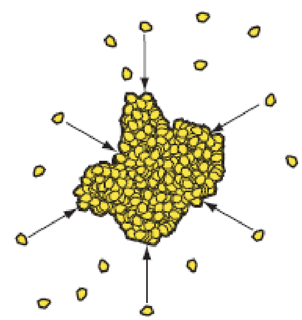

Melting and crystallization

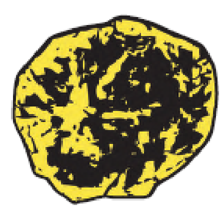

Internal isochron of an igneous CAI
(MacPherson et al., 2010b)

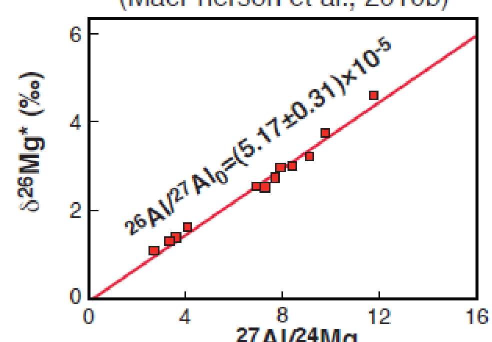

Dauphas & Chaussidon 2011

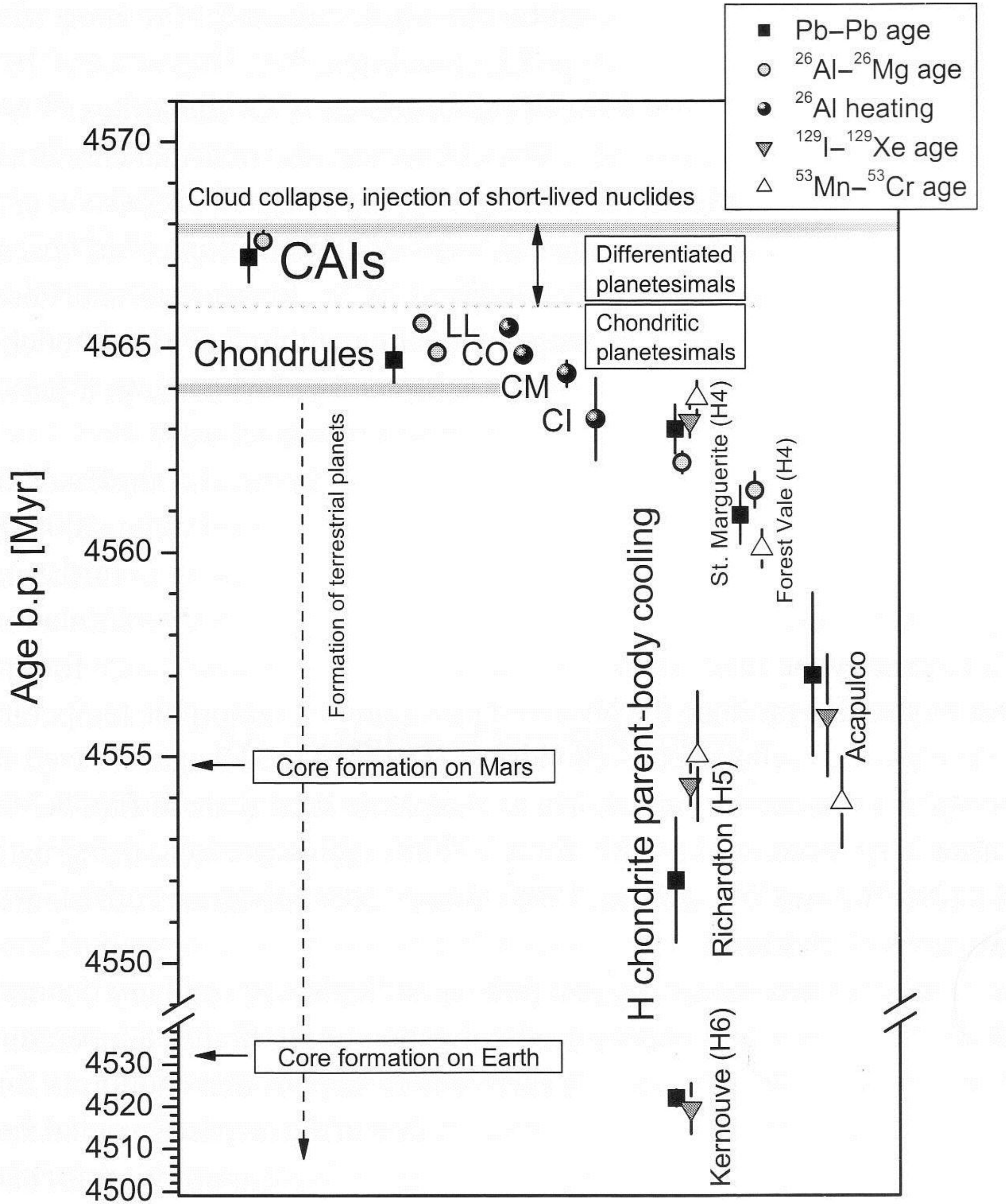

Trieloff & Palme 2006

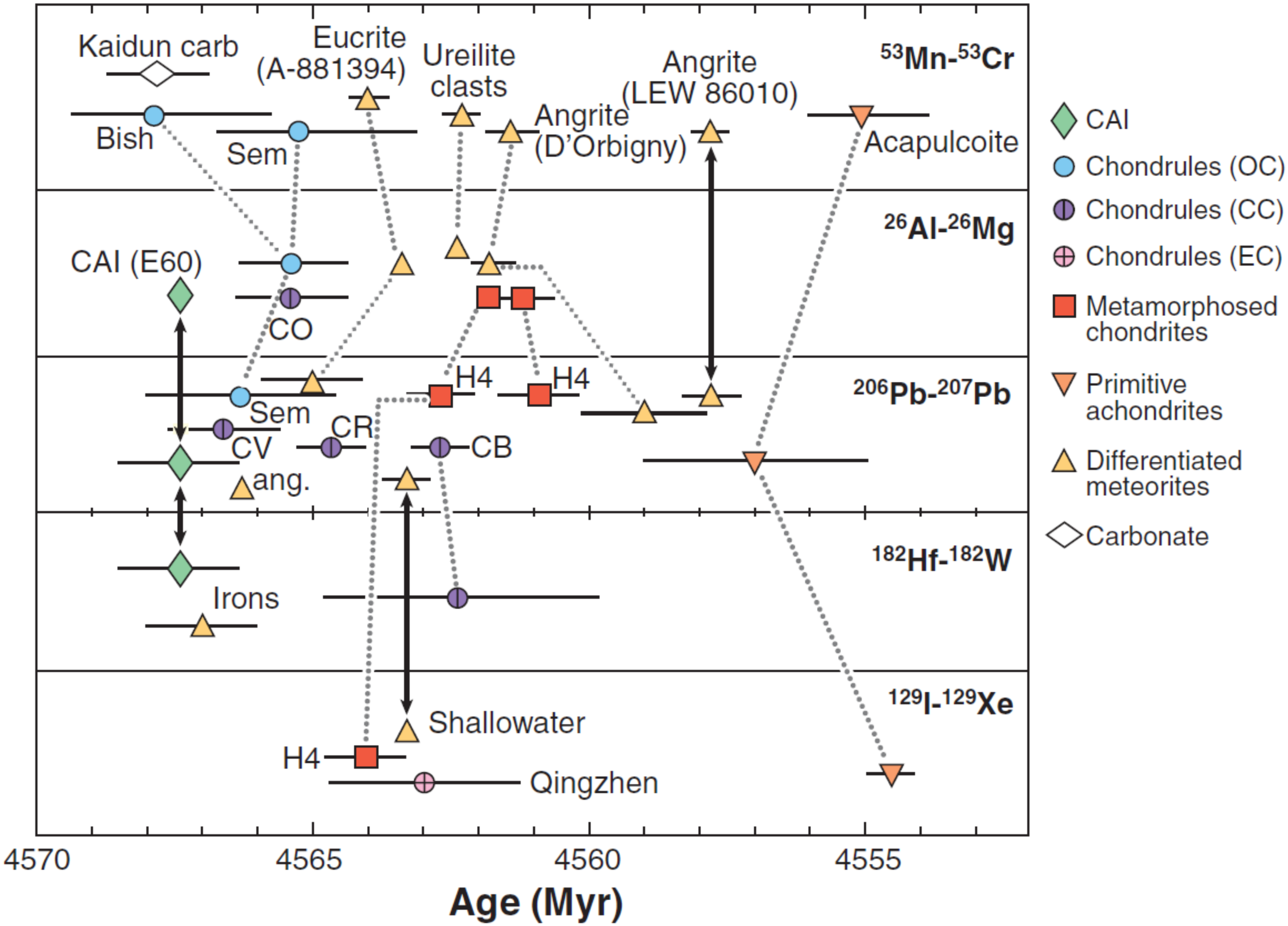

Kaidun carb
Eucrite
(A-881394)
Ureilite
clasts
Angrite
(LEW 86010)
53Mn-53Cr
Bish
Sem
Angrite
(D'Orbigny)
Acapulcoite
26Al-26Mg
CAI (E60)
CO
206Pb-207Pb
H4
H4
Sem
CR
CV
CB
ang.
182Hf-182W
Irons
129I-129Xe
Shallowater
H4
Qingzhen
4570
4565
4560
4555
Age (Myr)
CAI
Chondrules (OC)
Chondrules (CC)
Chondrules (EC)
Metamorphosed chondrites
Primitive achondrites
Differentiated meteorites
Carbonate

Scott 2007

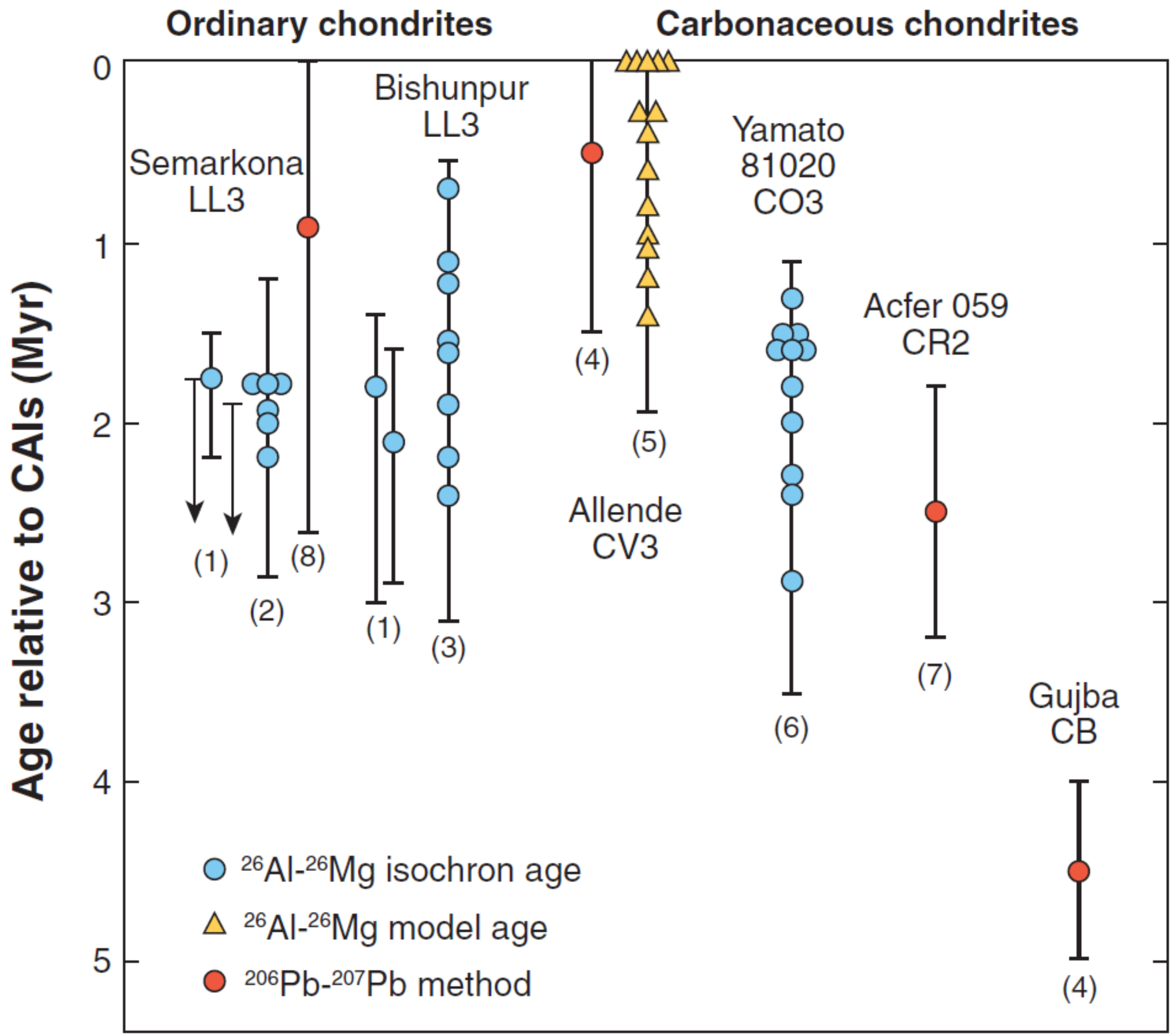
Ordinary chondrites
Carbonaceous chondrites
Age relative to CAIs (Myr)
0
1
2
3
4
5
Semarkona
LL3
Bishunpur
LL3
Allende
CV3
Yamato
81020
CO3
Acfer 059
CR2
Gujba
CB
(1)
(2)
(8)
(1)
(3)
(4)
(5)
(6)
(7)
(4)
^{26}Al-^{26}Mg isochron age
^{26}Al-^{26}Mg model age
^{206}Pb-^{207}Pb method

Scott 2007

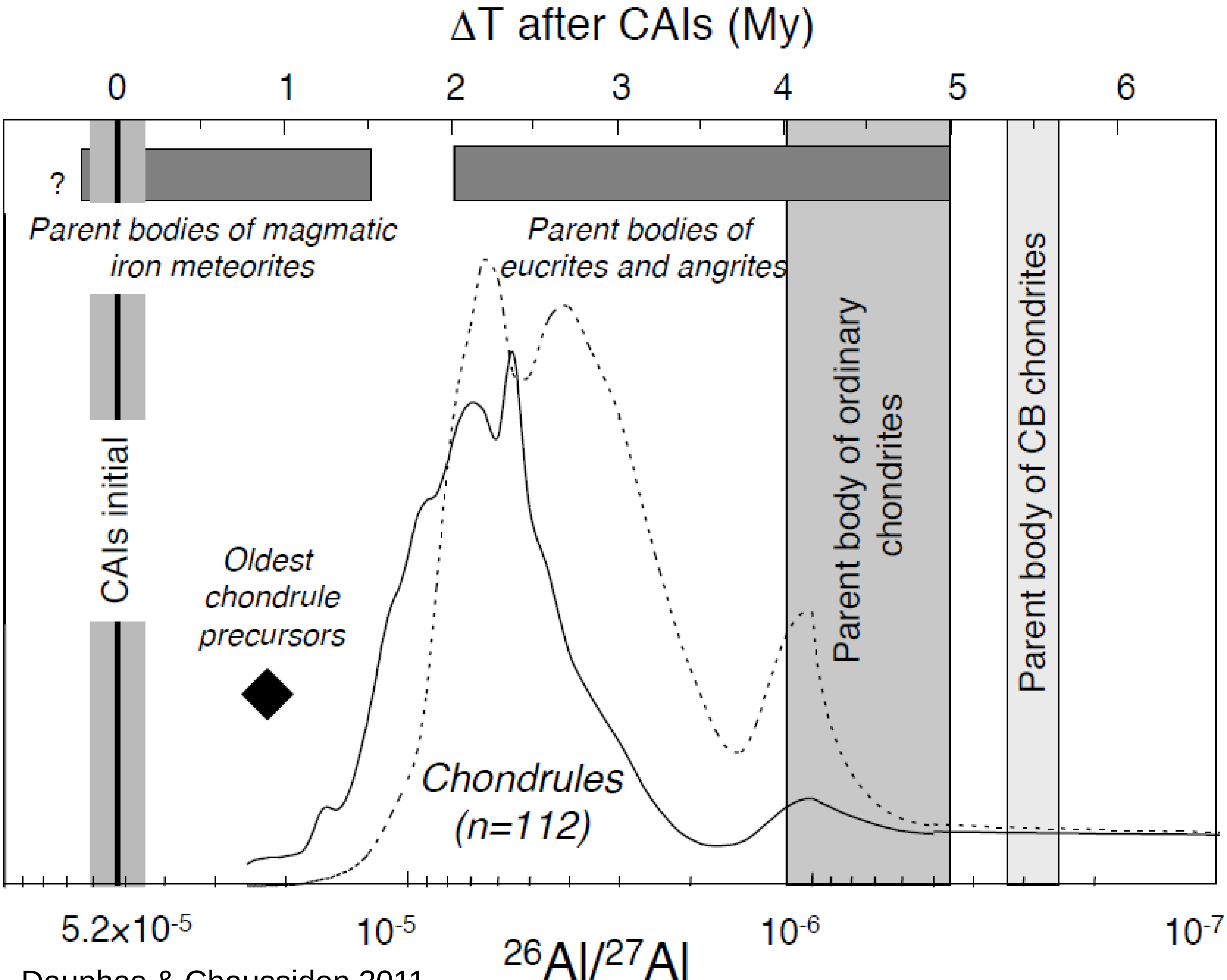

Dauphas & Chaussidon 2011

II. Observational constraints

i. Late heavy bombardment

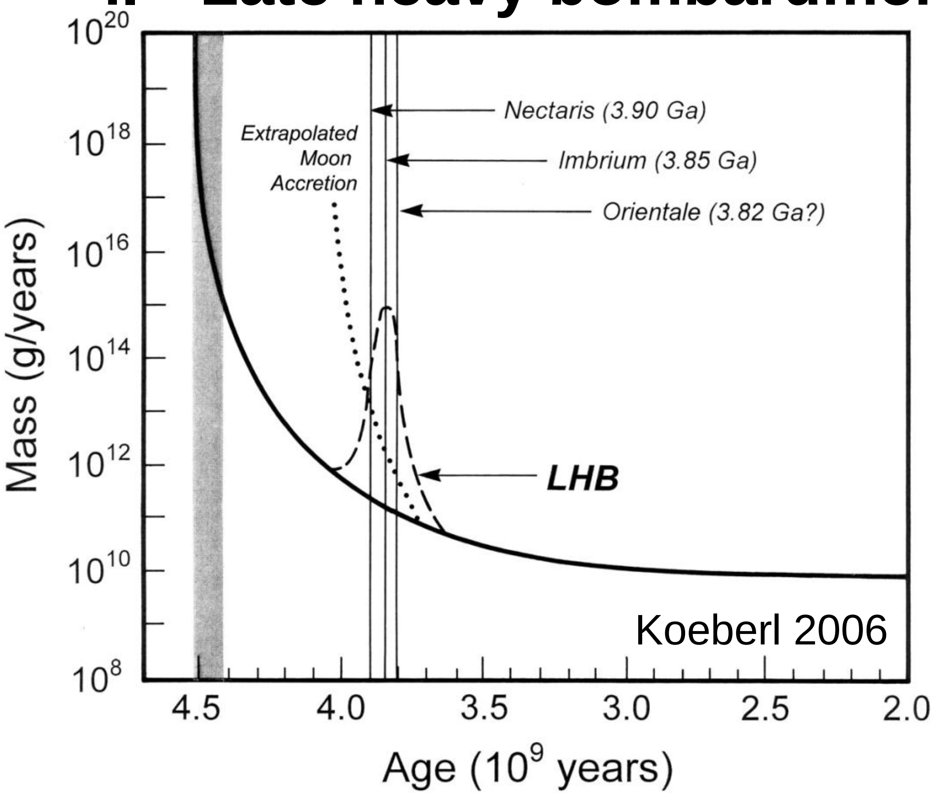

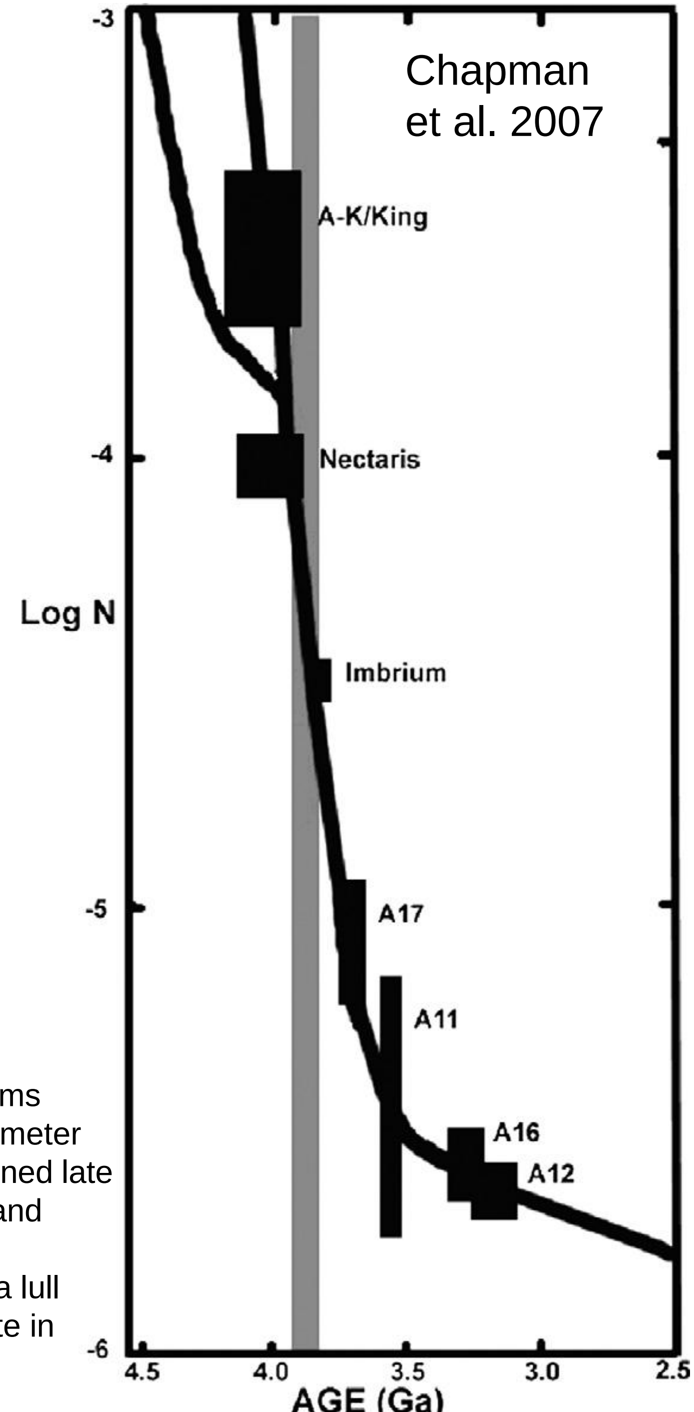

Fig. 1. Declining crater densities versus time, after Wilhelms (1987). *N* is the cumulative number of craters >20 km diameter per sq. km. The thin gray bar is the period of the well-defined late heavy bombardment, between the formation of Nectaris and Imbrium, when a dozen lunar basins were formed. Two extensions to the upper left indicate schematically either a lull prior to a cataclysm or a continued high bombardment rate in pre-nectarian times.

II. Observational constraints

j. Formation timescale and mass of Mars

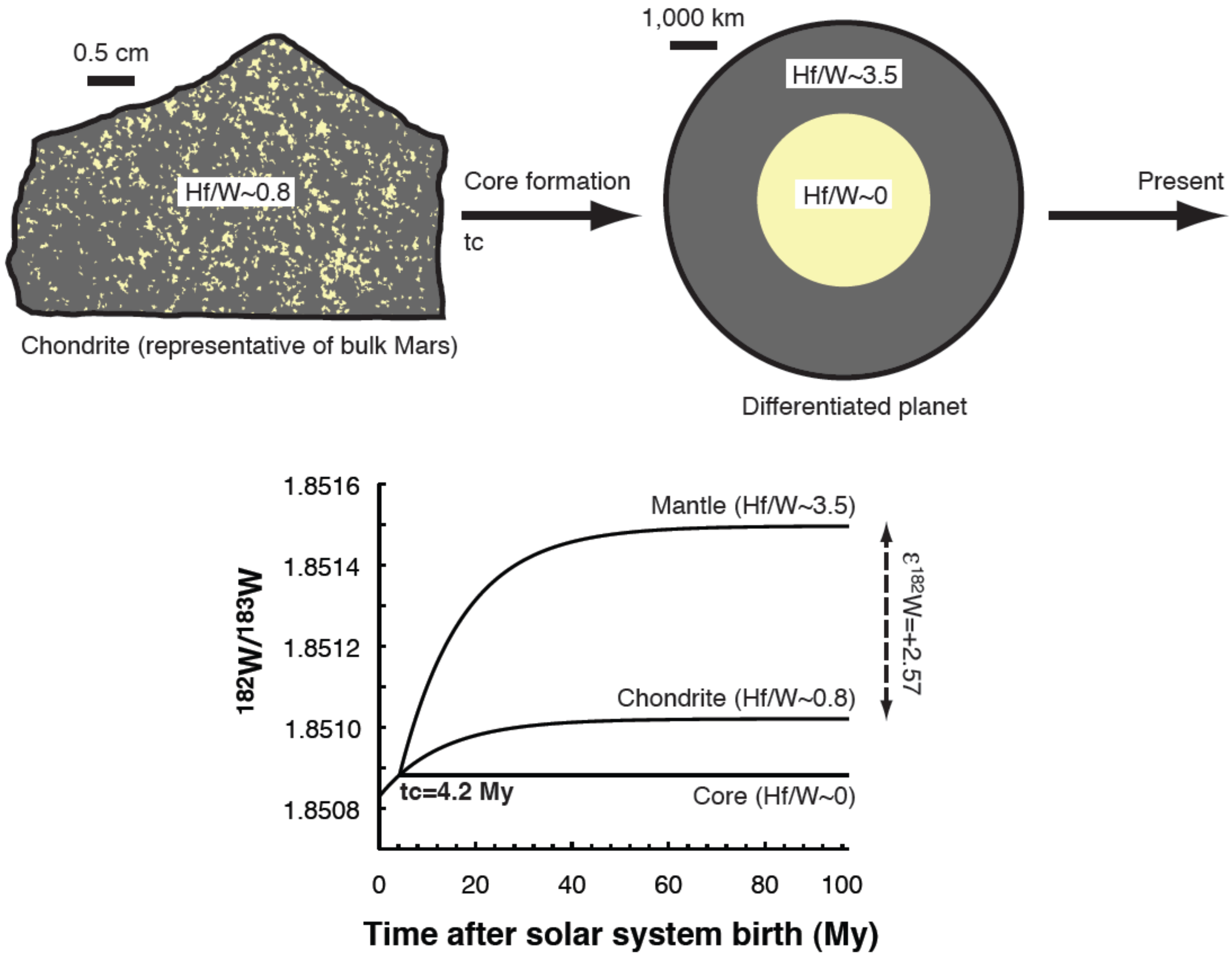

Dauphas & Chaussidon 2011

SNC (Martian) meteorites

SNC =
Shergottites,
Nakhlites,
Chassignites

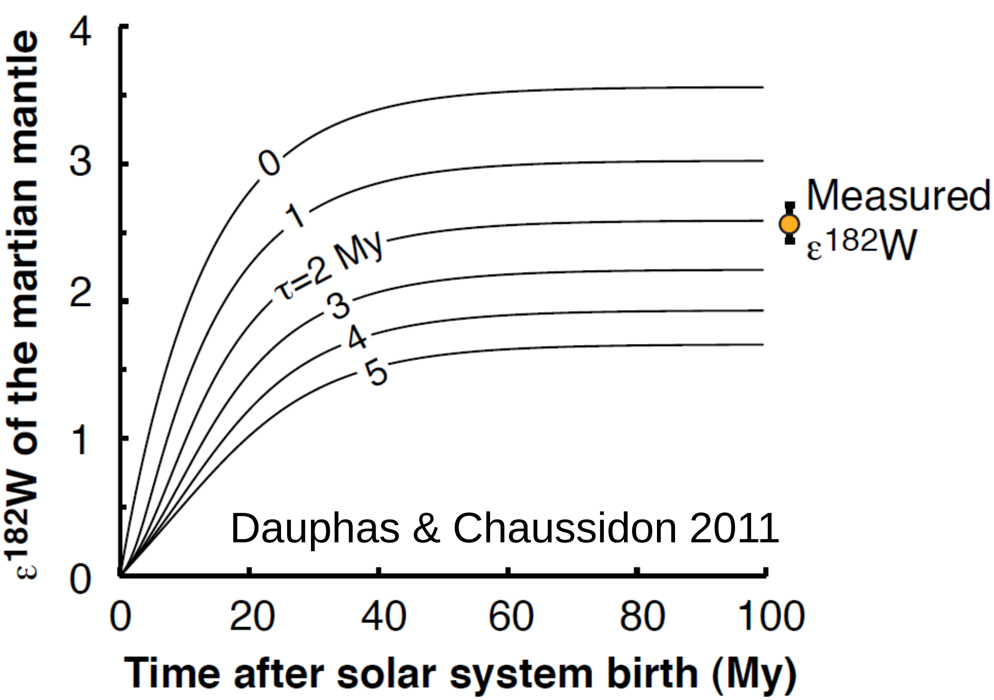

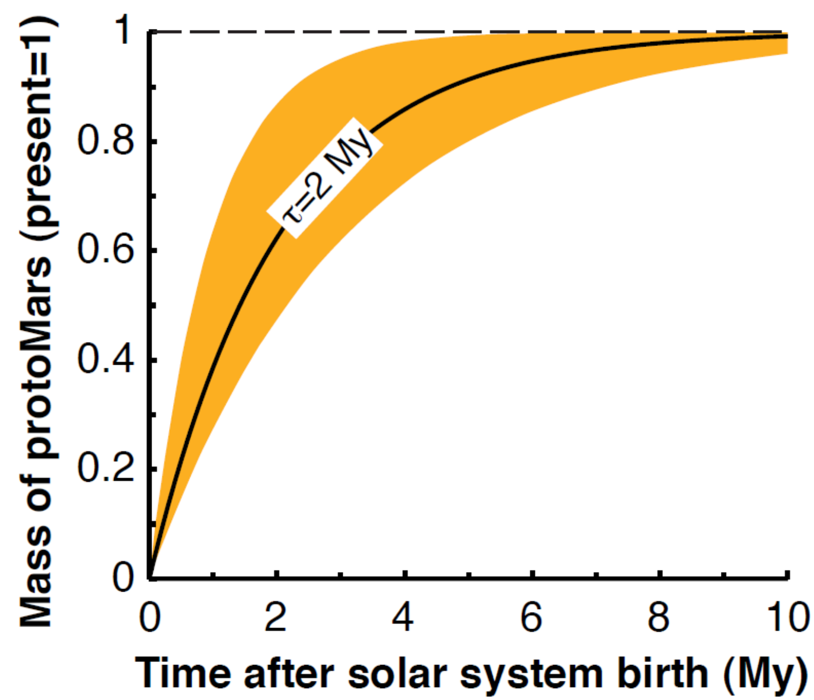

II. Observational constraints

k. Formation of the Earth and the Moon

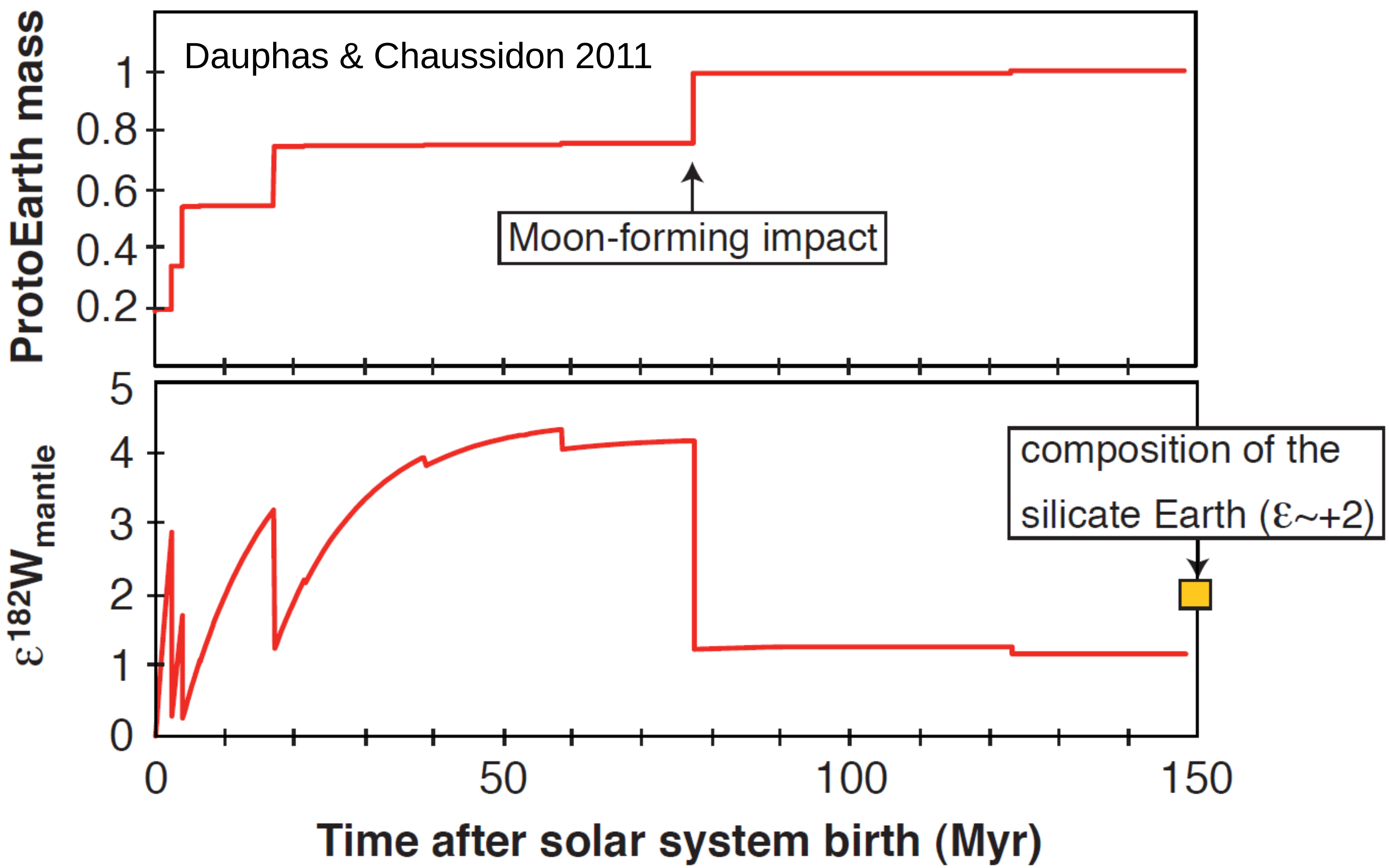

II. Observational constraints

I. Cosmochemical composition of planetary bodies as a function of distance to Sun

Planetary densities

Mercury - 5.427 g/cm^3
Venus - 5.204 g/cm^3
Earth - 5.515 g/cm^3
Mars - 3.934 g/cm^3
Jupiter - 1.326 g/cm^3
Saturn - 0.687 g/cm^3
Uranus - 1.27 g/cm^3
Neptune - 1.638 g/cm^3

Object	mean density	uncompressed density	semi-major axis
Mercury ☿	5.4 g cm^{-3}	5.3 g cm^{-3}	0.39 AU
Venus ♀	5.2 g cm^{-3}	4.4 g cm^{-3}	0.72 AU
Earth ⊕	5.5 g cm^{-3}	4.4 g cm^{-3}	1.0 AU
Moon ☾	3.3 g cm^{-3}	3.3 g cm^{-3}	1.0 AU
Mars ♂	3.9 g cm^{-3}	3.8 g cm^{-3}	1.5 AU
Vesta ⚶	3.4 g cm^{-3}	3.4 g cm^{-3}	2.3 AU
Pallas ⚴	2.8 g cm^{-3}	2.8 g cm^{-3}	2.8 AU
Ceres ⚳	2.1 g cm^{-3}	2.1 g cm^{-3}	2.8 AU

http://en.wikipedia.org/wiki/Terrestrial_planet

Material densities

Iron: 7.9 g/cm^3
Silicates: ~2.25-4.25 g/cm^3
Carbonaceous material: ~0.8-2.3 g/cm^3
Water ice: ~1.0 g/cm^3

II. Observational constraints

I. Cosmochemical composition of planetary bodies as a function of distance to Sun

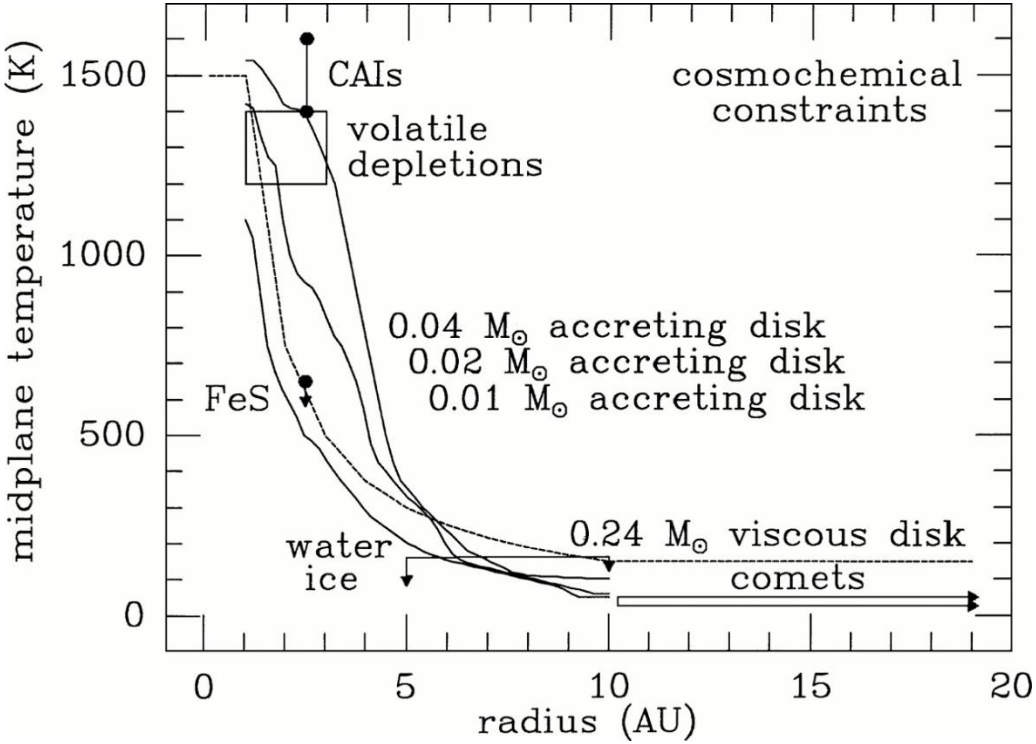

Boss 1998

Figure 1 Comparison with theoretical models of cosmochemically derived constraints on disk midplane temperatures (CAIs, volatile depletions, FeS, water ice, and comets; see text for references). *Solid lines* are values of *Tm* for three *Ansatz* disk models (Boss 1996a), labeled from top to bottom by the disk masses (inside 10 AU). *Dashed line* is *Tm* for a viscous accretion disk model (Morfill 1988) with $\dot{M} = 10^{-5}\ M_\odot$/year, and a mass of 0.24 $M_\odot$ inside 10 AU.

II. Observational constraints

m. The low (?) abundance of interstellar dust in meteorites and Stardust material

TABLE 3 Presolar grains in meteorites (Hoppe & Zinner 2000)

Composition	Diameter (μm)	Abundance[a]	Origins[b]
C (diamond)	0.002	5×10^{-4}	SN
SiC[c]	0.3–20	6×10^{-6}	AGB
C (graphite)[d]	1–20	1×10^{-6}	AGB, SN II, nova
SiC type X	1–5	6×10^{-8}	SN
Al_2O_3 (corundum)	0.5–3	3×10^{-8}	RG, AGB
Si_3N_4	$\sim$1	2×10^{-9}	SN II

[a] Overall abundance in primitive carbonaceous chondrite meteorites.

[b] SN = supernova; AGB = asymptotic giant branch star; RG = red giant.

[c] SiC grains sometimes contain very small TiC inclusions.

[d] Graphite grains sometimes contain very small TiC, ZrC, and MoC inclusions.

III.
The formation of planets and planetary systems

III. The formation of planets and planetary systems

a. The general picture

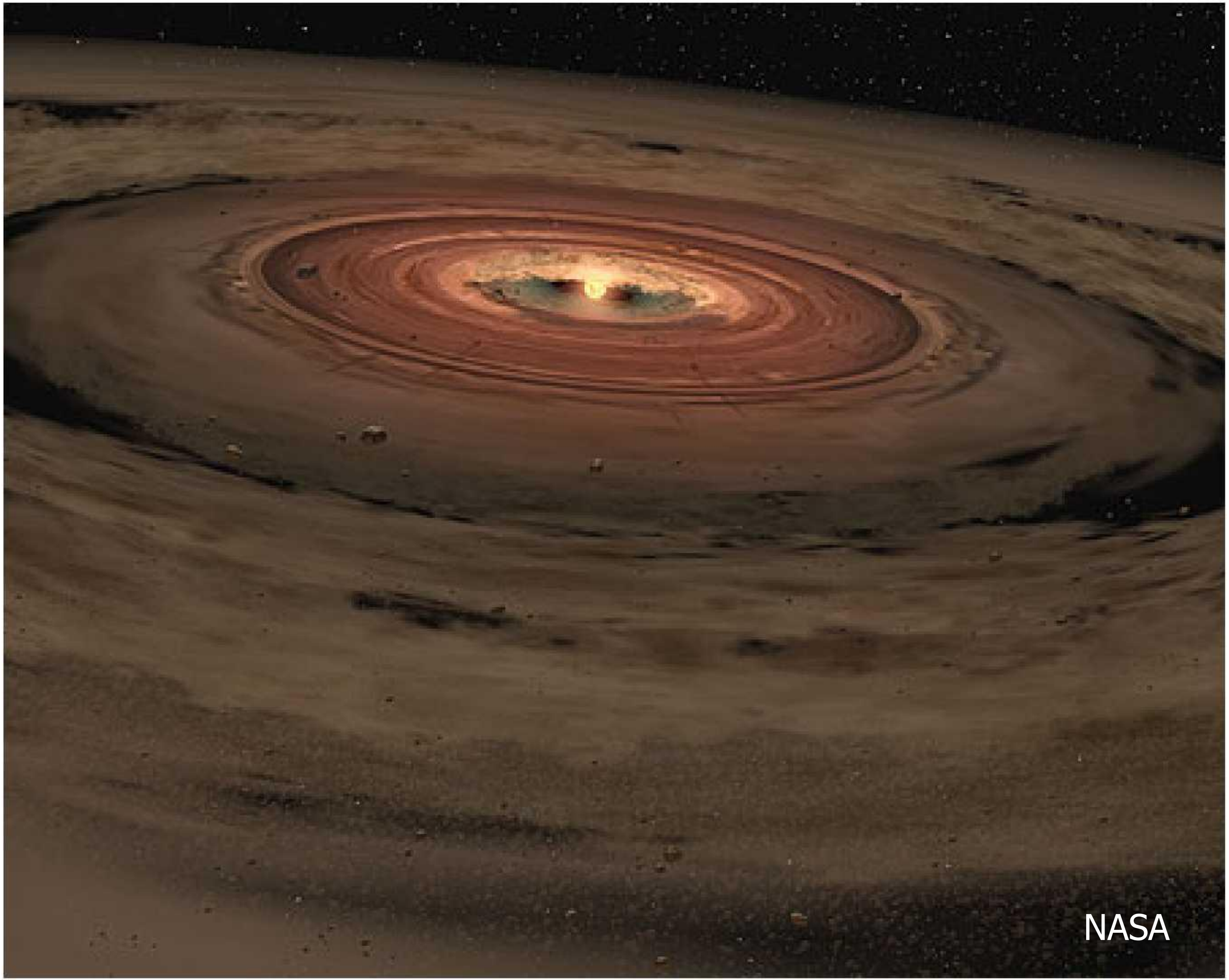

Star formation – an overview

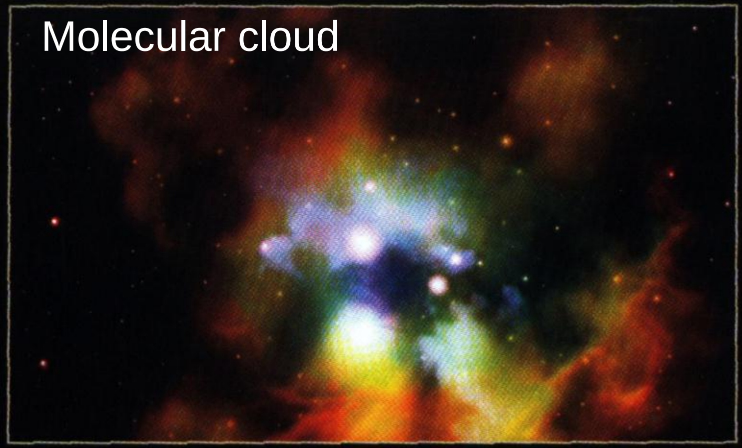

© GEO, after Shu et al. 1987

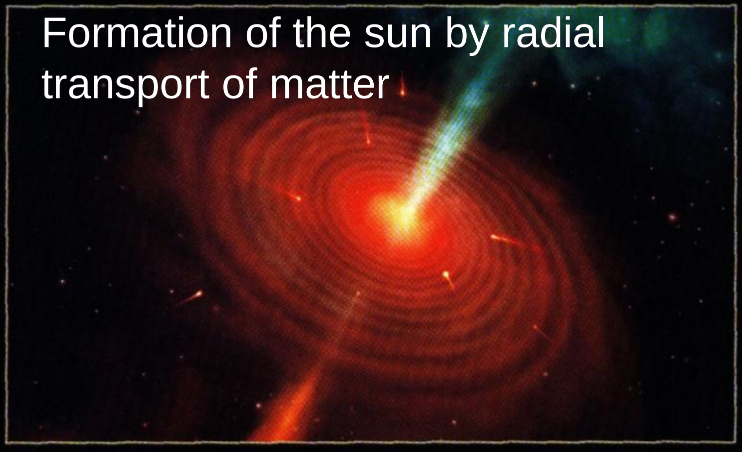

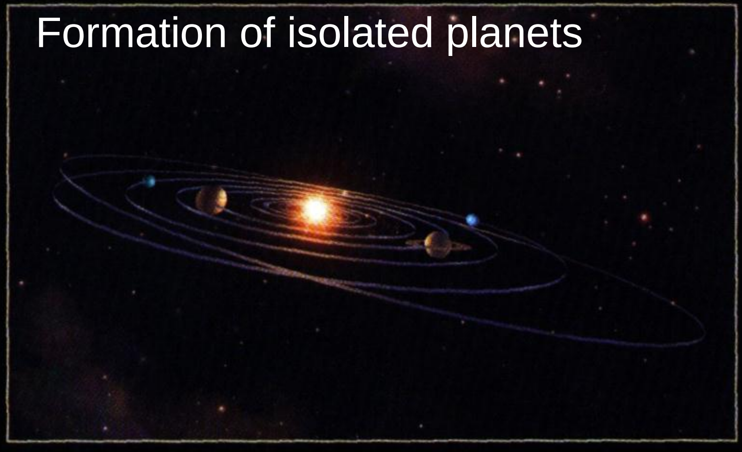

The five-stage process of planet formation

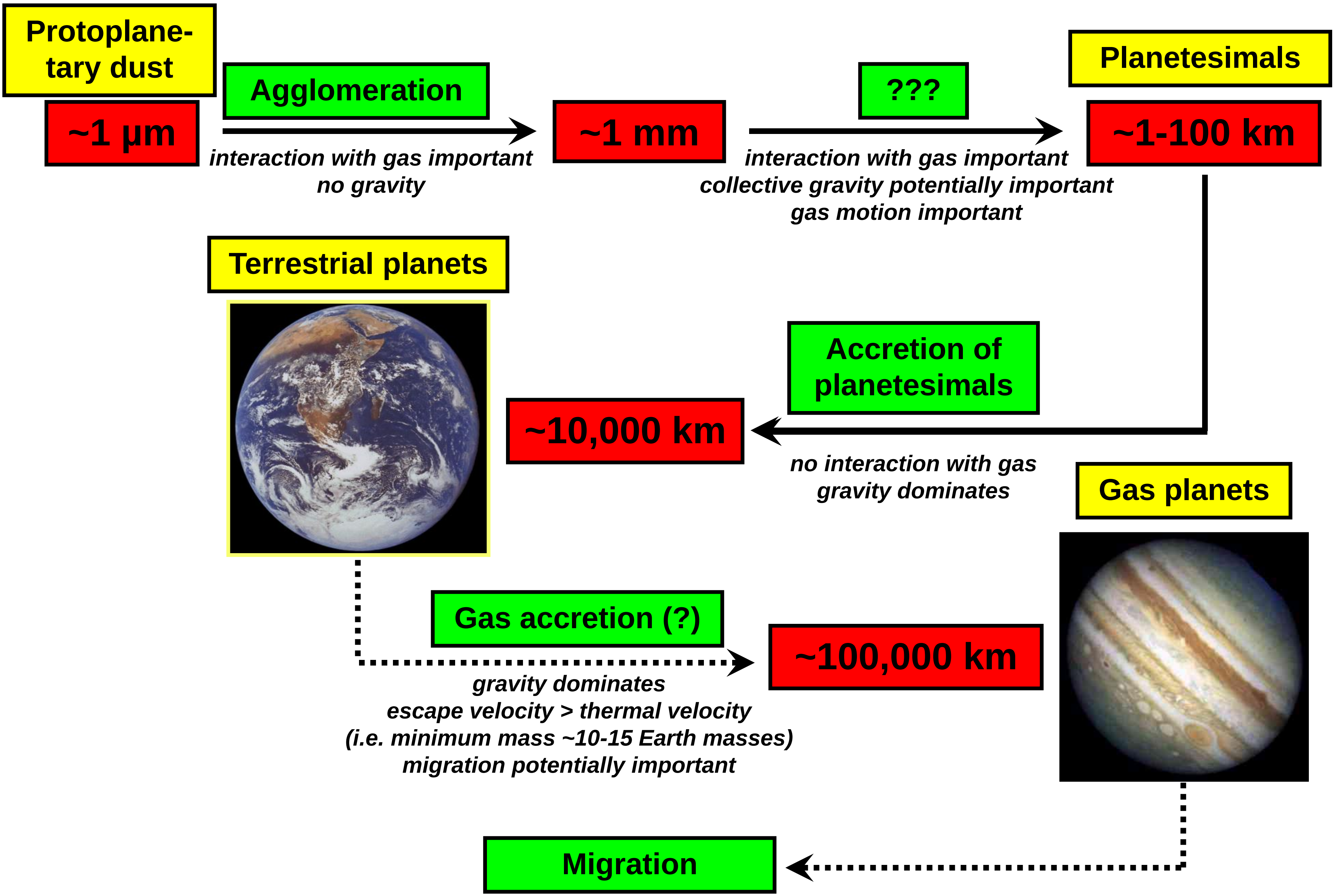

III. The formation of planets and planetary systems

b. Dust to planetesimals

i. Solar-nebula models

Planetary zones: masses and surface densities

	Mass ($M_\oplus$)	Fe mass fraction	Solar comp. mass ($M_\oplus$)	Zone limits (AU)	Surface density (g cm^{-2})
Mercury	0.053	0.62	27	0.22	880
Venus	0.815	0.35	235	0.56	4750
Earth	1	0.38	320	0.86	3200
Mars	0.107	0.30	27	1.26	95
Asteroids					
present	0.0005	0.25	0.1	2.0	0.13
original	0.15?		30		40
				3.3	
Jupiter	318	–	600–12 000	7.4	120–2400
Saturn	95	–	1000–6000	14.4	55–330
Uranus	14.6	–	700–2000	24.7	15–40
Neptune	17.2	–	800–2000	35.5	10–25

Weidenschilling 1977

Inferred surface densities

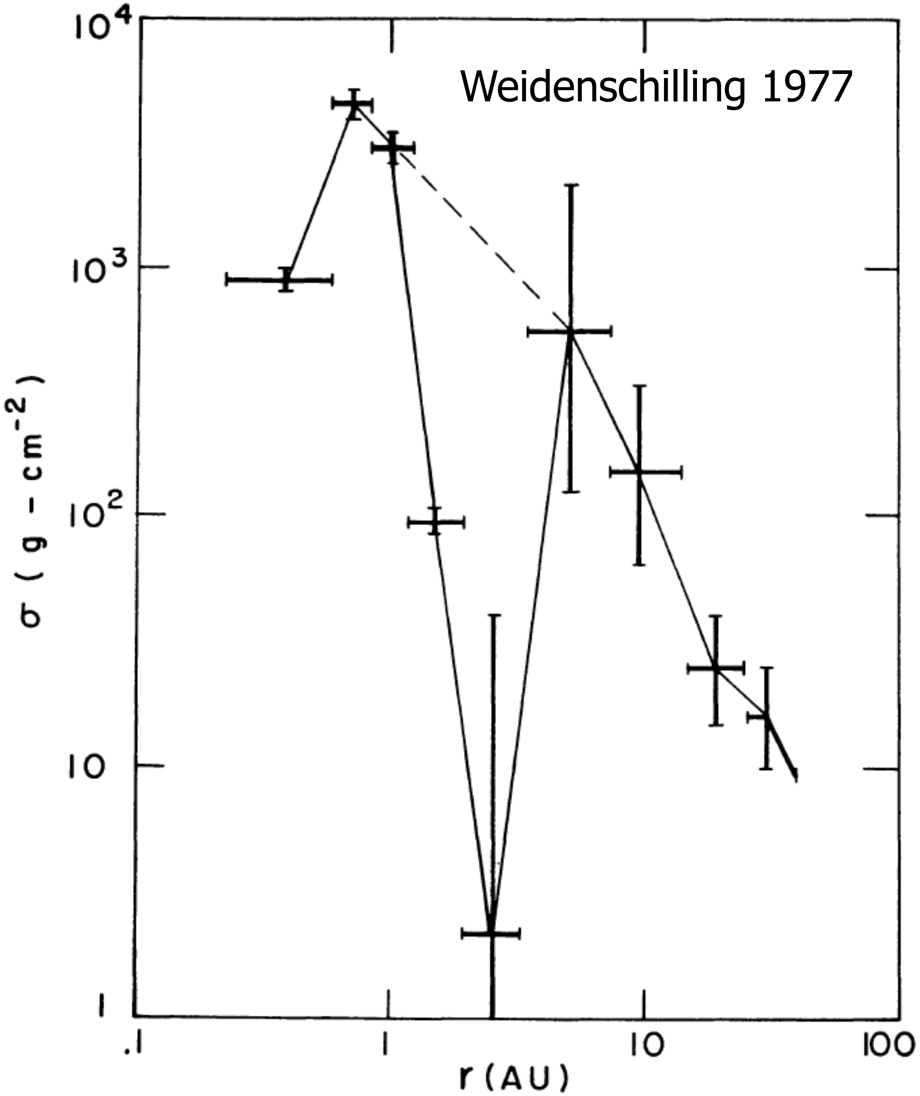

Fig. 1. Surface densities, σ, obtained by restoring the planets to solar composition and spreading the resulting masses through contiguous zones surrounding their orbits. The meaning of the 'error bars' is discussed in the text.

A power-law approximation:

$$\Sigma_s(r) = 1700\ \mathrm{g/cm^2} \cdot \left(\frac{r}{1\ \mathrm{AU}} \right)^{-3/2}$$

III. The formation of planets and planetary systems

b. Dust to planetesimals

ii. Metallicity of the solar nebula

TABLE 5

SOME INTERIOR CHARACTERISTICS OF THE SOLAR MODELS

Model	T_c	ρ_c	P_c	$Y_{\rm init}$	$Z_{\rm init}$	Y_c	Z_c
Standard	15.696	152.7	2.342	0.2735	0.0188	0.6405	0.0198
NACRE	15.665	151.9	2.325	0.2739	0.0188	0.6341	0.0197
AS00	15.619	152.2	2.340	0.2679	0.0187	0.6341	0.0197
GN93	15.729	152.9	2.342	0.2748	0.02004	0.6425	0.02110
Pre-M.S.	15.725	152.7	2.339	0.2752	0.02003	0.6420	0.02109
Rotation	15.652	148.1	2.313	0.2723	0.01934	0.6199	0.02032
Radius_{78}	15.729	152.9	2.342	0.2748	0.02004	0.6425	0.02110
Radius_{508}	15.728	152.9	2.341	0.2748	0.02004	0.6425	0.02110
No Diffusion	15.448	148.6	2.304	0.2656	0.01757	0.6172	0.01757
Old Physics	15.787	154.8	2.378	0.2779	0.01996	0.6439	0.02102
$S_{34} = 0$	15.621	153.5	2.417	0.2722	0.02012	0.6097	0.02116
Mixed	15.189	90.68	1.728	0.2898	0.02012	0.3687	0.02047

NOTE.—The quantities T_c (in units of 10^7 K), ρ_c (10^2 g cm^{-3}), and P_c (10^{17} ergs cm^{-3}) are the present-epoch central temperature, density, and pressure; Y and Z are the helium and heavy-element mass fractions, where the subscript "init" denotes the zero-age main-sequence model and the subscript "c" denotes the center of the solar model.

Bahcall et al. 2001

III. The formation of planets and planetary systems

b. Dust to planetesimals

iii. Condensation sequence: temporal or spatial (or both)?

© NASA, after Shu et al. 1987

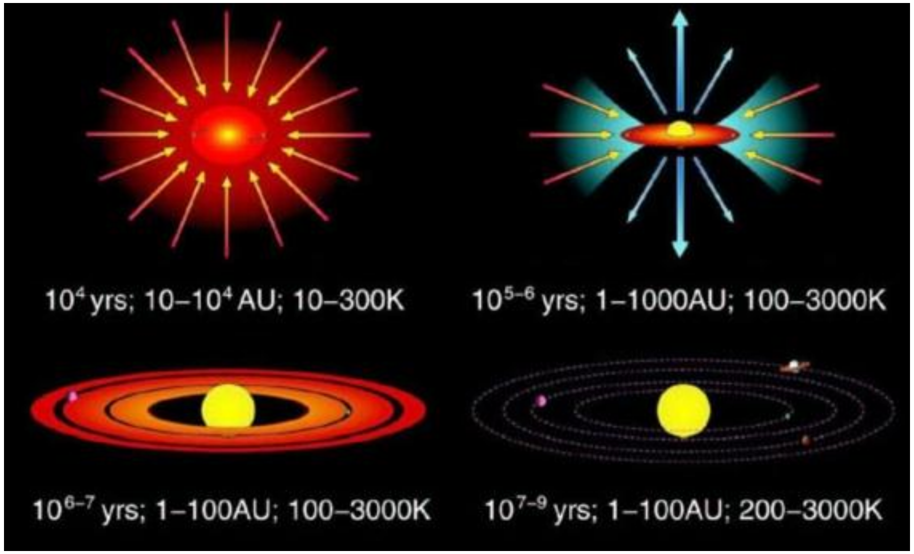

- ▷ Formation of an accretion disk.
- ▷ The disk is initially hot
  → few dust grains.
- ▷ As the disk cools down, dust particles condense.
- ▷ Dust materials: oxides, silicates, organics, ices.
- ▷ Particle sizes: sub-µm - µm.

TABLE II Condensation temperatures for selected materials

Armitage 2007

T	Material
1680 K	Al_2O_3
1590 K	$CaTiO_3$
1400 K	$MgAl_2O_4$
1350 K	Mg_2SiO_4, iron alloys
370 K	Fe_3O_4
180 K	water ice
130 K	$NH_3 \cdot H_2O$
40 K – 80 K	methane, methane ices
50 K	argon

Scott 2007

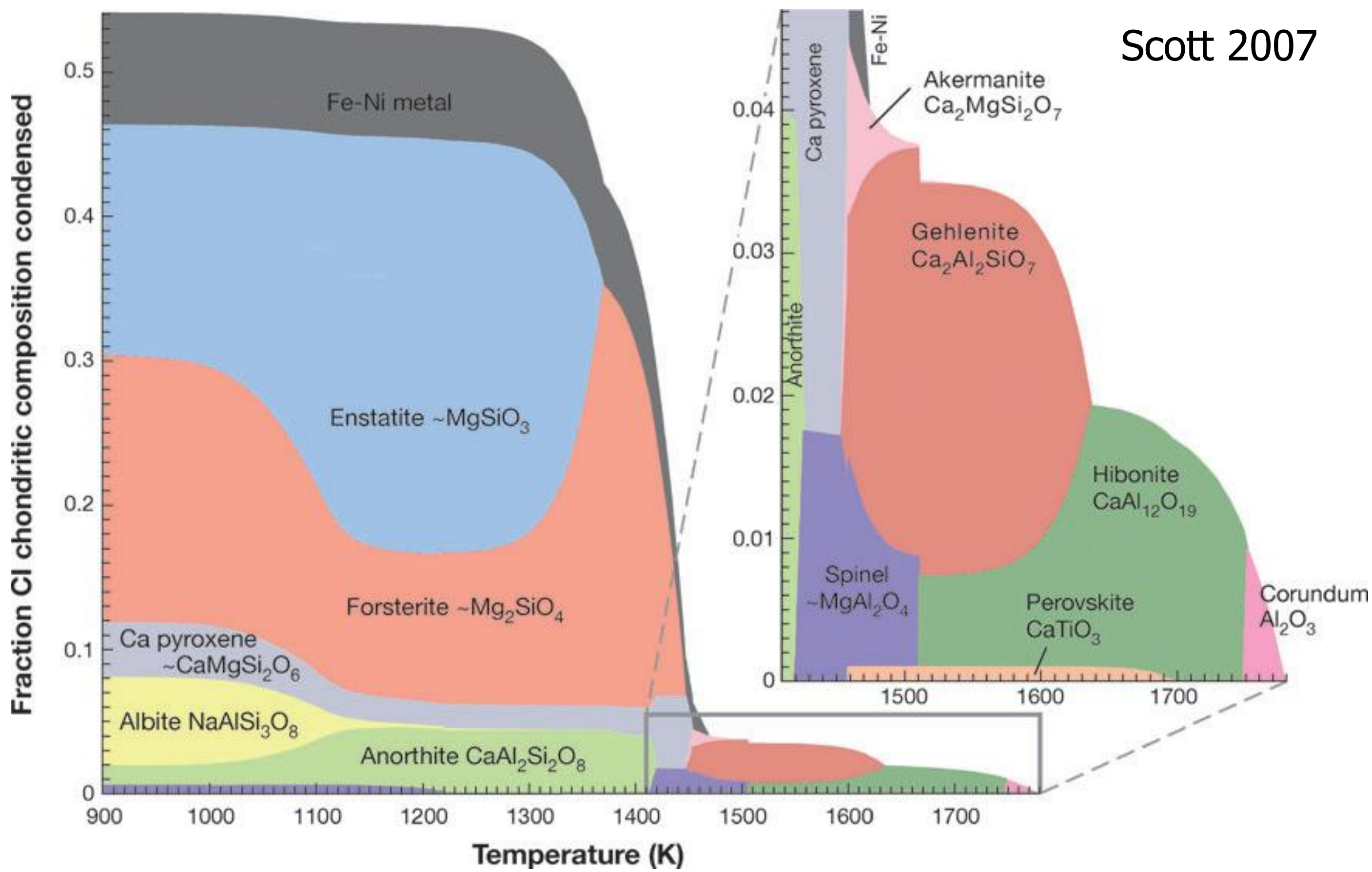

III. The formation of planets and planetary systems

b. Dust to planetesimals

iv. Dust-aggregate velocities in the solar nebula

- ▷ Brownian motion (Weidenschilling 1984)
- ▷ Vertical sedimentation, radial drift, azimuthal velocity differences (Weidenschilling 1984)
- ▷ Gas turbulence (magneto-rotational instability or self-induced) (Balbus & Hawley 1991; Johansen et al. 2006; Weidenschilling 1980; Sekiya 1998)

Motion of protoplanetary dust

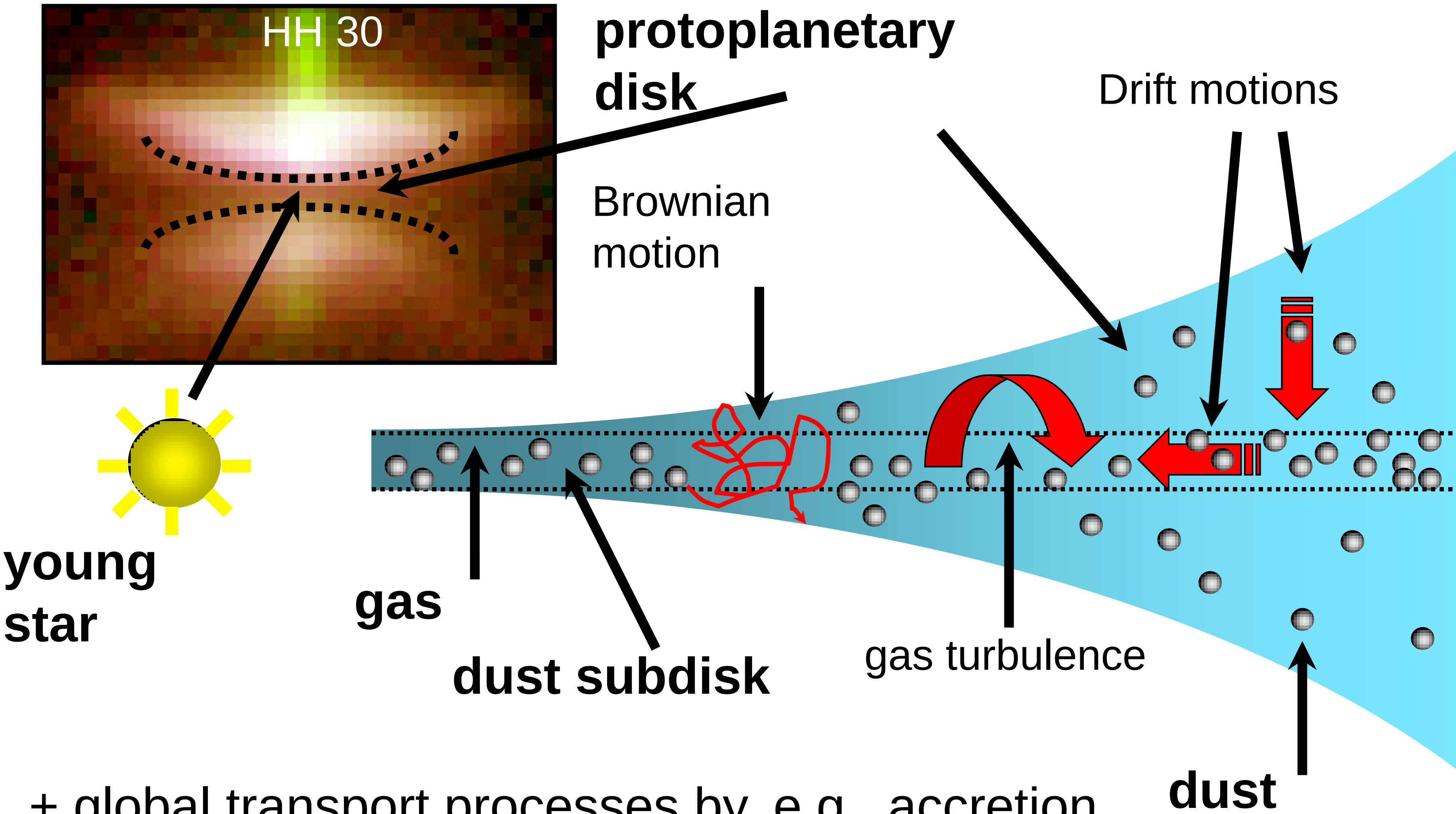

+ global transport processes by, e.g., accretion, turbulence, X-wind, photophoresis, …

Weidenschilling 1977

$$\Sigma_s(r) = 1700\ \mathrm{g/cm}^2 \cdot \left(\frac{r}{1\,\mathrm{AU}}\right)^{-3/2}$$

Critical velocity of 1 m/s reached for 5-cm particles

Andrews & Williams 2007

$$\Sigma_s(r) = 20\ \mathrm{g/cm}^2 \cdot \left(\frac{r}{1\,\mathrm{AU}}\right)^{-0.8}$$

Critical velocity of 1 m/s reached for 4-mm particles

Desch 2007

$$\Sigma_s(r) = 50500\ \mathrm{g/cm}^2 \cdot \left(\frac{r}{1\,\mathrm{AU}}\right)^{-2.17}$$

Critical velocity of 1 m/s reached for >1-m particles

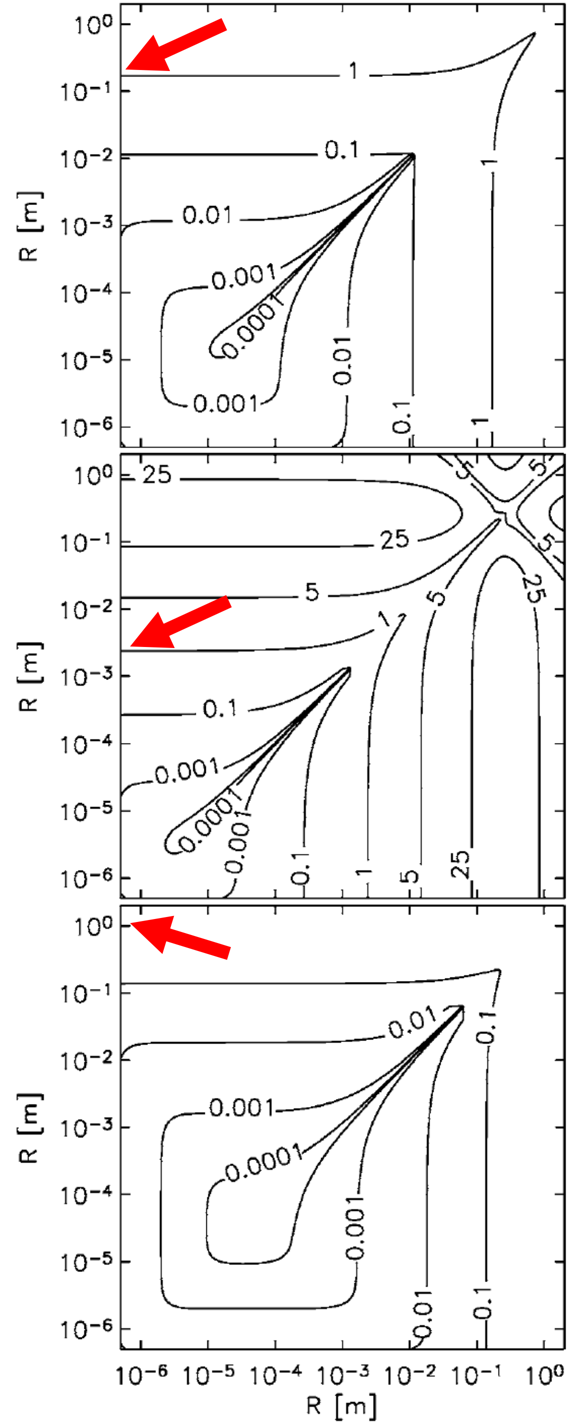

III. The formation of planets and planetary systems

b. Dust to planetesimals

v. Collisional dust growth

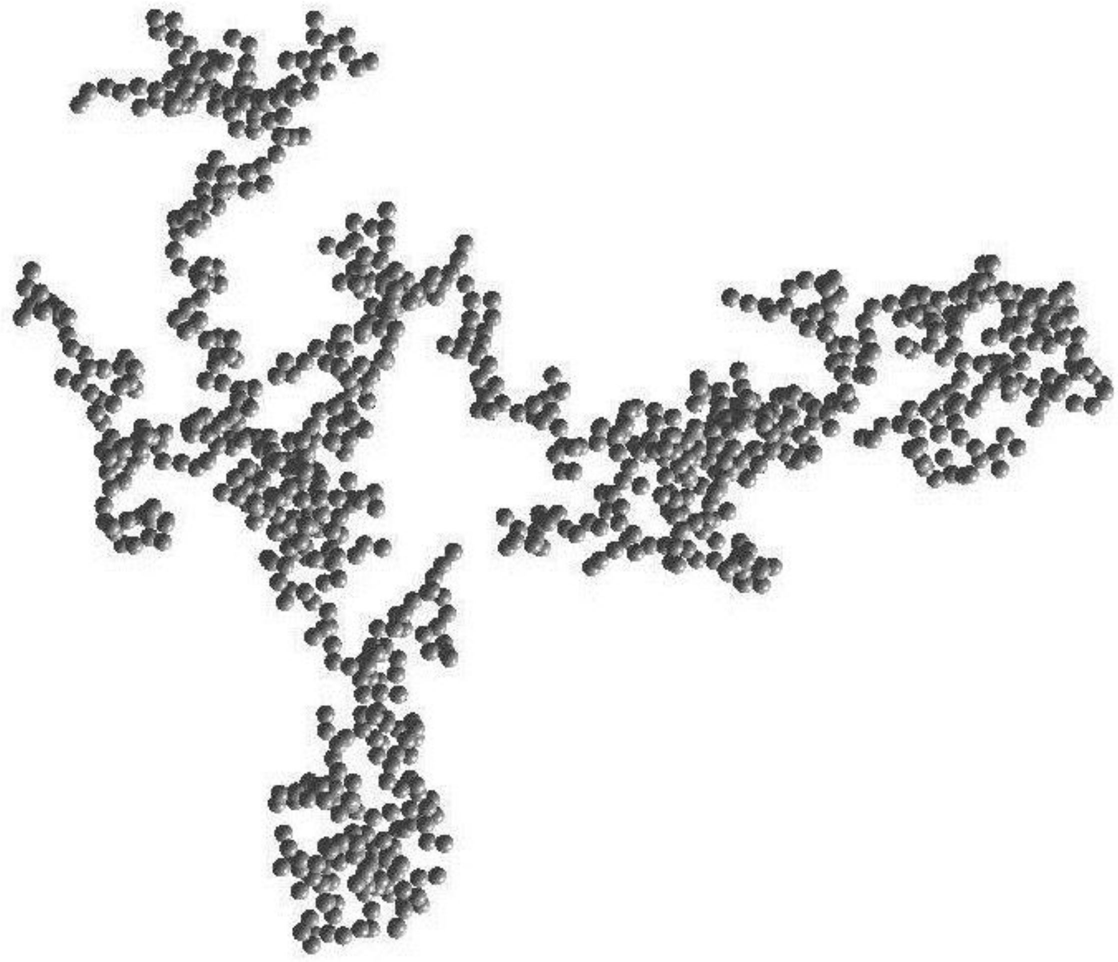

What happens in a collision between two dust particles/aggregates?

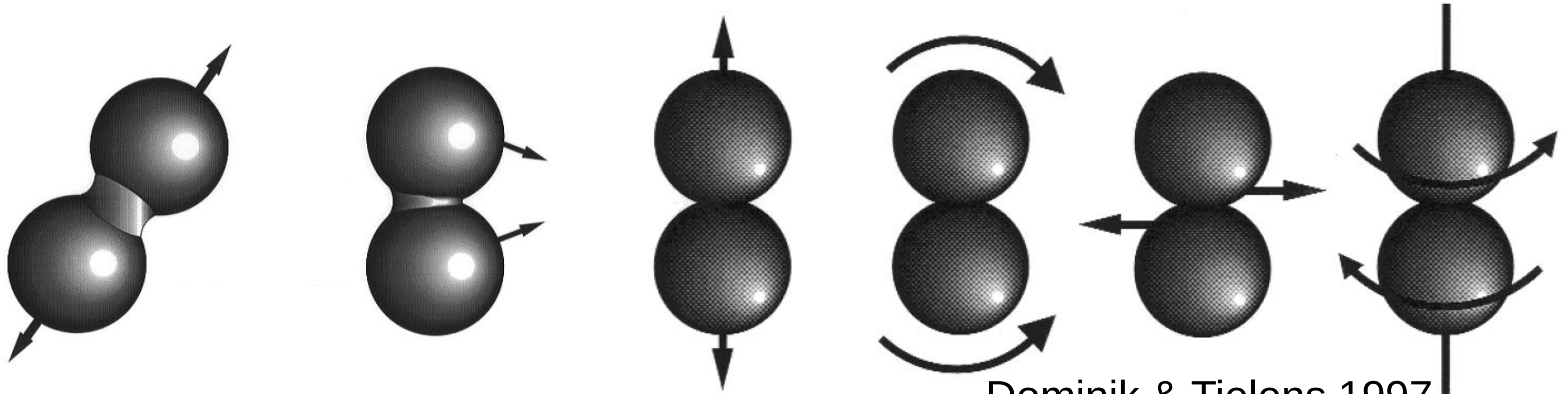

Dominik & Tielens 1997

Adhesion force
(van der Waals force)

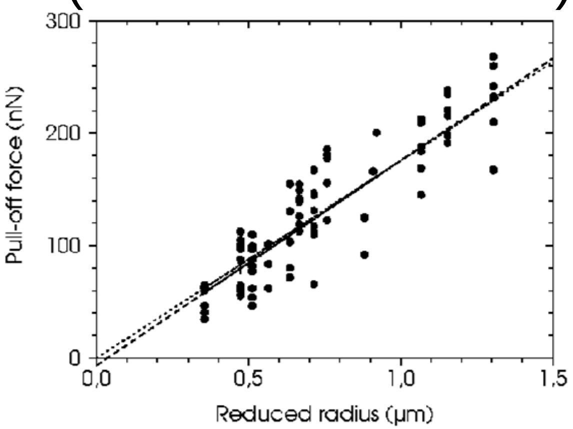

Heim et al. 1999

Threshold velocity
for sticking

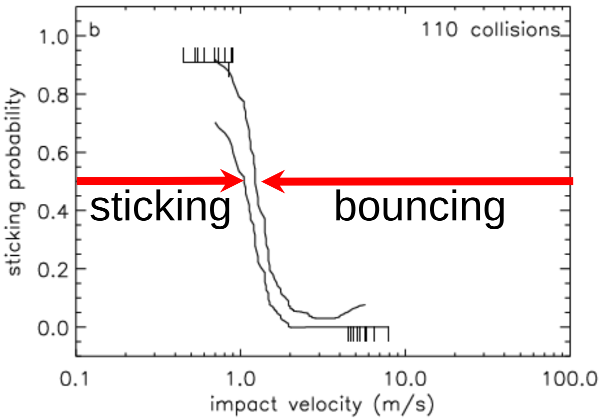

Poppe et al. 2000

Restructuring

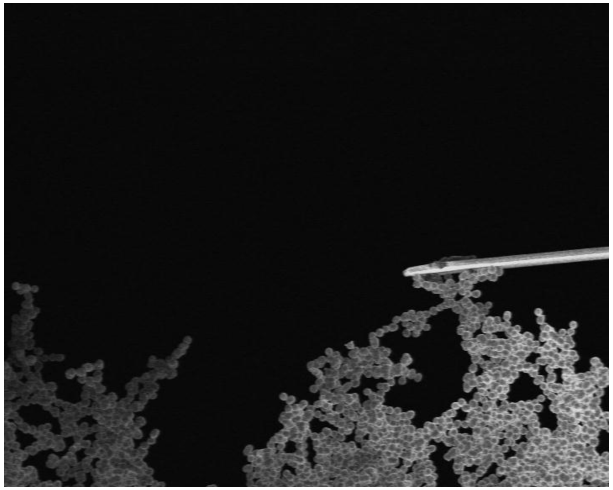

Heim et al. 2005

The importance of the threshold velocity for sticking

- $v_{SG} \approx v_{FR}$
  v_{SG}: threshold velocity for single-grain sticking
  v_{FR}: threshold velocity for dust-aggregate fragmentation.
- The threshold velocity for dust sticking is dependent on the monomer size.

Single-grain collisions

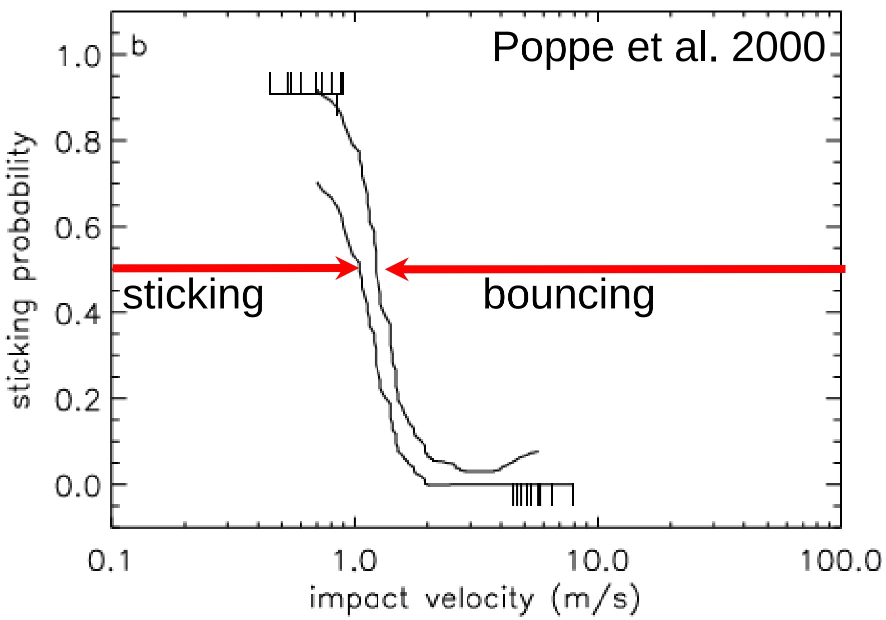

Dust-aggregate collisions

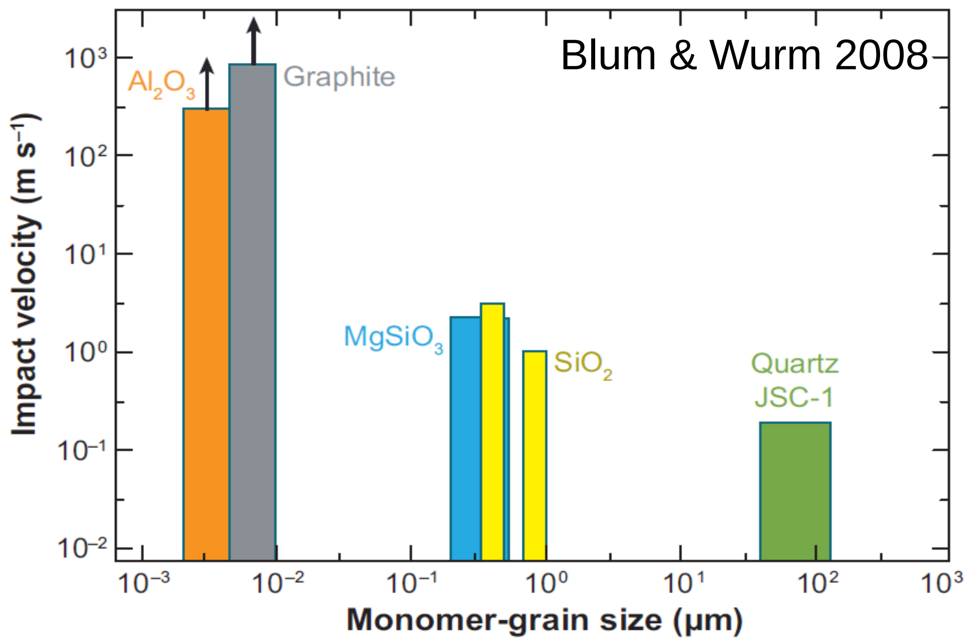

How does dust agglomeration start? The initial growth phase

PRINCIPLE

Start with monomers at $t_0 = 0$

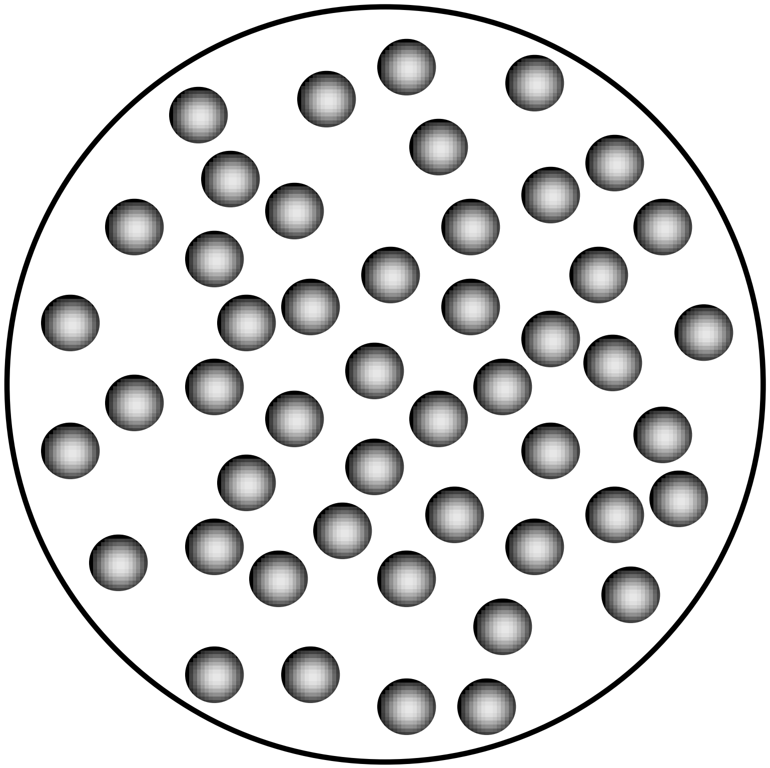

Relative velocities due to Brownian motion, drift, gas turbulence

Observe aggregate mass (distribution) and structure at $t > t_0$

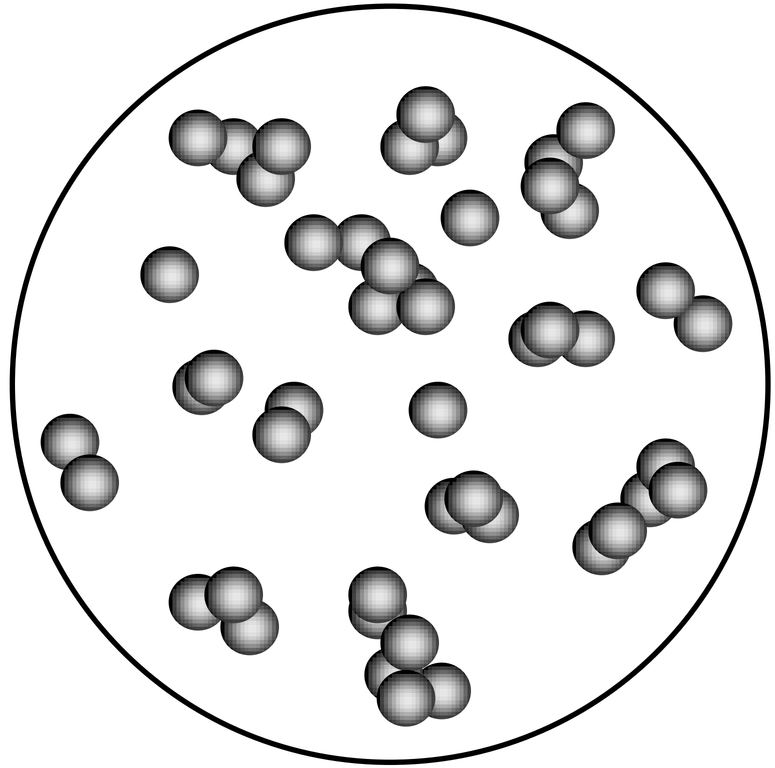

Consider the simplest cases

BPCA	BCCA
Ballistic Particle-Cluster Agglomeration	Ballistic Cluster-Cluster Agglomeration
⇓	⇓
ballistic hit-and-stick impacts of single dust particles into growing dust agglomerate	ballistic hit-and-stick collisions between equal-mass dust agglomerates

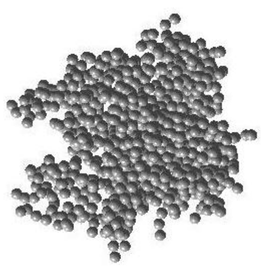

i = 1,024

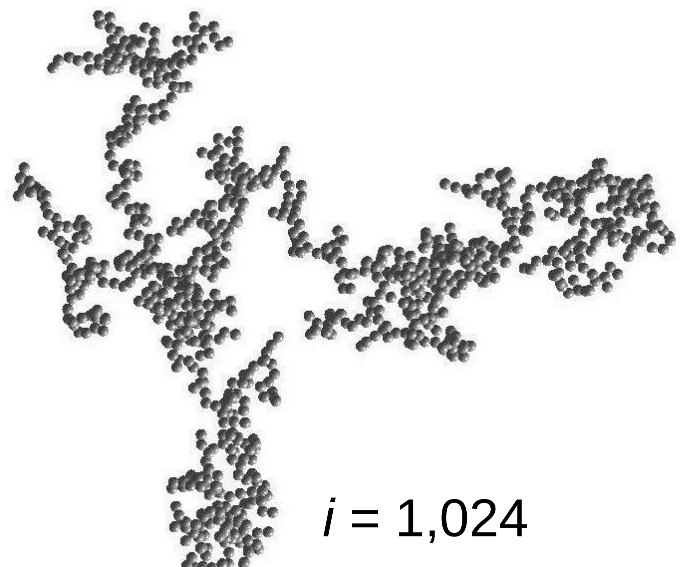

i = 1,024

BPCA

N=2

BPCA

N=4

BPCA

N=8

<u>BPCA</u>
N=16

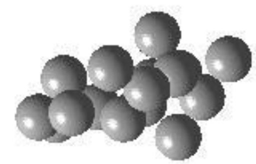

BPCA

N=32

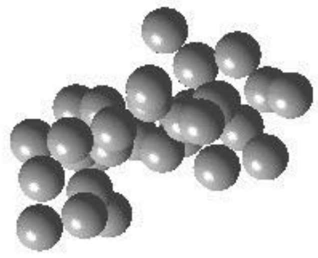

BPCA

N=64

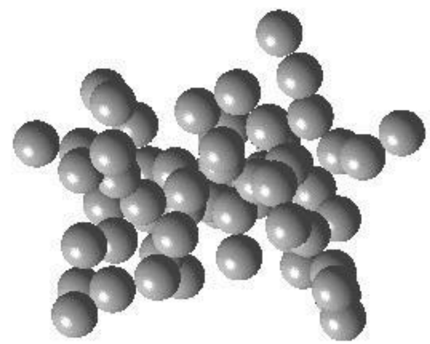

BPCA

N=128

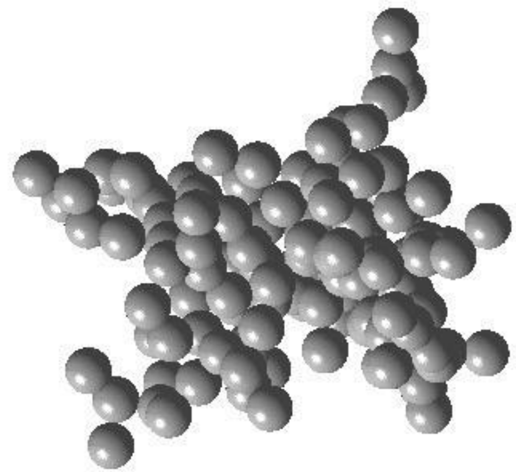

BPCA

N=256

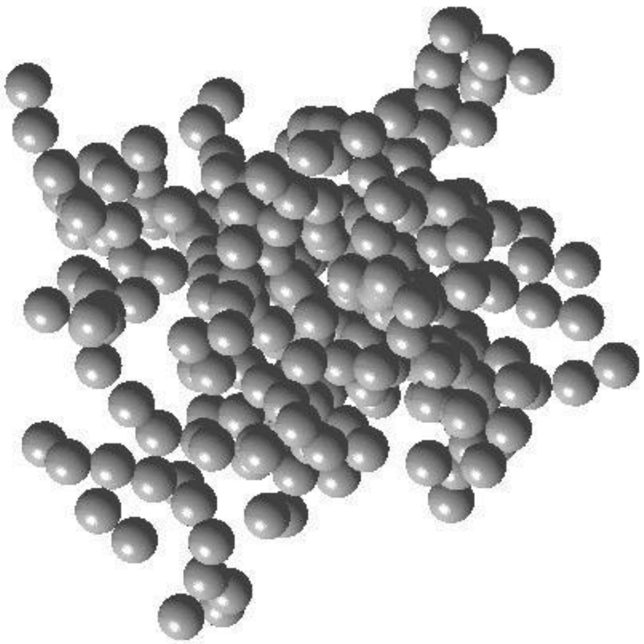

<u>BPCA</u>
N=512

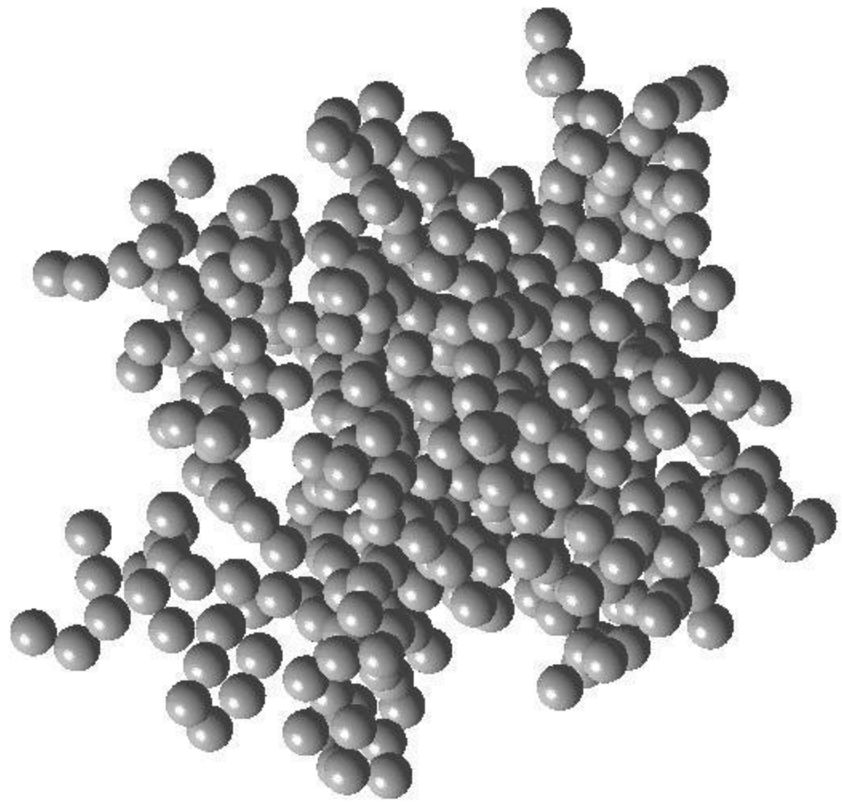

BPCA
N=1024

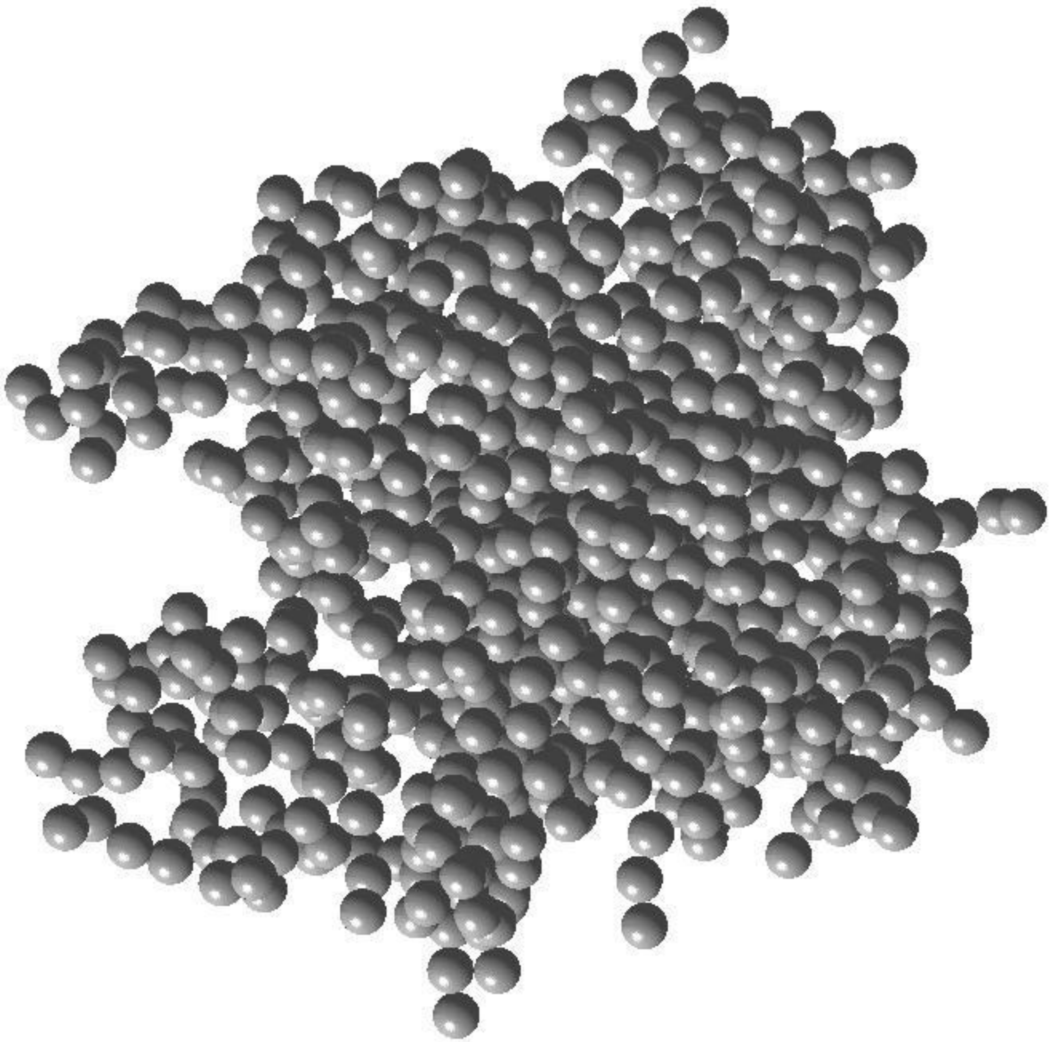

BCCA

N=2

BCCA

N=4

BCCA

N=8

BCCA

N=16

BCCA

N=32

BCCA

N=64

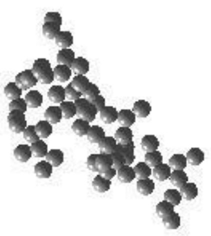

BCCA

N=128

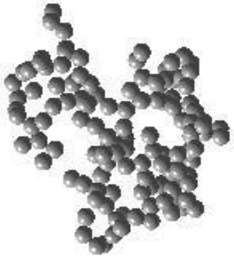

BCCA

N=256

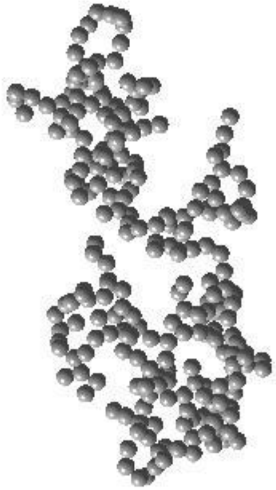

BCCA

N=512

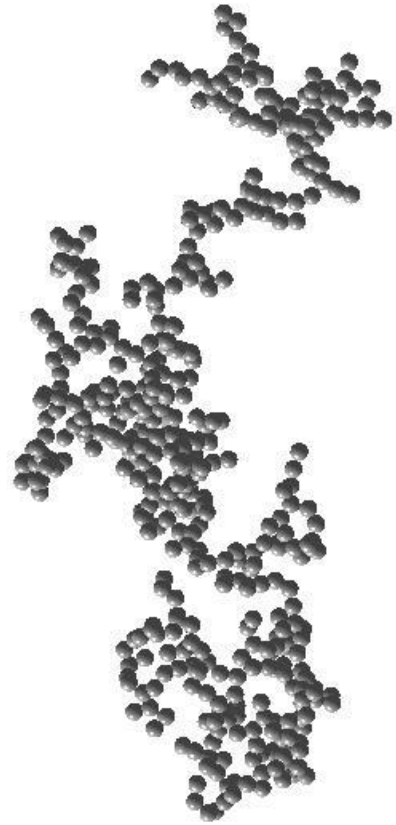

BCCA

N=1024

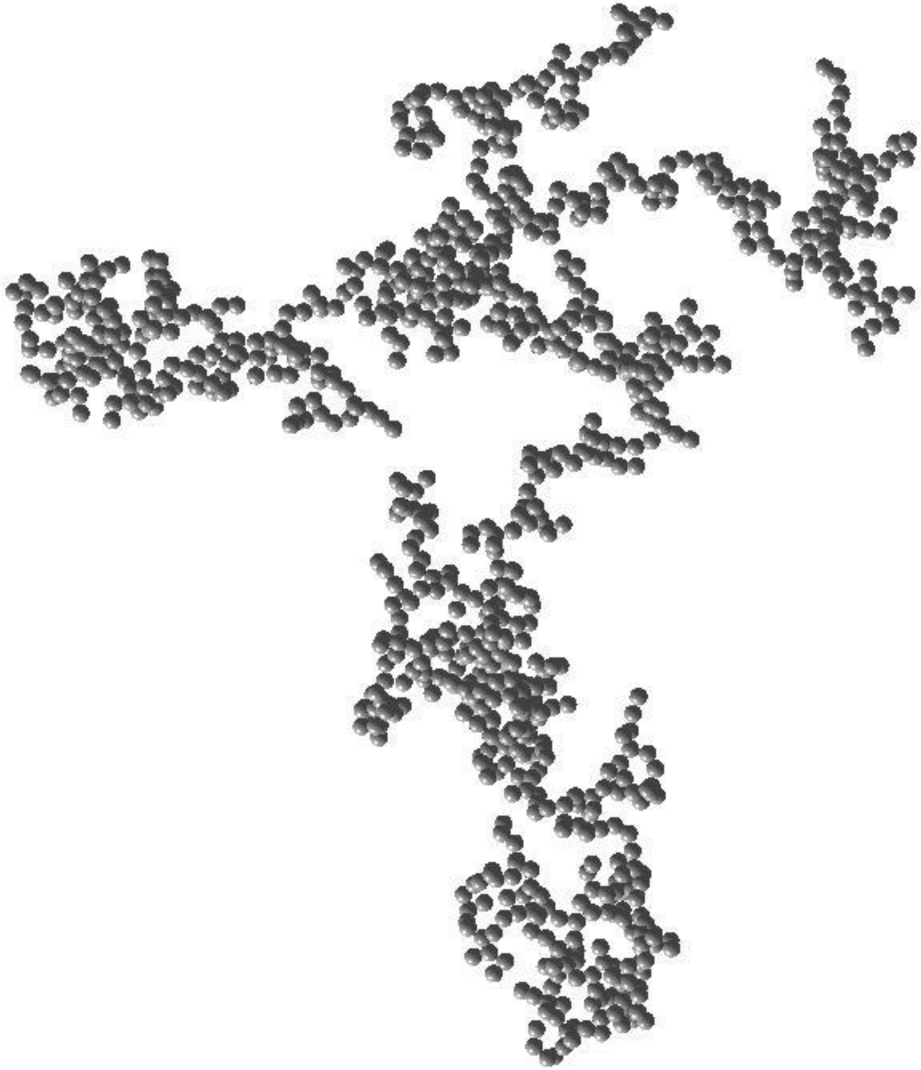

Consider the simplest cases

BPCA	BCCA
Ballistic Particle-Cluster Agglomeration	Ballistic Cluster-Cluster Agglomeration
⇓	⇓
ballistic hit-and-stick impacts of single dust particles into growing dust agglomerate	ballistic hit-and-stick collisions between equal-mass dust agglomerates

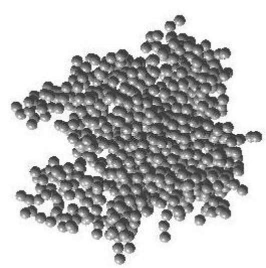

i = 1,024

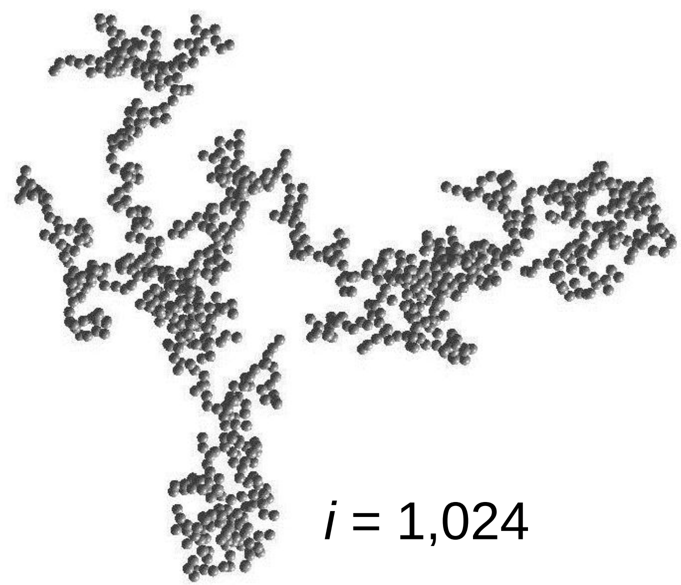

i = 1,024

The initial growth phase

E X P E R I M E N T S

Gas turbulence

Wurm & Blum 1998

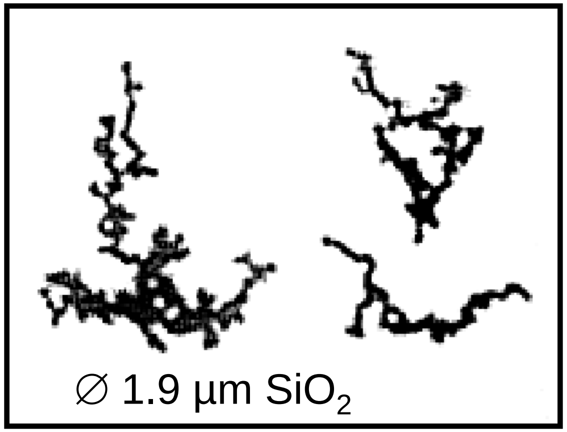

Differential sedimentation

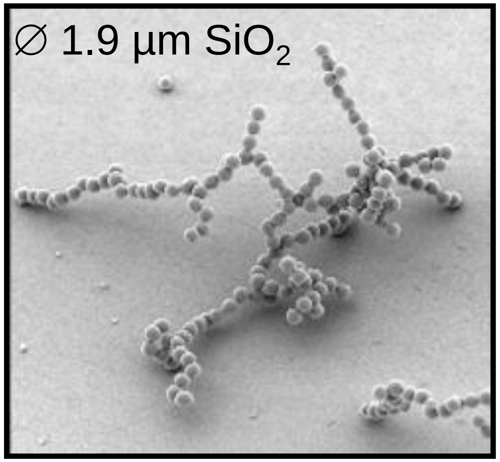

Blum et al. 1998

Brownian motion

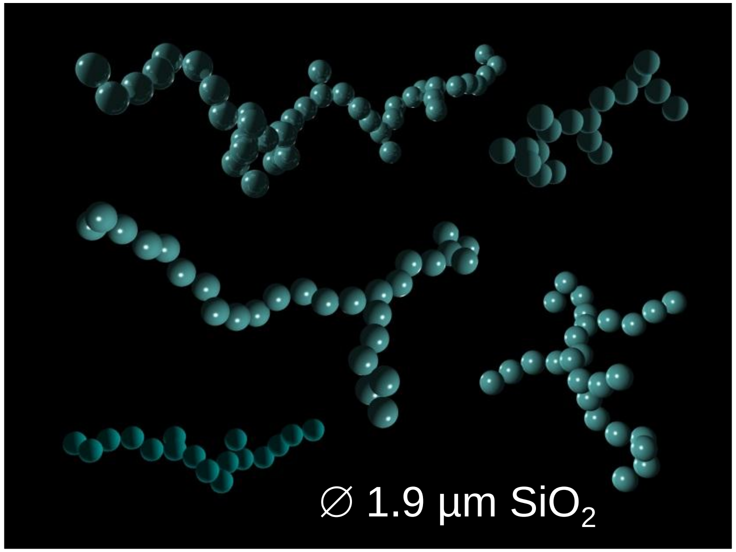

Blum et al. 2000

The initial growth phase

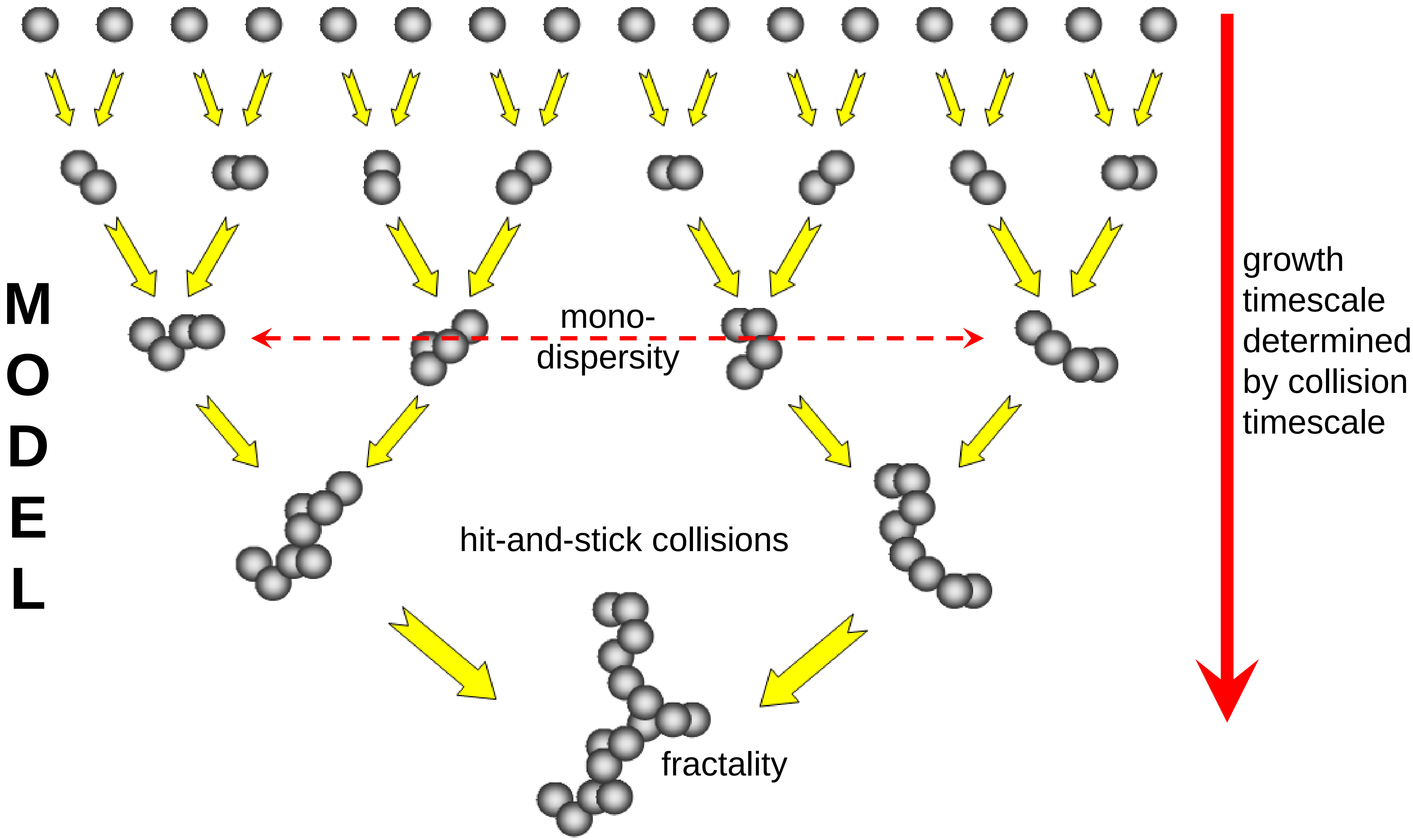

The initial growth phase

E X P E R I M E N T S

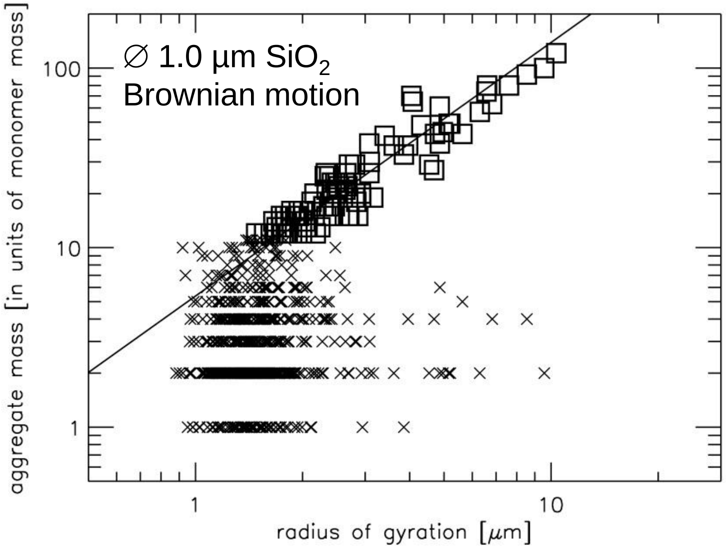

- ▷ Hit-and-stick collisions
- ▷ Mass-size relation $m \propto s^D$ with $D \leq 2$ (fractal aggregates)
- ▷ Narrow (quasi-monodisperse) mass spectra
- ▷ Temporal mass growth follows a power law

$$\frac{\bar{m}(t)}{m_0} = \left[(1-\gamma)\left(a\frac{t}{\tau} + c \right) \right]^{1/1-\gamma}$$

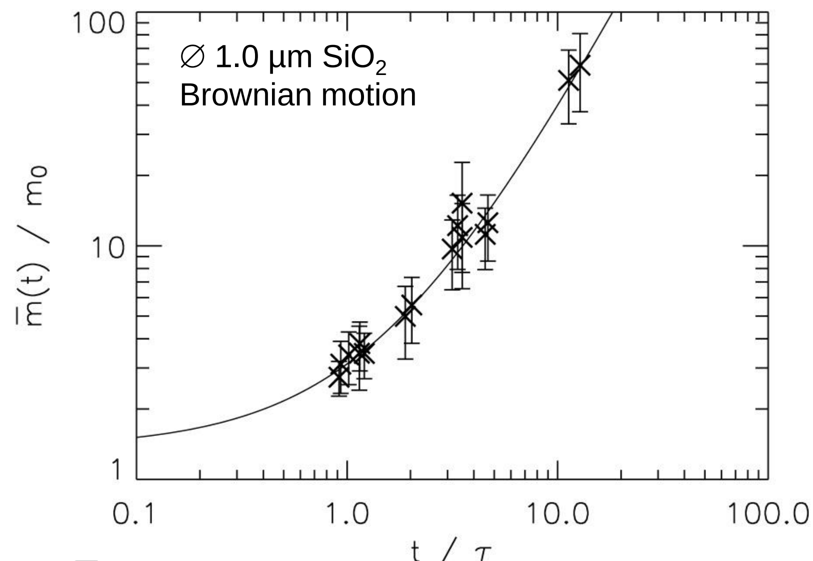

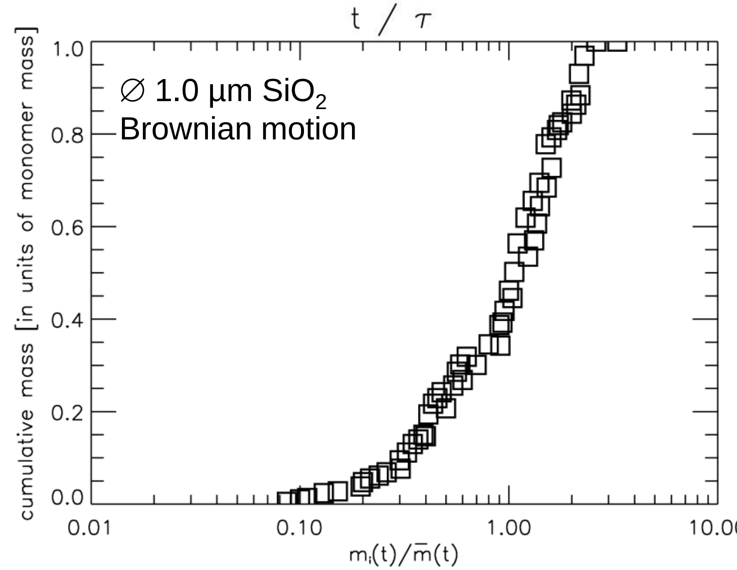

Krause & Blum 2004

The initial growth phase

SIMULATION

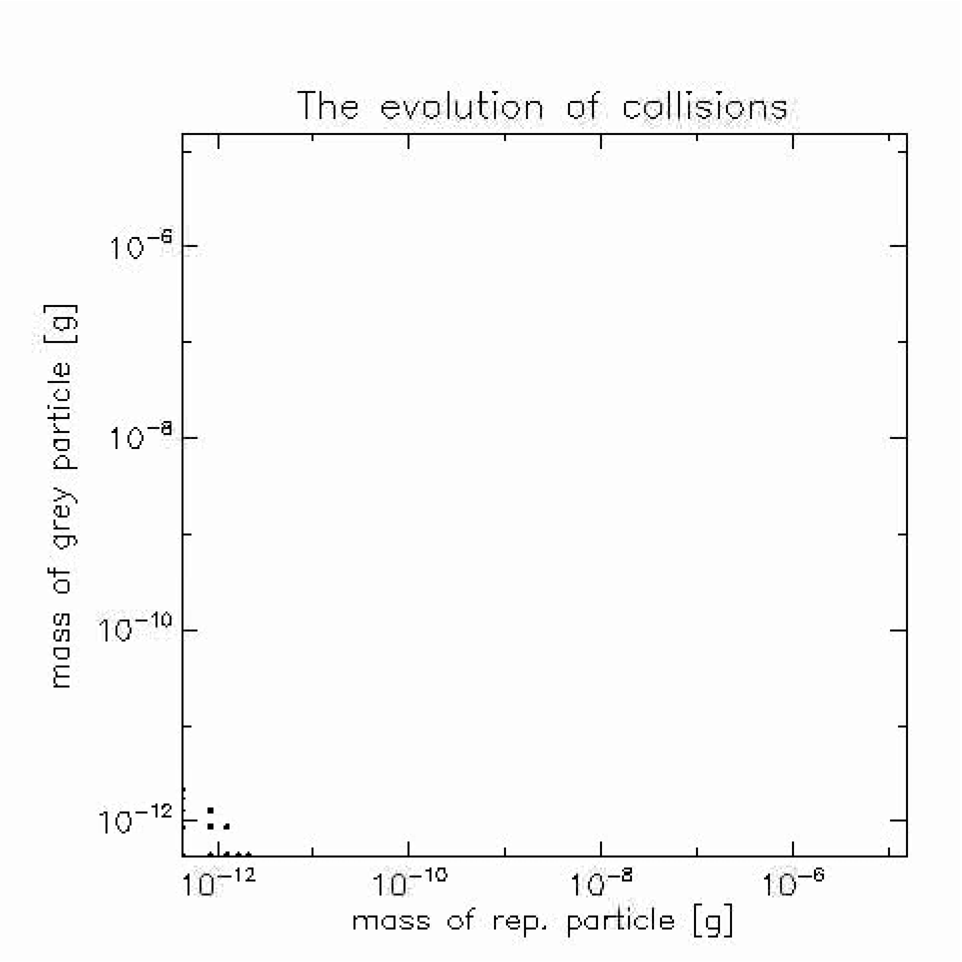

© Andras Zsom, MPIA Heidelberg

- ▷ "Minimum Mass Solar Nebula" model
- ▷ Hit-and-stick collisions
- ▷ Brownian motion + turbulence
- ▷ t = 0…30 yrs

The restructuring/compaction growth regime

Low impact energy: hit-and-stick collisions

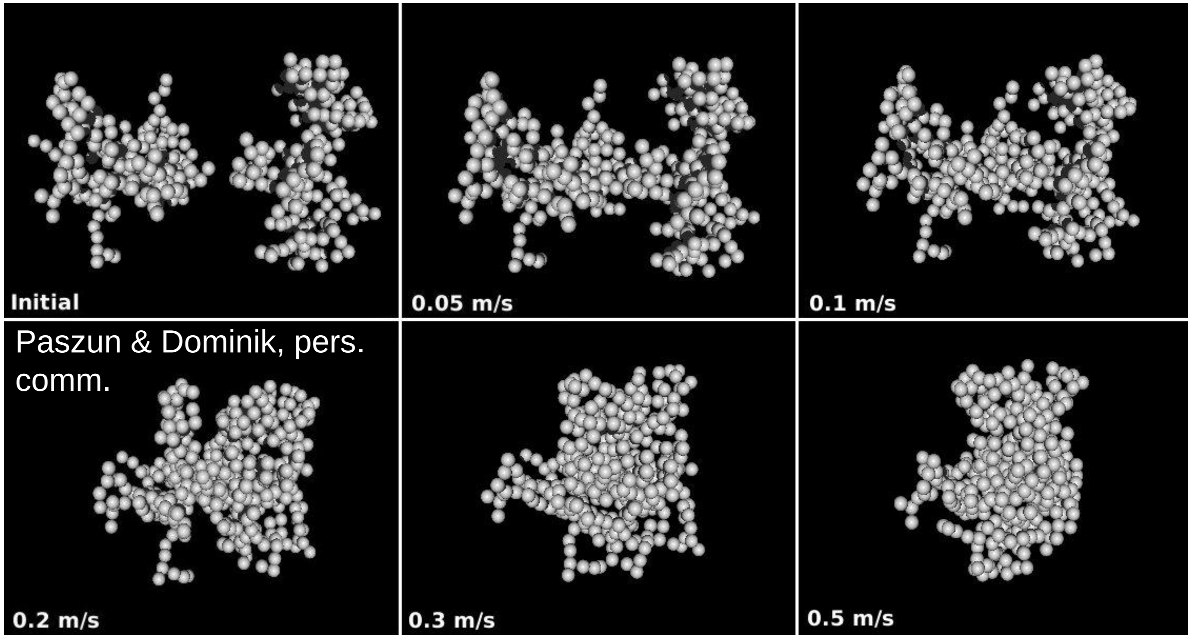

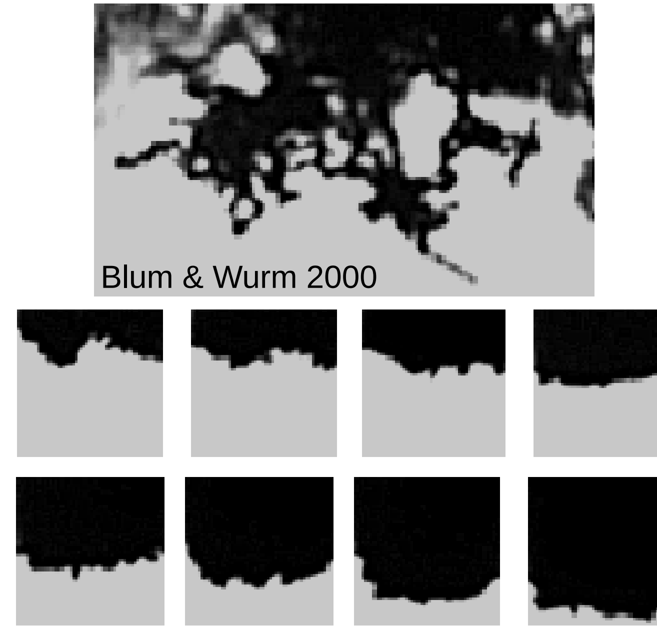

Intermediate impact energy: compaction

- ▷ Collisions result in sticking.
- ▷ Impact energy exceeds energy to overcome rolling friction
  (Dominik and Tielens 1997; Wada et al. 2007).
- ▷ Dust aggregates become non-fractal (?) but are still highly porous.

Overview of possible collisional outcomes

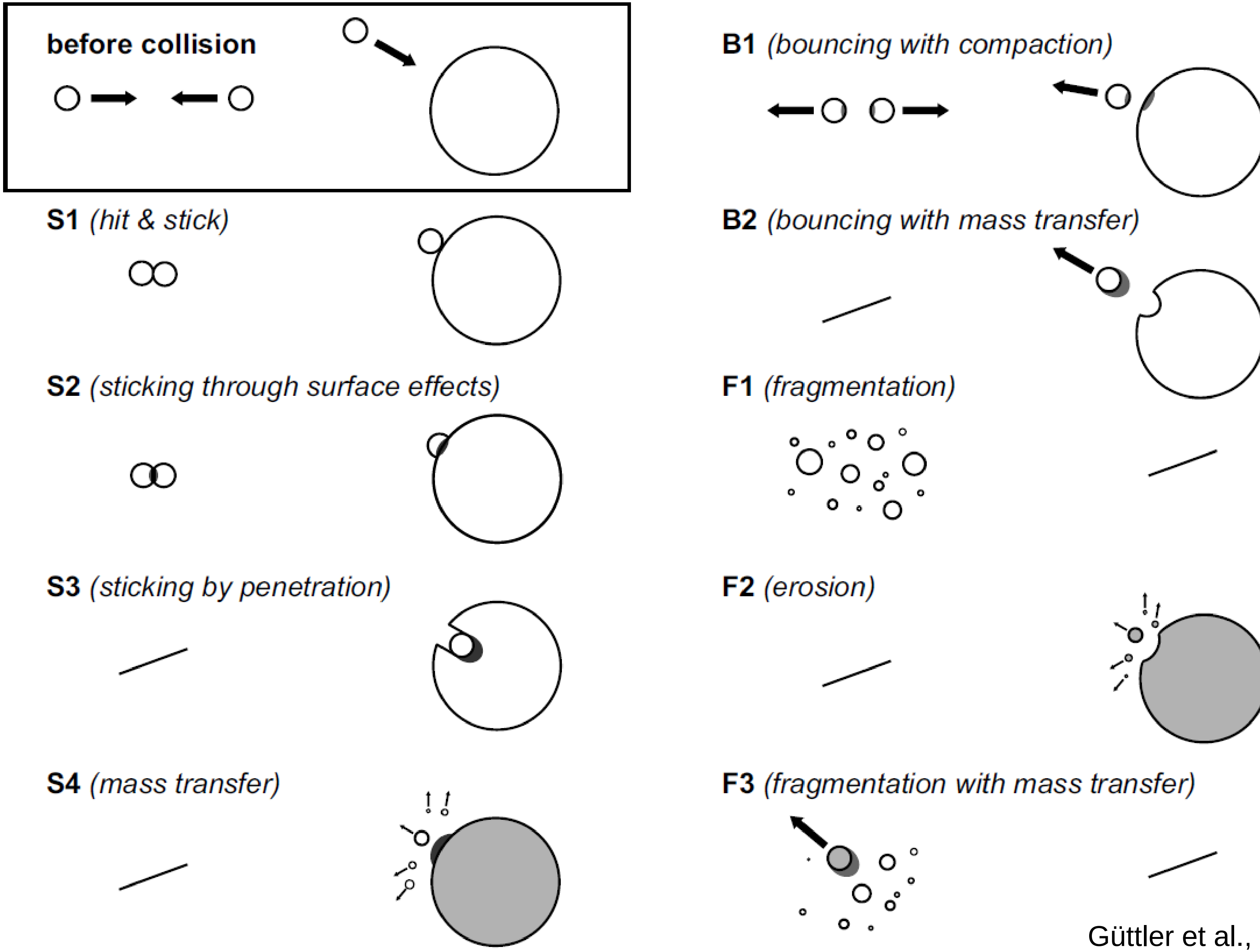

Güttler et al., 2010

A simplified collision model for dust aggregates

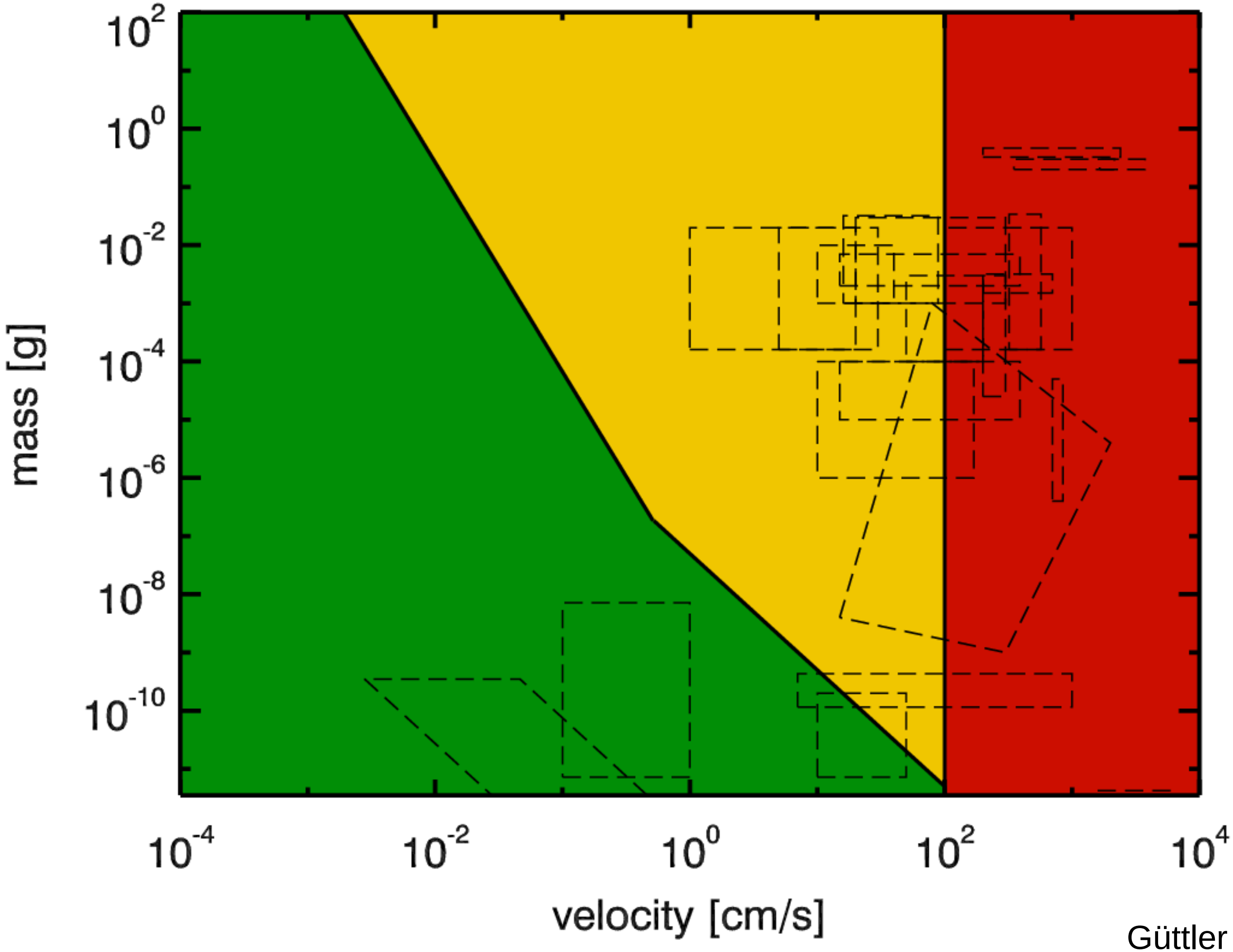

Güttler et al., 2010

The Full Collision Model

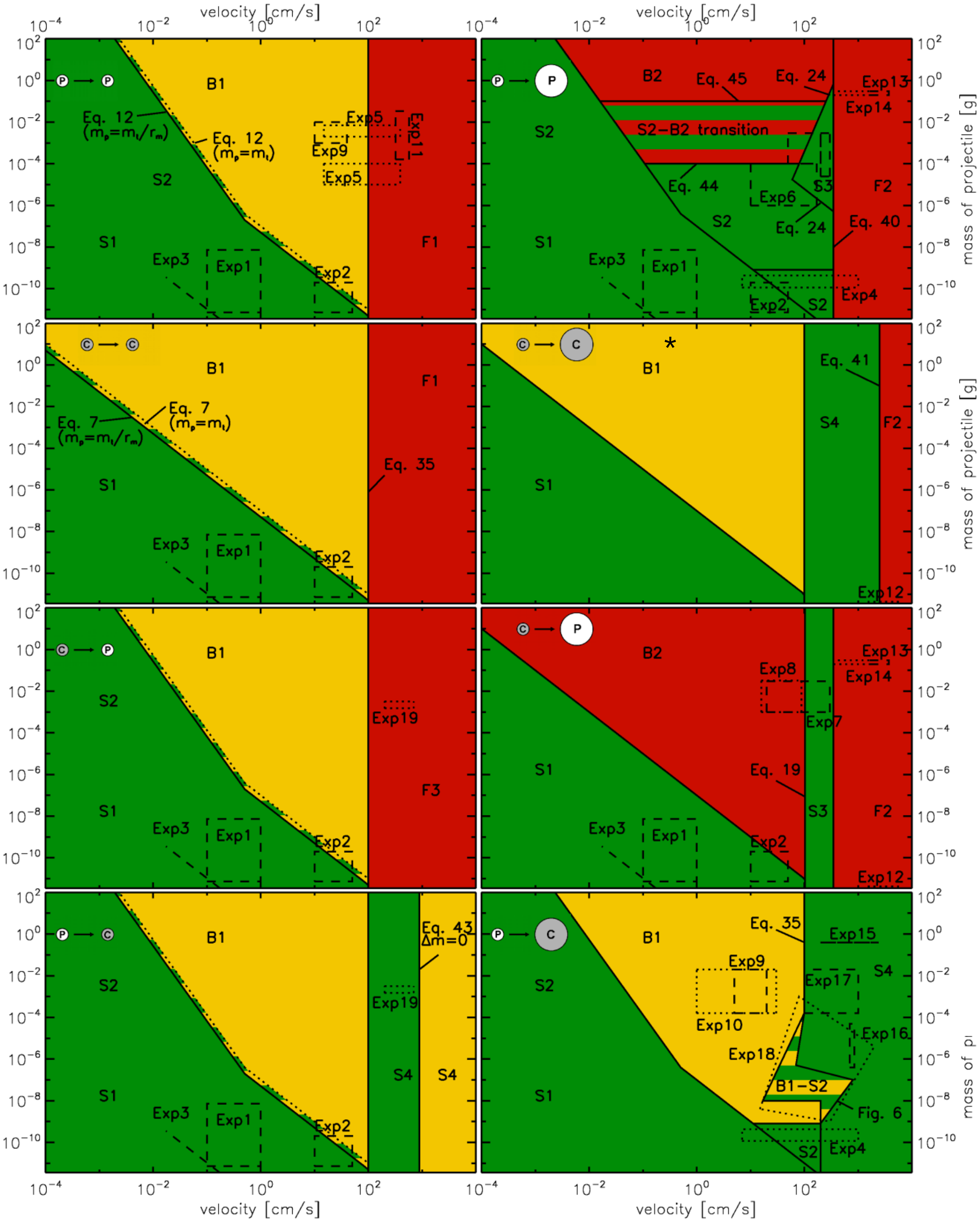

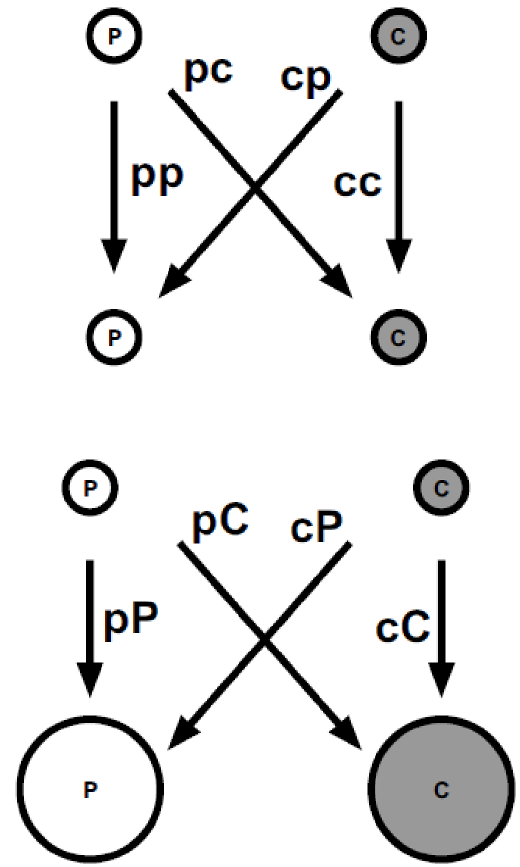

* pc ≠ cp

Güttler et al., 2010

A simplified collision model for dust aggregates

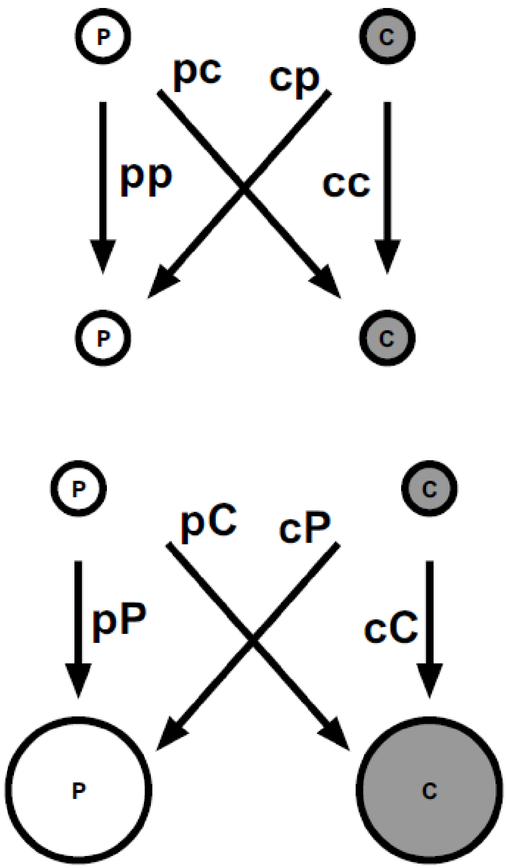

Güttler et al., 2010

- The current model has a binary nature
- No smooth transition in porosity and mass ratio
- Critical mass ratio of r_m=100
- Critical porosity of ϕ_c=0.4

An experiment to determine the sticking threshold for dust aggregates

Weidling et al. 2011

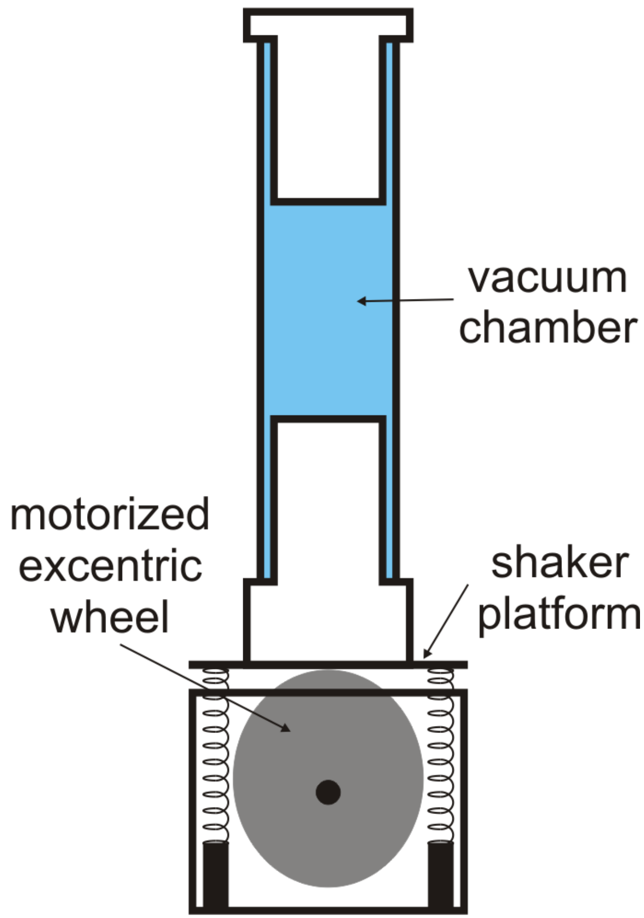

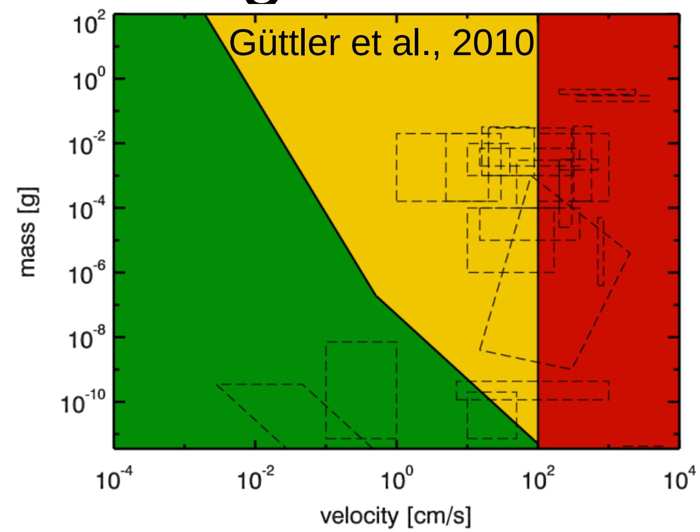

- Microgravity experiment (drop tower, suborbital flight)
- Particle diameter: 0.5-1.5 mm
- Initial velocity ~0.1m/s
- Collisional cooling down to mm/s

Example: bouncing collision

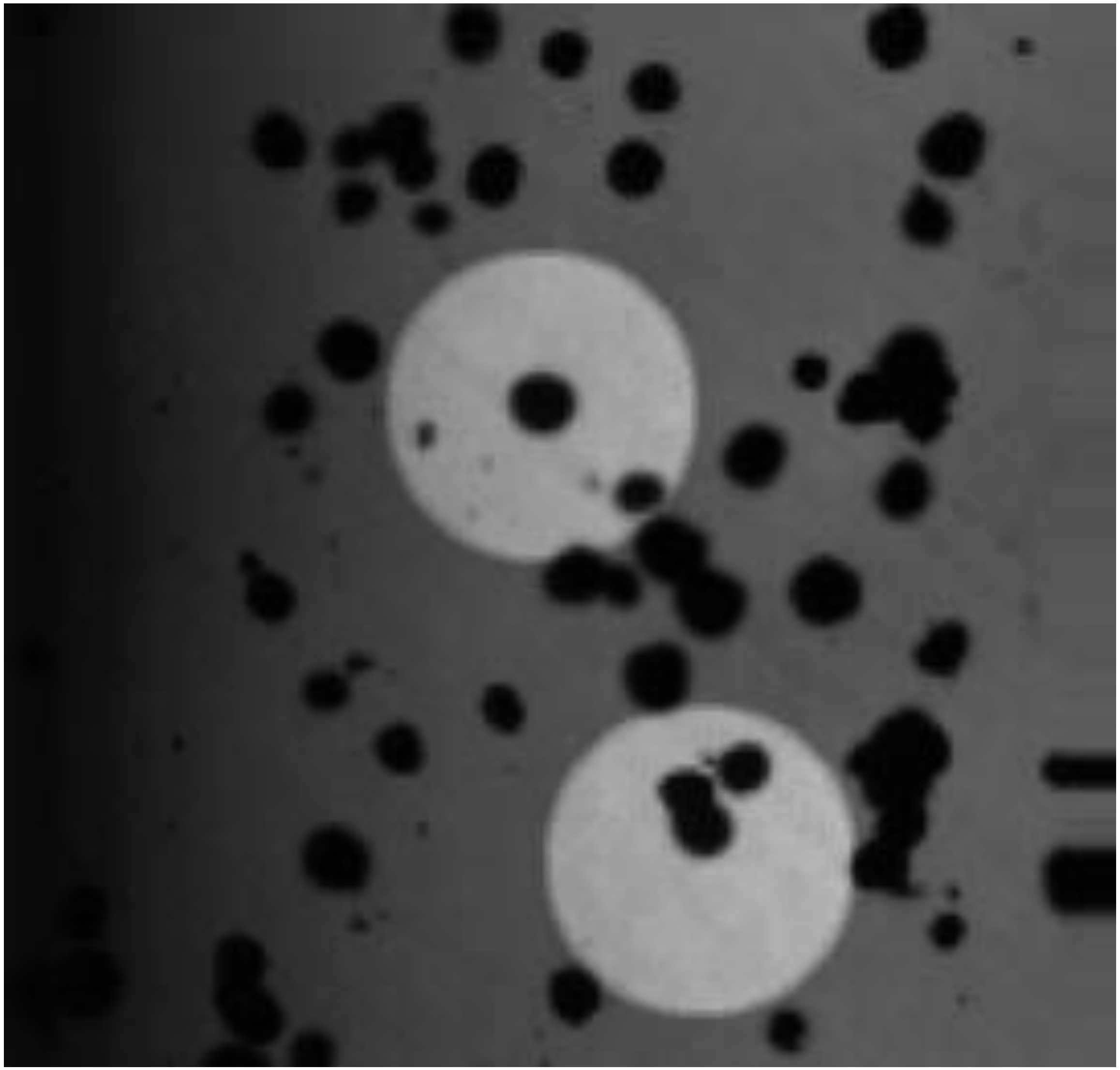

Bouncing collision

v = 12 mm/s

Dust-aggregate size:
0.5-1.5 mm

particle diameter: 1 mm
filling factor: 40%

<u>47 analyzed collisions:</u>
- 6x sticking
- 40x bouncing
- 1x fragmentation

Weidling et al. 2011

Example: sticking collision

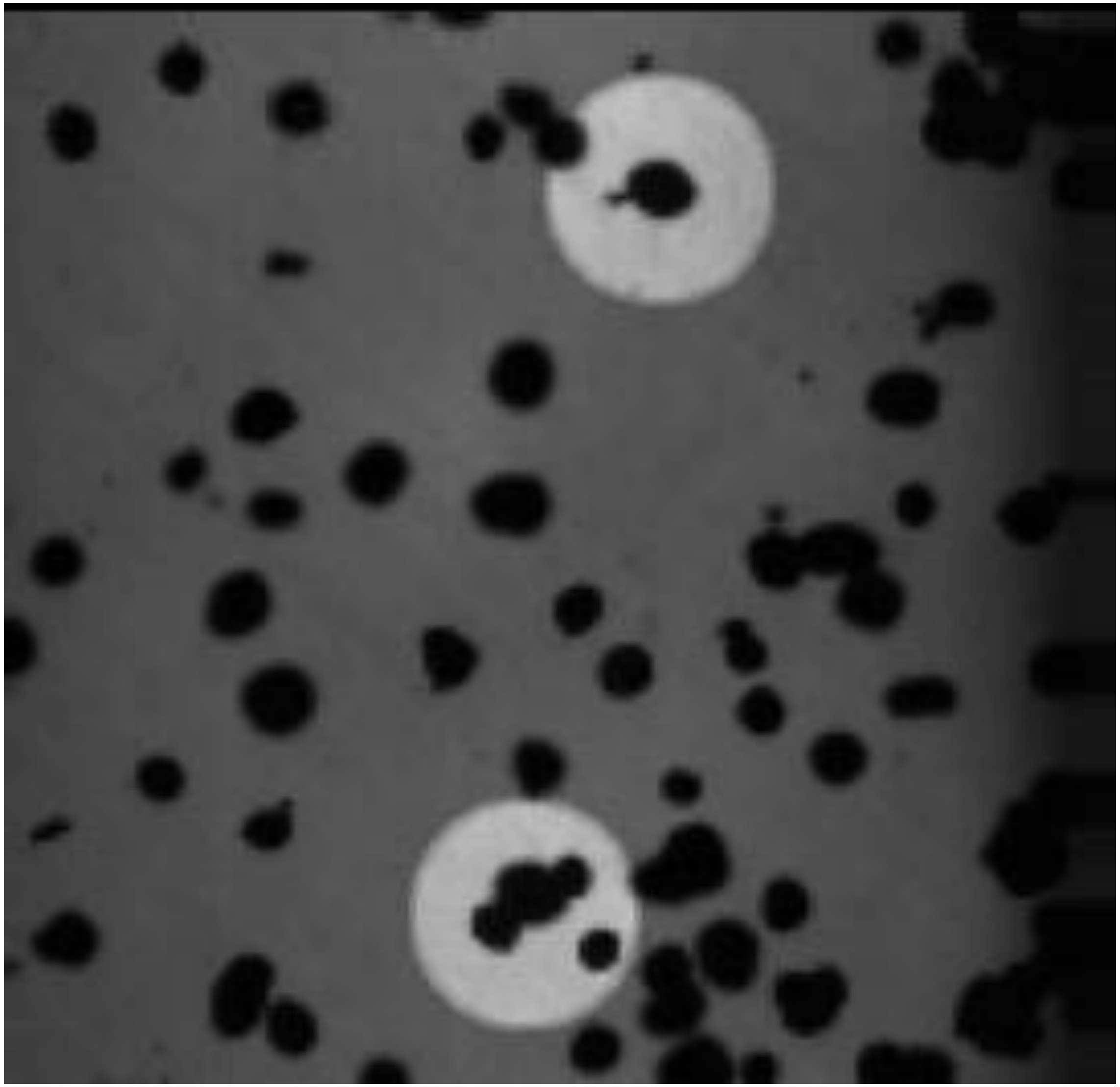

Sticking collision

v = 9 mm/s

Dust-aggregate size:
0.5-1.5 mm

particle diameter: 1 mm
filling factor: 40%

<u>47 analyzed collisions:</u>
- 6x sticking
- 40x bouncing
- 1x fragmentation

Weidling et al. 2011

Example: multiple sticking collisions

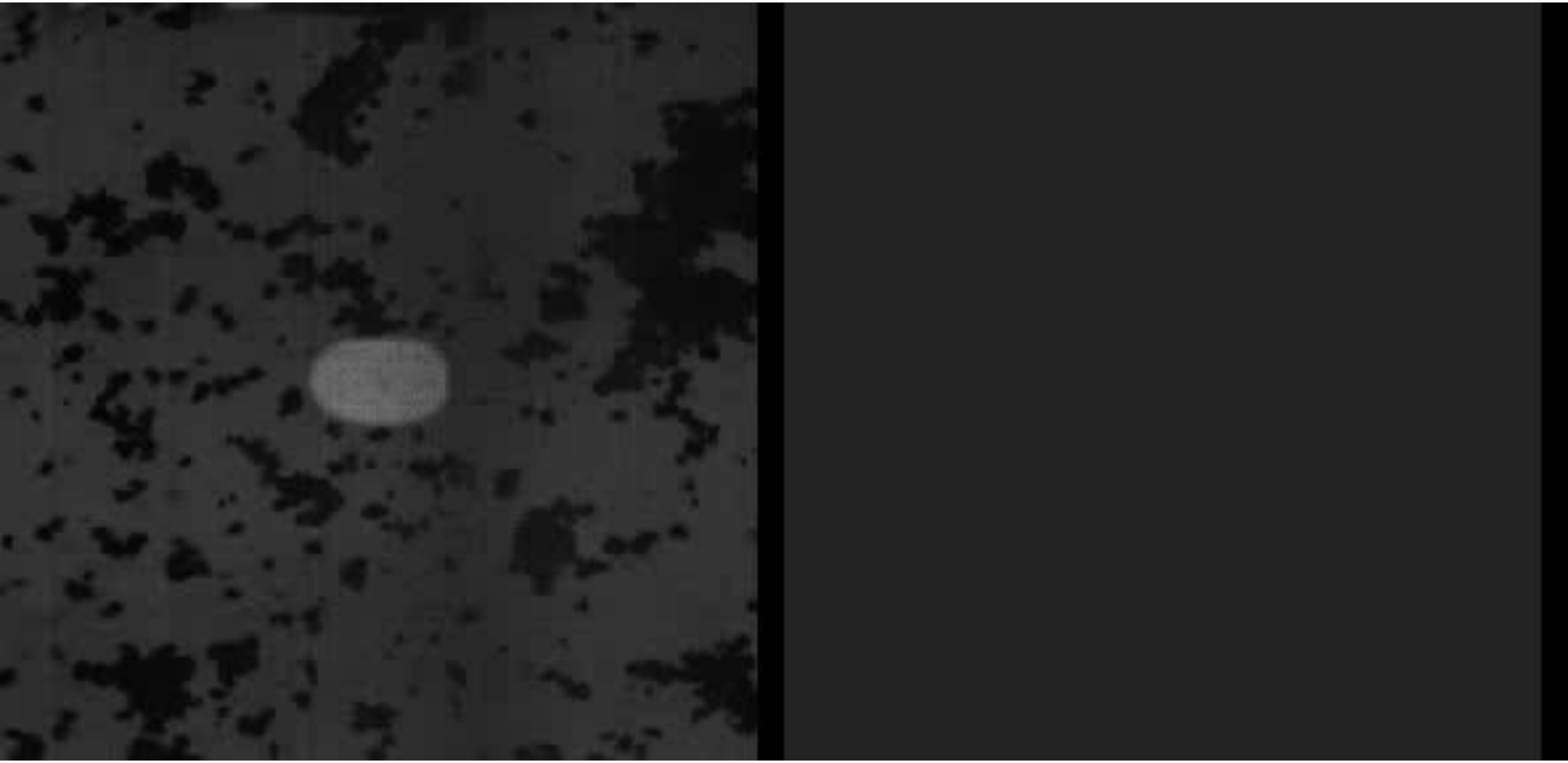

v = 1-10 cm/s; dust-aggregate size: 180 µm

The Braunschweig laboratory drop tower

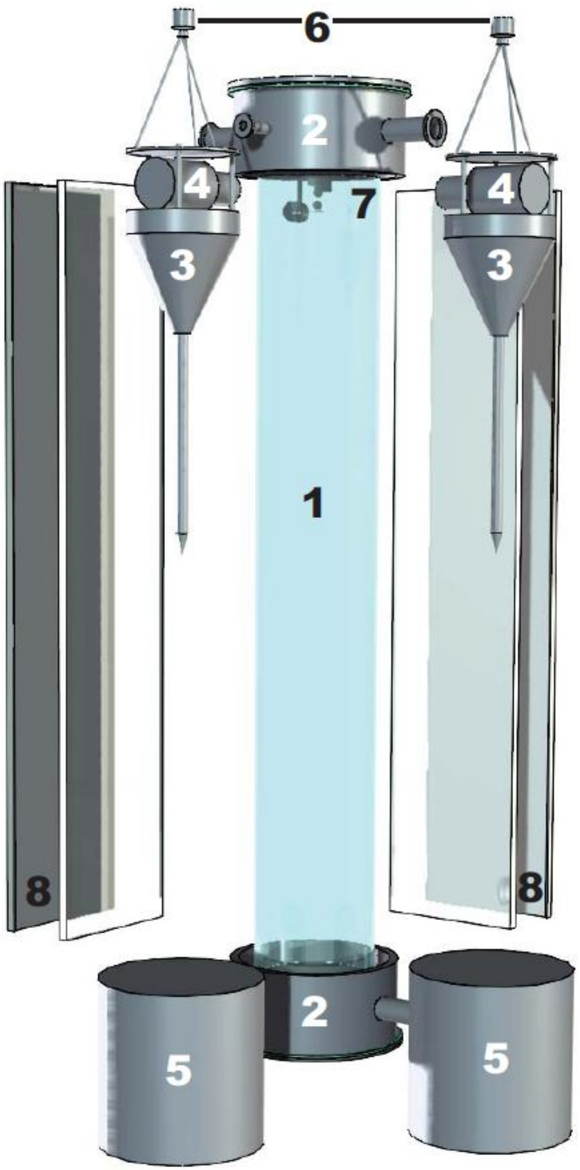

Beitz et al. 2011

- Laboratory drop tower
- Two aggregates collide in free fall
- Two falling cameras, 1.5 m drop height
- Velocities from 1 cm/s to 3 m/s

Low-velocity collisions between large dust aggregates

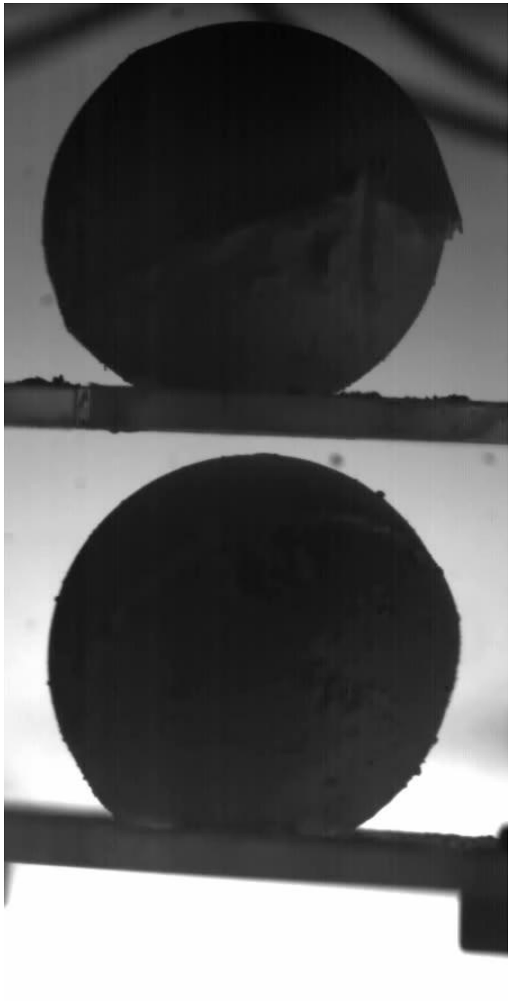

2 cm diameter, 50% filling factor, velocity: 10 mm/s

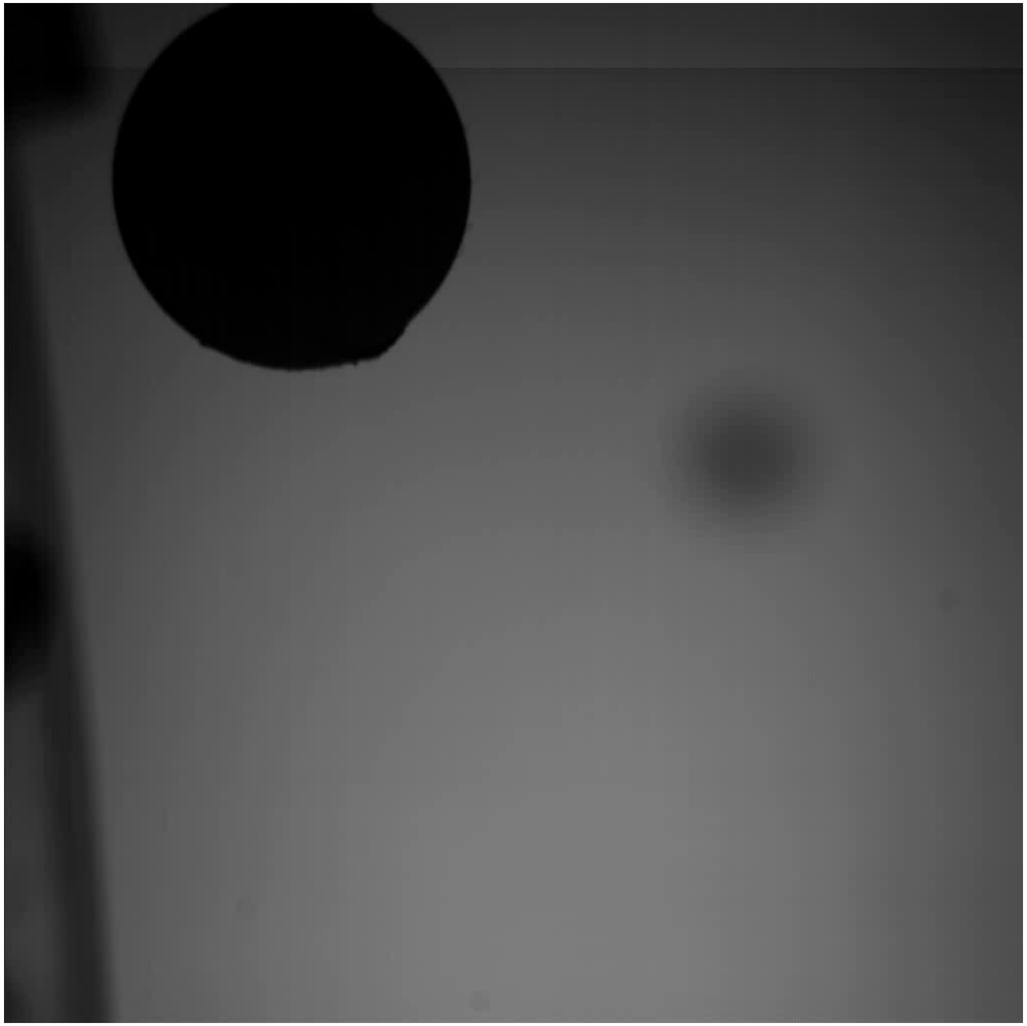

2 cm diameter, 50% filling factor, velocity: 1.8 m/s

Dust-aggregate fragmentation in moderate-velocity collisions

- **Bouncing** for v < 20 cm/s
- **Fragmentation** with mass transfer for v > 20 cm/s

S4 *(mass transfer)*

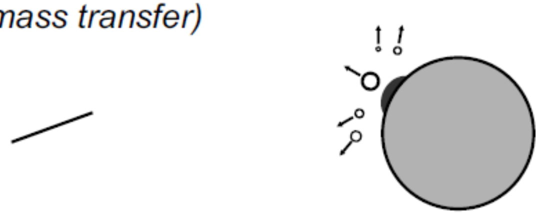

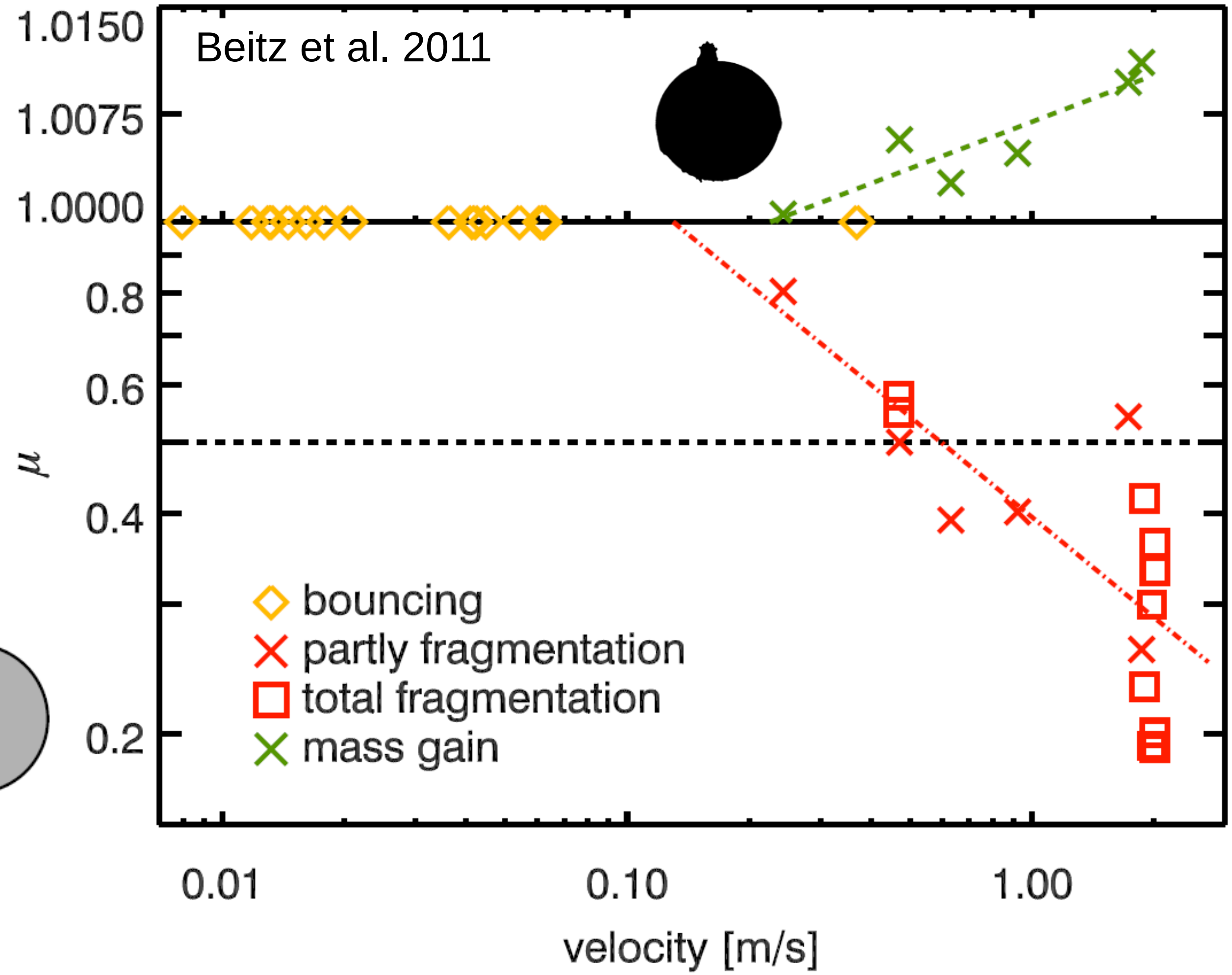

Accretion efficiency in moderate-velocity dust-aggregate collisions

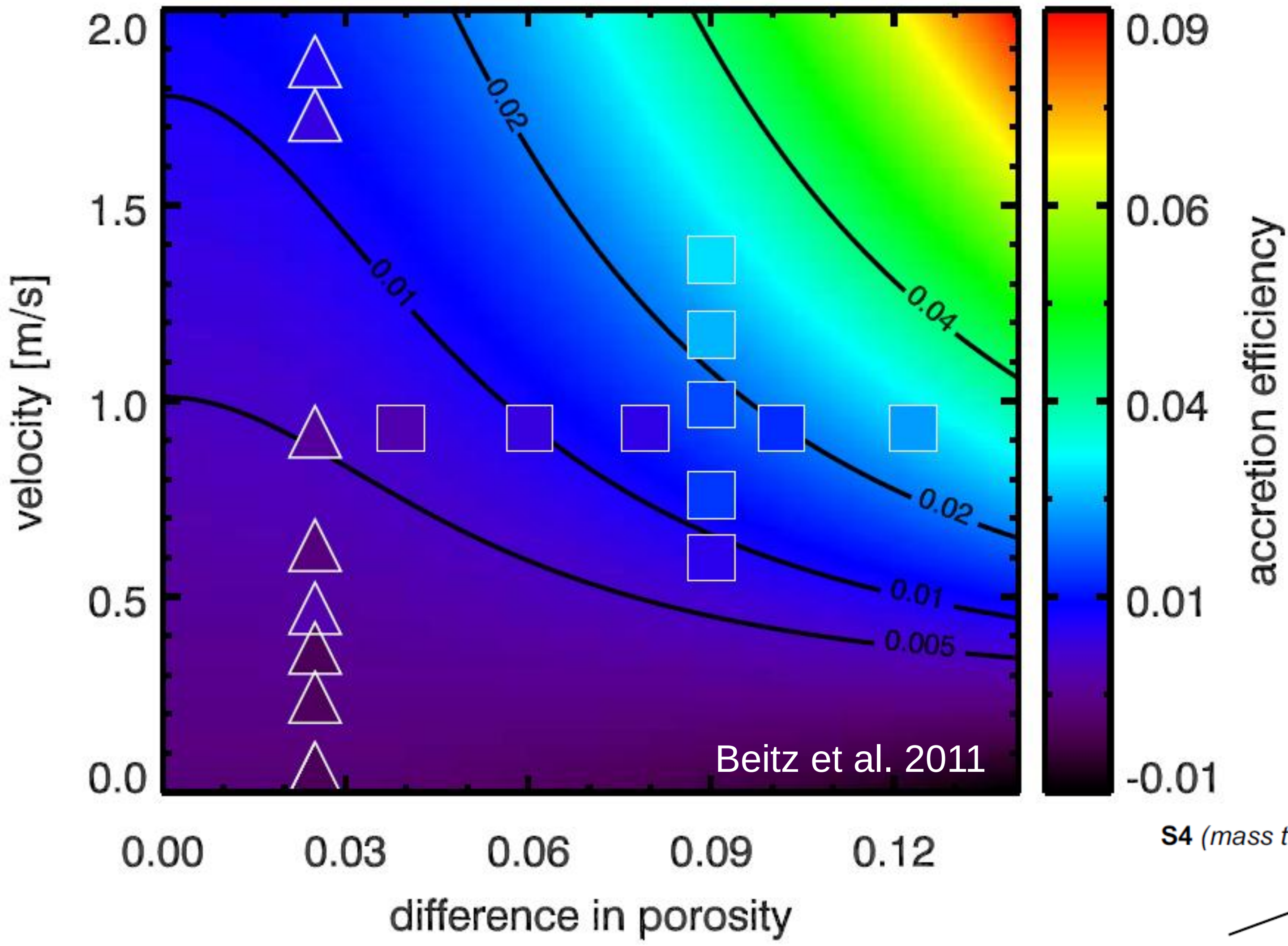

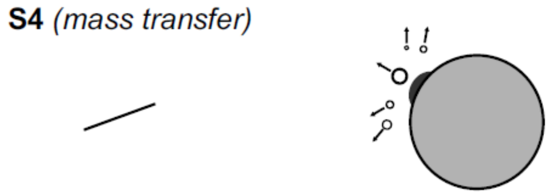

Accretion efficiency in moderate-velocity dust-aggregate collisions

- Projectiles: approx. 1mm, RBD aggregates, partly pre-fragmented
- Target: sintered SiO_2, filling factor 0.45
- Velocities: 2-6 m/s

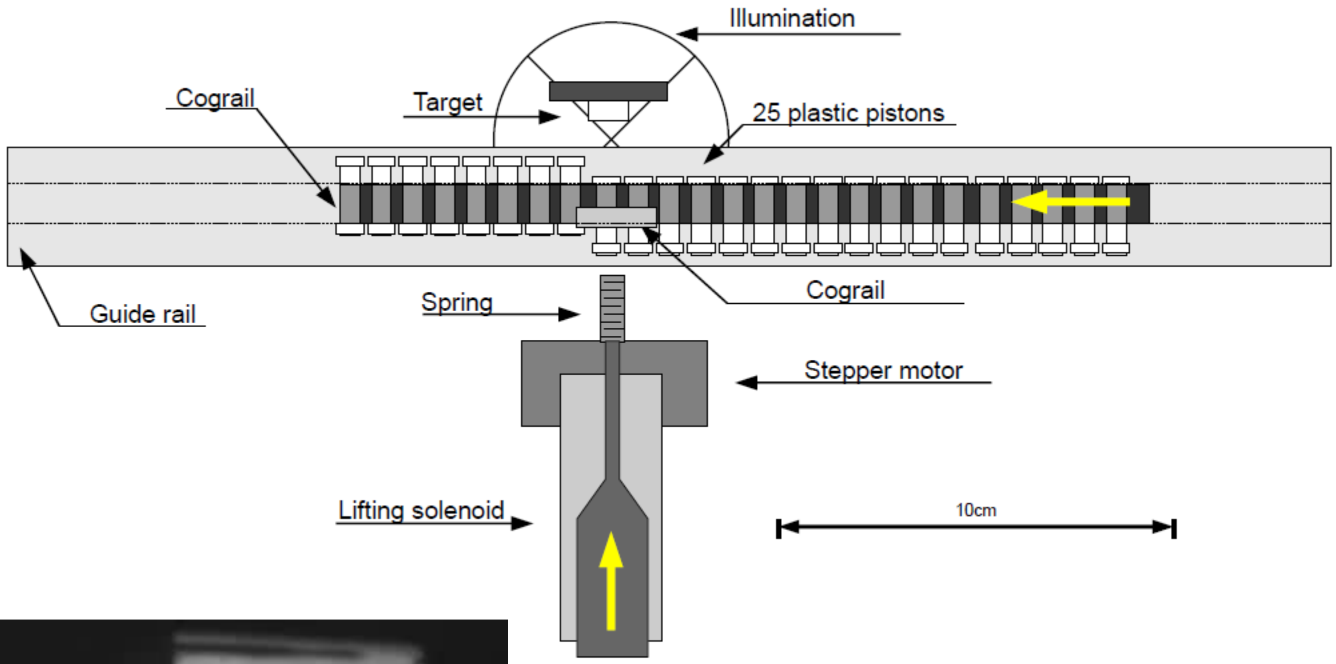

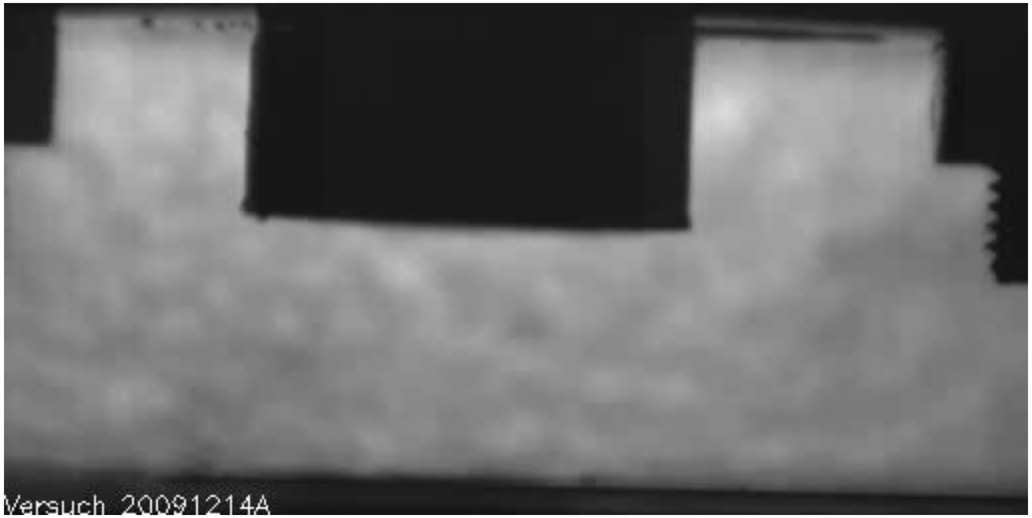

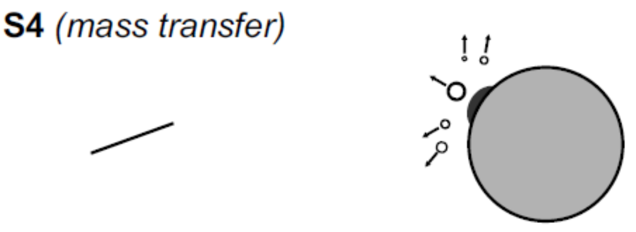

Kothe et al. 2010

Accretion efficiency in moderate-velocity dust-aggregate collisions

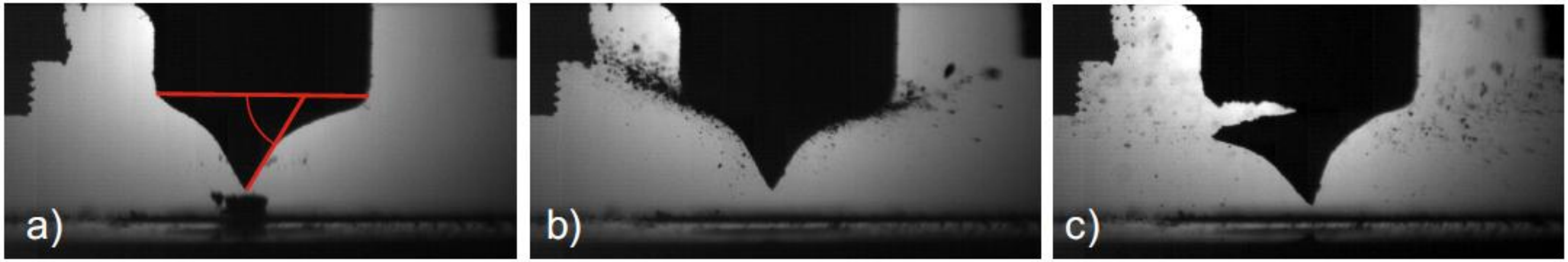

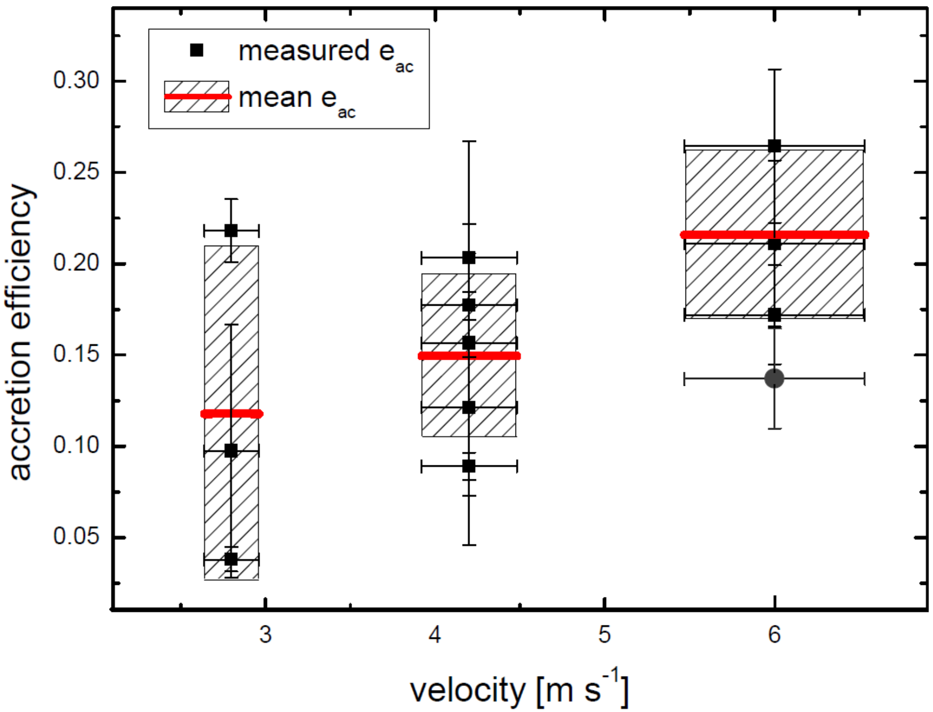

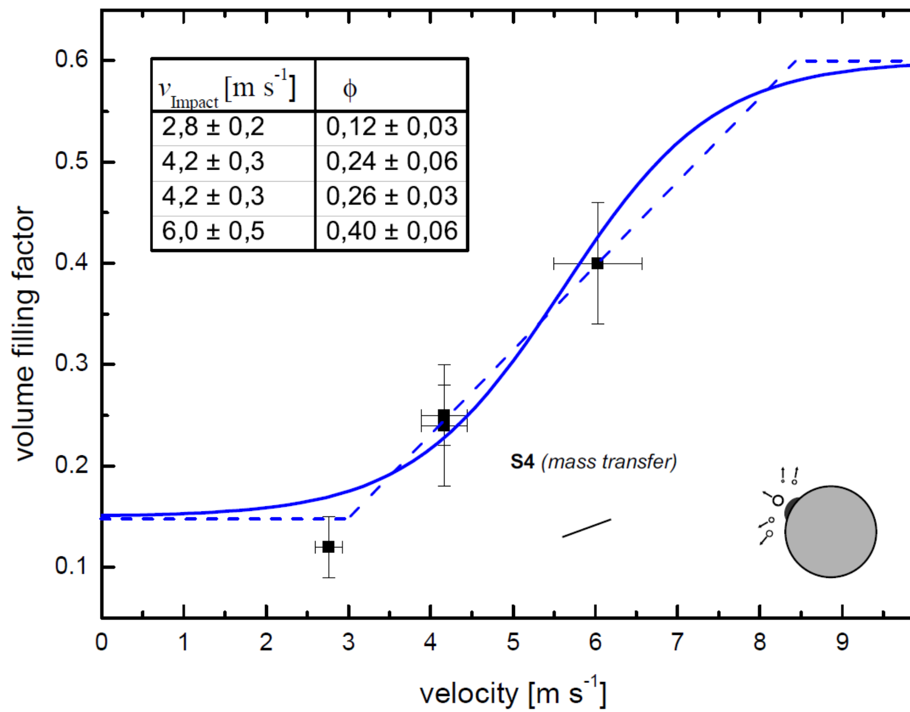

Kothe et al. 2010

A recent update of the collision model

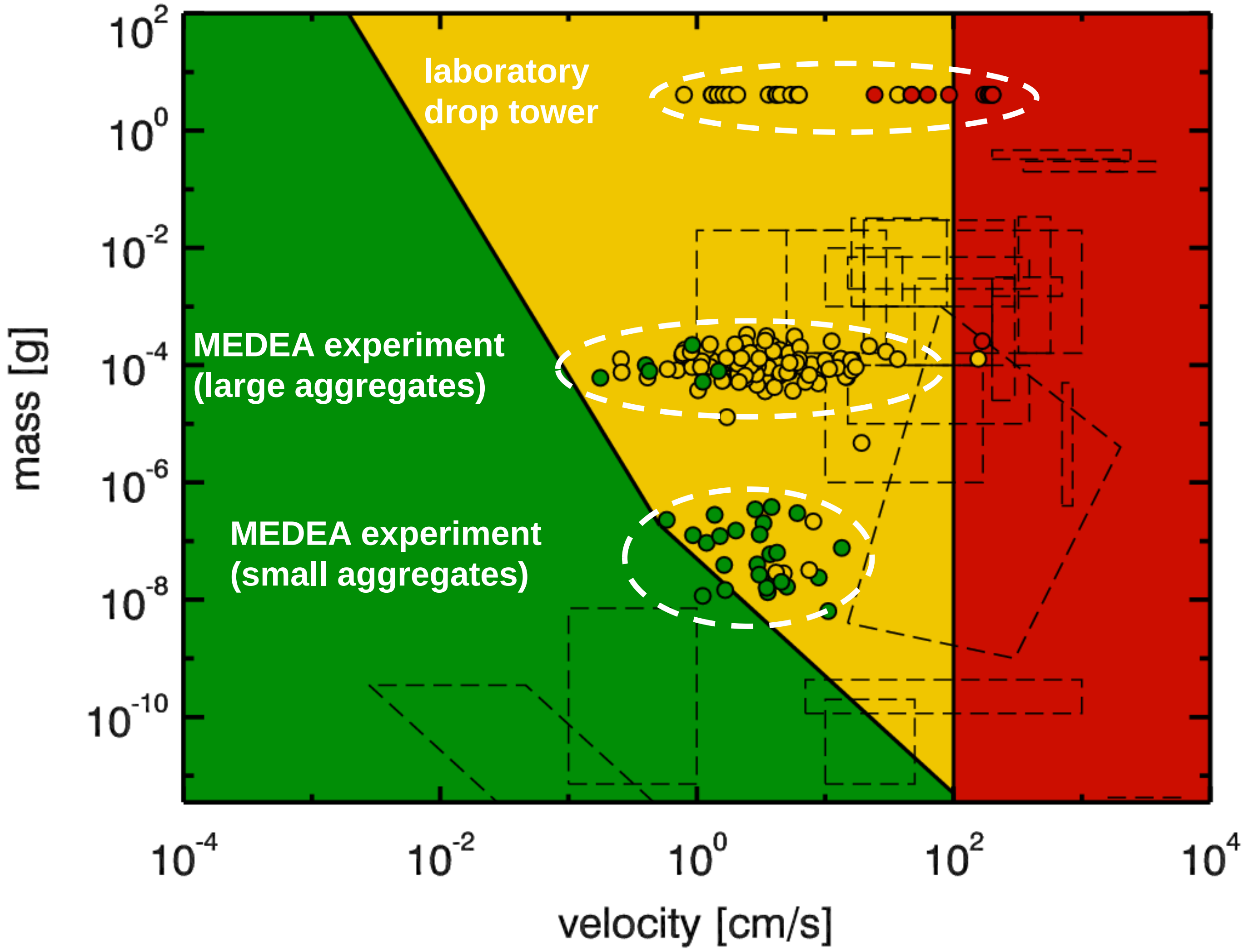

A recent update of the collision model

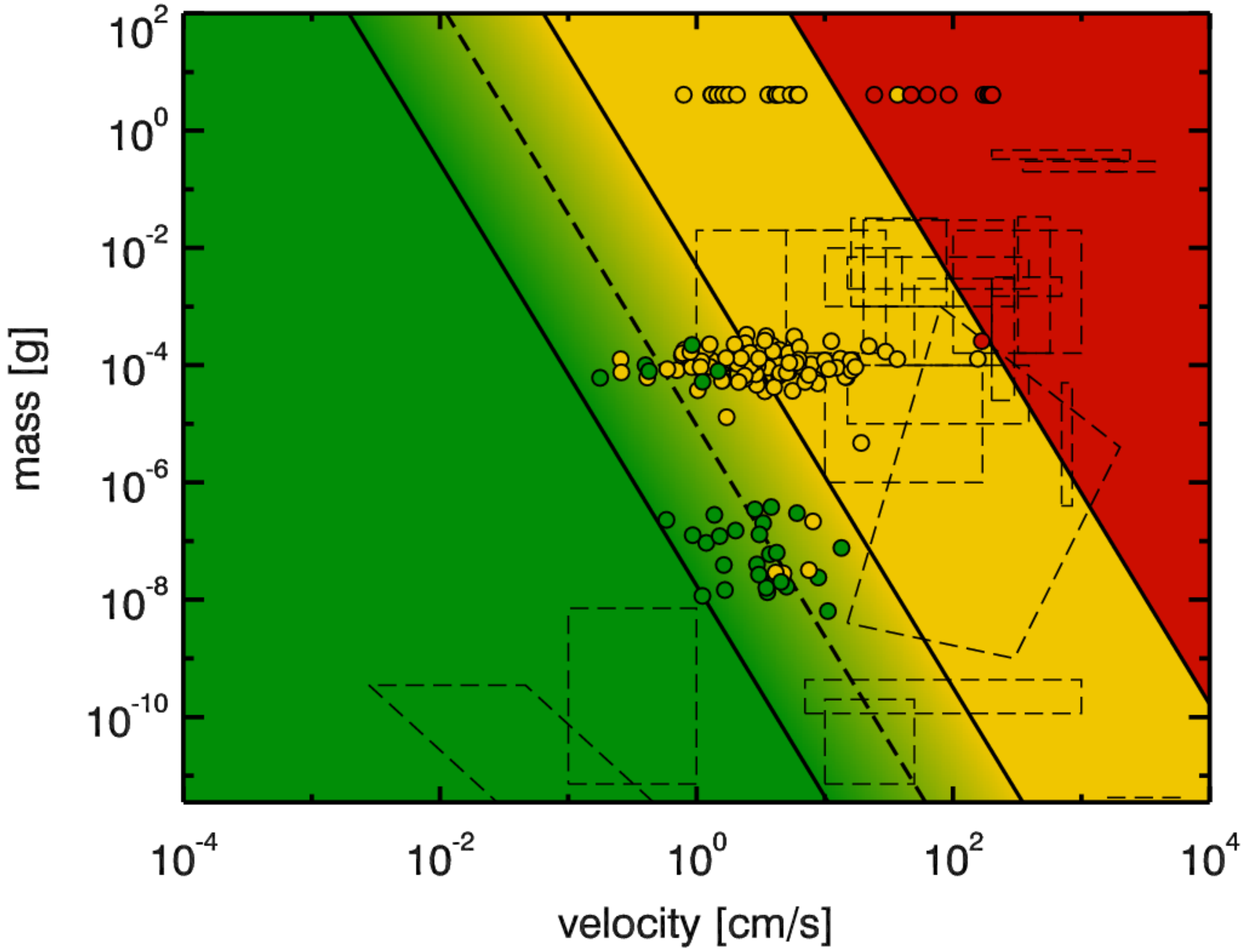

Numerical simulations of aggregate growth in PPDs using the Monte-Carlo method - Mass-porosity evolution

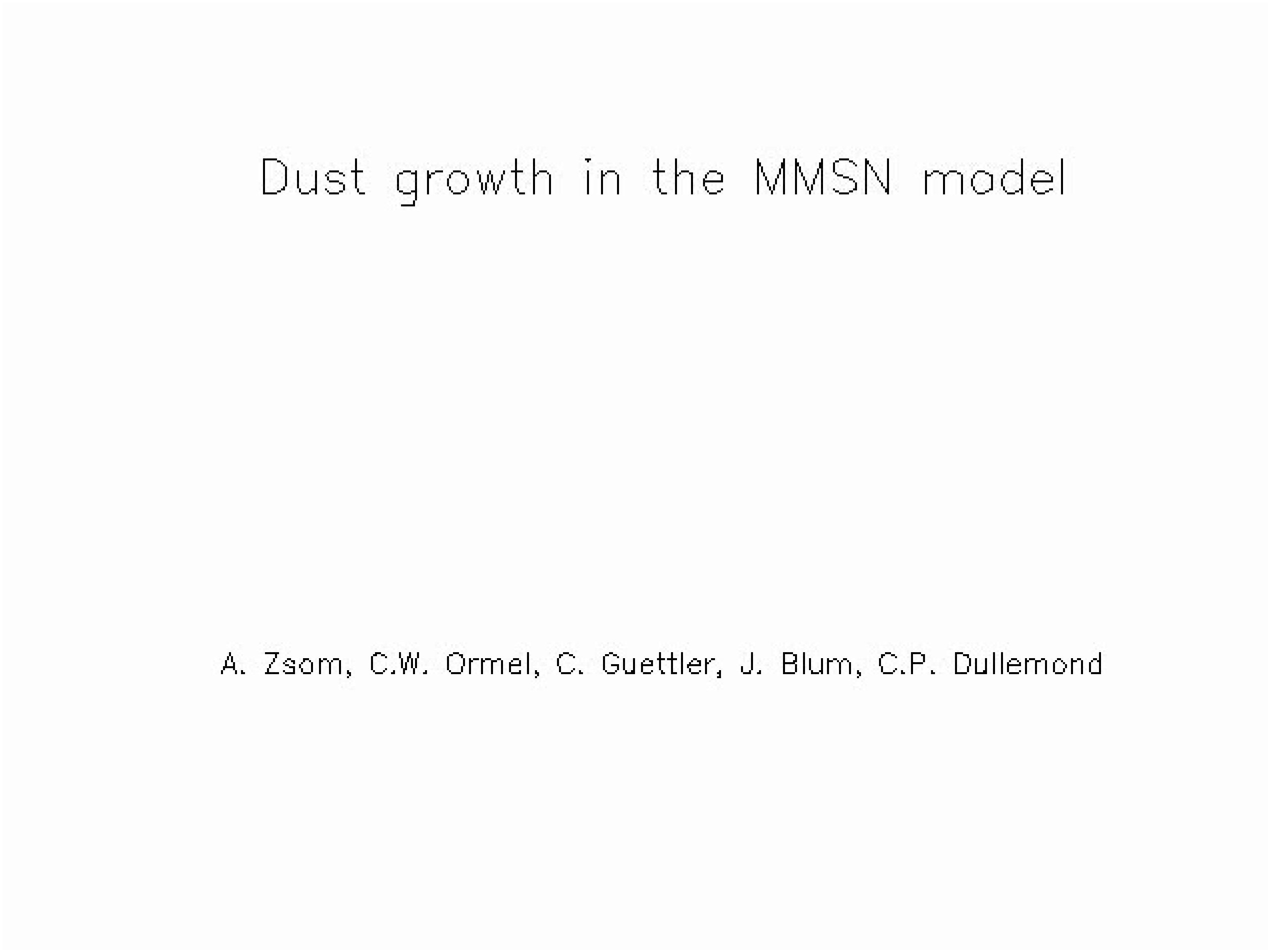

Zsom et al. 2010

Numerical simulations of aggregate growth in PPDs using the Monte-Carlo method - Results for the mass evolution

Zsom et al. 2010

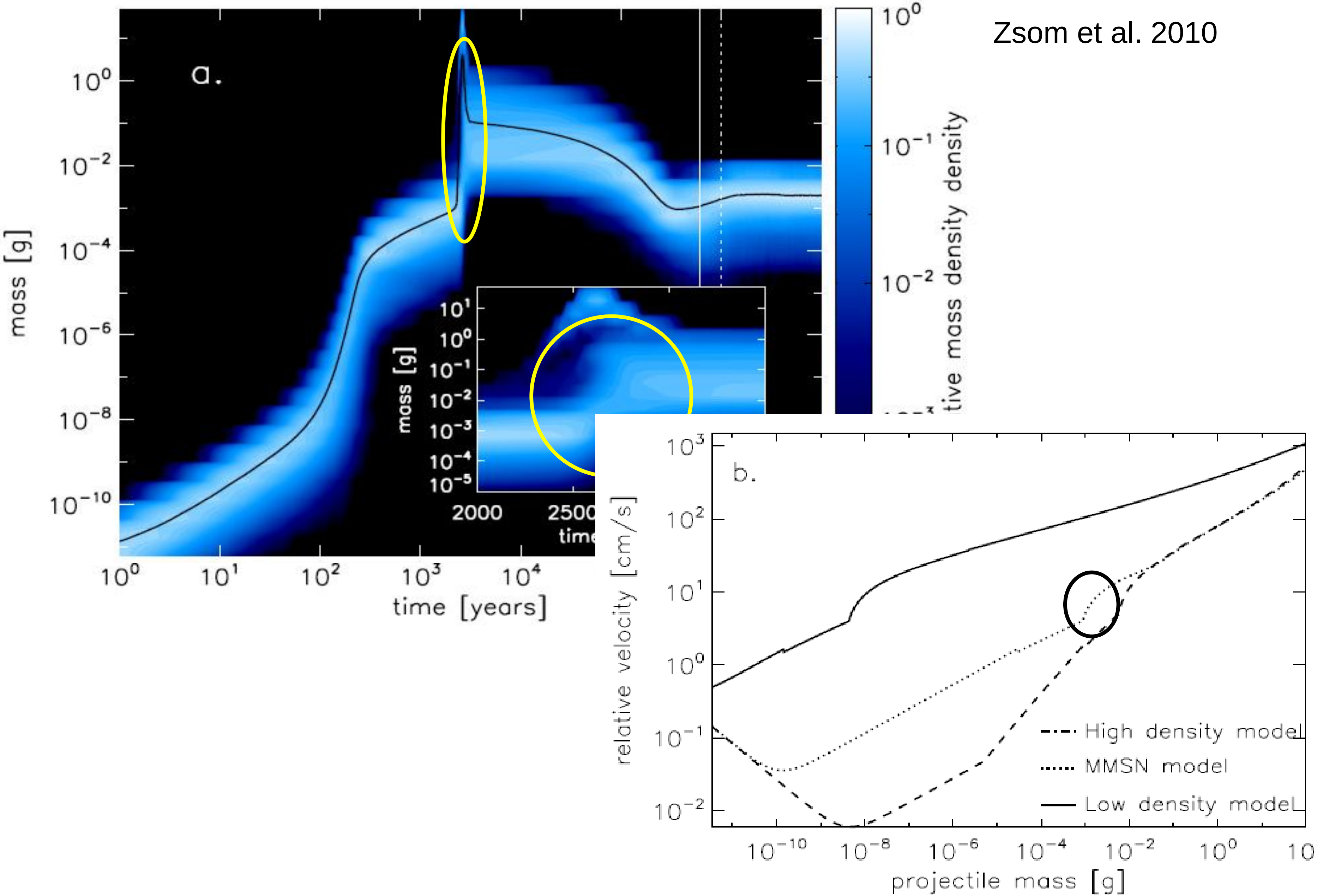

Numerical simulations of aggregate growth in PPDs using the Monte-Carlo method - Results for the porosity evolution

Zsom et al. 2010

97.5% porosity

90% porosity

85% porosity
(lab experiments)

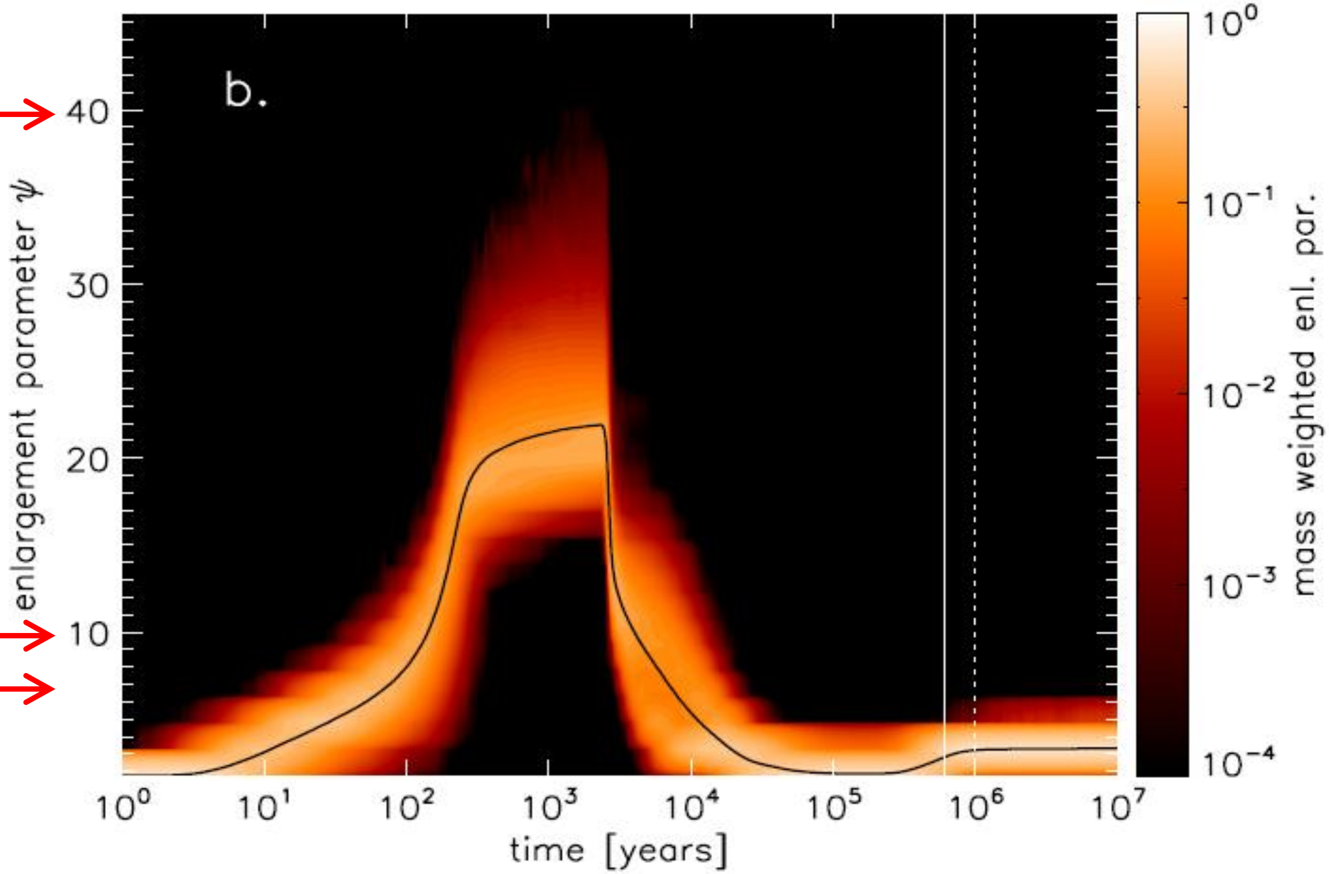

Lessons learned

1. Growth stops due to bouncing
   → "bouncing barrier"
2. Mass distribution stays narrow
3. Compaction in bouncing collisions is of eminent importance; final porosity "only" ~60-70%
4. Fragmentation regime is only reached for highest turbulence but does not invoke a new growth mode

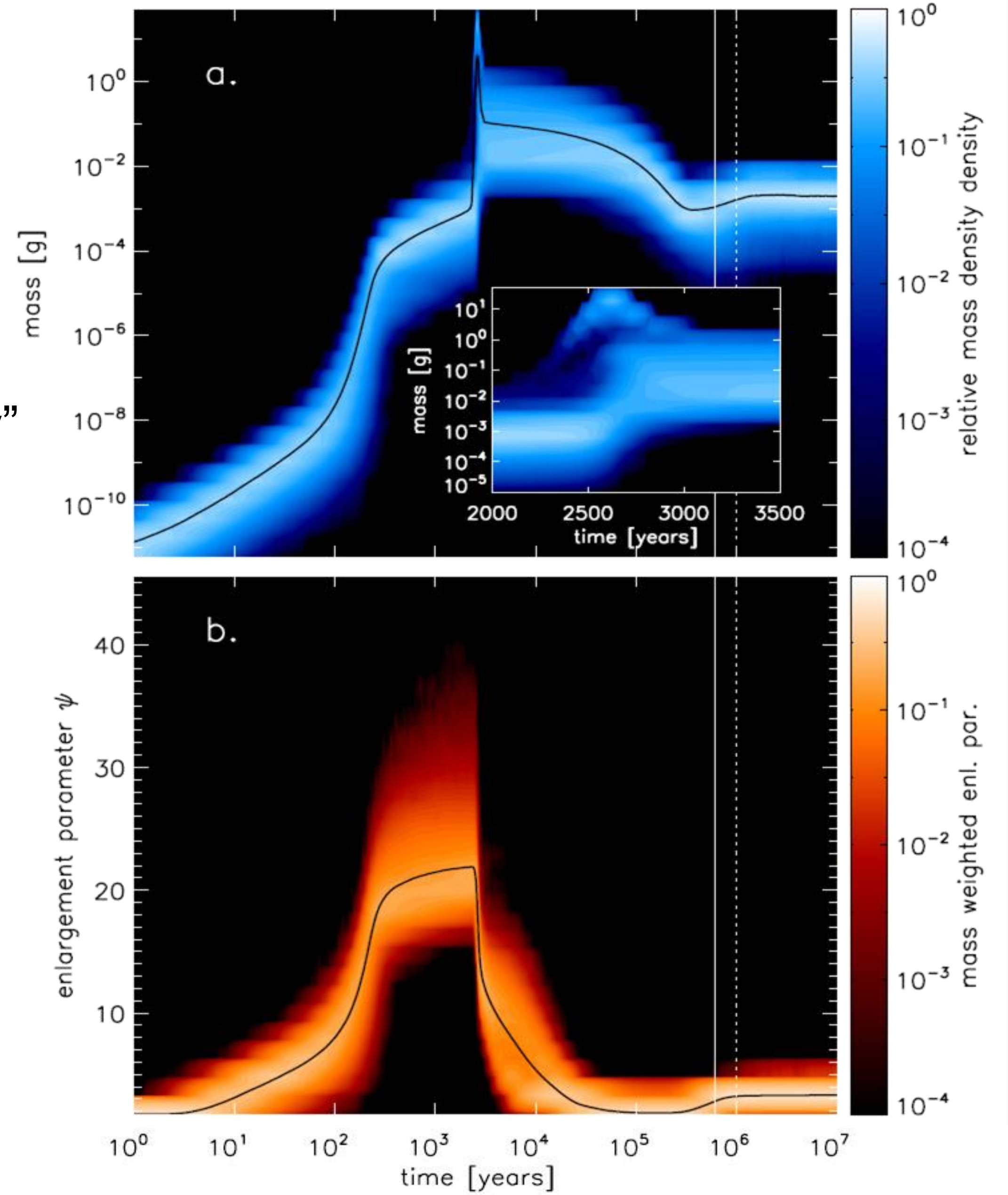

Where are we in terms of completeness ?

- Sizes of protoplanetary dust aggregates:

1 µm	1 mm	1 m	1 km

- Mass ratios of projectile and target:

0	1

- Collision velocities of protoplanetary dust aggregates:

10^{-4} m/s	10^{-2} m/s	1 m/s	100 m/s

- Porosities of protoplanetary dust aggregates:

compact	porous	very porous

- Protoplanetary dust materials and temperatures:

oxides/metals >1000 K	silicates ~300 K	organics ~200 K	ices ~100 K

no expt's	expt's

Can there be any collisional growth beyond the "bouncing barrier"?

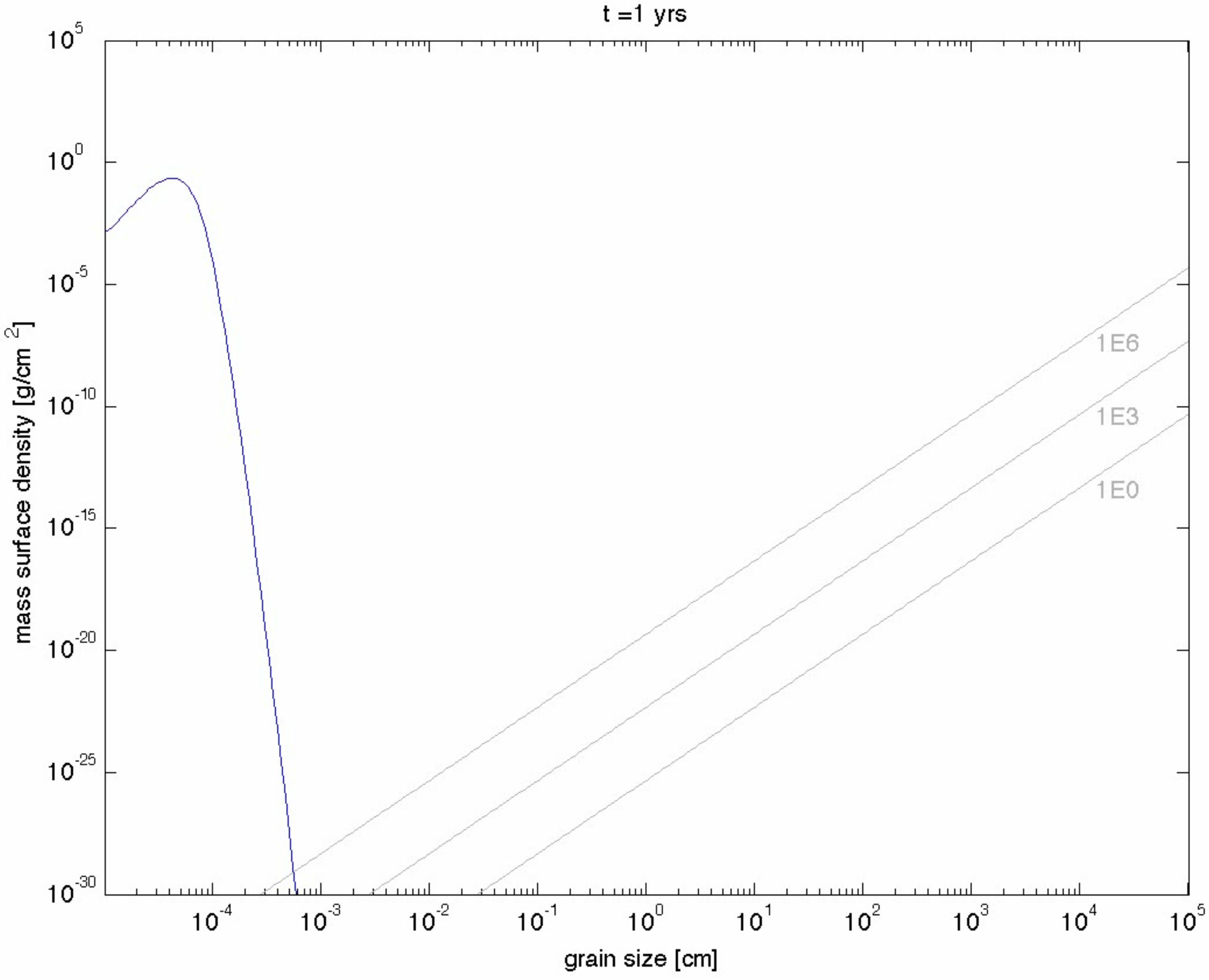

Windmark et al., pers. comm.

III. The formation of planets and planetary systems

b. Dust to planetesimals

vi. Gravitational instability models

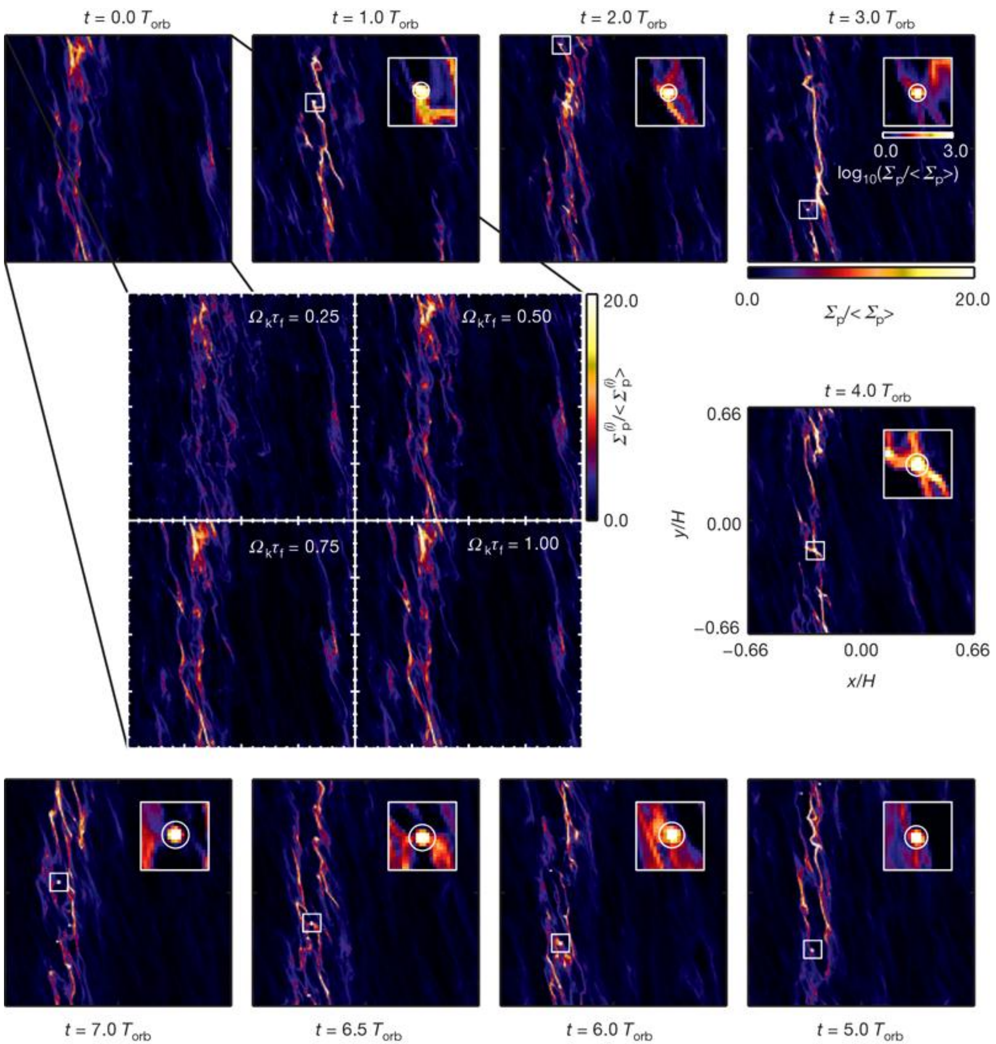

Johansen
et al. 2007

Capture of macroscopic particles by long-living gas vortices

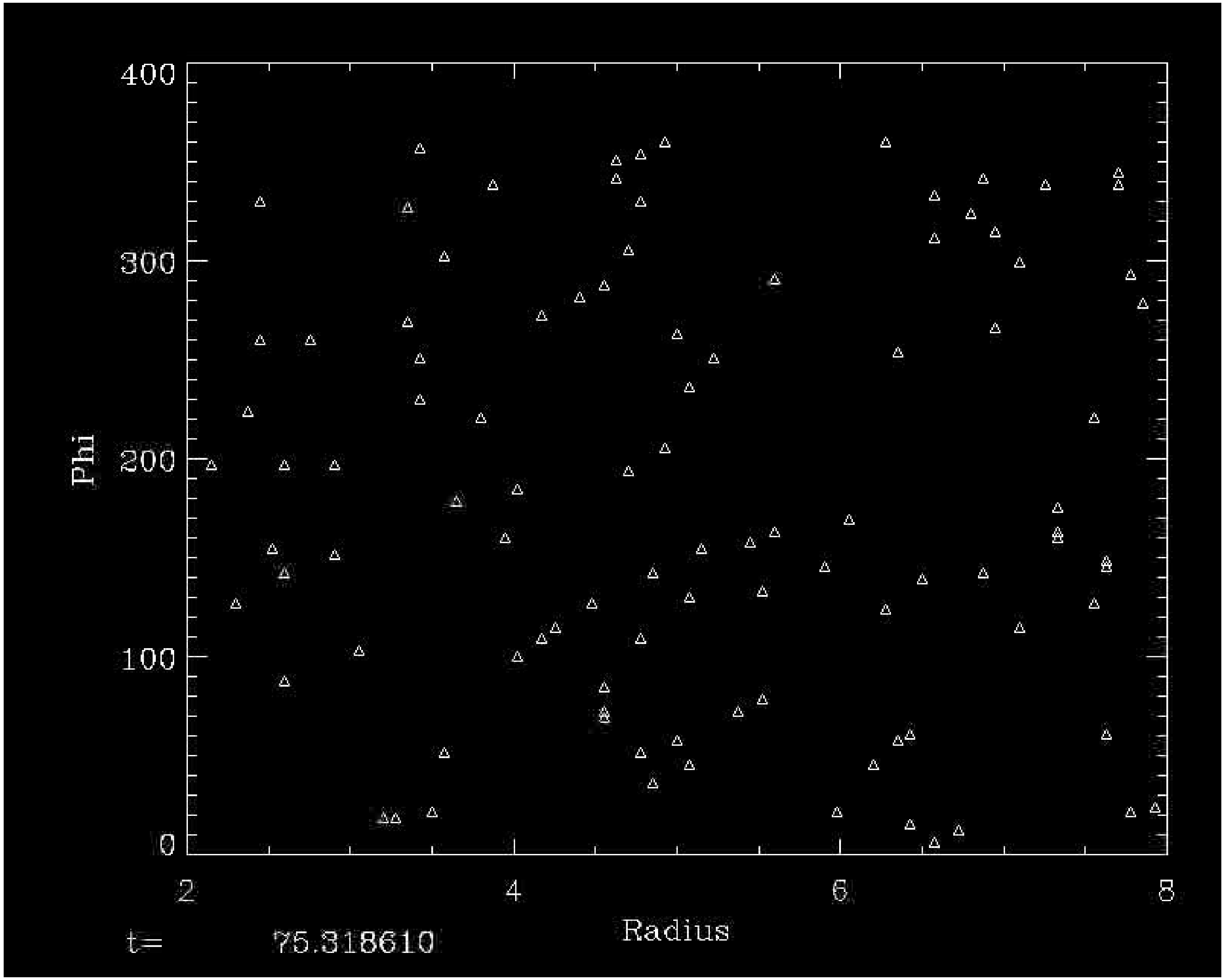

- ▷ Trapping of solid objects in pressure maxima and/or in anticyclonic vortices.
- ▷ Basically all solid bodies with sizes 0.1-10 m are efficiently captured.
- ▷ No escape of dust with sizes 0.1-1000 m from vortices.
- ▷ Low relative velocities within the vortices $\Rightarrow$ collisional growth ?
- ▷ No shear inside vortices.
- ▷ Concentration of the dust particles in the centers of the vortices $\Rightarrow$ gravitational instability ?

Δ: 1m dust particle

Gravitational instability

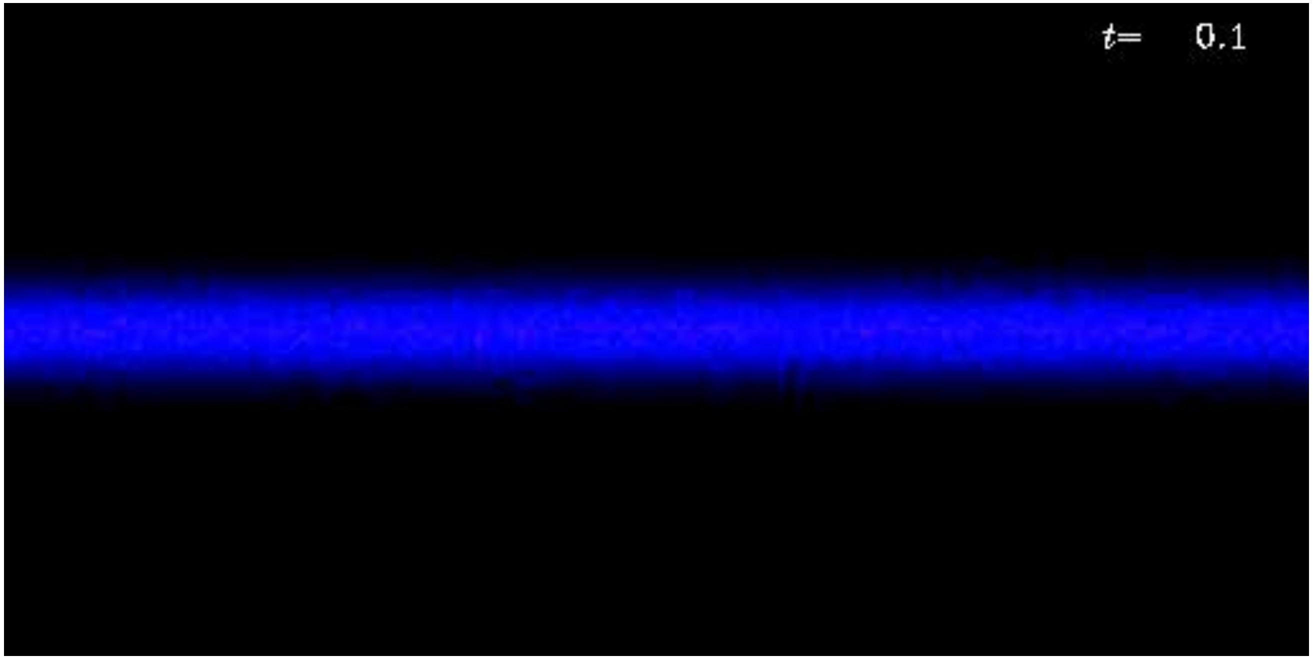

Johansen et al. 2007

nature06086-s2.mov

- In absence of turbulence, >cm-sized dust aggregates sediment towards the midplane of the protoplanetary disk.
- When the dust density exceeds the gas density, the gas in the midplane is forced to rotate at Keplerian velocity. Due to the shearing between the midplane rotation and the layers above/below the midplane, a Kelvin-Helmholtz instability forms.
- Due to a local variation of the dust-to-gas ratio and, thus, the rotation speed, a streaming instability occurs.
- Gravitationally-bound dust ensembles are formed when the dust size exceeds ~0.1 m.
- Direct formation of planetesimals with sizes up to 100-1 000 km, if fragmentation is negligible.
- However, if collisions results in fragmentation, no net growth occurs (Johansen et al. 2008).

III. The formation of planets and planetary systems

c. Planetesimals to planets

http://www.phys.boun.edu.tr/~semiz/universe/near/18.html#pix

Accretion of planetesimals

- ▷ Gas friction is negligible
- ▷ Typical collision velocity < escape velocity
  - ▶ Gravitational sticking
  - ▶ <u>Collision probability increased due to gravitational focussing</u>
    → large bodies grow faster than small bodies

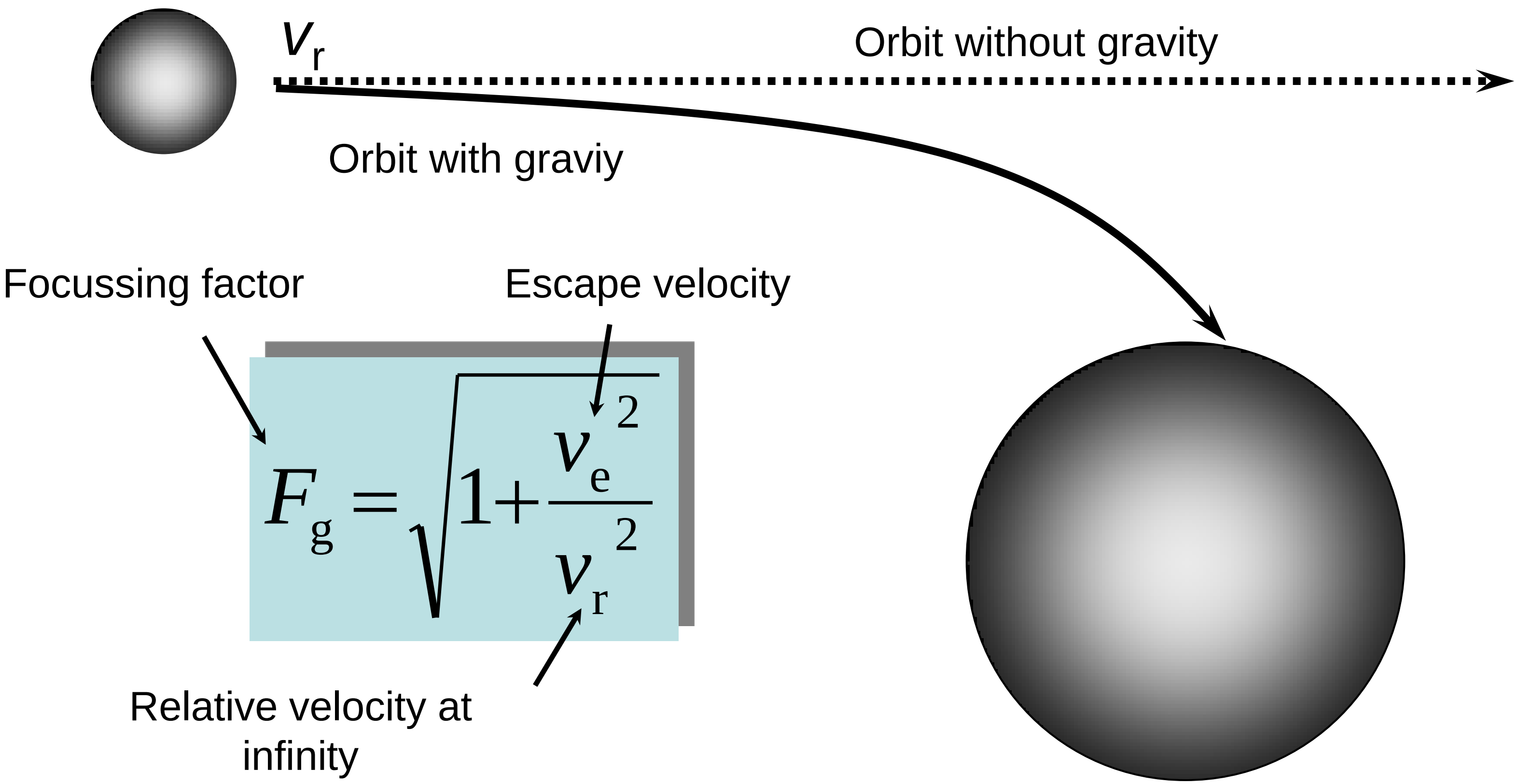

$$F_g = \sqrt{1 + \frac{v_e^2}{v_r^2}}$$

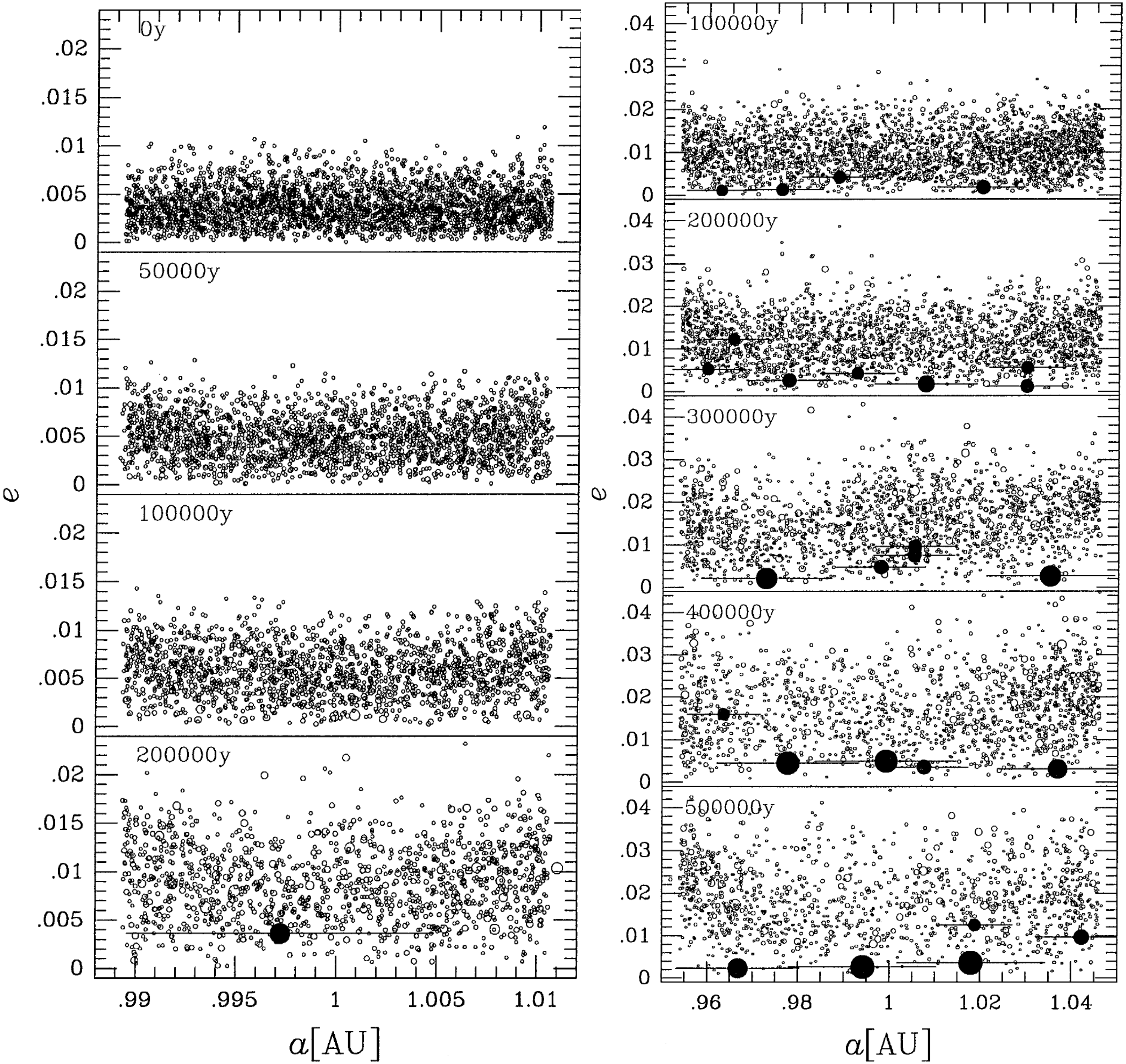

Kokubo & Ida 2000

Formation timescales of terrestrial planets

Time$^{\$}$ (yr)	*Size*	*Process*	
0	**10^{-6} m**	**Condensation of dust particles**	
~ 10^3-10^4	**0.1 m**	**Agglomeration with high sticking probability**	Stage 1
? (< 10^7)§	**10 km**	**Planetesimals with mass m_0**	Stage 2
Time$^{\#}$ (yr)	***Mass***	***Process***	
~ 10^3	**30 m_0**		
~ 7×10^3	**10^5 m_0**		
~ 2×10^4	**10^6 m_0**		
~ 6×10^4	**10^7 m_0**		Stage 3
~ 10^5	**$10^{7,5}$ m_0; 0,01-0,1 M_E**	**Planetary embryos (isolated)**	
~ 10^{6-7}	**0.1-0.5 M_E**	**Protoplanets (+ embryos; embryos are slowly consumed)**	
~ 10^{7-8}	**1 M_E**	**Planets on isolated orbits**	

$^{\$}$ Since the formation of the sun

§ Dispersion of the nebula after ~10^7 years

$^{\#}$ Since the formation of planetesimals

Making terrestrial planets

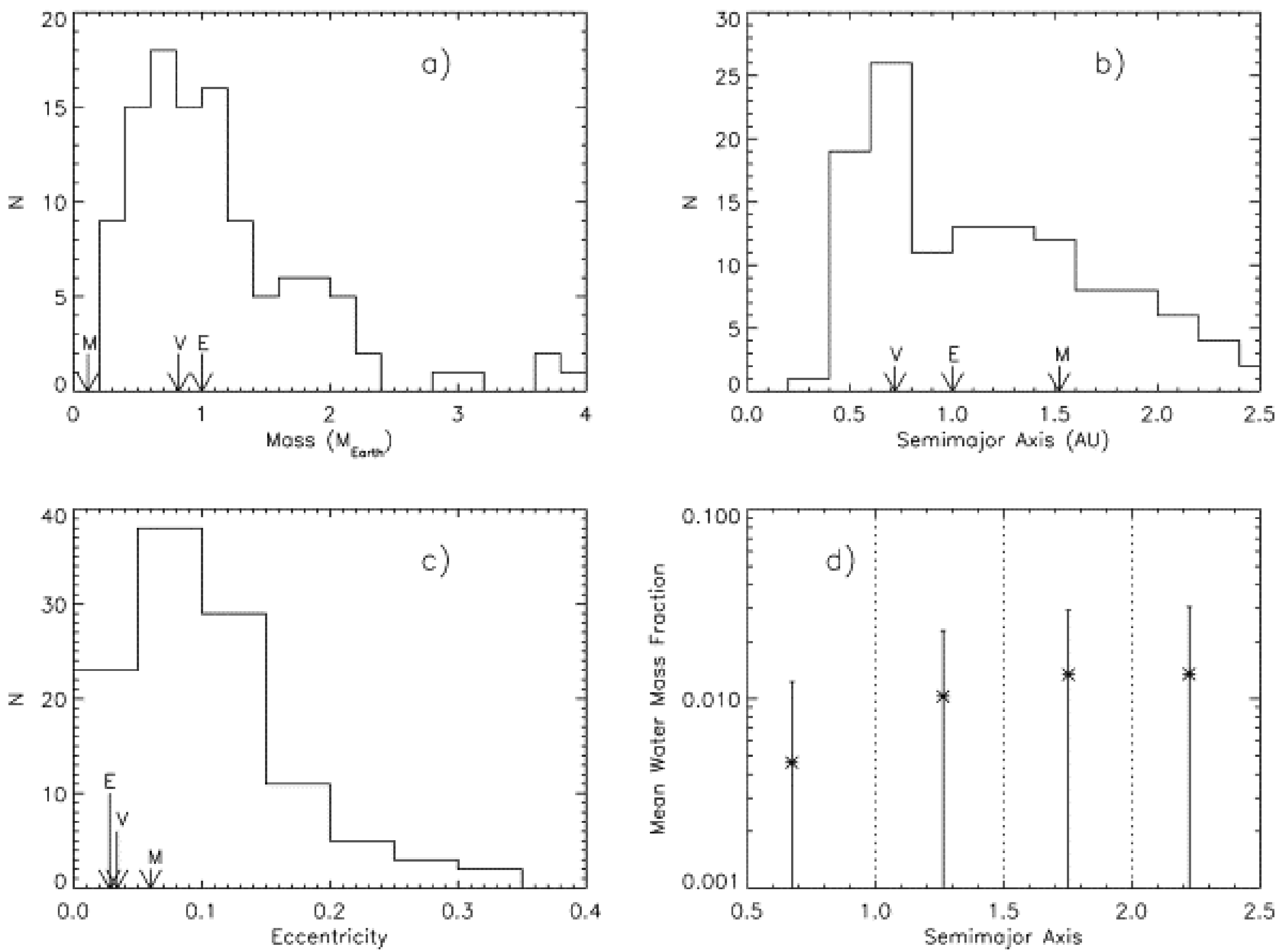

Raymond et al. 2004

Making terrestrial planets

Giant planets as today

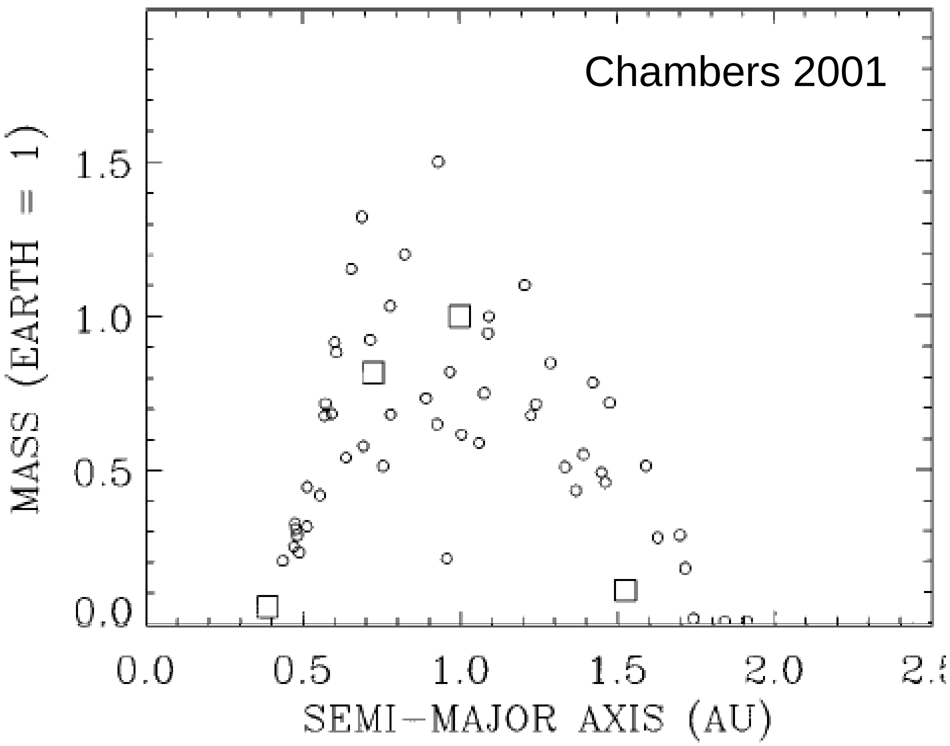

Giant planets in “compact” configuration

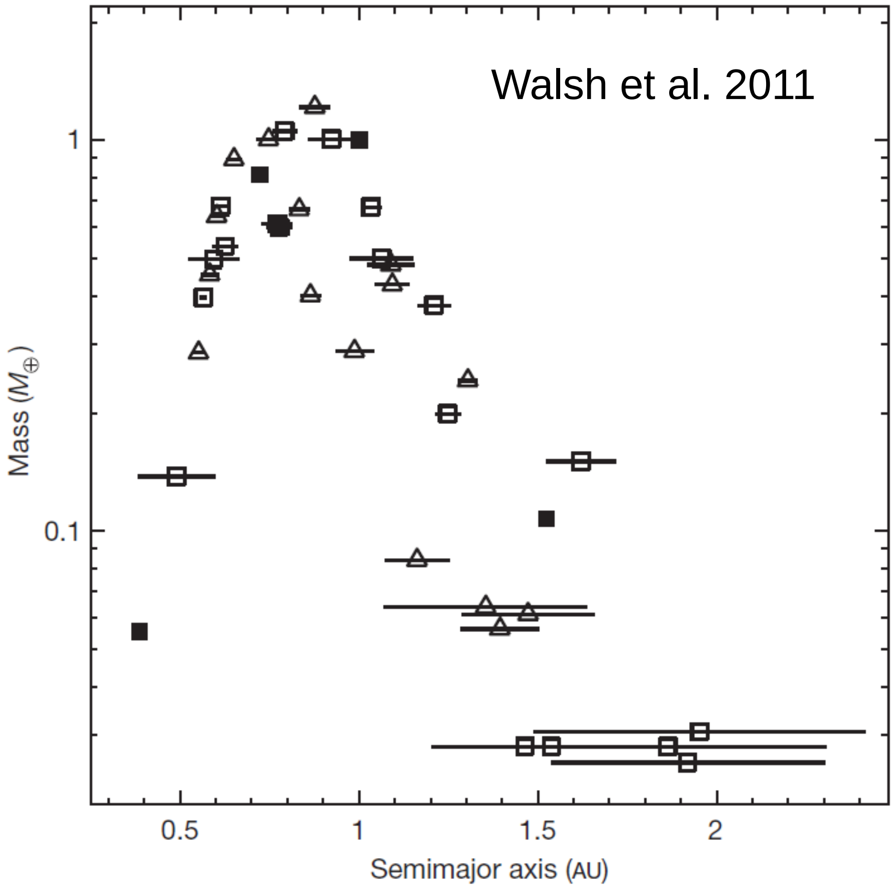

Overview of the formation of terrestrial planets

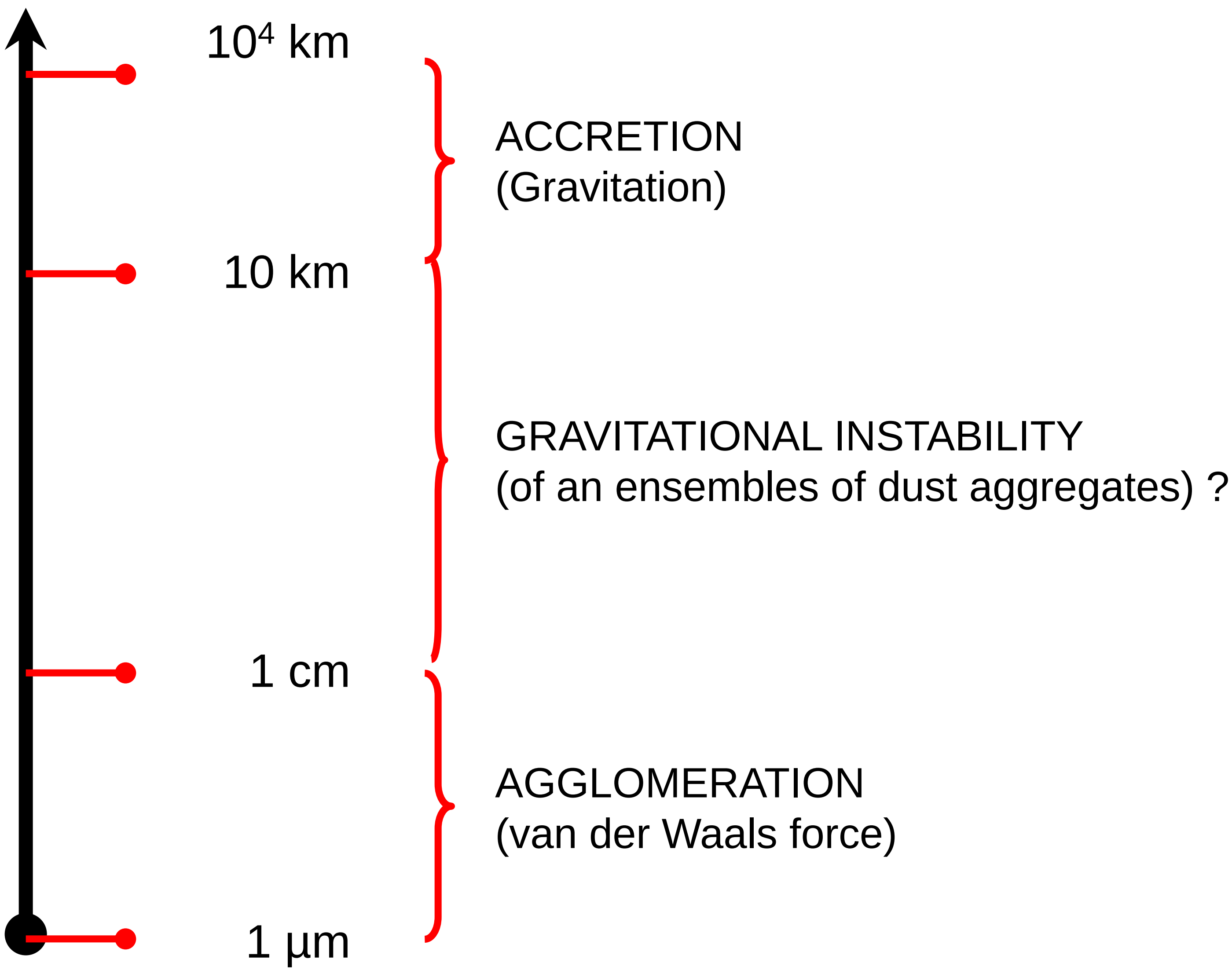

III. The formation of planets and planetary systems

d. Gas accretion

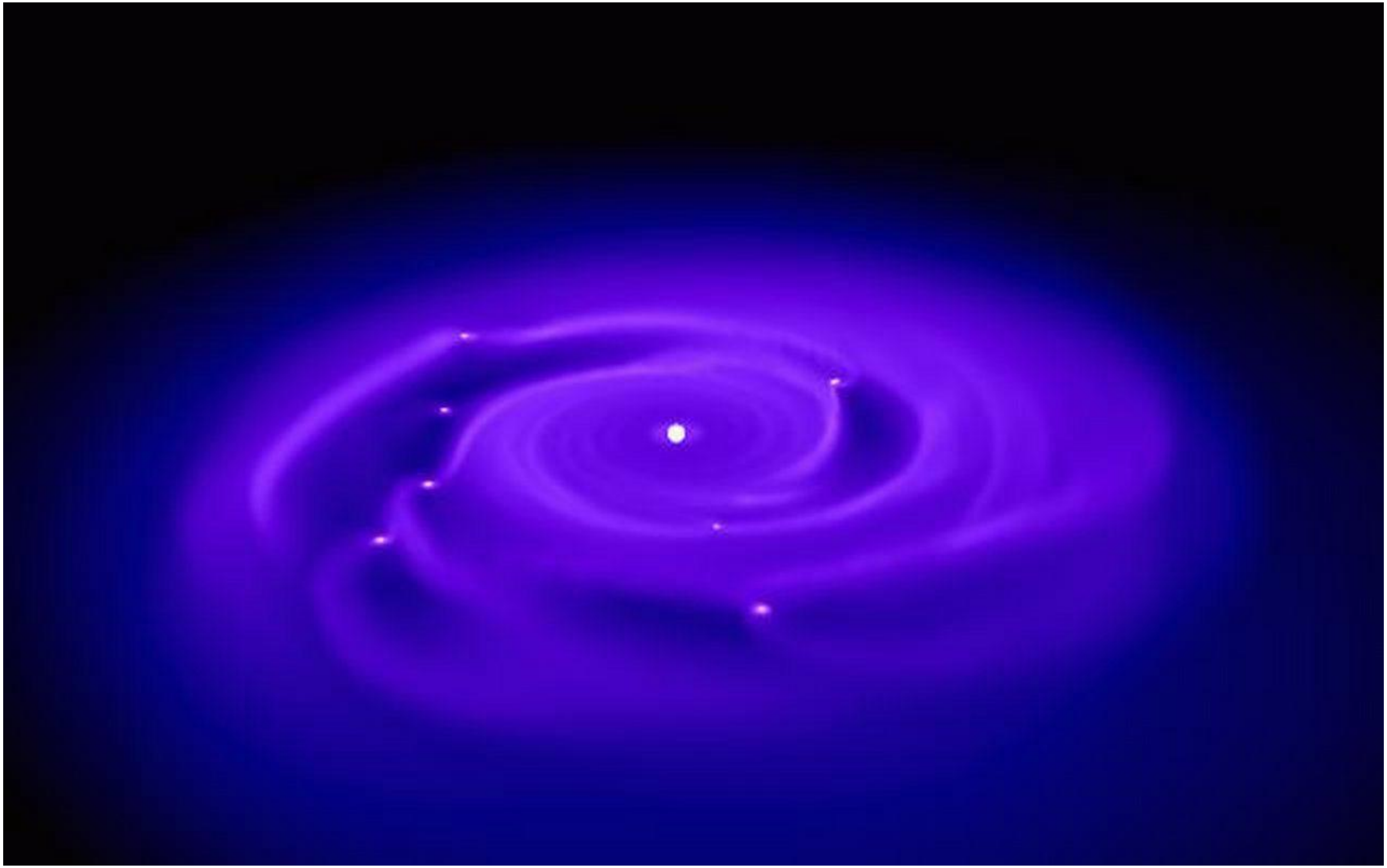

http://www.psc.edu/science/2003/quinn/how_to_cook_a_giant_planet.html

The formation of gas planets

Two hypotheses for the formation of the planets Jupiter, Saturn, Uranus and Neptune:

1. *Gravitational instability* (Boss 2001; 2003; 2007)
   - ▷ Pro: fast process.
   - ▷ Con: unclear whether the process is feasible (problems with radiation transport); "Brown Dwarf Desert".

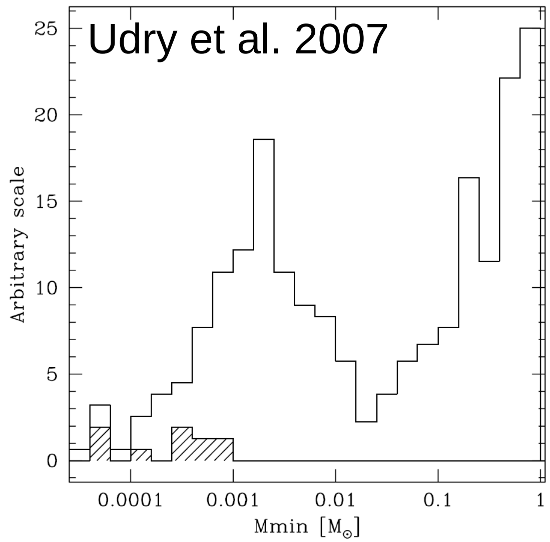

2. *Formation of a 10-15 M_E solid core; gravitational accretion of gas* (Pollack et al. 1996; Klahr & Bodenheimer 2006; Klahr & Kley 2006)
   - ▷ Pro: gas accretion on solid core well understood and fast (within ~300.000 yrs).
   - ▷ Con: formation of a 10-15 M_E terrestrial planet within < 10^7 yrs difficult; possible if (1) long-living eddies exist in the gas, which can efficiently trap m-sized bodies (in this case, no need for stages 2-3) or (2) if the mass density is sufficiently high.

Reminder: masses and sizes of extrasolar planets

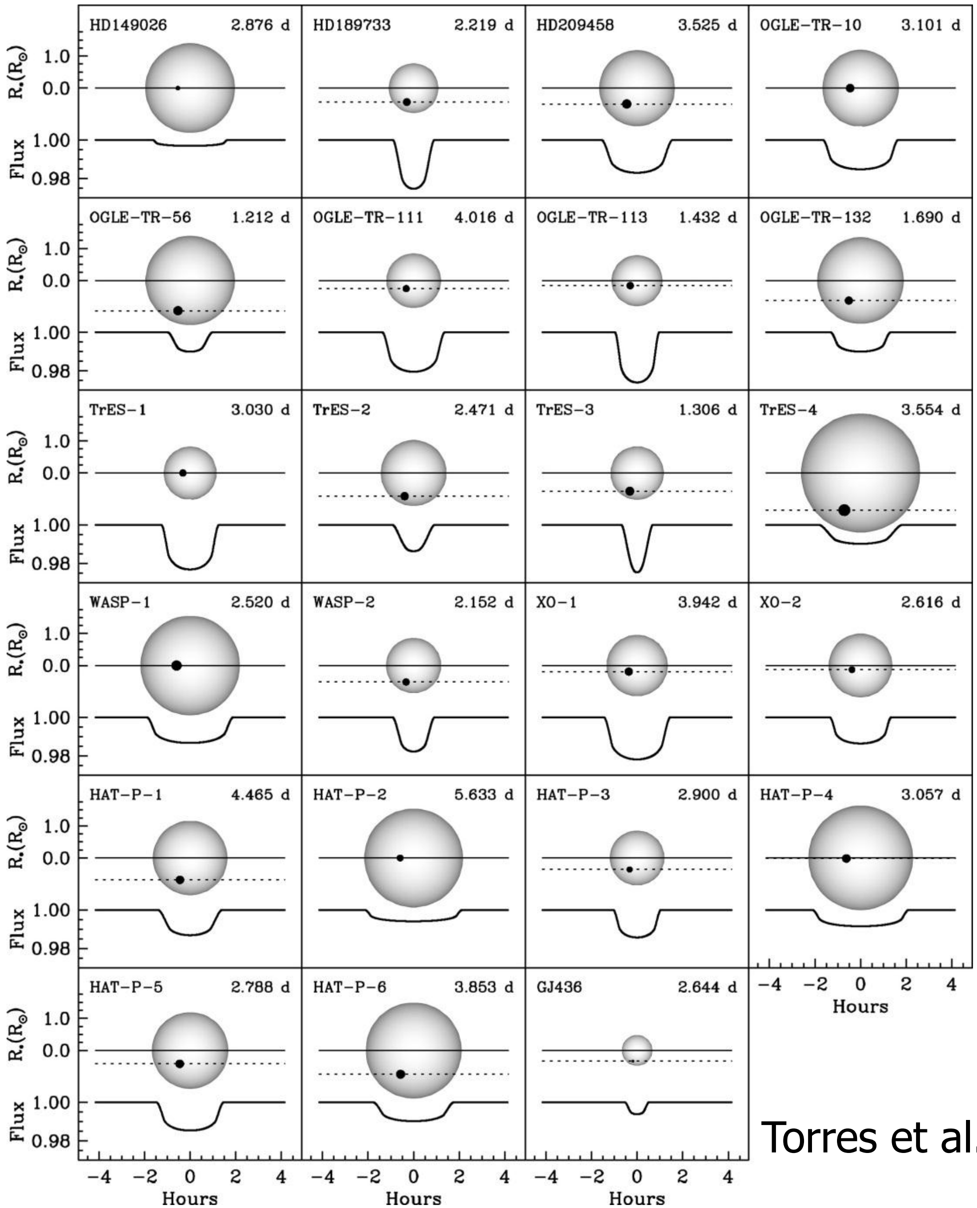

Torres et al. 2008

Tests of the formation hypotheses of gas planets:

→ Do extrasolar planets possess a core with more than ~2% of the planetary mass?
(→ solar metallicity ~2%)

→ Simultaneous measurement of mass and radius of extrasolar planets.

Reminder: masses and sizes of extrasolar planets

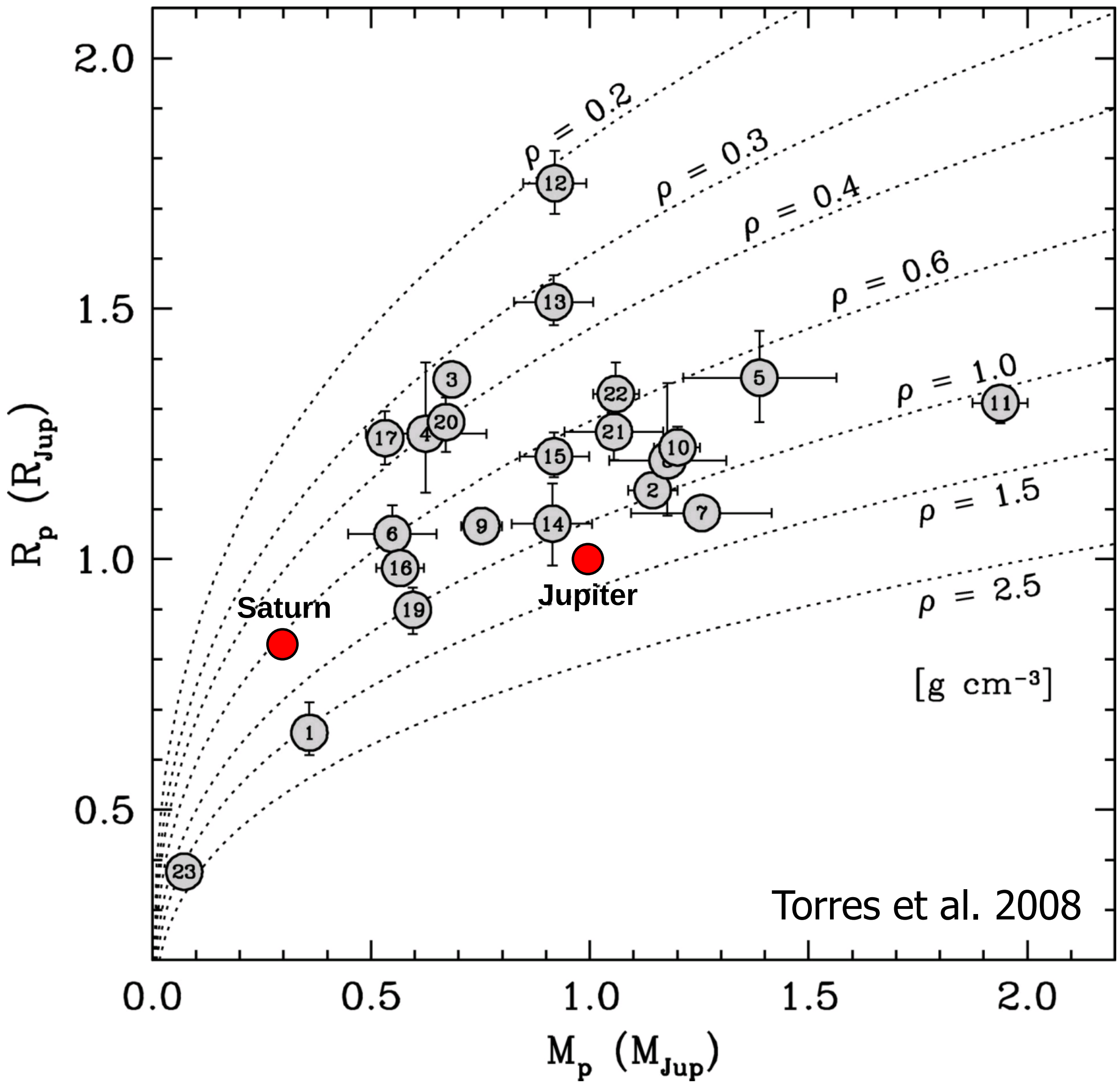

Core masses of extrasolar planets

Tests of the formation hypotheses of gas planets

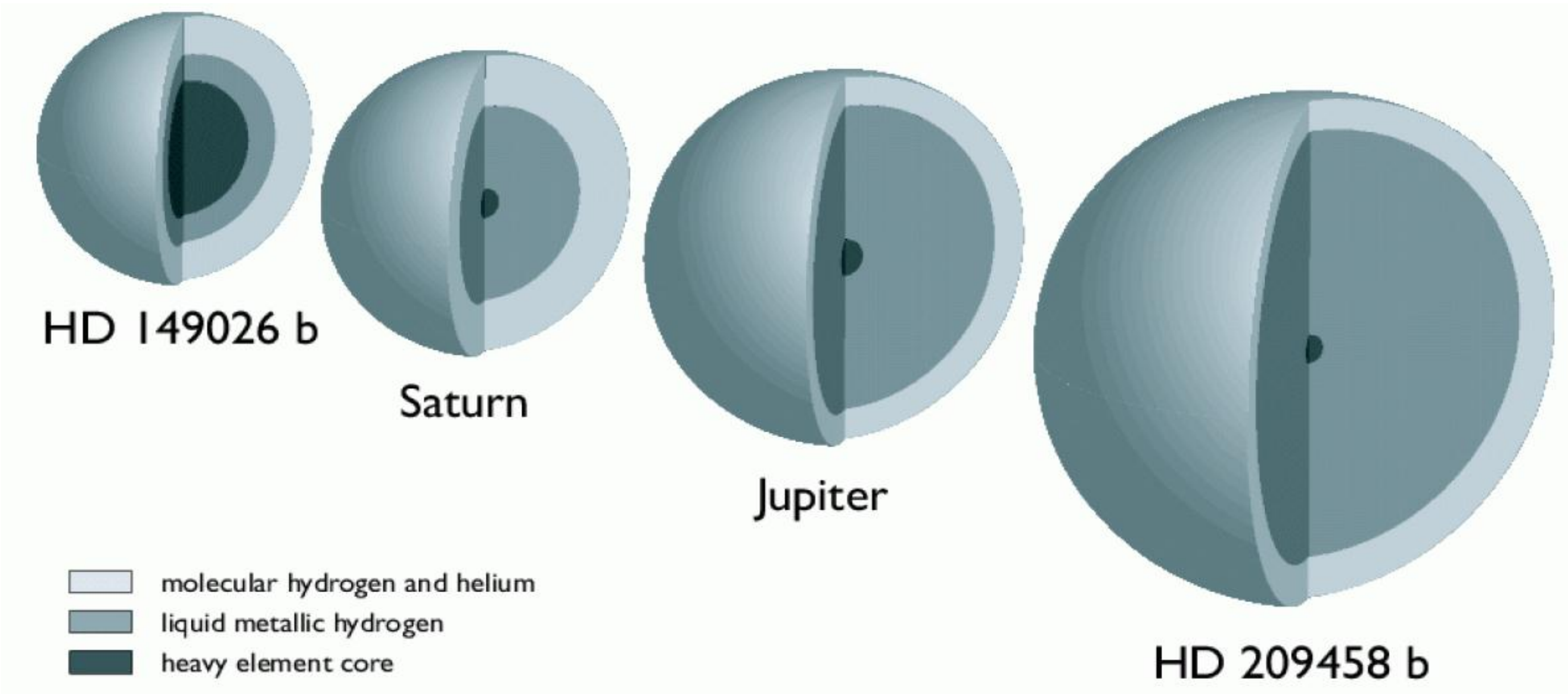

Charbonneau et al. 2007

Prediction model 1: core mass / total mass ~0.02.

Prediction model 2: core mass ≥10-20 earth masses.

Core masses of extrasolar planets

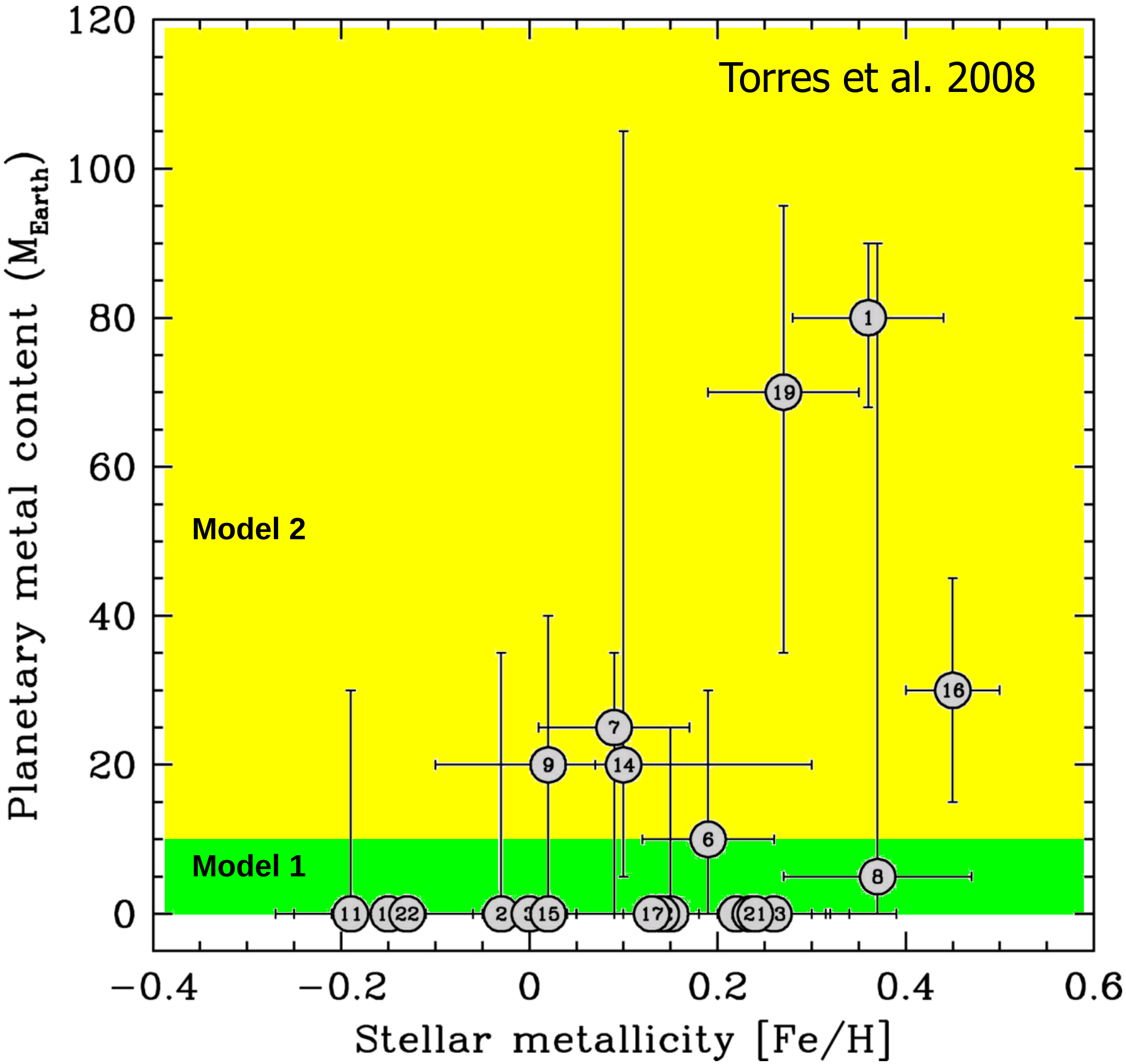

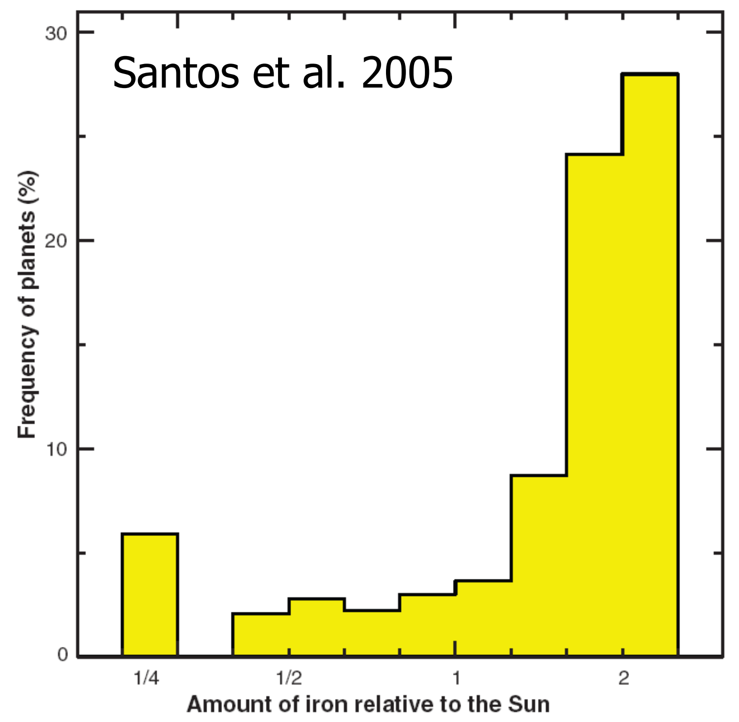

The formation of gas planets within 10^6-10^7 yrs

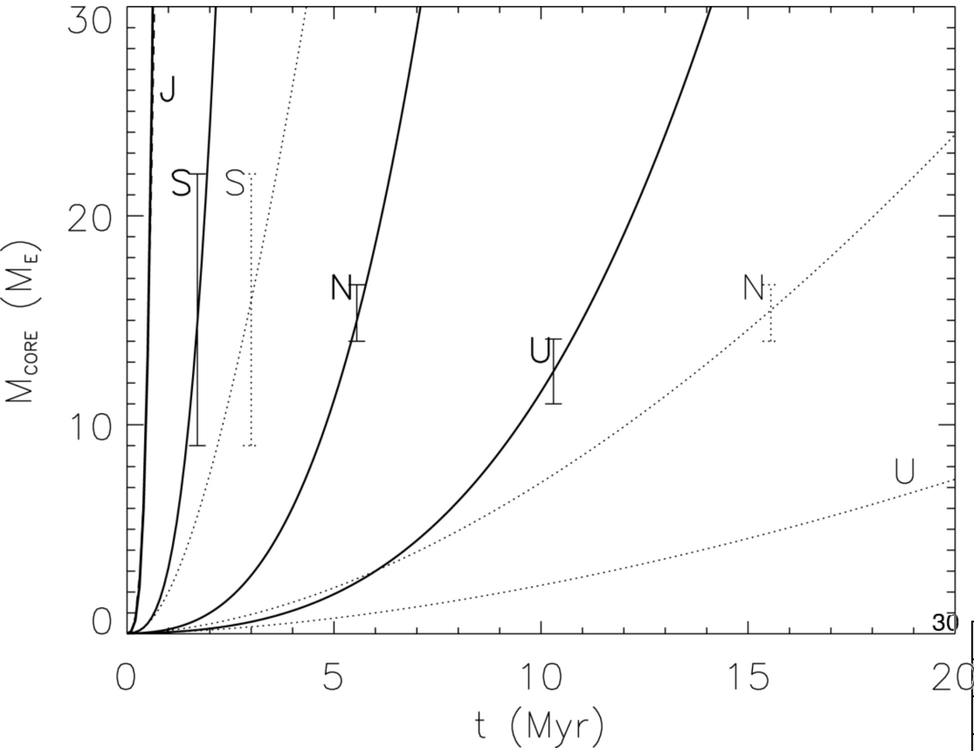

Desch 2007:
modified model of solar nebula,
based on Nice model

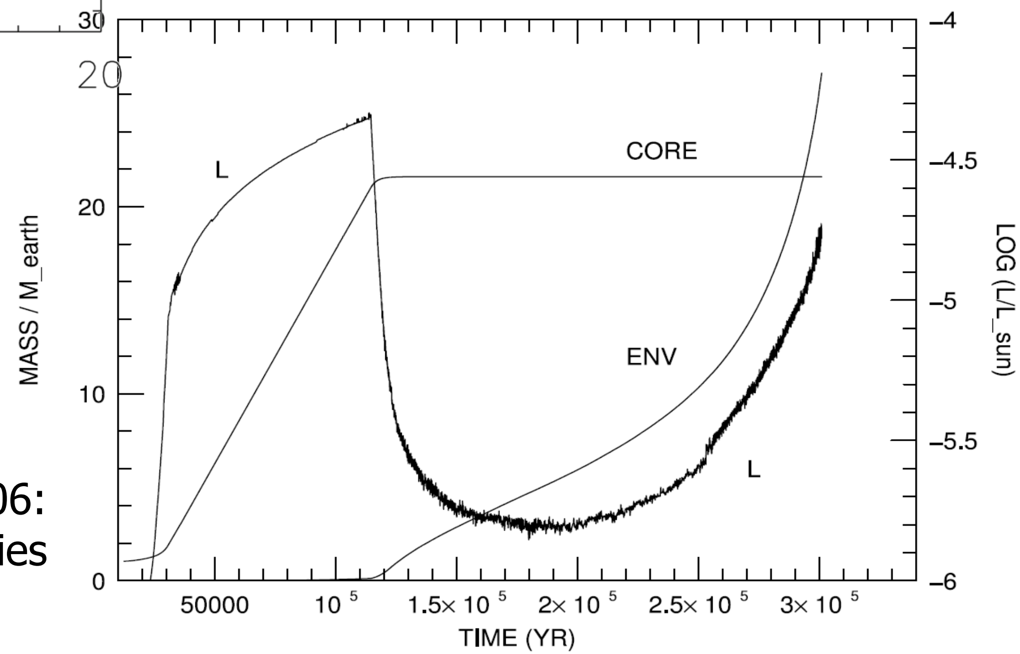

Klahr & Bodenheimer 2006:
particle shearing within turbulence eddies

The formation of gas planets within 10^6-10^7 yrs

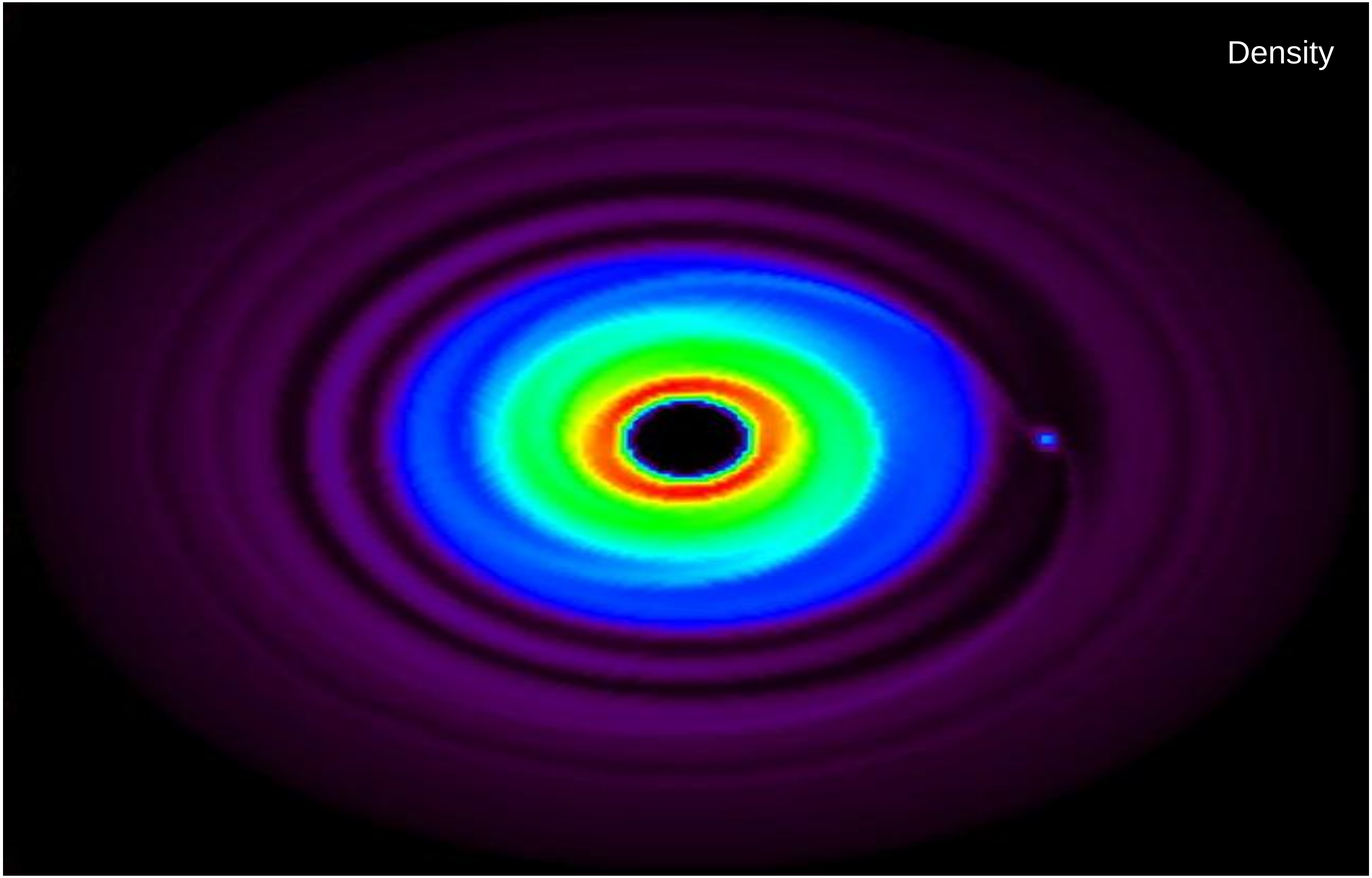

Klahr & Kley 2006

The formation of gas planets within 10^6-10^7 yrs

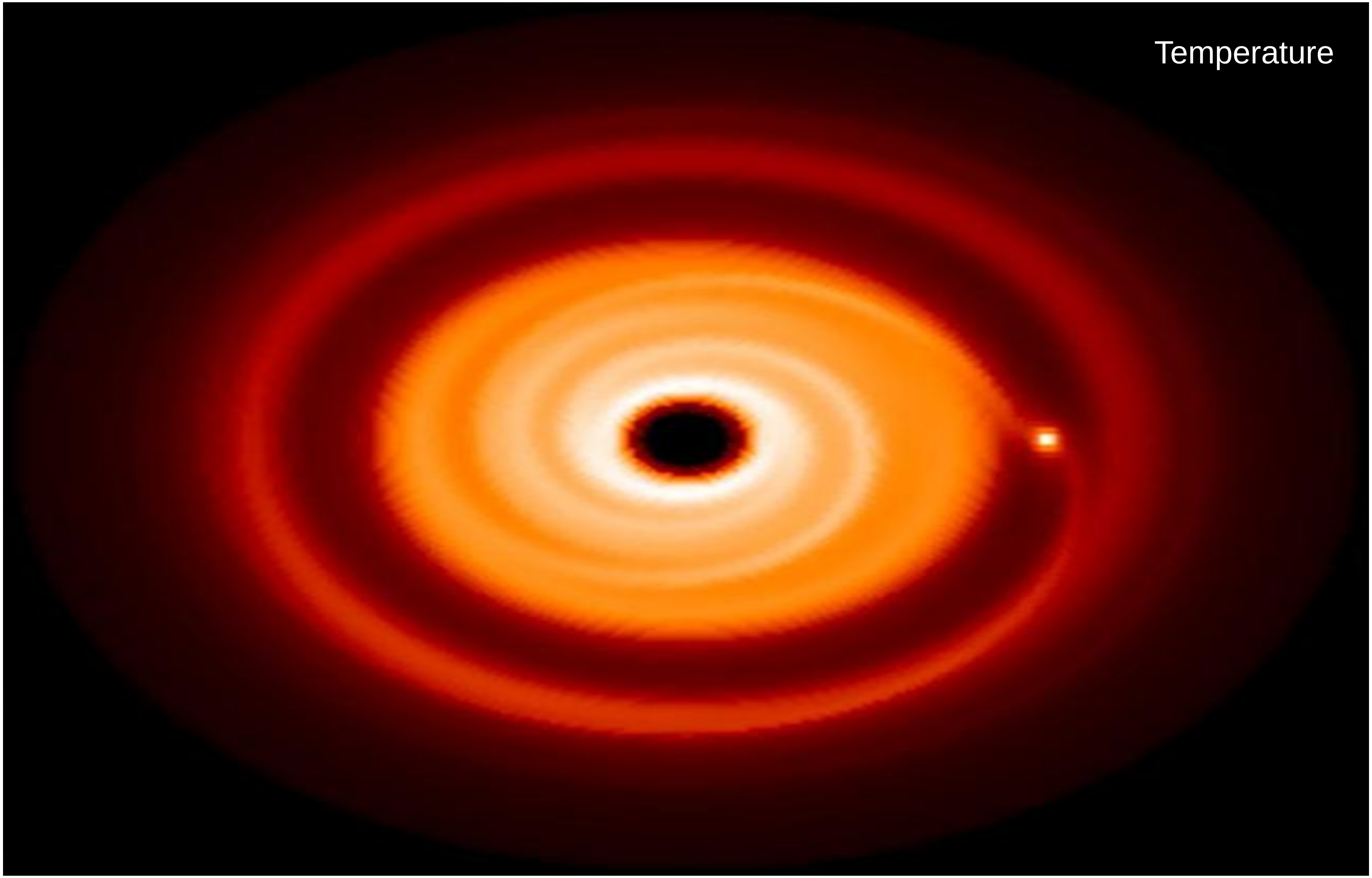

Klahr & Kley 2006

Has the formation of a gas planet been (indirectly) observed *in statu nascendi* ?

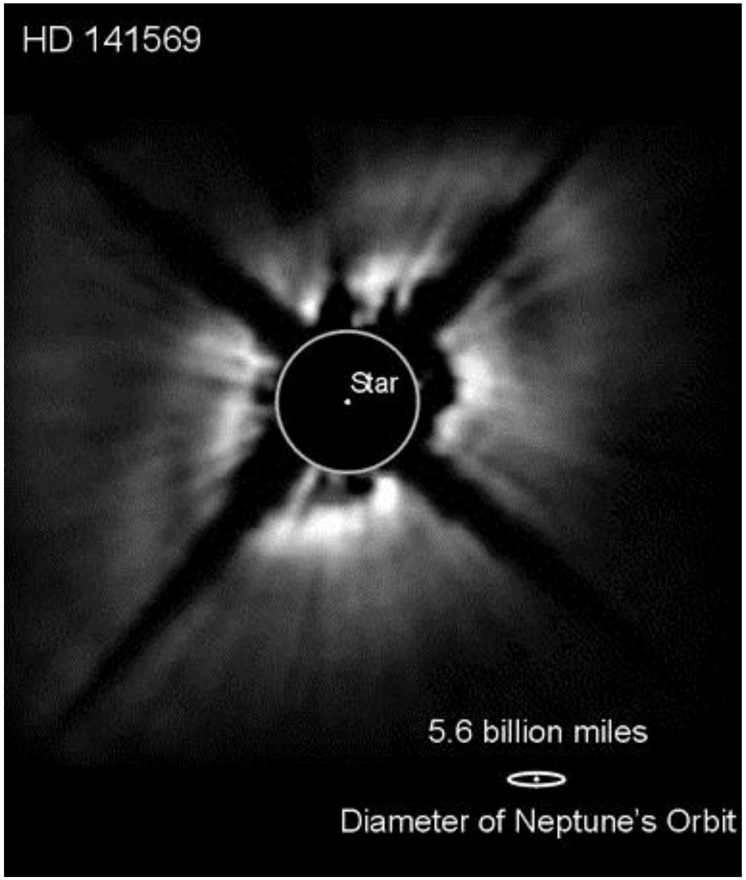

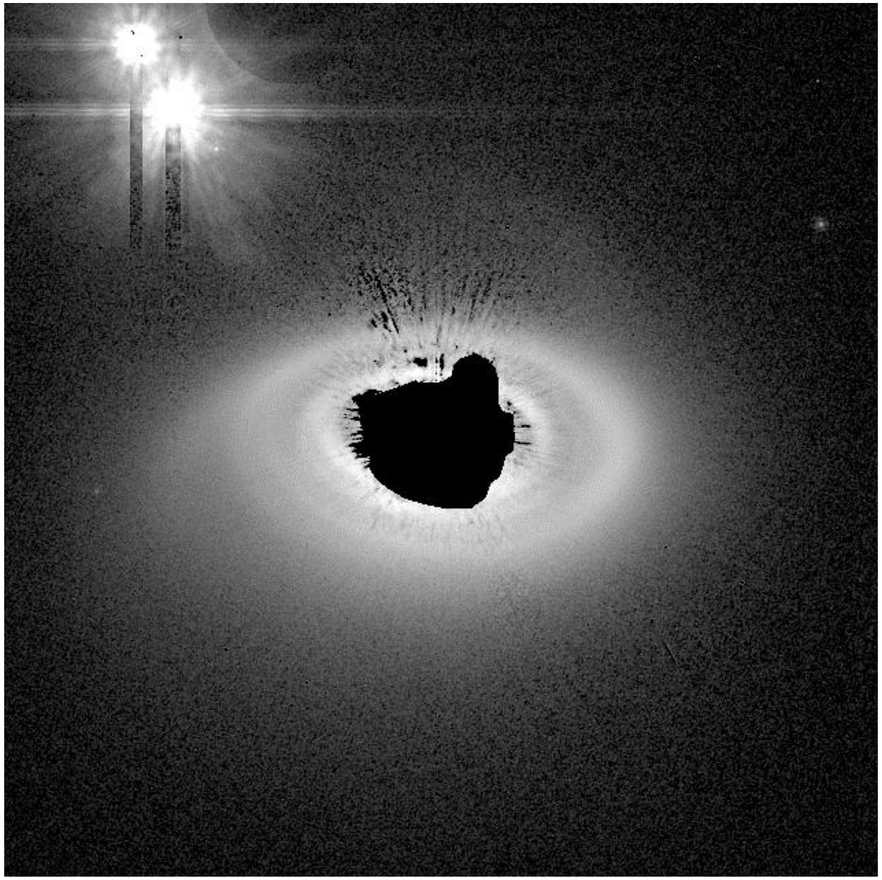

III. The formation of planets and planetary systems

e. Dynamical interaction and re-arrangement of planets

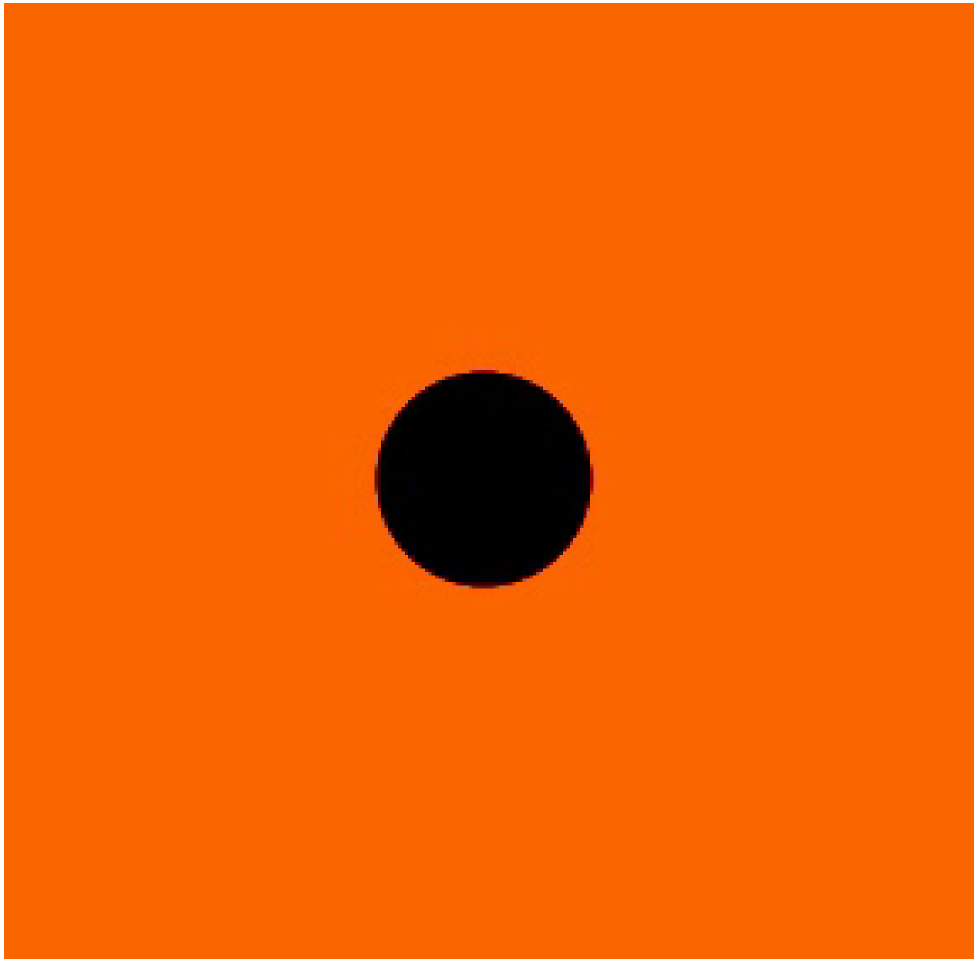

http://www.maths.qmul.ac.uk/~masset/moviesmpegs.html

Planet migration und reorganization

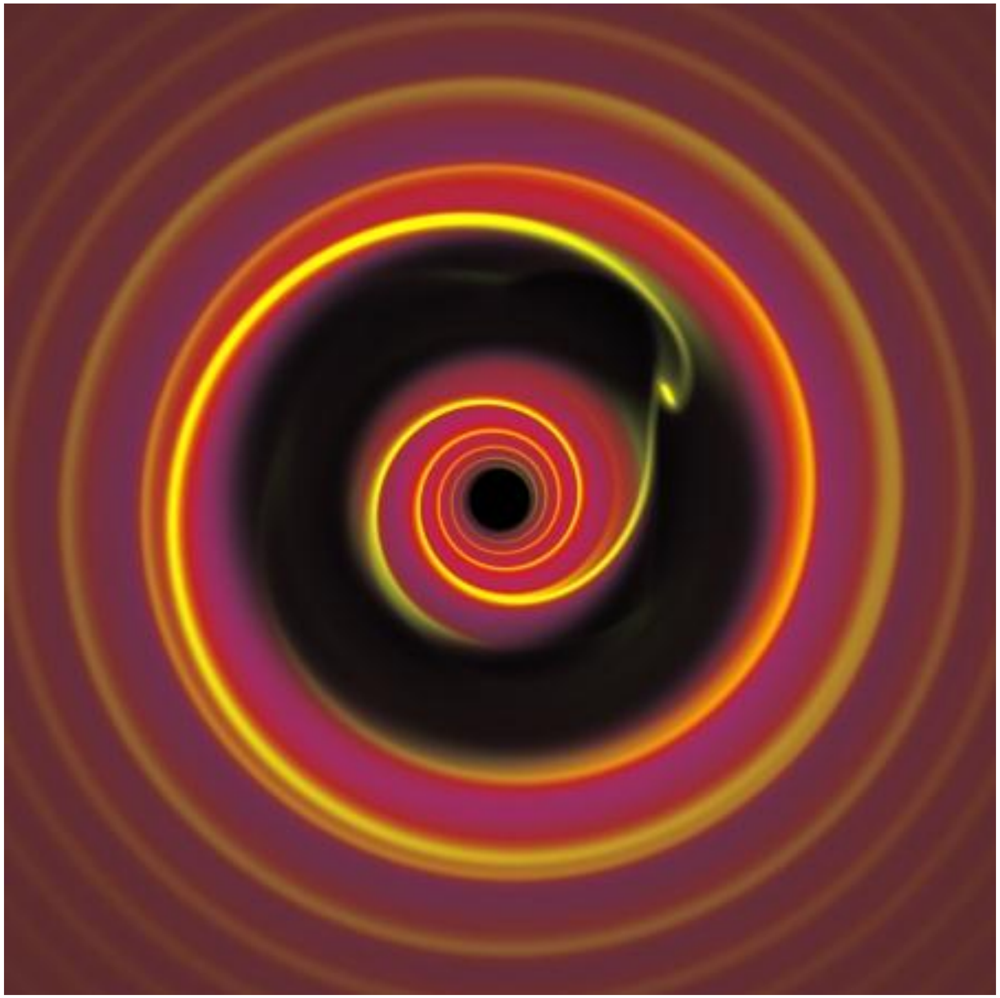

Excitation of spiral density waves in the gas by the planet; torque anisotropy between inner and outer disk; in most cases, the influence of the outer spiral wave dominates so that the planet loses angular momentum and spirals radially inward. Stop of migration by (a) clearing of the nebula or (b) tidal friction with the central star.

The *Nice* model for the dynamical evolution of the giant planets of the solar system

Gomes et al. 2005

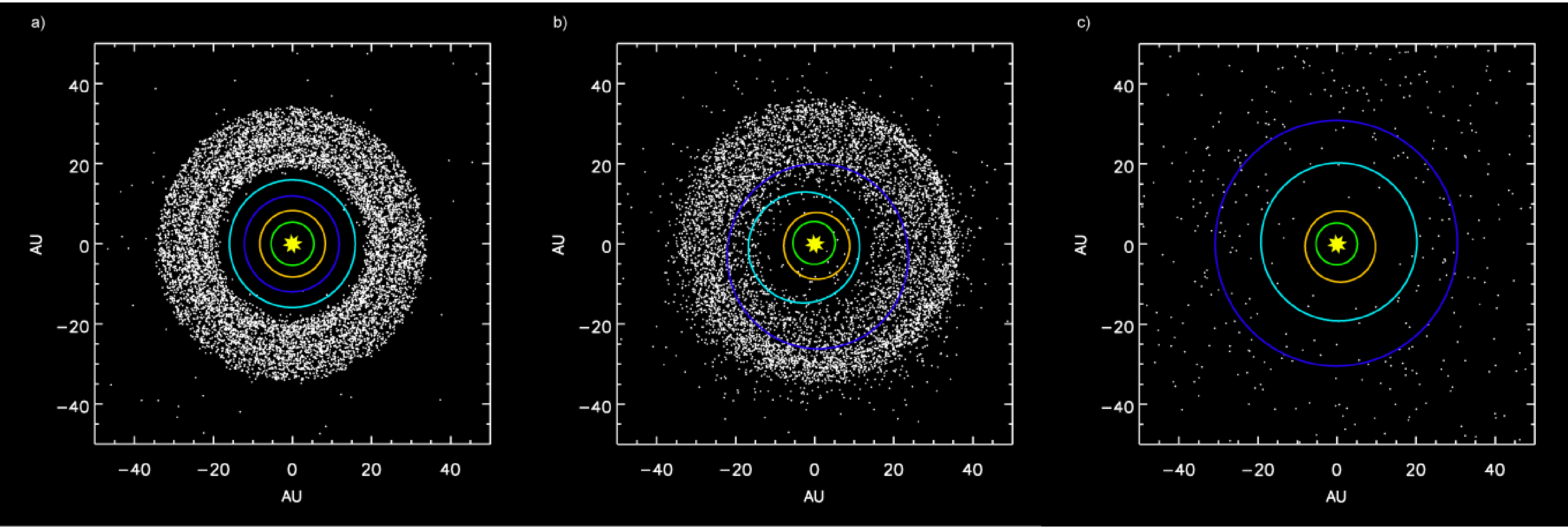

Left: before the 2:1 Jupiter-Saturn resonance, center: scattering of Kuiper-belt objects due to radial motion of Neptune, right: after scattering of the Kuiper-belt objects by Jupiter

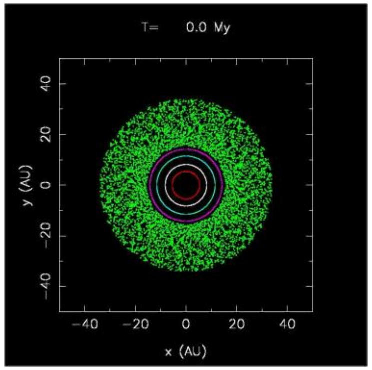

http://www.obs-nice.fr/morby/LHB/LHBxy.AVI

The *Nice* model for the dynamical evolution of the giant planets of the solar system

Morbidelli et al. 2007

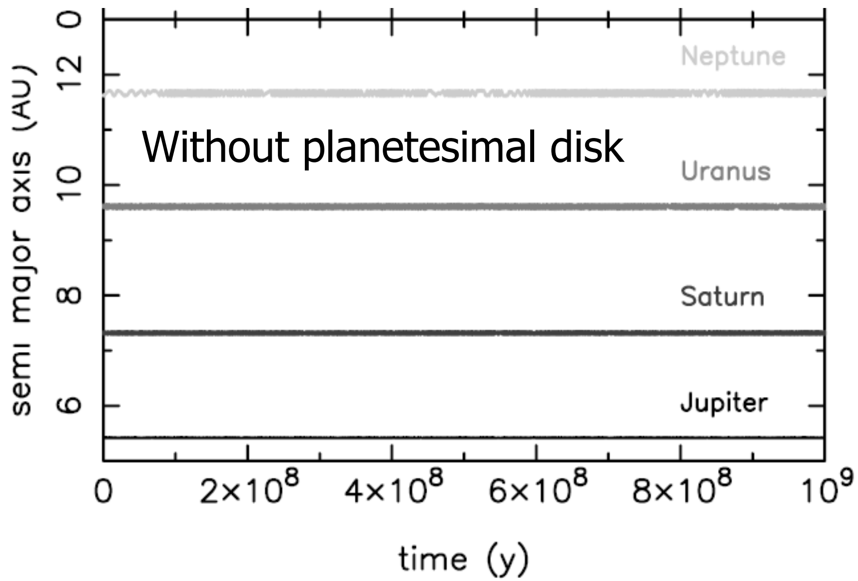

Gomes et al. 2005

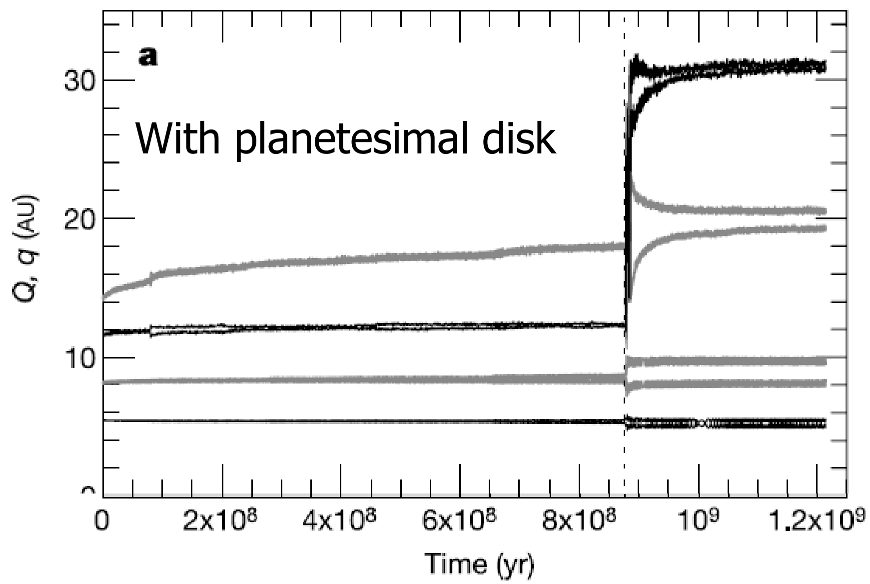

The *Nice* model for the dynamical evolution of the giant planets of the solar system

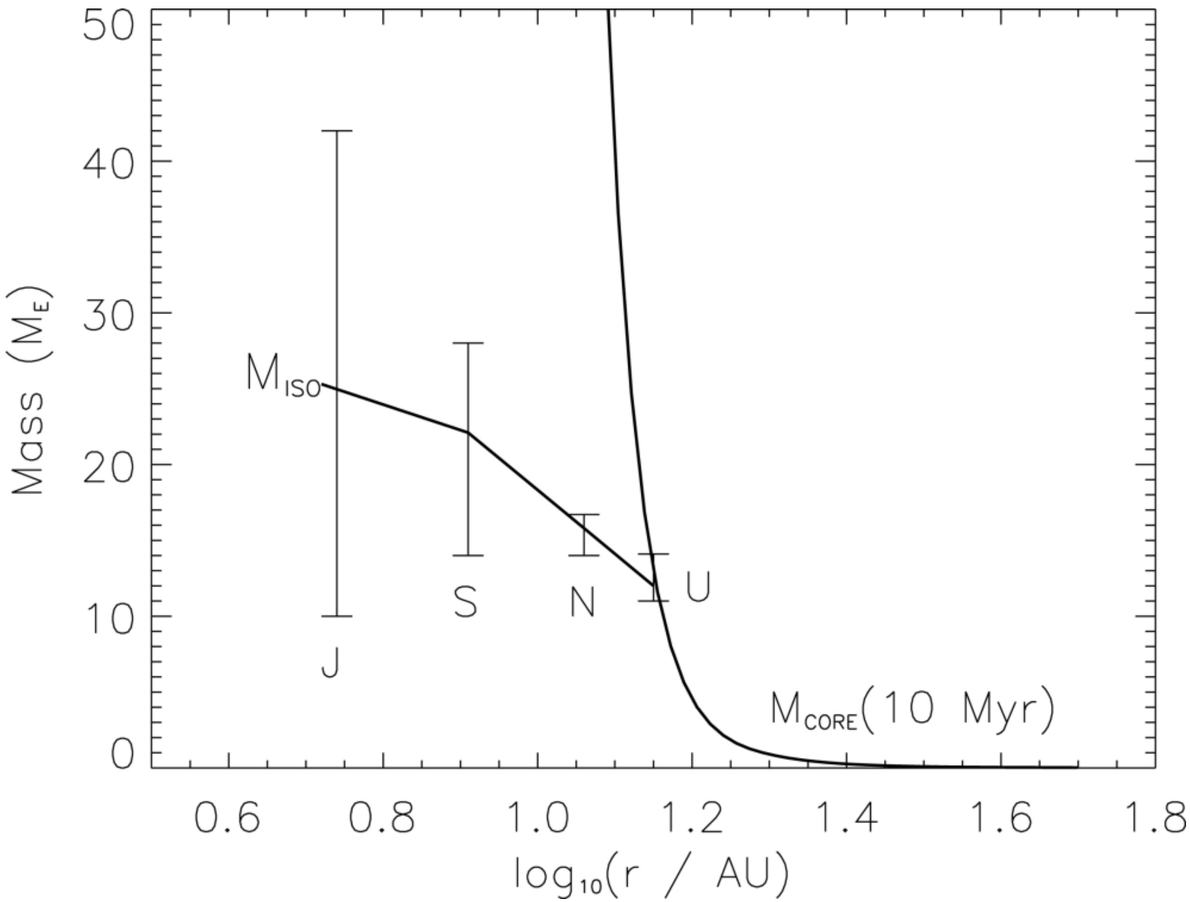

Desch 2007
(Prediction of the core masses of the giant planets; modified solar-nebula model, based upon Nice model)

III. The formation of planets and planetary systems

f. The late heavy bombardment

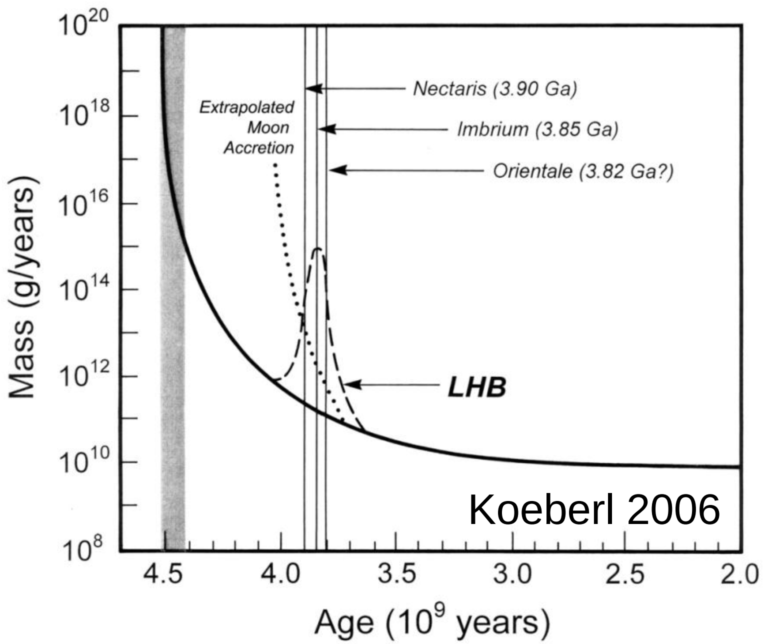

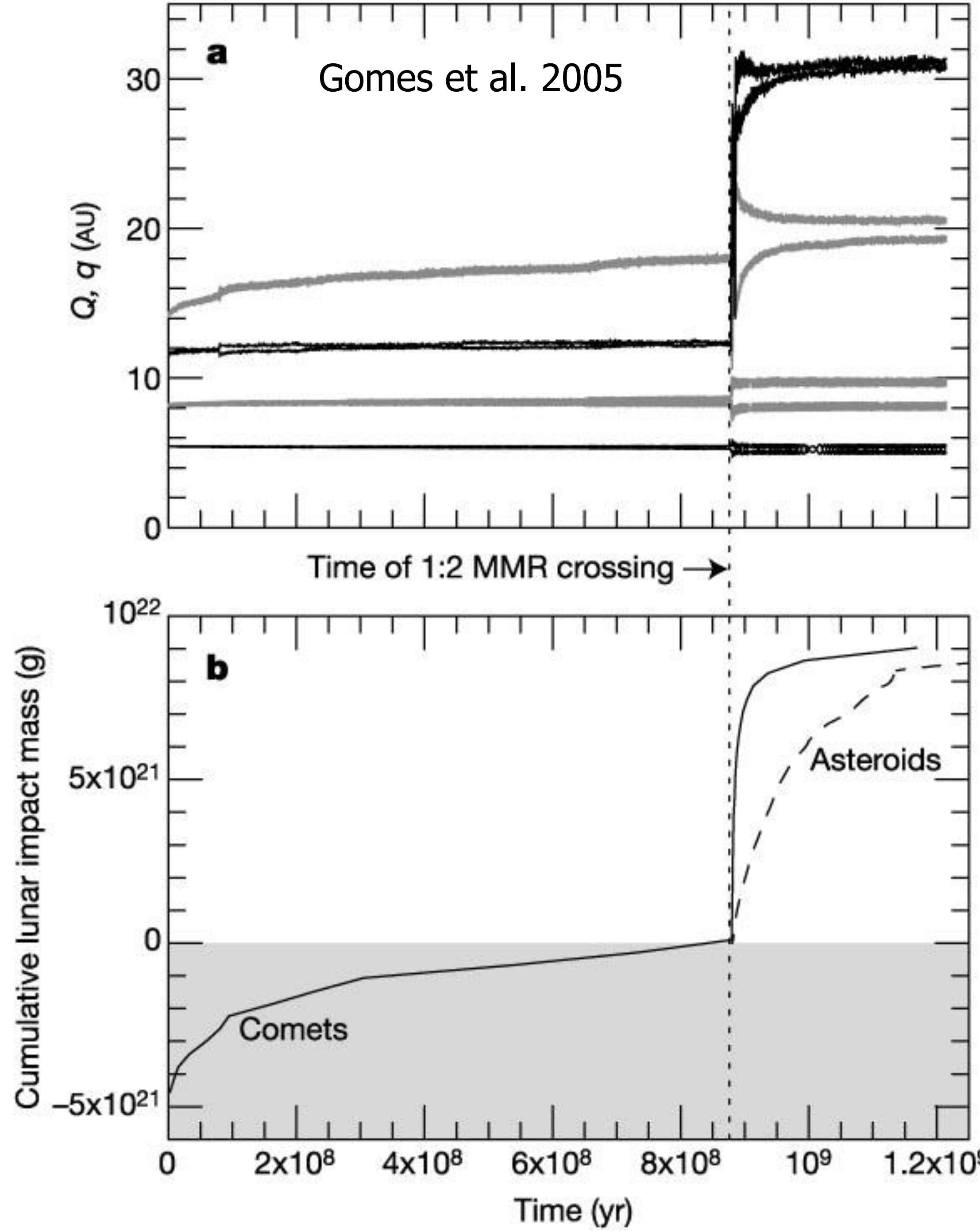

III. The formation of planets and planetary systems

g. Exchange of Oort cloud objects in young star clusters

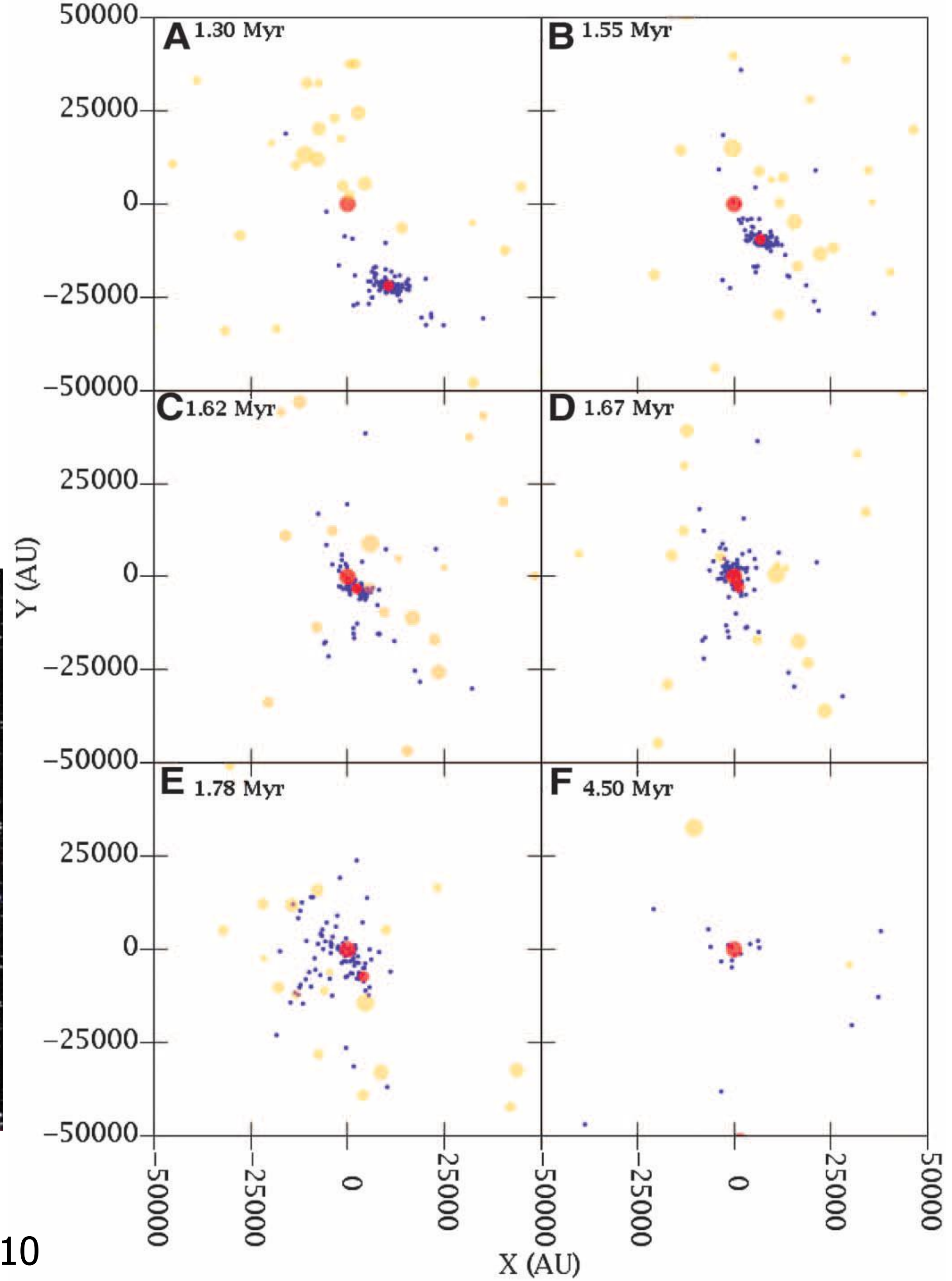

Levison et al. 2010

Conclusions

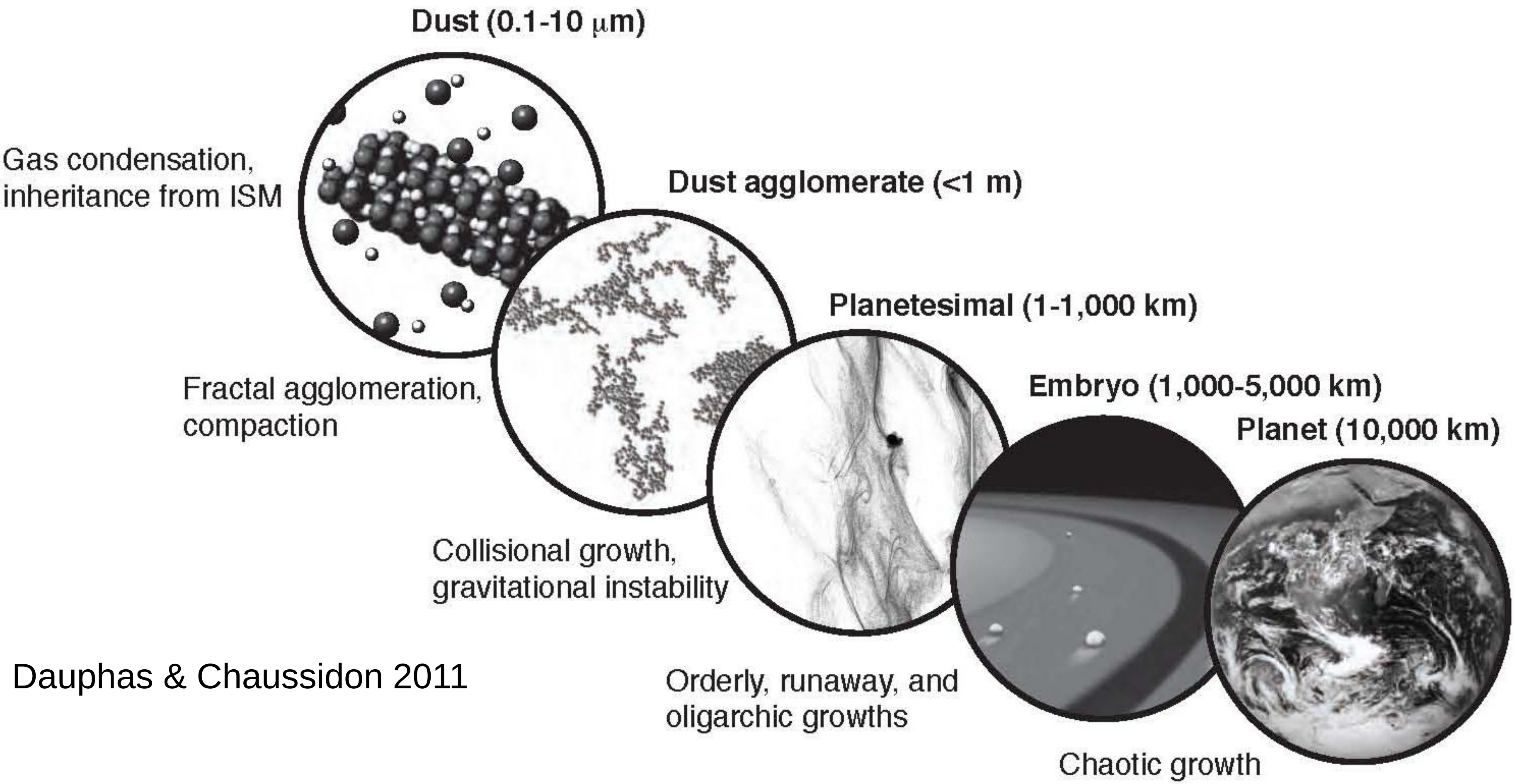

Dauphas & Chaussidon 2011

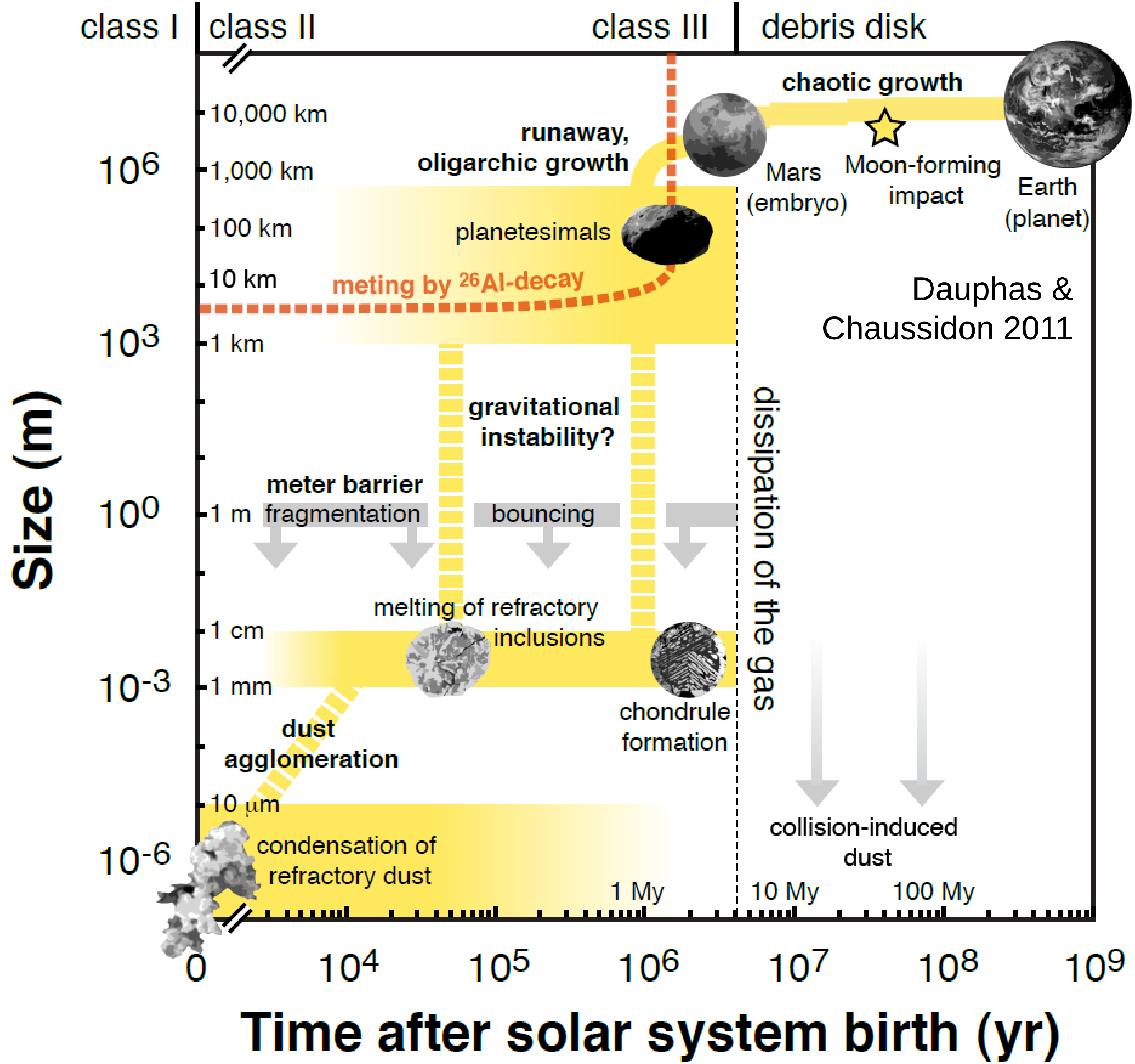
class I
class II
class III
debris disk
chaotic growth
10,000 km
runaway,
oligarchic growth
10^6
1,000 km
Mars
(embryo)
Moon-forming
impact
Earth
(planet)
100 km
planetesimals
10 km
meting by ^{26}Al-decay
Dauphas &
Chaussidon 2011
10^3
1 km
gravitational
instability?
dissipation of the gas
meter barrier
10^0
1 m
fragmentation
bouncing
melting of refractory
inclusions
1 cm
10^{-3}
1 mm
chondrule
formation
dust
agglomeration
10 μm
collision-induced
dust
10^{-6}
condensation of
refractory dust
1 My
10 My
100 My
Size (m)
0
10^4
10^5
10^6
10^7
10^8
10^9
Time after solar system birth (yr)

Conclusions

The five-stage process of planet formation

Protoplanetary dust

~1 µm

Agglomeration

interaction with gas important
no gravity

~1 mm

???

interaction with gas important
cumulative gravity potentially important
gas motion important

Planetesimals

~1-100 km

Accretion of planetesimals

no interaction with gas
gravity dominates

~10,000 km

Terrestrial planets

Gas accretion (?)

gravity dominates
escape velocity > thermal velocity
(i.e. minimum mass ~10-15 Earth masses)
migration potentially important

~100,000 km

Gas planets

Migration

Conclusions

The five-stage process of planet formation has the potential to explain/fulfil:

- The architecture of the Solar System ✓
- The architecture of other planetary systems ✓
- The gaseous-disk lifetime constraint ✓
- The existence and formation scenario of the Moon ✓
- Meteoritic constraints ✓
- The late heavy bombardment ✓
- The existence of debris disks ✓
- The stability of the Solar System over 5 Gyrs (?)

THANK YOU FOR YOUR ATTENTION !